

A Thesis Submitted for the Degree of PhD at the University of Warwick

Permanent WRAP URL:

<http://wrap.warwick.ac.uk/154356>

Copyright and reuse:

This thesis is made available online and is protected by original copyright.

Please scroll down to view the document itself.

Please refer to the repository record for this item for information to help you to cite it.

Our policy information is available from the repository home page.

For more information, please contact the WRAP Team at: wrap@warwick.ac.uk

An innovative organocatalyst for the chemical recycling of commodity polymers

A manuscript submitted to the
University of the Basque Country (UPV/EHU)

&

University of Warwick

For the degree of
DOCTOR IN SCIENCES

Presented by
Coralie Jehanno

Under the supervision of
Dr. Fernando Ruipérez (UPV/EHU)
Prof. Matthew I. Gibson (Warwick)

Donostia/San Sebastian

2019

**AUTHORISATION OF THE THESIS
SUPERVISORS FOR ITS PRESENTATION**

Dr. **Fernando Ruipérez**, with National ID Card n°

and Prof. **Matthew I. Gibson**, with National ID card n°

In their capacity as Supervisors of the Doctoral Thesis: **“An innovative organocatalyst for the recycling of commodity polymers”** completed within the Doctoral Programme **Chemistry and Polymers** by the PhD student Ms. **Coralie Jehanno**, hereby authorises the presentation of the aforementioned Doctoral Thesis, given that it fulfils the conditions necessary for its viva.

In on of 2019,

THE THESIS SUPERVISORS

Signed:

Signed:

Dr. Fernando Ruipérez

Prof. Matthew I. Gibson

**AUTHORISATION OF THE THESIS TUTOR
FOR ITS PRESENTATION**

Dr. Haritz Sardon and Prof. Andrew Dove, in their capacity as Tutors of the Doctoral Thesis: "An innovative organocatalyst for the recycling of commodity polymers" completed within the Doctoral Programme Chemistry and Polymers by the PhD student Ms. Coralie Jehanno, and supervised by Dr. Fernando Ruipérez and Prof. Matthew I. Gibson, hereby authorise the presentation of the aforementioned Doctoral Thesis, given that it fulfils the conditions necessary for its viva.

In on of 2019,

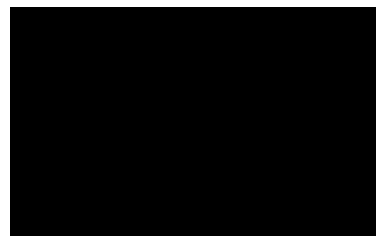
THE THESIS TUTORS

Signed:

Dr. Haritz Sardon

Signed:

Prof. Andrew Dove



**AUTHORISATION OF THE DOCTORAL
PROGRAMME'S ACADEMIC
COMMISSION**

The Academic Commission of the Doctoral Programme in **Chemistry and Polymers** during its meeting held on the of of 2019, agreed to authorise the presentation of the Doctoral Thesis entitled: **"An innovative organocatalyst for the recycling of commodity polymers"** supervised by **Dr. Fernando Ruipérez** and **Prof. Matthew I. Gibson** and presented by Ms. Coralie Jehanno and registered with the Department of Science and polymer technologies.

In on of 2019,

THE COORDINATOR OF THE DOCTORAL PROGRAMME

Signed:

DEPARTMENT APPROVAL

The Board of the Department of **Science and polymer technologies** during its meeting held on the of of 2019, agreed to authorise the processing of the Doctoral Thesis entitled: **“An innovative organocatalyst for the recycling of commodity polymers”** supervised by **Dr. Fernando Ruipérez** and **Prof. Matthew I. Gibson** and presented by **Ms. Coralie Jehanno**.

To this Department.

In on of 2019,

APPROVED BY THE DEPARTMENT DIRECTOR AND
DEPARTMENT SECRETARY

Signed:

Signed:

PHD DEGREE CERTIFICATE

DOCTORAL THESIS VIVA CERTIFICATE

PhD STUDENT Ms. Coralie Jehanno

TITLE OF THE THESIS: An innovative organocatalyst for the recycling of commodity polymers

After having witnessed the completion of the viva by the author and their response to any objections and/or suggestions made, the Panel appointed by the Postgraduate Commission of the University of the Basque Country to examine the Doctoral Thesis indicated above, meeting on the indicated date, agreed (unanimously or by majority vote) to award the following grade:

[Empty box for grade]

DISTINCTION / MERIT / PASS / FAIL

Viva language(s) (in the event of there being more than one language, please specify the percentage of the thesis defended in each):

Spanish

Others (specify which and the corresponding percentage): **English 100%**

In on of 2019,

CHAIRPERSON, Dr.

SECRETARY, Dr.

Signed:

Signed:

MEMBER 1,

MEMBER 2,

MEMBER 3,

Dr.

Dr.

Dr.

Signed:

Signed:

Signed:

PHD STUDENT

Signed:

A maman et papa, Justine et Enora,

“Rien ne se perd, rien ne se créé, tout se transforme”

Antoine Lavoisier

Acknowledgments

I would like to kindly acknowledge the European Union that funded this thesis through the SUSPOL-EJD 642671 project.

We say "words fly away, writings remain", so although I have at heart to verbally acknowledge all of you, I would like to let here something on the gratitude I have for the great people that accompanied me through this PhD. I crossed several borders, have worked in 5 laboratories, moved home 7 times, learned how to pack my entire life in two pieces of luggage and each of you somehow made these worth it.

My first acknowledgements will obviously go to my official, not-official-at-the-end, and non-official supervisors, Dr. Fernando Ruipérez, Pr. Andrew Dove and Dr. Haritz Sardon who accompanied me for more than three years. I learnt a lot from you and would like to sincerely acknowledge for the help and support, for the patience and the trust, and for the nice opportunities you offered me during this PhD. I also want to give a special thank to both Prof. David Mecerreyes and Dr. James Hedrick that provided me advices and assistance and with whom I had nice conversations, about chemistry, business and life. I would also like to thank other professors at POLYMAT for their advices and time dedicated to organise interesting seminars and discussions. I also have a special though for Prof. Maria Forsyth with whom I had rewarding talks and who I am considering as an example for the new female generation of academics that I am part of.

I consider myself very lucky to have been surrounded by so inspiring leaders and I hope to remember the best of what each of you taught me.

I will of course come now to the acknowledgements to all the people that worked with me in the Innovative Polymers group. It was a pleasure for me to work "hard and happy" with each of you guys! Starting with the "oldest" ones that welcomed me when I arrived in December 2015, Guiomar, Nerea, Ana, Maitane, Iñaki, Mehmet, Isabel, Luca and Alex, I saw all of you brilliantly defending your thesis and I can only wish you all the best for both you

personal and professional life! I have a special thought for the ones that started their PhD with me, Leire (mi primera vecina de despacho), Naroa (estas muy cerca de acabar guapa), Asier (para los Sabados de fiesta!), Antonio (Jueves, 20:30, sabemos donde estas) and Irma that collaborated with me on the first paper (depolymerización para mi, polimerización para ti, circular economy lab!). A thought also for the “new” ones in Korta, Esther, Marine, Soline, Marta, Jorge, I wish you all the best! And for the rest of you that made me happy to go to work every (most of) day(s), supporting me grumbling, singing, laughing and complaining! Ester, Liliana, Nicolas, Jeremy, the great team of post-docs as well as the new amazing generation of PhDs, Elena, Sara, Fermin, Alvaro. Thank you for everything and keep on working “hard and together”, this nice cheerful environment is the first step to good science! A thought also for the people that pass through our lab and with whom I spent nice time, Juan, Manoj, Klemen, Miguel-Angel and Antonella (guapa, tus sonrisas por la mañana, salvan vidas!) I finish with a special thank to Keita and Ion that held on with the depolymerisation experiments in the lab and did a great job. It was a pleasure to work with you, I wish you the best for what’s next!

I would like to thank a lot of other POLYMAT researchers with whom I shared scientific talks as well as extra work moments, I can not give all the names but, randomly, Giulia, Elodie, Boris, Stefano, Sil, Adrián, Sebastian, Nerea, Maialen, and others... It was a great pleasure to be part of this with you all! A very special thank to two persons that helped me a lot with administrative/bureaucracy/ renting things and much more: Inès and Mónica. I also want to acknowledge a bench of great people that sporadically shared with me pain and success in this PhD, my dear SUSPOL colleagues. Across 4 different countries, we had shared disappointments, joy and complains (yes, indeed we have complained a lot!). Jin and Leila, for the nice collaborations, Sètuhn and Panos for the help and support when I arrived in Warwick (and for the nice Thursday evenings with the Greek mafia), Beste for being the most joyful and smiling person I know, a bad day can only become a good day after a talk with you sweetyyyy, and Noé! Fue duro, penoso y largo pero lo has

hecho! Un día va a merecer la pena y hablaremos otra vez de todo eso con una caña sobre el sol de España! A special thank to Amaury who allowed me to start this PhD by sending me the offer. Profite de ta nouvelle vie parisienne! Un abrazo muy fuerte a Sufi! Acuérdate de pasar por Bretaña, que te ayudamos a olvidar este resentimiento que tienes por Francia y los Franceses... Y por fin, Andere, guapa, a ver como la historia sigue para nosotras, pero sabes que al peor, tenemos la opción de abrir un bar en una isla fuera, donde se puede surfear!

I also have to acknowledge quite a lot of people with whom I spent very fun moments in San Sebastian. Guys, I cannot cite you all but you will recognise yourself for the nice beach afternoons, DabaDaba Saturday evenings, pintxo pote Thursdays, salsa class Wednesdays and after work beers.

Un merci tout particulier à Mathias qui a supporté, avec son éternelle bonne humeur mes sauts d'humeur pendant la rédaction de cette thèse. A charge de revanche quand ce sera ton tour...

Now a special mention to the nice people that crossed my road in California! Ali, Nathan, Myron, with Daniele we were probably forming the weirdest afghano-americano-dutch-italo-french crew ever! But thanks for all the nice scientific and personal conversations with the terrible American coffee or the very good IPAs. I wish you all the best and hope we could meet sooner or later, in one part of the world or another.

Going in the chronological order, I have to acknowledge my English colleagues for their help and support while I arrived in the cold and windy East Midlands. I enjoyed spending time with you guys, Benoit, Jeff, Spiros, SUSPOL people I already mentioned, it was great and I wish you all the best for the future. I would like to add a special thank to Chiara and Mar for the writing support. I should also specially acknowledge three amazing persons with whom I share the worst flat ever! Jierong, Denisa, Davide, we could at least thank Mr. Bilkhu for having made our meeting possible! It was so much laughs, culinary discoveries, hilarious games and lanterns in the sky! Just finish

the PhDs and let's meet somewhere for another chino-roumanian-italo-french dinner!

Un énorme merci à Thibaut, pour m'avoir encouragé à me lancer dans cette aventure malgré ce que cela a impliqué. Sans ton soutien, la première année tout particulièrement, aurait été bien plus difficile.

Et parce que je ne serais pas là où j'en suis sans les PDGs de l'amour, il paraît qu'il va falloir vous remercier, vous dire que je vous aime et que ces 3 années d'écoles avec vous ont été aussi merveilleuses que fondatrices. Je pense donc que NB, AG, ELC, CG, CS, ALF, CS, MB, RB, MC, ES, GG, PP, AJ, TB, PP, 7A (BA) CP, méritent, un, applaudissement. Un merci émue à AP qui me supporte depuis plus longtemps encore, qui aurait pu se douter après des weekends entiers de souffrance sur les bancs de la BU de Beaulieu que j'en redemanderai encore 8 ans plus tard? Je voudrais ajouter un merci encore plus particulier à la personne qui méritera de figurer tout en haut de la liste, toutes périodes confondues, Vincent, merci de croire que je suis capable de faire les choses quand moi je suis persuadée que je n'y arriverai jamais...

Si on m'avait dit à l'époque où on organisait des soirées clandestines du 1^{er} mai à Péaule qu'un jour je vous remercierais officiellement dans un bouquin de 200 pages, je n'y aurais pas cru. Mais puisqu'il est évident que sans vous tout cela aurait été bien moins drôle, mille mercis à Marie, Lucie, Valentin, Fabien, Marion et Lou mais aussi à Pierre, Morgan, Adeline, Rémi, Estelle, Carole, Benoit, Ophélie, Baptiste, et j'en oublie sûrement! Merci pour les soirées, les discussions, les engueulades, les weekends, les festivals, les plages et les expos, les campings et les cinés, que ce fut à San Sebastian ou à Péaule, à Paris ou à Le Cours, à Budapest ou à Questembert, rien n'est à jeter...

Daniele, mereces un págrafo para ti mismo, para haberme seguido en cualquier lugar durante casi 3 años. Gracias para las charlas, para la ciencia, para las explicaciones de RMNs y las columnas de los carbonatos del infierno, gracias para soportarme, para enfadarte y entenderme, para haber saltado de

un avión conmigo (literalmente!), para los cafés y los f*****g huge american burgers!, y simplemente, para ser ti mismo.

Et pour terminer ces éloges et ces mercis, ma Jenny bien sûr, qui a été là dans les bons comme dans les mauvais moments. Celle qui m'a connue au berceau, quand chez tata Danielle on goûtait des pains au lait au Nutella et du jus de raisin. Je ne compte pas rentrer tout de suite mais où que je sois, je sais que je peux compter sur toi.

Mille mercis à ma famille au sens large du terme, je ne peux pas tous vous citer ici mais vous vous reconnaissez bien sûr ! Merci de penser à moi régulièrement, bien que je sois loin de vous, de supporter mes blagues, mes positions tranchées et même parfois mes coups de sang pendant nos repas de famille ! Si je pense à mamie qui depuis Rinsquivy doit se demander dans quel pays lointain est-ce que je compte encore m'exiler l'année prochaine, je n'oublie pas ceux qui n'auront pas eu le temps de me voir commencer cette thèse mais qui auraient sûrement été à la fois fiers et inquiets pour leur petite-fille trop souvent au loin.

Enfin, et puisque vous êtes et resterez ceux qui comptent le plus, ceux qui m'ont tout donné. Papa, maman, merci de me faire confiance, de toujours croire en moi et de me soutenir dans mes choix de vie, même lorsque vous n'êtes pas d'accord, même lorsque vous avez peur pour moi. Enora, Justine, mes sœurs chéries, sachez que peu importe à quel point vous êtes fières de moi, je le suis toujours encore plus de vous. Cette thèse est pour vous, je vous aime tout les quatre, bien plus qu'il ne m'est possible de l'écrire ici, et je sais tout ce que je vous dois!

Abstract

Over the past century, synthetic plastics have become ubiquitous in our daily life, occupying an ever-expanding range of uses. Their global production has exponentially increased in the past half-century, from 15 to 311 million tons between 1964 and 2014, and is expected to double again by 2035. Many of those materials have extremely short lifetimes and the direct consequence is the tremendous quantities of plastic wastes accumulating in the environment for years. Produce, buy, use and dispose, this linear way of consuming more and more plastics is nowadays raising concerns, not only from governments, interstate institutions and companies but also by citizens themselves. The treatment of plastic wastes is a global problem which requires innovative solutions to collect, sort, degrade, and re-process these materials. Thus, recycling is a crucial matter from an environmental point of view but also taking into account the plastic production and the tremendous income recycling could be for the global economy.

Currently, most of the recycled plastics are by means of mechanical methods that involve grinding and re-processing of the material into lower value plastic products. The structural deteriorations lead to recycled product which does not share the same properties as the virgin polymer and also rapidly ends up as waste. Another approach relies on their direct conversion into high calorific value fuels through pyrolysis, but this thermal deterioration only postpones their unsustainable end-of-life since the resulting combustible will typically be burnt releasing mainly green-house gases such as CO₂ and potentially affecting to the global warming. In comparison, chemical recycling involves the depolymerisation of polymers into monomers or oligomeric fragments that can then be subsequently polymerised to yield recycled materials, it represents an attractive long-term strategy to create a sustainable polymer supply chain. Recently, the chemical recycling of polymers has attracted a lot of attention among the scientific community, mainly driven by the current public awareness of the plastic pollution problem. However, as a

consequence of the high stability of most polymers, depolymerisation processes are generally conducted in very harsh conditions and in the presence of catalysts, principally organometallics, which can present several drawbacks: possible presence of metal in the final product, low monomer yields or challenging purification procedures. Organocatalysts are promising "green" substitutes to classic organometallic catalysts. Although they are currently widely investigated for various polymerisation techniques, they have been much less explored in depolymerisation processes. One of the main reason behind this is that typically organic catalysts show poor thermal stability at temperatures that would be practical for recycling reactions. Thus, the partial or full degradation of the catalyst hinders the perspective of reusing it for several reactions and entails colouration of the final products, low conversion or undesirable side-reactions.

In **Chapter 1**, an innovative series of acid and base mixtures have been explored as catalyst for depolymerisation reactions. Not only these acid-base mixtures displayed unique thermal stability, a tremendous advantage compared to most of organocatalysts which usually degrade at relatively low temperatures, but also reveals very good abilities for the depolymerisation of commodity polymers. Indeed, both poly(ethylene terephthalate) (PET) and Bisphenol A-based polycarbonate (BPA-PC) have been depolymerised using an equimolar mixture of 1,5,7-triazabicyclo[4.4.0]dec-5-ene (TBD) and methanesulfonic acid (MSA) as catalyst in a solvent-free procedure. The comparison with already reported procedures have demonstrated the superior control of the reaction employing the present organocatalyst.

Chapter 2 has explored the influence of different parameters on the PET glycolysis catalysed by TBD:MSA (1:1). Using the adequate amount of reagent and catalyst, over 90% of Bis(hydroxyethyl)terephthalate (BHET) is obtained and easily recovered. Kinetics have emphasised the high selectivity of the reaction to form the desired monomer compared to well-known organocatalyst. Both the reagent and the catalyst can be easily recycled, demonstrating no loss of catalytic activity even after 6 cycles. Finally, it was

demonstrated that this catalyst could even be used in the self-condensation of BHET to obtain recycled PET exhibiting good thermal and physical properties, closing the polymer to monomer to polymer loop.

In a similar way, **Chapter 3** has investigated the same procedure for the depolymerisation of BPA-PC into both Bisphenol A (BPA), its industrial monomer, and valuable building blocks. By wisely choosing the starting reagent and tuning the reaction conditions, 5- and 6-membered cyclic carbonates were obtained in reasonable to excellent yields (up to 97 %), constituting a phosgene-free, 100% atom economy procedure for the ring-closing of valuable carbonates widely reported for the synthesis of high-performance materials. Similarly, innovative linear carbonates and ureas were obtained.

Density functional theory (DFT) methodology was employed for determining the mechanisms involved for both reactions – with PET and with BPA-PC. The obtained pathways exhibited similar chemical interactions but with a large energetic difference, inspiring the possibility for these two polymers to be recycled selectively. Thus, in **Chapter 4**, using different reagents and different reaction conditions investigated in the previous chapters, the simultaneous depolymerisation of BPA-PC and PET was explored using different reagents and in the presence of other plastics (i.e. polyolefins).

Resumen

Desde un siglo, los plásticos sintéticos han ganado cada vez más importancia en nuestra vida cotidiana hasta el punto de que se ha vuelto un material indispensable en muchos aspectos. Desde los años sesenta la producción mundial ha aumentado de manera exponencial, pasando de 15 millones de toneladas en 1964 a 311 en 2014, y las predicciones anuncian que este número se va a ver multiplicado por dos para el 2035. Muchos de estos productos tienen un tiempo de vida útil muy corta y la consecuencia directa son los billones de toneladas de plásticos que se acumulan en el medio ambiente. Producir, comprar, usar y desechar, esta manera lineal de producir cada año más plásticos es actualmente una verdadera preocupación tanto para los gobiernos e instituciones como para la industria y los ciudadanos. El tratamiento de los desechos de plástico es un problema mundial que necesita de soluciones innovadoras para recolectar, clasificar y reciclar estos materiales. Esta preocupación actualmente se ha vuelto de mayor importancia tanto por la protección del medio ambiente como por la pérdida económica que representa la no valorización de dichos plásticos.

Hoy en día, el reciclaje mas usado en el mundo es el reciclaje "físico" o "mecánico" que supone el molido de los desechos en gránulos de plástico posteriormente utilizado para hacer un nuevo material. Sin embargo, el deterioro de las propiedades del nuevo plástico no permite obtener un producto de la misma calidad que el producto original. De este modo solo se puede reciclar pocas veces el mismo material antes de obtener un producto demasiado dañado que terminará en la basura. Otra posibilidad para los desechos de plástico es la pirolisis, la combustión del material a altas temperaturas en ausencia de oxígeno para obtener un combustible de alta valor calorífica, pero la emisión de CO₂ y de gases tóxicos que este proceso provoca también contribuye a la contaminación del medio ambiente. Por lo contrario, el reciclaje "químico" es la depolimerización de un polímero en monómeros u oligómeros, los cuales pueden ser seguidamente utilizados para otras polimerizaciones. Recientemente, este método sostenible ha

comenzado a interesar en la comunidad científica, que también siguen la tendencia general de incremento del interés por el medio ambiente, en general, y el reciclaje en particular. La mayoría de los polímeros que usamos diariamente son macromoléculas muy estables que necesitan condiciones severas como temperaturas altas, presión o presencia de catalizador. En la literatura, muchas reacciones funcionan gracias al uso de catalizadores organometálicos pero esta familia de moléculas muestra inconvenientes, como la presencia de metales en el producto final, bajo rendimiento, o complicaciones en la purificación. En cambio, los organocatalizadores constituyen una alternativa prometedora, más "verde". Aunque la investigación y el uso de dichos catalizadores en diferentes polimerizaciones ha tenido éxito desde las últimas dos décadas, los estudios sobre el uso de moléculas orgánicas como catalizadores para reacciones de depolimerización son casi inexistentes. El problema principal de los catalizadores orgánicos es la pobre resistencia que tienen a las altas temperaturas, lo que los hacen poco prácticos para las reacciones de depolimerización que son típicamente procesadas a altas temperaturas. La degradación del catalizador durante la reacción genera varias dificultades como la coloración del producto final, la promoción de reacciones indeseables o bajo rendimiento al mismo tiempo que impide la reutilización del catalizador para más reacciones.

En el **Capítulo 1**, mezclas de ácidos y bases demuestran excelente resistencia térmica, superior a los catalizadores orgánicos usuales. En particular, la mezcla estequiométrica de 1,5,7-triazabicyclo[4.4.0]dec-5-ene (TBD) y ácido metanosulfónico (MSA) resiste excepcionalmente, hasta más de 400 °C. Además, las primeras pruebas efectuado con tereftalato de polietileno (PET) y policarbonato común (BPA-PC) han demostrado las capacidades del TBD:MSA (1:1) como catalizador para la depolimerización de polímeros comunes. Usando un procedimiento sin disolventes orgánicos, el producto de cada depolimerización fue recogido puro en un tiempo razonable.

El **Capítulo 2** explora la influencia de diversos parámetros sobre la glicólisis del PET con el catalizador TBD:MSA (1:1). Usando cantidades adecuadas de

reactivos y catalizador, mas de 90% de bis(hidroxietyl) tereftalato (BHET) fueron recogidos después de su cristalización en agua. Cinéticas han demostrado la alta selectividad de este catalizador en comparación con otros catalizadores encontrados en la literatura. El reactivo, utilizado en exceso, y el catalizador fueron reciclados hasta 5 veces sin cambiar el rendimiento de la reacción. Seguidamente, el mismo catalizador fue empleado también para polimerizar el BHET en PET con propiedades térmicas y físicas similares a los de un PET no reciclado, cerrando así el círculo polímero-monómero-polímero. De la misma manera, en el **Capítulo 3**, el mismo procedimiento ha sido aplicado a la depolimerización del BPA-PC en Bisphenol A (BPA), su monómero industrial, y moléculas valiosas. Con el reactivo adecuado y con el control de los parámetros de la reacción, carbonatos cíclicos de 5 y 6 carbonos fueron obtenidos, hasta 97% de rendimiento. Así, el cierre de estos carbonatos cíclicos – utilizados en la síntesis de materiales de alto performance – es posible, sin utilizar fosgeno o sus derivados tóxicos. Carbonatos lineares y ureas también fueron obtenidos con el mismo método. Cálculos cuánticos DFT (Teoría del funcional de la densidad) fueron utilizados para entender el mecanismo implicado en las dos reacciones descritas en los capítulos 2 y 3 – con PET y BPA-PC. Los diagramas de energía muestran interacciones químicas similares con el catalizador para los dos polímeros pero la barrera de activación implica mucho más energía en el caso del PET que para el BPA-PC. En el **Capítulo 4**, esta diferencia fue utilizada para depolimerizar a la vez dos plásticos. Diferentes reactivos fueron empleado para observar el efecto de la presencia de un polímero con el otro sobre la depolimerización de los dos. Además, la presencia de otros plásticos (i.e. poliolefinas), demostró no interferencia en el resultado de la depolimerización ni del BPA-PC ni del PET.

Résumé

Depuis près d'un siècle, les plastiques de synthèse se sont progressivement imposés dans nos vies jusqu'à devenir omniprésents dans la plupart de nos tâches quotidiennes. La production mondiale a augmenté de façon exponentielle et, entre 1964 et 2014, on est ainsi passé de 15 à 311 millions de tonnes de plastique produit annuellement, des prédictions annonçant le doublement de ce chiffre d'ici à 2035. La plupart de ces produits plastiques ont une durée de vie très courte, il en résulte une pollution visible – sur nos côtes et dans nos rues – mais pire encore, une pollution invisible sous la forme de gigantesques gisements de plastiques au milieu des océans et de milliards de micro-fragments de plastiques disséminés sous les eaux. Produire, acheter, utiliser puis jeter, cette linéarité dans notre consommation du plastique est aujourd'hui remise en cause, tant par les gouvernements et les organisations supra-étatiques que par les entreprises et les citoyens. Le traitement des déchets plastiques est un problème global qui nécessite des solutions techniques innovantes pour collecter, trier puis réutiliser efficacement ces matériaux dans une approche circulaire de nos modes de production et de consommation. Le recyclage est donc un sujet central pour nos sociétés modernes, d'un point de vue du respect de l'environnement, mais également d'un point de vue économique puisque le non-traitement de millions tonnes de plastiques chaque année entraîne un manque à gagner colossal pour l'économie mondiale.

Aujourd'hui la méthode de recyclage la plus utilisée reste le recyclage dit "physique" ou "mécanique" qui consiste en un broyage des déchets plastiques en petites billes qui seront ensuite utilisées pour produire un nouveau matériau. Cependant, la détérioration intrinsèque au plastique recyclé, due notamment aux additifs et aux contaminants, conduit à une qualité inférieure qui ne permet pas de produire un plastique aussi performant que celui du produit initial. Ce type de recyclage est donc limité et ne peut être appliqué que quelques fois avant que le plastique ne finisse irrévocablement sa course, au mieux à l'incinérateur, au pire dans la nature.

Une autre approche, la pyrolyse, consiste à transformer les plastiques en un combustible à haute valeur calorifique, mais l'émission de CO₂ et de fumées toxiques qui en découle requiert de nombreux traitements et il ne s'agit alors que d'une autre forme de pollution. A l'inverse, le recyclage dit "chimique" implique la dépolymérisation d'un polymère en monomères ou en fragments oligomériques qui pourront ensuite être utilisés pour de nouvelles polymérisations. Récemment, cette méthode durable a concentré de plus en plus d'intérêts de la part de la communauté scientifique, poussée par l'engouement général autour de cette problématique. Cependant, la plupart des polymères que nous utilisons quotidiennement sont des macromolécules très stables qui demandent de sévères conditions de traitement : haute température, forte pression, présence de catalyseurs... Si la plupart des réactions présentes dans la littérature utilisent des catalyseurs organométalliques, cette famille de molécules présente certains désavantages lorsqu'il s'agit de dépolymérisation : présence de résidus métalliques dans le(s) produit(s), rendements faibles, purification difficile.

Ainsi, les organocatalyseurs se présentent comme une alternative plus "verte" aux catalyseurs métalliques. Et bien que leur application en polymérisation soit très étudiée depuis deux décennies, seuls de rares exemples existent en dépolymérisation. L'une des principales raisons réside dans le fait que la plupart de ces molécules organiques ne résistent pas à de fortes températures, les rendant peu pratiques pour des réactions de dépolymérisations typiquement conduites à haute température. La dégradation du catalyseur lors de la réaction menant à diverses complications : coloration du produit, faible rendement, promotion de réactions secondaires, etc, et rendant, dans le même temps, la perspective de le réutiliser impossible.

Dans le **Chapitre 1**, différents mélanges d'acides et de bases organiques ont montrés de meilleures résistances à la température que la plupart des organocatalyseurs. En particulier, le mélange équimolaire de 1,5,7-triazabicyclo[4.4.0]dec-5-ene (TBD) et d'acide methanesulfonique (MSA)

présente une exceptionnelle stabilité thermique alors que des tests effectués sur deux polymères de consommation courante, le polytéréphtalate d'éthylène (PET) et le polycarbonate usuel (BPA-PC), ont démontrés la capacité du mélange TBD:MSA (1:1) à catalyser des réactions de dépolymérisation. Une procédure sans solvant organique permet d'obtenir le produit de chaque dépolymérisation en quelques heures.

Le **Chapitre 2** explore l'influence de divers paramètres sur la glycolyse du PET en utilisant l'organocatalyseur précédemment synthétisé et testé. Après optimisations des conditions, plus de 90% de Bis(hydroxyethyl)terephthalate (BHET) furent collectés à la suite d'une simple cristallisation dans l'eau. Un contrôle cinétique de la réaction a permis de démontrer la sélectivité supérieure du TBD:MSA (1:1) comparé aux autres organocatalyseurs présents dans la littérature. Dans une démarche d'optimisation durable de la réaction, le réactif utilisé en excès ainsi que le TBD:MSA (1:1) ont été recyclés, jusqu'à 5 fois, sans perte significative de la capacité du catalyseur. Enfin, le BHET obtenu par dépolymérisation peut être polymériser à l'aide du même catalyseur pour obtenir à nouveau du PET, les propriétés de ce dernier étant similaires à celles du polymère initial.

De la même façon, le **Chapitre 3** étudie l'application de la même procédure à la dépolymérisation du BPA-PC en deux produits : le Bisphenol A (BPA), le monomère utilisé industriellement, et une molécule à haute valeur ajoutée. En choisissant le réactif approprié, et en ajustant les conditions de réactions, des carbonates cycliques à 5 et à 6 carbones sont obtenus (jusqu'à 97% de rendement). Cette procédure constitue ainsi une méthode n'utilisant pas de phosgène ou ces dérivés toxiques pour la fermeture de carbonates cycliques ensuite très largement utilisés dans la synthèse de matériaux haute performances. Des carbonates linéaires ainsi que des urées ont également pu être synthétisés par cette méthode.

Enfin, des calculs DFT (Density functional theory) ont été utilisés pour tenter de comprendre le mécanisme à l'œuvre pour ces deux réactions – PET et BPA-PC. Les diagrammes énergétiques résultant présentent des interactions

chimiques similaires, impliquant cependant des niveaux d'énergies différents. Cet état de fait permet d'imaginer la possibilité de dépolymériser les deux polymères lors d'une même réaction, ce qui est décrit dans le **Chapitre 4**. En utilisant différents réactifs et conditions de réaction, la dépolymérisation successive du BPA-PC puis du PET mène à des rendements équivalents à ceux obtenus lors des dépolymérisations individuelles des deux polymères, également en présence d'autres plastiques, en particulier, de polyoléfines.

Table of content



Introduction 1

1 On the importance of recycling	3
1.1 In a world of polymers	3
1.2 From a linear to a circular economy	5
1.3 Different recycling methodologies	6
1.4 Chemical recycling	7
2 Organocatalysed recycling of commodity polymers	9
2.1 organic bases	9
2.2 Organic acids	12
2.3 Ionic liquids and Acid-Base mixtures	13
3 Upcycling towards innovative polymers	18
3.1 From polymer to monomers	19
3.2 From polymer to polymer	21
4. Approach and objectives of the thesis	22
References	24



Organocatalysis 31

Introduction	35
1 Acid-base mixtures	37
1.1 Synthesis & characterisation	37
1.2 Thermal Stability	39
2 Catalytic activity for PET depolymerisation	42
2.1 TBD:MSA mixtures	42
2.2 Comparison with other acid-base mixtures	45
3 Catalytic activity for BPA-PC depolymerisation	47
Conclusion	50
References	52

BPA-PC depolymerisation 79

Introduction 83

1 Comparison between –OH, –NH₂ and –SH groups 85

1.1 Reactions with symmetric nucleophiles 86

1.2 Reactions with asymmetric nucleophiles 88

1.3 Further investigations on amino-alcohols 90

2 Renewable feedstocks as nucleophiles 91

2.1 Screening of bio-based feedstocks 91

2.2 Optimisation of the reaction using *meso*-erythritol (1l) 93

2.3 Isolation of the cyclic carbonates 94

2.3.1 General procedure 94

2.3.2 Example of the diglycerol dicarbonate (2m) 95

3 Synthesis of valuable 6-membered cyclic carbonates 96

3.1 The specific case of 1,3-propanediol 97

3.2 Alkyl groups in α position of the hydroxyl groups 983.3 Alkyl groups in β position of the hydroxyl groups 100

3.3.1 Kinetic of the reaction with 1s 100

PET depolymerisation 55

Introduction 59

1 Glycolysis optimisation salts 61

1.1 Influence of ethylene glycol and catalyst contents 61

1.2 Kinetic study 63

2 Recycling of catalyst 64

3 Scaling-up and limitations 66

3.1 Scaling-up the reaction 66

3.2 Reactions with coloured PET 66

4. Polymerisation of BHET 68

5. Quantum chemical modelling 71

Conclusion 73

References 75

3.3.2 Temperature and catalyst loading	101
3.3.3 Amount of reagent	103
3.3.4 Optimised conditions	104
3.4 Functional groups in β position of the hydroxyl groups	106
3.5 Influence of the substituent bulkiness on the ring-closure of the carbonate	108
4. Quantum chemical modelling	109
4.1 Model reaction with ethylene glycol	109
4.2 Comparison between 5- & 6-membered cyclic carbonate	113
4.2.1 Comparing reaction time	113
4.2.2 Comparing ability to ring-close	114
Conclusion	116
References	118

04

Selective depolymerisation 123

Introduction	127
1 PET vs BPA-PC reaction pathways	129
2 Depolymerisation of BPA-PC and PET in ethylene glycol	131
2.1 Preliminary trial	131
2.2 Kinetics using ethylene glycol as reagent	133
3 Depolymerisation of BPA-PC and PET in other reagents	137
3.1 Ethylene diamine and ethanolamine	137
3.2 Glycerol and allyl ether	140
4 Reactions in the presence of other polymers	142
4.1 Depolymerisation in the presence of PP	142
4.2 Depolymerisation in the presence of PVC	143
Conclusion	143
References	146

Appendix 181

Appendix Chapter 1	183
Appendix Chapter 2	192
Appendix Chapter 3	194
Appendix Chapter 4	223

Curriculum Vitae 228

Contact	231
Working experience	231
Education	232
Skills	233
References	234
Bibliography	236
Conference contributions	239

05

Conclusions & Perspectives 147

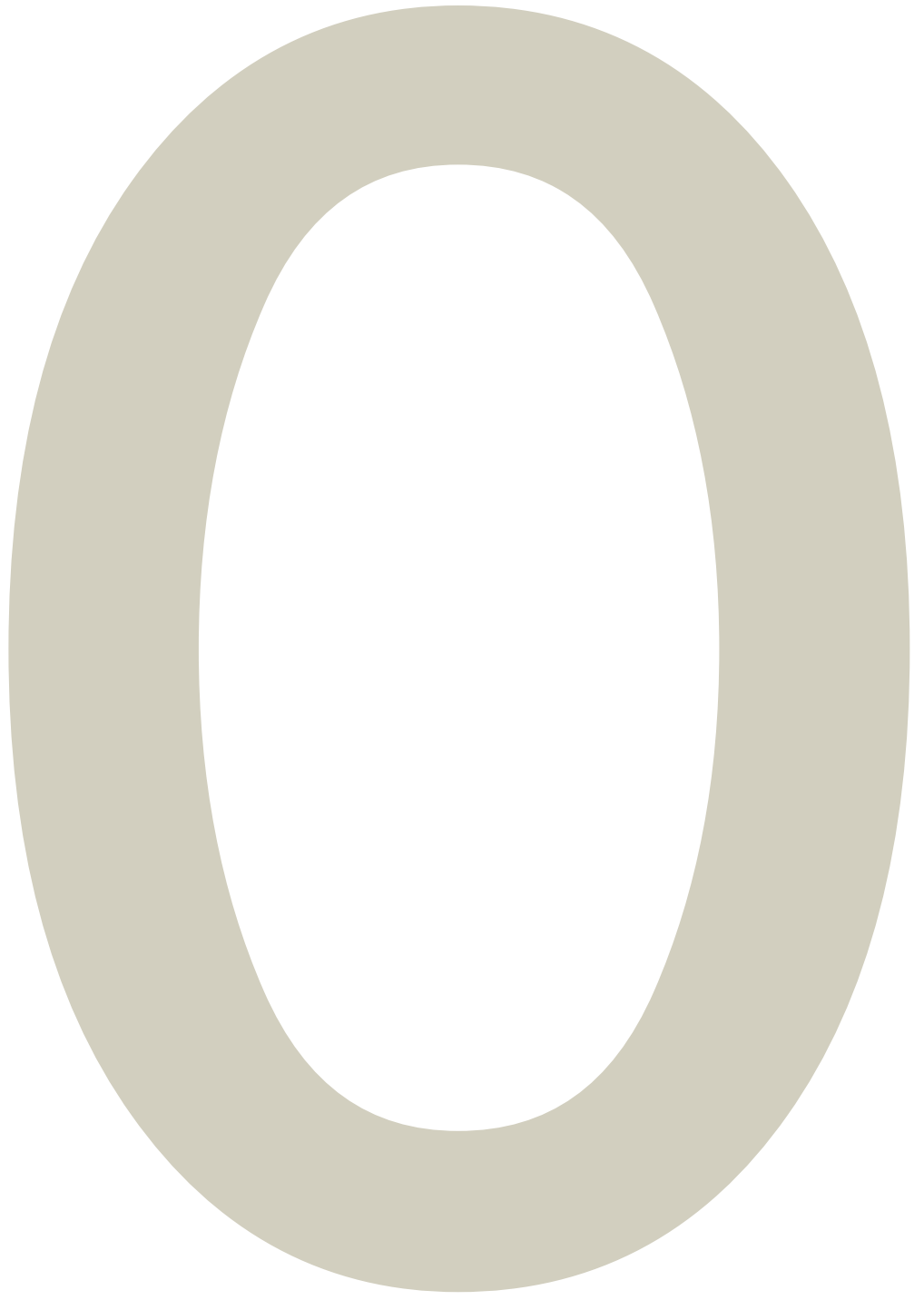
Methods 155

Instrumentation	157
Materials	158
Experimental part	158
Preparation of the catalyst	158
Re-crystallisation of TBD:MSA (1:1)	159
PET depolymerisation	160
BPA-PC depolymerisation	160
Polymerisation of recycled BHET	161
Isolation of carbonates	161
Selective depolymerisation procedures	167
Computational methodology	169
Introduction to quantum chemistry	169
Quantum chemical methods	171
References	178

List of Abbreviation

ATR	Attenuated total reflectance
BA	Benzoic acid
BAETA	N ¹ ,N ⁴ -bis(2-aminoethyl)terephthalamide
BHET	Bis(hydroxyethyl)terephthalate
BHETA	N ¹ ,N ⁴ -bis(2-hydroxyethyl)terephthalamide
BHEU	1,3-Bis(2-hydroxyethyl)urea
BPA	Bisphenol A
BPA-PC	Bisphenol A-based polycarbonate
DABCO	1,4-Diazabicyclo[2.2.2]octane
DBN	1,5-Diazabicyclo [4.3.0]non-5-ene
DBU	1,8-Diazabicyclo(5.4.0)undec-7-ene
DES	Deep-eutectic solvent
DFT	Density functional theory
DMA	Dimethylaniline
DMAP	4-Dimethylaminopyridine
DMC	Dimethyl carbonate
DMSO	Dimethyl sulfoxide
DMT	Dimethyl terephthalate
DSC	Differential scanning calorimetry
EEA	European Environment Agency
GPC	Gel permeation chromatography
IL	Ionic liquid
IR	Infra red
IRC	Intrinsic reaction coordinate
MSA	Methanesulfonic acid
NIPU	Non-isocyanate polyurethane
NMI	1-Methylimidazole
NMR	Nuclear magnetic resonance

PA	Polyamide
PCM	Polarised continuum model
PE	Polyethylene
PET	Poly(ethylene terephthalate)
PG	Polyglycolide
PHB	Poly(3-hydroxybutyrate)
PLA	Poly(lactic acid)
poly(TMC)	Poly(trimethyl carbonate)
PP	Polypropylene
PU	Polyurethane
PVC	Poly(vinyl chloride)
rPET	recycled Poly(ethylene terephthalate)
SCRF	Self consistent reaction field
TBD	1,5,7-Triazabicyclo[4.4.0]dec-5-ene
TFA	Trifluoroacetic acid
TGA	Thermogravimetric analysis
TMC	Trimethyl carbonate
TPA	Terephthalic Acid
TS	Transition state
ZPVE	Zero-point vibrational energy



Introduction

1 On the importance of recycling polymers

1.1 In a world of polymers

Polymers have become ubiquitous materials in our daily life on account of their low cost production and safety combined with their remarkable functional properties. Their global production has exponentially increased in the past half-century, from 15 million tons in the late 1960's to 311 million tons in 2014. Far from reducing, this number is estimated to triple by 2050.^{1,2} (Fig. 0.1)

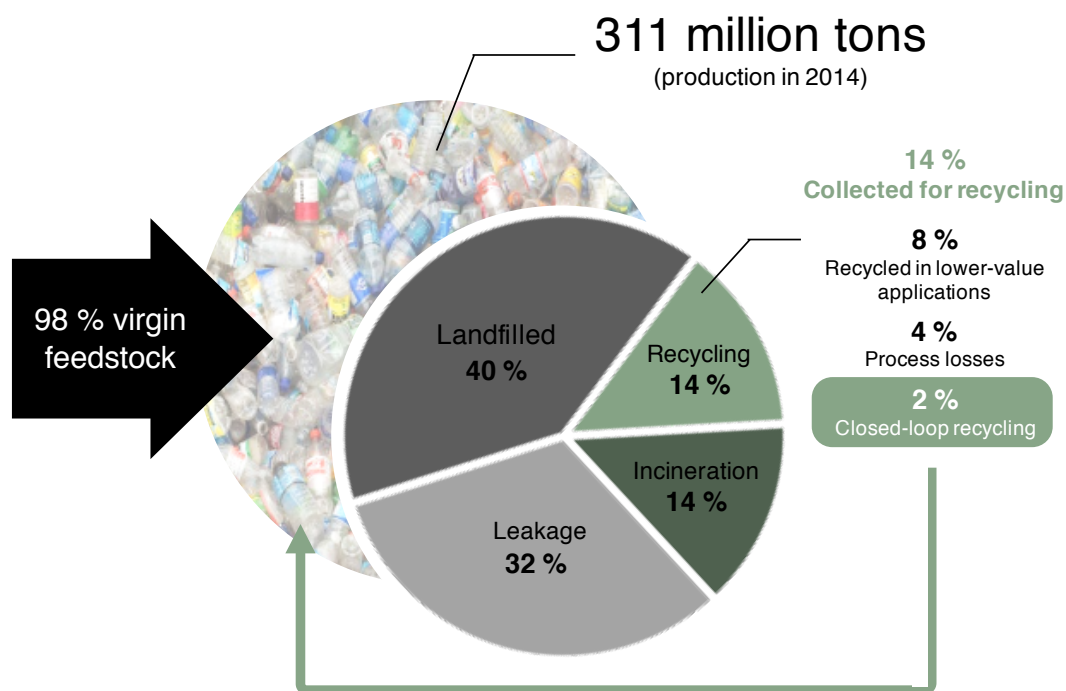


Figure 0.1. Production of plastics and their end-of-life treatment for the year 2014.

Many of the materials that we use, however, have extremely short lifetimes and are commonly limited to a single use. Consequently, plastic waste has been accumulating in the environment for years, and it is only very recently that this linear way of consuming plastics has raised concerns. If we are now fully leaving the "plastic age" as Yarsley and Couzens anticipated it in the 40's, "It is a world free from moth and rust and full of colour, [...] a world in which man, like a magician, makes what he wants for almost every need out of what is beneath and around him", the issues associated with plastic wastes management are not.³ Indeed, while the abundance of "disposable" plastics

for a variety of daily actions was considered as a considerable step to modernity in the post second world war context, (Fig. 0.2A) today, the exact same items are considered harmful for both human health and the environment (Fig. 0.2B).



Figure 0.2. Evolution of the public point of view on plastics, from (A) a cover of "Time" in 1955 considering single-use plastic items as a sign of modernity to (B) a cover of "National Geographic" in 2018 revealing the ecological disaster that these same plastics nowadays entail – The photographer freed this stork from a plastic bag at a landfill in Spain.

In 2015, it was calculated that 6 300 million tons of plastic waste have been generated since the 1950's with only 12% incinerated, less than 9% recycled and the resulting 79% released in the environment.¹ (Fig. 0.3) Worst, predictions indicate that with the growing of plastic production going hand-in-hand with the growing of the world population, this number could raise 12 000 million tons of plastic waste lost in the environment by 2050 if no actions are taken. Hence, the treatment of plastic waste is a global societal and environmental problem which requires innovative solutions to collect, sort, degrade, and re-process these materials. If the collecting and sorting policies and legislations are the matter of governments and interstate organisations,

the efficiency and viability of recycling processes is incumbent to the scientific community: scientists, engineers, industrials and academics.

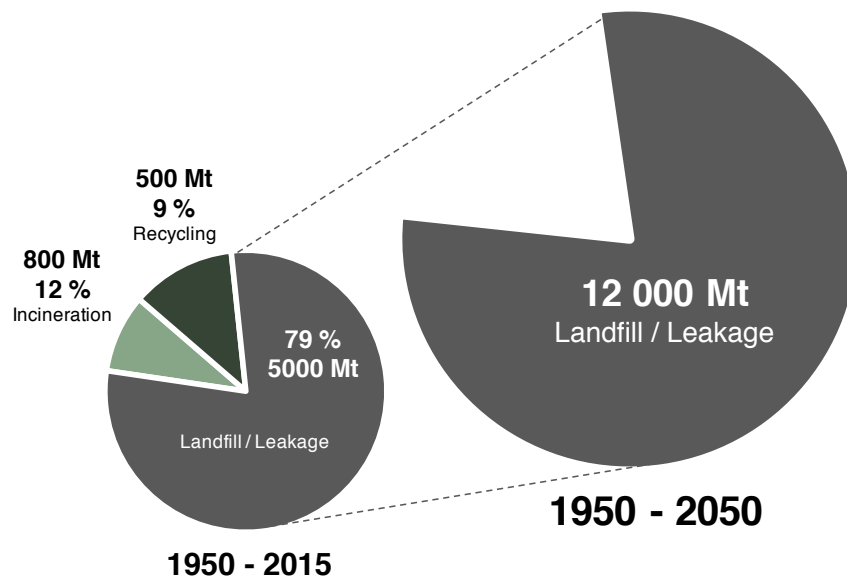


Figure 0.3. Growing production of plastic and their end of life from 1950-2015 period to 1950-2050 period.

1.2 From a linear to a circular economy

Recycling and in particular recycling plastic waste is a crucial problem considering the world that we want to bequeath to the next generations. Beyond the ecological considerations, the waste of millions of tons of plastic that currently cannot be recycled results in an estimated economic loss of 80 to 120 billion dollars each year, only for the plastic packaging sector.⁴ Counting that only 14% of packaging wastes are collected and recycled, and considering the loss during collection, sorting as well as the performance losses of the recycled material, estimations reveal that 95% of the possible economical value of discarded plastics is lost. (Fig. 0.4) Despite economic and environmental incentives to promote plastic waste treatment, current alternatives are very limited. The Ellen MacArthur foundation recently suggested three different strategies for a sustainable plastic packaging economy based on (1) reusing 20% of the packaging items in the long-term, (2) re-designing 30% of them and (3) recycling the remaining 50%.⁵ This last category mainly concerns the most commonly used plastics, such as polyethylene (PE), polyesters, polycarbonates, or polyurethanes. More than

350 entities including international companies, governments, financial institutions, universities and research organisations have taken resolutions through a global commitment to answer the plastic wastes issue with ambitious targets for 2025 and 2030. By eliminating non-necessarily plastic items, innovate for reusable, recyclable, and/or compostable plastics and globally design circularity for the plastic economy, these actors of the plastic industry are now engaged to reduce their environmental impact.⁶

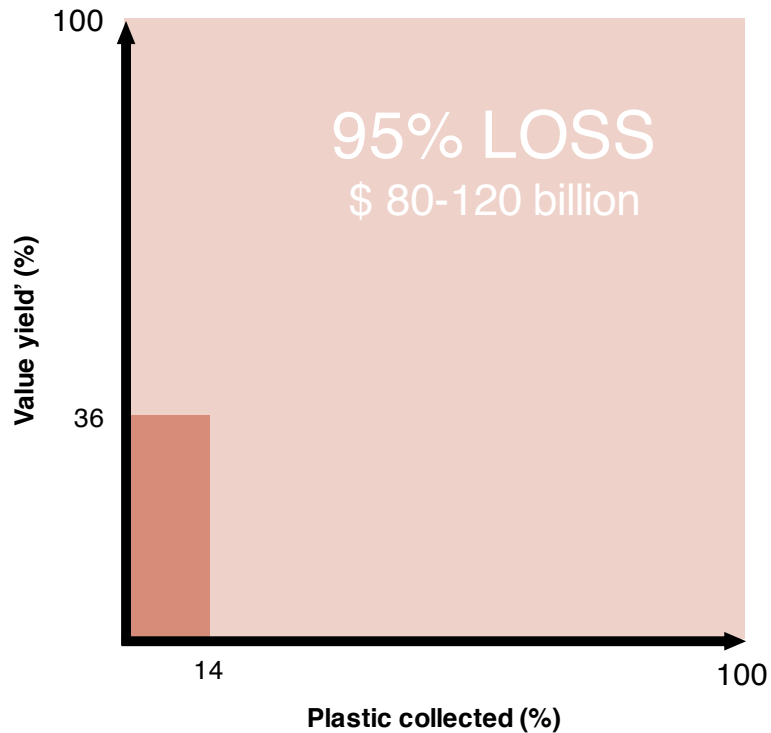


Figure 0.4. Estimation of the economic losses for plastic economy for the year 2016. *Value yield = volume yield x price yield, where volume yield = output volumes / input volumes, and price yield = USD per tonne of reprocessed material / USD per tonne of virgin material. Situation in 2016 based on 14% recycling rate, 72% volume yield and 50% price yield. Total volume of plastic packaging of 78 million tons, given a weighted average price of 1 100 – 1 600 USD/ton.⁷*

1.3 Different recycling methodologies

Currently, physical recycling is the most practiced method for commodity polymers but it involves the grinding and re-processing of the material into low-value plastic products. The inferior properties of the resulting material compared to the initial polymer has been qualified as *downcycling*, owing to the chemical or food contamination, discoloration, loss of strength, or decrease in molecular weight, for example.⁸ (physical recycling – **Fig. 0.5**) Another approach for treating post-consumed plastics relies on their direct

conversion into a high calorific value fuel through pyrolysis, a treatment that requires elevated pressure and temperature. However, this thermal deterioration only postpones their unsustainable end-of-life since the resulting combustible will typically be burnt to produce energy, releasing undesirable gases into the environment. (pyrolysis – Fig. 0.5) Additionally, pyrolysis is not suitable for some commodity polymers because of the undesirable toxic or corrosive compounds synthesised during the procedure, in the case of PET for example, the large portion of benzoic acid in the resulting oil obtained leads to poor quality fuel because of the acid corrosiveness'.^{9–11}

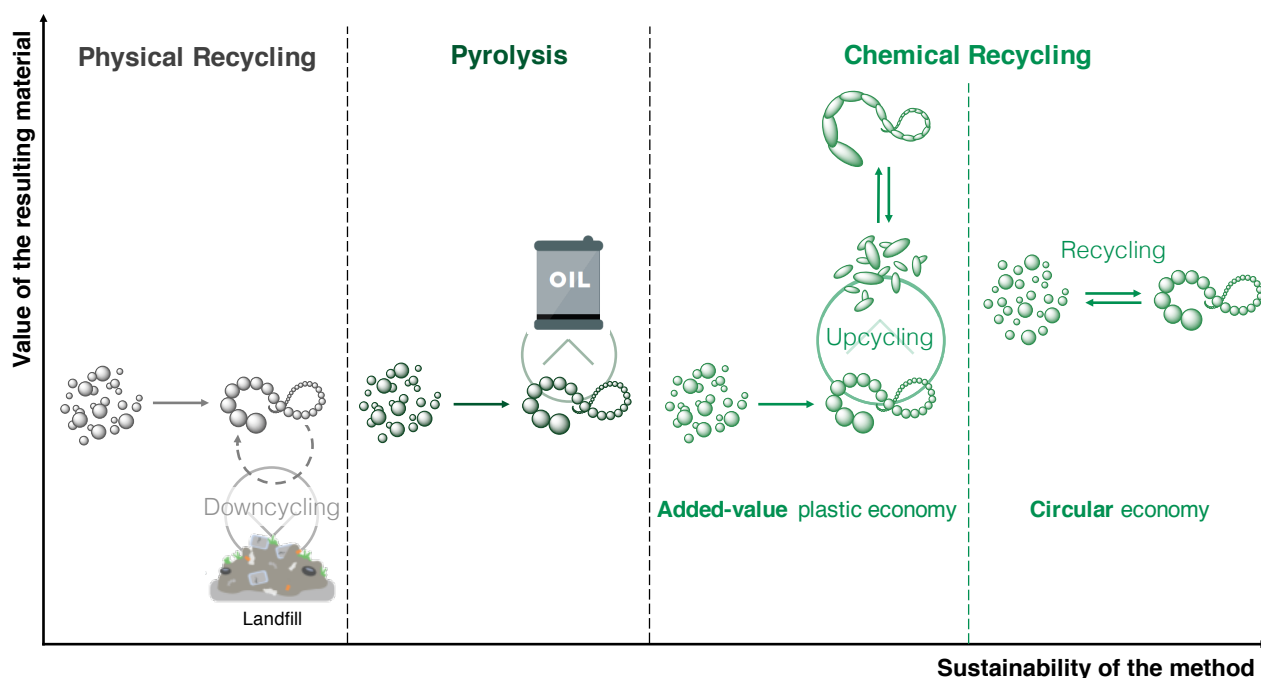


Figure 0.5. The different methodologies for the recycling of polymers.

The last and less implemented method is the chemical recycling which represents an attractive long-term strategy to create a sustainable polymer supply chain. Recently, it has attracted a lot of attention among the scientific community,^{12–15} mainly driven by the current public awareness of the plastic waste problem.

1.4 Chemical recycling

Chemical recycling means transforming polymers from plastic waste into high purity small molecules in outstanding yield. Specifically, chemical

depolymerisation either produces the initial monomers that can be subsequently re-polymerised into high quality polymers (circular economy – **Fig. 0.5**), or innovative small molecules that can be used as high added-value building blocks for synthesising unique polymeric materials or other chemicals (added-value plastic economy – **Fig. 0.5**).¹⁶ This process involving economic input is named *upcycling* to take the counterpart of the mechanical recycling leading to *downcycling*.

However, as a consequence of the high stability of polymeric materials, forcing conditions, such as microwave assistance,^{17–21} supercritical conditions,^{22–26} or the use of catalysts^{27–31} are usually required to enhance the efficiency of the depolymerisation reactions. In particular, stable and highly active organometallic catalysts, such as zinc or lead acetates, sodium/potassium sulphate, or titanium phosphate, which are already well-established for organic chemistry reactions, have been largely applied to depolymerisation processes. Despite their advantages, these metal-based catalysts display several drawbacks: (1) they are challenging to separate from the crude product, thus leading to lower-quality materials while molecules obtained from the depolymerisation are polymerised, (2) they have poor selectivity during the depolymerisation process, which results in a mixture of oligomers that are difficult to re-process and (3) the use of metal-based catalysts entails a high environmental and economic cost – some widely used metals risk complete disappearance in the next 100 years (e.g. zinc or silver), while others will be seriously threatened in the future if their consumption continues to increase (e.g. ruthenium, lithium, or copper).³²

As an emerging alternative, organocatalysts have appeared as promising “green” substitutes to traditional organometallic complexes. While a wide range of organic catalysts are being applied in an increasing number of polymerisations,^{33–38} to date, the translation to depolymerisation processes is limited. When applied to polymer degradation, in particular to transesterification reactions, organocatalysts can promote mechanisms that may lead to the formation of highly pure small molecules that are in turn

suitable for subsequent polymerisations. In many cases, hydrogen-bonds are playing an important role in controlling the catalytic activity and selectivity of the depolymerisation, as well as the architecture of the resulting polymer.^{39–41} Although few examples are available in literature, some recent advances have been made by using organic bases, organic acids, and ionic mixture catalysts, their performances are, for some of them, comparable to that displayed by typical organometallic, but even more interesting, the use of organocatalyst can promote, in some cases, reactions non-affordable with classical metal catalysts.

2 Organocatalysed recycling of commodity polymers

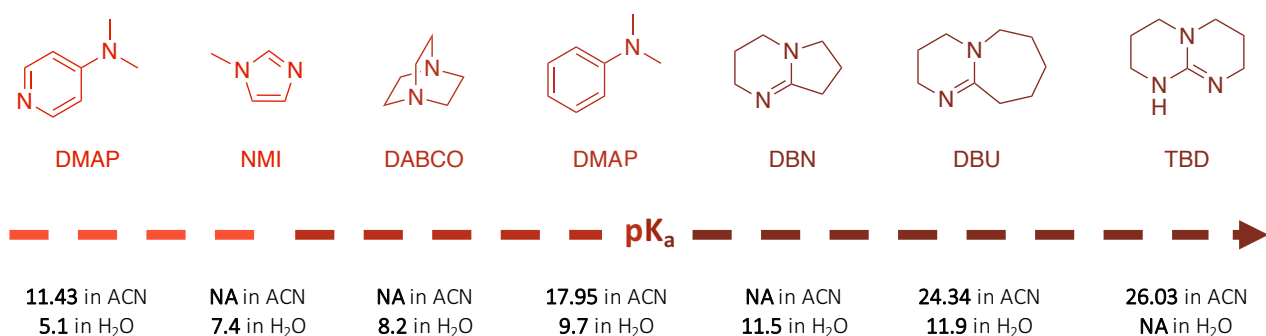
An important technological challenge involves the design of suitable pathways for the degradation of oxygen-containing commonly used polymers, mainly, polycarbonates, polyesters or polyurethanes. These materials are extensively used across a range of sectors that includes packaging, building, automotive and electronics and the majority of those produced will never be recycled. Several catalytic approaches have been investigated for the organocatalysed depolymerisation of these materials.

2.1 Organic bases

Organic bases are efficient catalysts for a large variety of base-mediated transformations both in organic and polymer synthesis. They are a powerful tool that have found particular use in a range of transesterification reactions.^{42–45} The so-called “superbases”, such as amidines, guanidines or phosphazenes have been found to be extremely active catalysts for the ring opening polymerisation (ROP) of cyclic esters,^{46–49} and in particular lactide.^{50,51} (**Scheme 0.1**) As therefore may be expected, their ability to catalyse depolymerisation via similar ‘general base’ mechanisms have driven interest in depolymerisation as it demands precise scission of the polymer backbone to obtain unique building blocks. In 2011, Hedrick and co-workers reported for the first time the glycolysis of PET using an organocatalyst, TBD (**Scheme 0.1**).⁵² In a large excess of ethylene glycol (16 eq.), at 190 °C, pellets of waste PET beverage

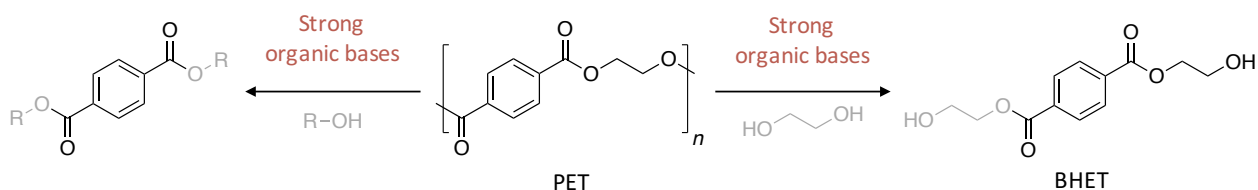
00. Introduction

bottles were degraded in 3.5 h. The major product (78% after crystallisation from water) of this reaction was BHET, a convenient monomer for a subsequent polymerisation back to PET. (Scheme 0.2)



Scheme 0.1. Organic bases described in this chapter, arranged according to their basicity

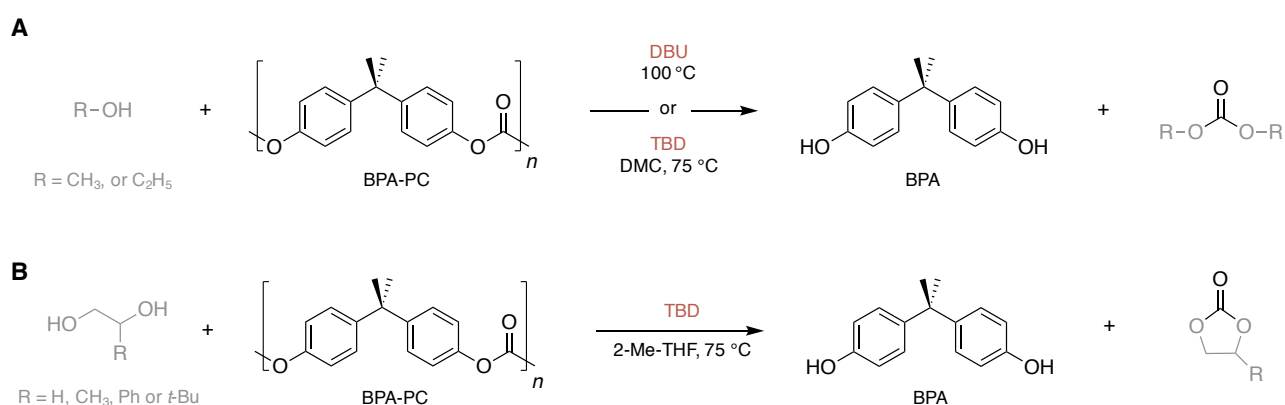
Insoluble impurities were identified as short oligomers of PET and additives to the polymer (isophthalic acid, diethylene glycol, and cyclohexane dimethanol). Additional experiments using coloured PET bottles led to slower glycolysis with a lower BHET yield (64%). These results are comparable to ones, encountered in the literature, obtained with usual organometallic catalysts employed for this reaction such as acetate (Zinc, Manganese).^{53,54} A complementary DFT computational study has demonstrated that both TBD and ethylene glycol played a role in the depolymerisation mechanism, activating transesterification via H-bonding.⁵⁵



Scheme 0.2. Depolymerisation of PET through glycolysis or alcoholysis.

In a subsequent work, the efficiency of a range of other nitrogen bases was investigated to establish a correlation between their basicity (pK_a) and catalytic activity.⁵⁶ Glycolysis appeared to be more efficient (more rapid with lower undesirable oligomers content) in the case of strong bases such as TBD, DBU, or DBN compared to bases with a lower pK_a such as NMI or DMA. (Scheme 0.1)

More recently, organic bases as catalysts have gained attention for the depolymerisation of other polymers. Thus, the recycling of BPA-PC has been also investigated using organic bases as catalysts. Using DBU (10 mol%) at 100 °C in an excess of ethanol or methanol, BPA-PC was degraded within 30 min to provide a reasonable yield of BPA and the respective organic carbonates.⁵⁷ (Scheme 0.3A) Reutilisation of the catalyst was explored, via subsequent addition of BPA-PC *in situ*, demonstrating the ability of DBU to catalyse the degradation for several cycles. Notably however, the reaction time increased with successive loads of fresh polymer, from 30 min for the first feed to 4 h for the 5th one. Further investigation into the nature of the catalytic species revealed that a DBU-BPA adduct was formed in the crude reaction product. While still catalytically active, it is less active than DBU itself hence explaining the sequential loss in activity. The investigation of other bases has shown that weaker bases, DABCO and DMAP (Scheme 0.1) are less active than DBU requiring 4 to 6 time longer reaction duration to reach equilibrium. These observations support the tendency previously reported that catalytic performances of organic bases for depolymerisation increases with their basicity.



Scheme 0.3. Organocatalysed depolymerisation of BPA-PC using (a) alcohols as reagent, (b) diols as reagent.

In another recent publication, the use of TBD as catalyst was reported for the methanolysis of BPA-PC into BPA and DMC.⁵⁸ Investigations into solvents and catalysts have demonstrated that the best result was obtained using DMC as solvent, at 75 °C, with 2 mol% of TBD and 10 eq. of methanol. (Scheme 0.3B) The use of DMC, one of the products of the depolymerisation, as solvent for

the reaction enables an easier and faster separation, which simplifies the overall process. Additionally, the authors explored the depolymerisation of BPA-PC in 2-methyltetrahydrofuran, using small diols, to obtain 5-membered cyclic carbonates in reasonable yields.

Finally, Leibfarth *et al.* recently reported the efficiency of TBD to degrade PLA, at room temperature, to obtain valuable building blocks.⁵⁹ Similarly to PET depolymerisation with different alcohols, the degradation of PLA led to a mixture of products, here lactate esters and their dimers. However, tuning the reaction parameters, the ethanolysis of PLA reached more than 95% of ethyl lactate. Moreover, its tolerance regarding the incorporation of various polymerisable groups to the ester products presented the opportunity to produce then new polymers by step growth methods. The same process was also applied to PG.

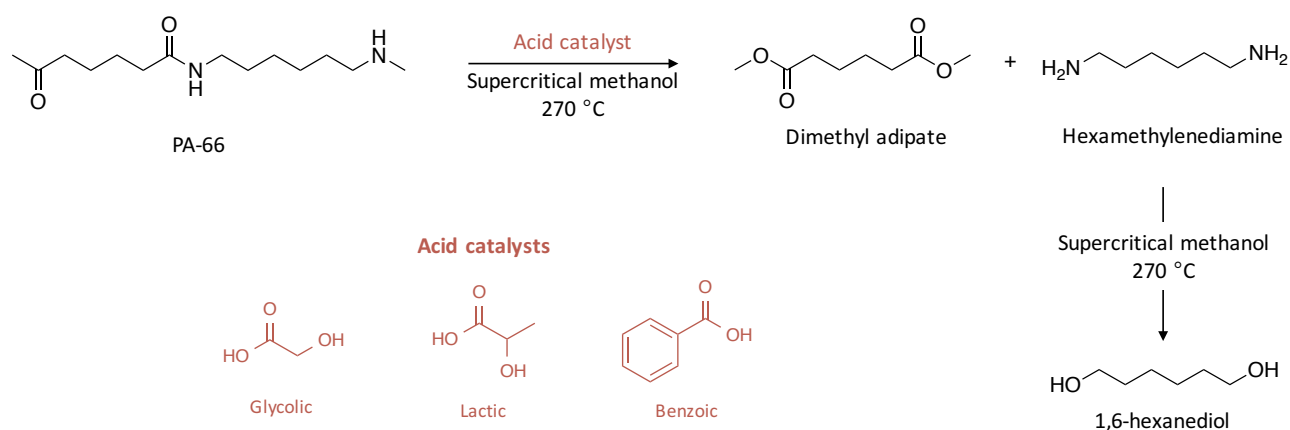
2.2 Organic acids

Unlike organic bases currently widely explored as organocatalysts and although they are attractive building blocks for polymerisation, few examples of organic acids as catalyst are reported in the literature.

In the first report of using acid catalysts for polymer degradation, typical aqueous acidic solutions were used as catalyst for the degradation of discarded PA-6 waste fibres ($M_n = 12 \text{ kg}\cdot\text{mol}^{-1}$).⁶⁰ After dissolution in concentrated solution of formic acid, degradation products of different molecular weights were recovered through fractional precipitation, raising a minimal M_n of $580 \text{ g}\cdot\text{mol}^{-1}$ in 20 h. Interestingly, with hydrochloric acid and sulfuric acid, aminocaproic acid was identified as the major component (94% and 78%, respectively) and was isolated in high purity, eventually also allowing for subsequent polymerisation.

More recently, Kamimura and co-workers reported the degradation of PA-66 into valuable chemicals using the combination of supercritical methanol as solvent and organic acids as catalyst.⁶¹ Depolymerisation with 8 eq. of glycolic acid in methanol, at $270 \text{ }^\circ\text{C}$ for 6 h, yielded 75% of dimethyl adipate and 50%

of 1,6-hexanediol. Similar yields were obtained with other acids such as lactic or benzoic acid while use of esters or weaker acids provided comparable yields of dimethyl adipate, but lower yields of 1,6-hexanediol. The authors proposed that the scission of the amide bond was promoted by the acid catalyst to yield dimethyl adipate and hexamethylenediamine before the subsequent degradation of the diamine into various compounds, including 1,6-hexanediol, was promoted by supercritical methanol (**Scheme 0.4**). This diol being a relevant monomer for subsequent preparations of polyesters or polyurethanes, its synthesis from commercial PA-6 constitutes a step towards economically viable depolymerisation processes.



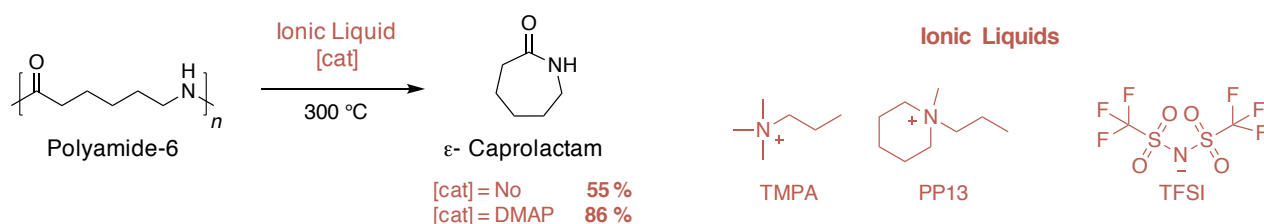
Scheme 0.4. Depolymerisation of PA-66 catalysed by organic acids in supercritical methanol

2.3 Ionic liquids and acid-base mixtures

The use of ILs – defined as a salt in the liquid state with melting point lower than 100 °C – or other acid-base salts is appealing on account of their higher thermal stability which prevents their degradation under the demanding, high temperature conditions required for many depolymerisation processes. As well as retaining activity for multiple cycles of depolymerisation – satisfying the need for low cost catalysts – this property prevents from the highly undesirable colouration of the final product. ILs have the added advantage of being liquid and hence the use of organic solvents can also be prevented.

The use of ILs as an efficient media has been primarily developed for the depolymerisation of PA-6. (**Scheme 0.5**) Quaternary ammonium salts such as N-methyl-N-propylpiperidinium (PP13) and N,N,N-trimethyl-N-propyl

ammonium (TMPA), together with bis(trifluoromethane sulphonyl)imide (TFSI) as counter anion, successfully depolymerised PA-6 in 5 to 6 h, at 300 °C.⁶² The polymer was converted into ϵ -caprolactam in satisfactory yield (43-55%), without requiring addition of a further catalyst. Adding 5 wt% of DMAP as added catalyst, improved the depolymerisation efficiency such that 86% of monomer was recovered. Further investigations into optimisation of the reaction conditions demonstrated the importance of the temperature with 7% monomer isolated at 270 °C, 55% at 330 °C and 6% at 360 °C. For temperatures below 300 °C, a large portion of oligomeric polyamides in the crude product explained the low quantity of ϵ -caprolactam collected. For temperatures above 300 °C, formation of by-products such as N-methyl- and N-propyl lactams indicated that ILs decomposed at these temperatures, which hinders the depolymerisation to reach good yield.



Scheme 0.5. Depolymerisation of PA-6 into ϵ -caprolactam using ILs as catalyst

Extension of this methodology to polyamide-12 (PA-12) also led to isolation of the corresponding lauractam, however, the yield did not exceed 17%, most likely a consequence of the closing of a 12-member ring being energetically disfavoured.⁶³ The ILs were able to be recycled, with the process being repeated up to 5 times, without observing any loss of depolymerisation efficiency. In a subsequent work, the same group demonstrated the possibility of depolymerising PA-6 using DMAP salts in the same ionic liquids. DMAP salts prepared with iodine and imidazolium as counter anion were able to catalyse the reaction, several times, reaching up to 79% of monomer recovered. However, this performance being under the yield obtained with DMAP alone, this catalyst was not investigated further for depolymerisation reactions.⁶⁰

Urea and urea-based ionic liquids were also applied to the catalysis of polymer degradation. Musale and Shukla have shown that choline chloride ([Ch][Cl]) urea salts are highly efficient catalysts for the aminolysis of PET.⁶⁵ Compared to glycolysis, depolymerisation of PET using amines is faster and generally more selective. Using ethanolamine or diethanolamine, degradation of PET under reflux is complete in less than 30 min, providing the corresponding amides in reasonable to good yields. [Ch][Cl] urea mediated depolymerisation demonstrated an improved performance compared to urea, 69 and 80% for EA and DEA, respectively, against 55 and 66% for urea alone. **(Fig. 0.6A)** However, the reaction using the corresponding zinc salt, namely [Ch][Cl] ZnCl₂, afforded higher monomer yields, until 82 and 95% respectively. Similar results were obtained for the urea-catalysed glycolysis of PET wastes. At 180 °C, using ethylene glycol as nucleophile and solvent, monomer was collected with a yield of 78 %.⁶⁶ **(Fig. 0.6B)** Moreover, residual ethylene glycol and urea were recycled, up to 10 times, and every recycling step yielded similar final ratio of BHET, demonstrating that no loss of activity was experienced. *In situ* IR and DFT calculations emphasised the predominant role of the H-bonds formed between urea and ethylene glycol. As they are known to form H-bond with alcohol groups, tetraalkylammonium-based amino acid-functionalised ILs were used as catalyst to further enhance the efficiency of the depolymerisation. Using tetramethylammonium alaninate [N₁₁₁₁][Ala], a similar yield of monomer was obtained in a reduced time, 50 min at 170 °C against 190 min for urea alone. This last result consolidates the key role of H-bonding in the depolymerisation mechanism.

In an environmental-friendly perspective, Sun *et al.* studied the application of low-cost and biocompatible ionic liquids to the solubilisation and depolymerisation of PET.⁶⁷

The authors demonstrated the ability for cholinium Phosphate ([Ch]₃[PO₄]) to solubilise PET at relatively low temperature (120 °C) and subsequent glycolysis of PET led to BHET being obtained in 60% yield before recycling the IL for subsequent depolymerisations. **(Fig. 0.6G)** NMR and IR spectroscopic analysis

suggested a bifunctional activation of the system with the cation activating the carbonyl group of PET while the anion simultaneously activated one hydroxyl group of ethylene glycol.

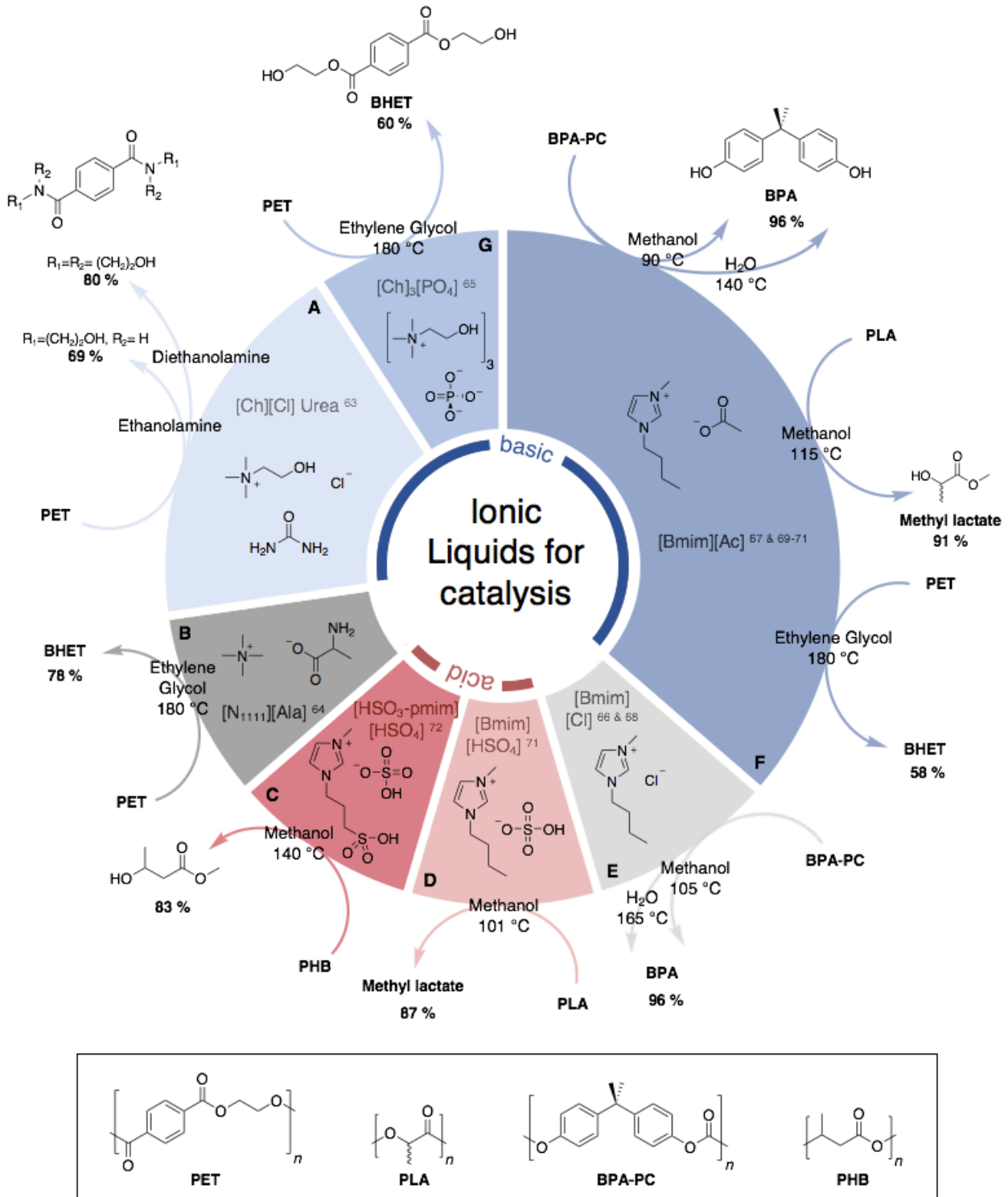


Figure 0.6. Ionic liquids as catalyst for the depolymerisation of commodity polymers

In 2010, imidazolium-based ILs were investigated by Liu *at al.* for the depolymerisation of BPA-PC. ILs with different inorganic anions (Cl, Br, BF₄,

PF₆) and various chain natures for the *N*-alkyl imidazolium moieties have been synthesised to catalyse the methanolysis of the polymer.⁶⁸ Although most of the ILs did not display any catalytic activity, 1-Butyl-3-methylimidazolium Chloride ([Bmim][Cl]) provided complete depolymerisation of BPA-PC after 2.5 h at 105 °C. High yields (up to 96 %) of both monomers, BPA and DMC, were isolated and the ionic liquid was reused up to 8 times with no significant loss of the catalytic activity being observed. (Fig. 0.6E)

Subsequently, Al Sabagh *et al.* showed that [Bmim][Cl] and [Bmim][Br] did not display any catalytic activity for the glycolysis of PET however the more basic [Bmim][Ac] fully degraded the polymer in 3 h.⁶⁹ (Fig. 0.6F) Once again, the IL was, then, recycled for subsequent polymerisation with no loss in the catalytic activity.

In successive studies, the same conditions were applied to the hydrolysis and methanolysis of BPA-PC testing both [Bmim][Cl] and 1-butyl-3-methylimidazolium acetate ([Bmim][Ac]) as catalyst, obtaining BPA in very good yields for each reaction. Using [Bmim][Cl] as catalyst with water at 165 °C, the polymer fully depolymerised in 3 h, to afford up to 95% yield of BPA.⁷⁰ (Fig. 0.6E) Similarly, with [Bmim][Ac], in the same amount of time, 0.5 g of methanol for 1 g of BPA-PC was needed to provide high yield of BPA (96%), at 90 °C.⁷¹ The same monomeric yield was afforded through hydrolysis of the BPA-PC using 1.5 g of the same IL and 0.35 g of water, at 140 °C.⁷² (Fig. 0.6F) Notably, in hydrolysis, the catalyst requires higher temperatures and higher loading to afford the same performance as in methanolysis. Furthermore, [Bmim][Ac] exhibited higher catalytic activity than [Bmim][Cl], depolymerising BPA-PC under milder conditions, using lower temperatures and a smaller amount of catalyst. The authors suggested that the enhanced performance of [Bmim][Ac] in depolymerising BPA-PC is related to the better solubility of the polymer in this IL. Finally, the methanolysis of PLA into methyl lactide has also been investigated using different imidazolium ionic liquids.⁷³ Comparison of the catalytic activity of [Bmim][Cl], [Bmim][PF₆], [Bmim][Ac] and [Bmim][HSO₄] revealed that the neutral ILs ([Bmim][Cl] and [Bmim][PF₆]) were inactive for

depolymerisation whereas the basic [Bmim][Ac] and acidic [Bmim][HSO₄] completed degradation of the polymer in 3 h at 115 °C. The efficacy of acid and base catalysts for PLA depolymerisation by transesterification is well known and hence this result is not surprising. [Bmim][Ac] appeared to be slightly more active than its acidic homologue, reaching 96% conversion of PLA for an isolated methyl lactide yield of 91%. (Fig. 0.6D & 0.6F)

As described earlier, basic ILs have been widely investigated for alcoholysis of oxygen-containing polymers, in particular, PET, BPA-PC or PLA. In contrast, acidic ILs have received much less attention. One notable application has explored the methanolysis of the polyester, PHB, a bio-sourced and biodegradable polymer, using 1-methyl-3-(3-sulfopropyl) imidazolium hydrogen sulfate [HSO₃-pmim][HSO₄] as catalyst.⁷⁴ Efficient depolymerisation to methyl 3-hydroxybutyrate monomer in 83% yield after 3 h occurred at 140 °C. Interestingly, the ionic liquid prepared with the same cation but with dihydrogen phosphate (H₂PO₄⁻) anion was not active for depolymerisation, most likely a consequence of the less acidic nature of H₂PO₄⁻, (pK_a = 7.21)⁷⁵ compared to HSO₄⁻ (pK_a = 1.99).⁷⁵ (Fig. 0.6C).

3 Upcycling towards innovative polymers

Upcycling was first employed by Gunter Pauli in 1999 in the eponymous book and refers to a process transforming by-products, undesired, unwanted or waste products into new materials of better quality – regarding economic value, aesthetic or sustainability.⁷⁶ *Upcycling* in the polymer context means use a discarded plastic as a feedstock for the synthesis of a new molecule or polymeric material profitable for higher value applications. The direct consequence is to implement an economic value to a materials intended to be landfilled or burnt. This involves (1) the recycling of polymers into innovative monomers or building blocks for subsequent polymerisation for high-added value applications, (2) the depolymerisation of commodity polymers into valuable molecules that could be re-used in other fields of chemistry as solvent, additive or catalyst for example, or (3) the post-

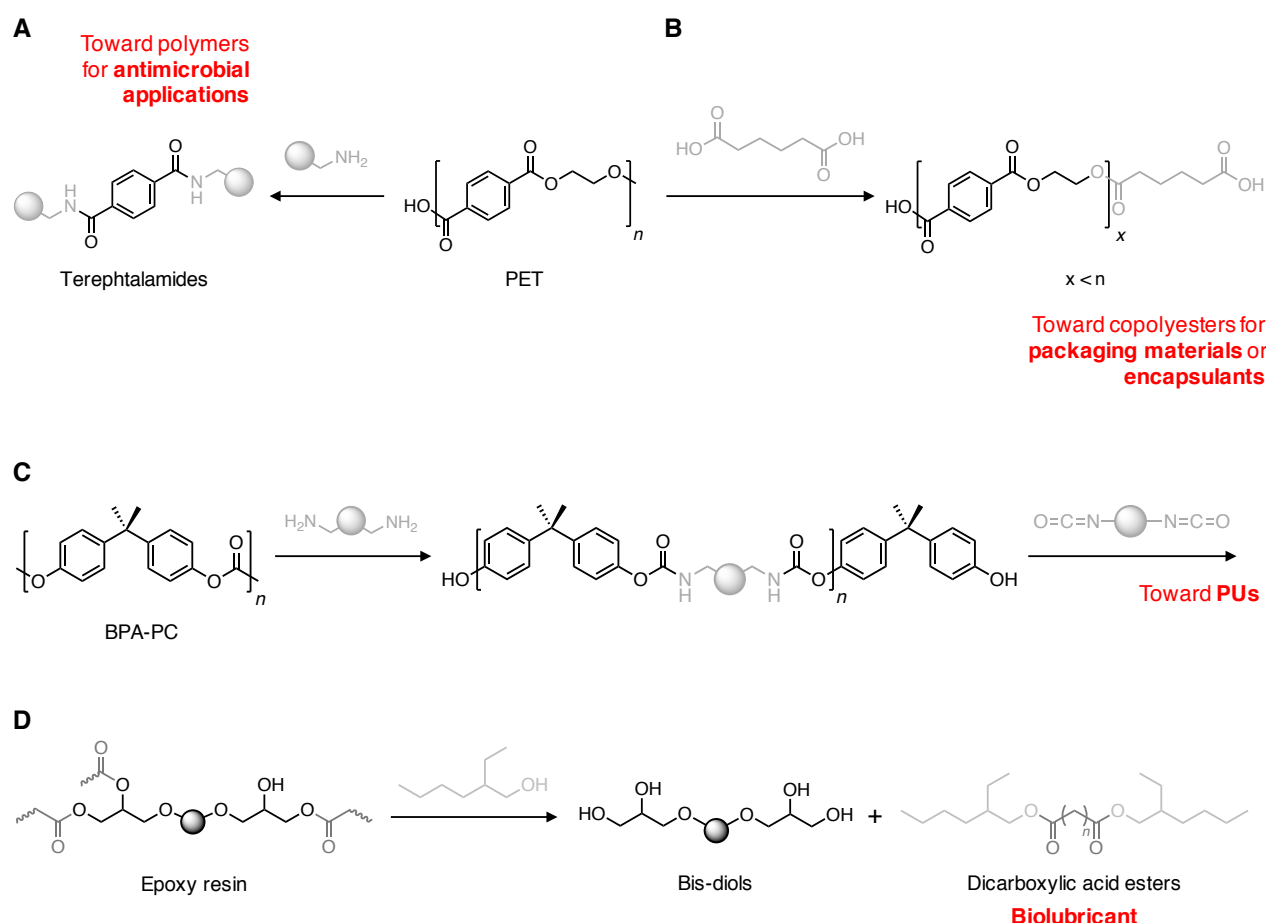
functionalisation or direct re-use of discarded polymers to yield high-performance materials. The two former options referring to a polymer-to-monomer-to-polymer loop while the last alternative consist in a direct polymer-to-polymer transformation.

3.1 From polymer to monomers

In order to implement economic value to recycling processes, the easiest strategy consist in choosing an appropriate reagent for depolymerising polymers into valuable building blocks for subsequent polymerisations.

One well-studied example is the aminolysis of PET which provides terephthalamides, valuable monomers for the synthesis of functional biomaterials, in particular for supramolecular structures demonstrating antimicrobial properties^{77,78} or cross-linked polymers with adhesive properties.⁷⁹ The ability of TBD to catalyse such reaction has been investigated to produce a large range of crystalline terephthalamides in reasonable yields.⁸⁰ (**Scheme 0.6A**) The thermal and mechanical properties were dependant on the amine used as reagent and provided building blocks for high performance materials. The computational support studies suggested that the bifunctionality of TBD plays an important role in the mechanism, especially in the activation of the carbonyl group *via* H-bonding, which makes it more efficient than other organic bases for aminolysis.

Similarly, Geyer *et al.* investigated the use of carboxylic acids, in particular adipic acid as chain scission agent for the depolymerisation of PET into oligomeric fragments of defined compositions. (**Scheme 0.6B**) Indeed, depending on the quantity of acid used for the reaction, predictable depolymerisation degrees were afforded to yield products then re-used for the synthesis of block copolyesters. These materials demonstrated improved performances – enhanced glass transition temperature – compared to original PET. This is of specific interest for the synthesis of special materials such as encapsulants or specific packaging.⁸¹



Scheme 0.6. Depolymerisation of PET (A) using amines and (B) adipic acid, (C) chemical recycling of BPA-PC using diamine and (D) epoxy resins depolymerisation with 2-ethyl hexanol

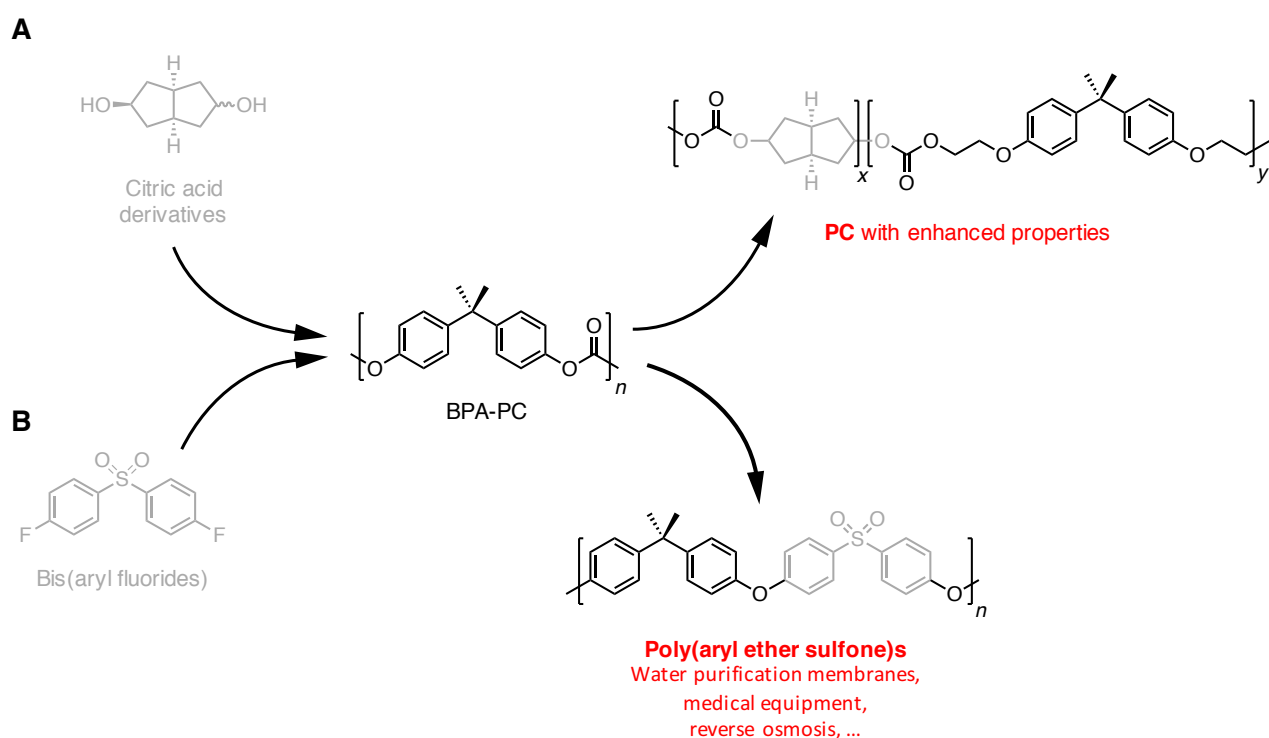
Wu *et al.* also reported the aminolysis of BPA-PC to obtain versatile building blocks used for the synthesis of PU.⁸² (Scheme 0.6C) The depolymerisation under mild conditions – less than 80 °C – without catalysts has led to different carbamates depending on the diamine used as reagent that were then polymerised with diisocyanates to reach PU in a two-step, one-pot procedure in a 100% atom economy.

Thermosets are a class of polymer, in which chemical bonds maintain a permanent network, resulting in a cross-linked material very difficult to reprocess or recycle by conventional heating or melting procedures. Nowadays, they account for 15 to 20% of the global plastic production,⁸³ therefore growing efforts are made for encountering innovative solutions for recycling these materials. The chemical recycling into valuable building block is an attractive option as they can then be re-used for high added value applications. Very recently, thermosetting epoxy resins synthesised with TBD

were chemically treated with a commercial catalyst – $\text{Zn}(\text{Ac})_2$ – and 2-ethyl hexanol at relatively mild conditions to reach recycled oligomers of dicarboxylic acid esters which can be used as biolubricant.⁸⁴ (Scheme 0.6D)

3.2 From polymer to polymer

Another way of *upcycling* plastic materials is the utilisation of a waste polymer in a combination with a monomer for direct obtaining of a new material. Pang *et al.* very recently reported the melt polymerisation of a bicyclic diol derived from citric acid with a depolymerisation product of BPA-PC resulting from its recycling with ethylene glycol at very high temperatures. (Scheme 0.7A) While the polymerisation of this bicyclic diol alone is leading to a very thermally stable but also very brittle polymer, the incorporation of BPA-PC recycled chemical enhanced the low reactivity of the monomer and increased the mechanical properties of the resulting material.⁸⁵



Scheme 0.7. *Upcycling* of discarded BPA-PC (A) using citric acid to yield PC with improved thermal and mechanical properties and (B) using bis(aryl fluorides) to yield poly(aryl ether sulfone)s.

The same polymer, BPA-PC, has been depolymerised using bis(aryl fluorides) and carbonate salts as catalyst to reach poly(aryl ether sulfone)s through polycondensation. (Scheme 0.7B) This one-step, one-pot repurposing allows

the synthesis of high-performance thermoplastics demonstrating thermal properties suitable for water purification membranes, medical equipment or reverse osmosis for instance.⁸⁶

On a different approach, Gooneie *et al.* have used an organic phosphorus multifunctional additive known for its flame retardant properties for incorporation into waste PET to gain into chemical structure stability and viscosity in order to improve the properties of the rPET after several mechanical recycling. Extrusion trials confirmed the enhanced lubrication effect of the modified-PET resulting in better processability and chemical stability in recycling.⁸⁷

Here are only few examples showing what could be the possibilities for using recycled polymers as a feedstock for improved-properties materials using organic molecules and solvent-free procedures while possible.

4 Approach and objectives of the thesis

The objectives of the present thesis involve the design of an efficient procedure for the chemical recycling and *upcycling*, in a circular economy approach, of commodity polymers.

In order to built an efficient and sustainable process, **Chapter 1** will depict the synthesis and characterisation of an innovative organocatalyst resisting to severe thermal conditions in the aim of using it for depolymerisation reactions. Different ratio of organic acids and bases are mixed to yield chemicals subsequently tested for different polymer's depolymerisation to evaluate their capacity as catalyst.

As PET is the most studied commodity polymer for chemical recycling, in **Chapter 2**, an efficient solvent-free procedure will be implemented to the glycolysis of PET to yield highly pure monomer in outstanding yields. The catalyst is recycled and the molecule obtained from the depolymerisation is polymerised using the same catalyst to yield rPET with pristine-like properties. A DFT mechanistic study is performed in order to understand the behaviour of the acid-base mixture as catalyst.

In **Chapter 3**, the depolymerisation of BPA-PC is investigated, in the aim of obtaining both the starting material, in a closed polymer-monomer-polymer loop, and high added value chemicals. By wisely choosing the reagent, the versatility of the reaction allows the synthesis of a library of cyclic and linear carbonyl-containing molecules, 5- and 6-membered cyclic carbonates are obtained in reasonable to excellent yields (up to 97 %), constituting a phosgene-free procedure for the ring-closing of valuable carbonates widely reported for the synthesis of high-performance materials. Using the same procedure, innovative linear carbonates and ureas are also obtained. DFT calculations are performed to unveil the depolymerisation mechanistic pathway.

In a last important step, both PET and BPA-PC are successively depolymerised using different reagents in **Chapter 4**. Kinetics of the simultaneous depolymerisations of PET and BPA-PC are performed under different conditions to encounter the best parameters for yielding high quantities of both reactions product' highly pure.

Results will be then summarised and commented in regard of the challenges faced by the field.

References

- 1 R. Geyer, J. R. Jambeck and K. L. Law, *Sci. Adv.*, 2017, **3**, e1700782.
- 2 World Economic Forum, *The new plastics economy*, 2016.
- 3 V. E. Yarsley and E. G. Couzens, *Plastics*, Allen Lane, Penguin Books, Penguin., 1945.
- 4 *The new plastics economy - Catalysing action*, 2017.
- 5 Catalysing action, <https://newplasticseconomy.org/publications>, (accessed May 9, 2018).
- 6 *New plastics economy global commitment*, Ellen MacArthur foundation, 2019.
- 7 *The new plastics economy - Rethinking the future of plastics*, Ellen MacArthur Foundation, 2016.
- 8 W. McDonough and M. Braungart, *Cradle to Cradle - Remaking the Way We Make Things*, North Point Press., 2002.
- 9 S. D. Anuar Sharuddin, F. Abnisa, W. M. A. Wan Daud and M. K. Aroua, *Energy Convers. Manag.*, 2016, **115**, 308–326.
- 10 N. Dimitrov, L. Kratofil Krehula, A. Ptiček Siročić and Z. Hrnjak-Murgić, *Polym. Degrad. Stab.*, 2013, **98**, 972–979.
- 11 T. Yoshioka, G. Grause, C. Eger, W. Kaminsky and A. Okuwaki, *Polym. Degrad. Stab.*, 2004, **86**, 499–504.
- 12 X. Zhang, M. Fevre, G. O. Jones and R. M. Waymouth, *Chem. Rev.*, 2018, **118**, 839–885.
- 13 D. K. Schneiderman and M. A. Hillmyer, *Macromolecules*, 2017, **50**, 3733–3749.
- 14 M. Hong and E. Y.-X. Chen, *Green Chem.*, 2017, **19**, 3692–3706.
- 15 A. Rahimi and J. M. García, *Nat. Rev. Chem.*, 2017, **1**, 41570-017-0046–017.
- 16 H. Sardon and A. P. Dove, *Science*, 2018, **360**, 380–381.
- 17 V. Jamdar, M. Kathalewar and A. Sabnis, *J. Coat. Technol. Res.*, 2018, **15**, 259–270.
- 18 E. Bäckström, K. Odelius and M. Hakkarainen, *Ind. Eng. Chem. Res.*, 2017, **56**, 14814–14821.
- 19 Y. Hongmei, M. Yongshuai, Z. Weilu and Z. Dong, *Adv. Mater. Res.*, 2012, **550**, 280–283.

- 20 A. Kamimura, S. Yamamoto and K. Yamada, *ChemSusChem*, 2011, **4**, 644–649.
- 21 F. Scé, I. Cano, C. Martin, G. Beobide, Ó. Castillo and I. de Pedro, *New J. Chem.*, 2019, **43**, 3476–3485.
- 22 W.-T. Chen, K. Jin and N.-H. Linda Wang, *ACS Sustain. Chem. Eng.*, 2019, **7**, 3749–3758.
- 23 A. Kamimura, K. Ikeda, S. Suzuki, K. Kato, H. Matsumoto, K. Kaiso and M. Yoshimoto, *Polym. Degrad. Stab.*, 2017, **146**, 95–104.
- 24 C. Chaabani, E. Weiss-Hortala and Y. Soudais, *Waste Biomass Valorization*, 2017, 1–13.
- 25 C. S. Nunes, P. R. Souza, A. R. Freitas, M. J. V. da Silva, F. A. Rosa and E. C. Muniz, *Catalysts*, 2017, **7**, 43.
- 26 C. S. Nunes, M. J. V. da Silva, D. C. da Silva, A. dos R. Freitas, F. A. Rosa, A. F. Rubira and E. C. Muniz, *RSC Adv.*, 2014, **4**, 20308–20316.
- 27 Y. Chujo, H. Kobayashi and Y. Yamashita, *J. Polym. Sci. Part Polym. Chem.*, 1989, **27**, 2007–2014.
- 28 C.-H. Chen, C.-Y. Chen, Y.-W. Lo, C.-F. Mao and W.-T. Liao, *J. Appl. Polym. Sci.*, 2001, **80**, 943–948.
- 29 M. Ghaemy and K. Mossaddegh, *Polym. Degrad. Stab.*, 2005, **90**, 570–576.
- 30 Z. Maeno, S. Yamada, T. Mitsudome, T. Mizugaki and K. Jitsukawa, *Green Chem.*, 2017, **19**, 2612–2619.
- 31 H. Liu, R. Zhao, X. Song, F. Liu, S. Yu, S. Liu and X. Ge, *Catal. Lett.*, 2017, **147**, 2298–2305.
- 32 A. J. Hunt and J. H. Clark, *Element Recovery and Sustainability*, Royal Society of Chemistry, 2013.
- 33 W. N. Ottou, H. Sardon, D. Mecerreyes, J. Vignolle and D. Taton, *Prog. Polym. Sci.*, 2016, **56**, 64–115.
- 34 D. W. C. MacMillan, *Nature*, 2008, **455**, 304–308.
- 35 A. Bossion, K. V. Heifferon, L. Meabe, N. Zivic, D. Taton, J. L. Hedrick, T. E. Long and H. Sardon, *Prog. Polym. Sci.*, 2019, **90**, 164–210.
- 36 N. E. Kamber, W. Jeong, R. M. Waymouth, R. C. Pratt, B. G. G. Lohmeijer and J. L. Hedrick, *Chem. Rev.*, 2007, **107**, 5813–5840.
- 37 M. K. Kiesewetter, E. J. Shin, J. L. Hedrick and R. M. Waymouth, *Macromolecules*, 2010, **43**, 2093–2107.

- 38 H. Sardon, A. Pascual, D. Mecerreyes, D. Taton, H. Cramail and J. L. Hedrick, *Macromolecules*, 2015, **48**, 3153–3165.
- 39 C. Thomas and B. Bibal, *Green Chem.*, 2014, **16**, 1687–1699.
- 40 A. P. Dove, *ACS Macro Lett.*, 2012, **1**, 1409–1412.
- 41 M. K. Kiesewetter, E. J. Shin, J. L. Hedrick and R. M. Waymouth, *Macromolecules*, 2010, **43**, 2093–2107.
- 42 F. Nederberg, E. F. Connor, M. Möller, T. Glauser and J. L. Hedrick, *Angew. Chem. Int. Ed.*, 2001, **40**, 2712–2715.
- 43 B. G. G. Lohmeijer, R. C. Pratt, F. Leibfarth, J. W. Logan, D. A. Long, A. P. Dove, F. Nederberg, J. Choi, C. Wade, R. M. Waymouth and J. L. Hedrick, *Macromolecules*, 2006, **39**, 8574–8583.
- 44 L. Zhang, R. C. Pratt, F. Nederberg, H. W. Horn, J. E. Rice, R. M. Waymouth, C. G. Wade and J. L. Hedrick, *Macromolecules*, 2010, **43**, 1660–1664.
- 45 J. M. W. Chan, X. Zhang, M. K. Brennan, H. Sardon, A. C. Engler, C. H. Fox, C. W. Frank, R. M. Waymouth and J. L. Hedrick, *J. Chem. Educ.*, 2015, **92**, 708–713.
- 46 R. C. Pratt, B. G. G. Lohmeijer, D. A. Long, R. M. Waymouth and J. L. Hedrick, *J. Am. Chem. Soc.*, 2006, **128**, 4556–4557.
- 47 S. Venkataraman, V. W. L. Ng, D. J. Coady, H. W. Horn, G. O. Jones, T. S. Fung, H. Sardon, R. M. Waymouth, J. L. Hedrick and Y. Y. Yang, *J. Am. Chem. Soc.*, 2015, **137**, 13851–13860.
- 48 C. Tan, S. Xiong and C. Chen, *Macromolecules*, 2018, **51**, 2048–2053.
- 49 S. Naumann, P. B. V. Scholten, J. A. Wilson and A. P. Dove, *J. Am. Chem. Soc.*, 2015, **137**, 14439–14445.
- 50 A. Chuma, H. W. Horn, W. C. Swope, R. C. Pratt, L. Zhang, B. G. G. Lohmeijer, C. G. Wade, R. M. Waymouth, J. L. Hedrick and J. E. Rice, *J. Am. Chem. Soc.*, 2008, **130**, 6749–6754.
- 51 T. S. Stukenbroeker, J. S. Bandar, X. Zhang, T. H. Lambert and R. M. Waymouth, *ACS Macro Lett.*, 2015, **4**, 853–856.
- 52 K. Fukushima, O. Coulembier, J. M. Lecuyer, H. A. Almegren, A. M. Alabdulrahman, F. D. Alsewailem, M. A. Mcneil, P. Dubois, R. M. Waymouth, H. W. Horn, J. E. Rice and J. L. Hedrick, *J. Polym. Sci. Part Polym. Chem.*, 2011, **49**, 1273–1281.

- 53 R. López-Fonseca, I. Duque-Ingunza, B. de Rivas, S. Arnaiz and J. I. Gutiérrez-Ortiz, *Polym. Degrad. Stab.*, 2010, **95**, 1022–1028.
- 54 D. E. Nikles and M. S. Farahat, *Macromol. Mater. Eng.*, 2005, **290**, 13–30.
- 55 H. W. Horn, G. O. Jones, D. S. Wei, K. Fukushima, J. M. Lecuyer, D. J. Coady, J. L. Hedrick and J. E. Rice, *J. Phys. Chem.*, 2012, **116**, 12389–12398.
- 56 K. Fukushima, D. J. Coady, G. O. Jones, H. A. Almegren, A. M. Alabdulrahman, F. D. Alsewailem, H. W. Horn, J. E. Rice and J. L. Hedrick, *J. Polym. Sci. Part Polym. Chem.*, 2013, **51**, 1606–1611.
- 57 E. Quaranta, D. Sgherza and G. Tartaro, *Green Chem.*, 2017, **19**, 5422–5434.
- 58 T. Do, E. R. Baral and J. G. Kim, *Polymer*, 2018, **143**, 106–114.
- 59 F. A. Leibfarth, N. Moreno, A. P. Hawker and J. D. Shand, *J. Polym. Sci. Part Polym. Chem.*, 2012, **50**, 4814–4822.
- 60 S. R. Shukla, A. M. Harad and D. Mahato, *J. Appl. Polym. Sci.*, 2006, **100**, 186–190.
- 61 H. Matsumoto, Y. Akinari, K. Kaiso and A. Kamimura, *J. Mater. Cycles Waste Manag.*, 2017, **19**, 326–331.
- 62 A. Kamimura and S. Yamamoto, *Org. Lett.*, 2007, **9**, 2533–2535.
- 63 A. Kamimura and S. Yamamoto, *Polym. Adv. Technol.*, 2008, **19**, 1391–1395.
- 64 S. Yamamoto and A. Kamimura, *Chem. Lett.*, 2009, **38**, 1016–1017.
- 65 R. M. Musale and S. R. Shukla, *Int. J. Plast. Technol.*, 2016, 1–15.
- 66 Q. Wang, X. Yao, S. Tang, X. Lu, X. Zhang and S. Zhang, *Green Chem.*, 2012, **14**, 2559–2566.
- 67 Sun Jian, Liu Dajiang, Young Robert P., Cruz Alejandro G., Isern Nancy G., Schuerg Timo, Cort John R., Simmons Blake A. and Singh Seema, *ChemSusChem*, 2018, **11**, 781–792.
- 68 F. Liu, Z. Li, S. Yu, X. Cui and X. Ge, *J. Hazard. Mater.*, 2010, **174**, 872–875.
- 69 A. M. Al-Sabagh, F. Z. Yehia, A.-M. M. F. Eissa, M. E. Moustafa, G. Eshaq, A.-R. M. Rabie and A. E. ElMetwally, *Ind. Eng. Chem. Res.*, 2014, **53**, 18443–18451.
- 70 L. Li, F. Liu, Z. Li, X. Song, S. Yu and S. Liu, *Fibers Polym.*, 2013, **14**, 365–368.

- 71 F. Liu, L. Li, S. Yu, Z. Lv and X. Ge, *J. Hazard. Mater.*, 2011, **189**, 249–254.
- 72 X. Song, F. Liu, L. Li, X. Yang, S. Yu and X. Ge, *J. Hazard. Mater.*, 2013, **244–245**, 204–208.
- 73 X. Song, X. Zhang, H. Wang, F. Liu, S. Yu and S. Liu, *Polym. Degrad. Stab.*, 2013, **98**, 2760–2764.
- 74 X. Song, H. Wang, F. Liu and S. Yu, *Polym. Degrad. Stab.*, 2016, **130**, 22–29.
- 75 Bjerrum J., *Stability Constants of Metal-ion Complexes, with Solubility Products of Inorganic Substances: Inorganic ligands*, Chemical Society, 1958.
- 76 G. Pauli and J. F. Hartkemeyer, *UpCycling.*, Chronik Verlag im Bertelsmann LEXIKON Verlag GmbH, München, 1999.
- 77 K. Fukushima, *Polym. J.*, 2016, **48**, 1103–1114.
- 78 K. Fukushima, J. P. K. Tan, P. A. Korevaar, Y. Y. Yang, J. Pitera, A. Nelson, H. Maune, D. J. Coady, J. E. Frommer, A. C. Engler, Y. Huang, K. Xu, Z. Ji, Y. Qiao, W. Fan, L. Li, N. Wiradharma, E. W. Meijer and J. L. Hedrick, *ACS Nano*, 2012, **6**, 9191–9199.
- 79 P. Sharma, B. Lochab, D. Kumar and P. K. Roy, *ACS Sustain. Chem. Eng.*, 2016, **4**, 1085–1093.
- 80 K. Fukushima, J. M. Lecuyer, D. S. Wei, H. W. Horn, G. O. Jones, H. A. Al-Megren, A. M. Alabdulrahman, F. D. Alsewailem, M. A. McNeil, J. E. Rice and J. L. Hedrick, *Polym. Chem.*, 2013, **4**, 1610–1616.
- 81 B. Geyer, S. Röhner, G. Lorenz and A. Kandelbauer, *J. Appl. Polym. Sci.*, 2014, **131**, 39786–39798.
- 82 C.-H. Wu, L.-Y. Chen, R.-J. Jeng and S. A. Dai, *ACS Sustain. Chem. Eng.*, 2018, **6**, 8964–8975.
- 83 D. J. Fortman, J. P. Brutman, G. X. De Hoe, R. L. Snyder, W. R. Dichtel and M. A. Hillmyer, *ACS Sustain. Chem. Eng.*, 2018, **6**, 11145–11159.
- 84 X. Kuang, E. Guo, K. Chen and H. J. Qi, *ACS Sustain. Chem. Eng.*, 2019, **7**, 6880–6888.
- 85 C. Pang, X. Jiang, Y. Yu, X. Liu, J. Lian, J. Ma and H. Gao, *ACS Sustain. Chem. Eng.*, 2018, **6**, 17059–17067.
- 86 G. O. Jones, A. Yuen, R. J. Wojtecki, J. L. Hedrick and J. M. García, *Proc. Natl. Acad. Sci.*, 2016, **113**, 7722–7726.

87 A. Gooneie, P. Simonetti, K. A. Salmeia, S. Gaan, R. Hufenus and M. P. Heuberger, *Polym. Degrad. Stab.*, 2019, **160**, 218–228.



Organocatalysis

The synthesis of an innovative and thermoresistant organocatalyst



This picture comes from a series of images created by the artist Mandy Barker and named **SOUP** after the description given to plastic debris suspended in the sea. As Barker told herself, "The series of images aim to engage with, and stimulate an emotional response in the viewer by combining a contradiction between initial aesthetic attraction and social awareness".

All the plastic pieces in the photography have been salvaged from coasts around the world and represents the variety of debris encountered in the oceans today.

SOUP

Introduction

“Organocatalysis” depicts the adding of a sub-stoichiometric amount of organic molecule(s) with the aim of fasten a chemical reaction. If the use of small organic molecules as catalysts has been known since more than a century, their use as a replacement for classical organometallic catalysts or their direct application for innovative reactions has literally blossomed over the last couple of decades. Data illustrates this fact as, while the number of publications referring to organocatalysis barely reached 1000 for the year 1998, in 2018, more than 8 000 studies involved “organocatalysis” or a derivative term in their abstract, title or key words. (Fig. 1.1)

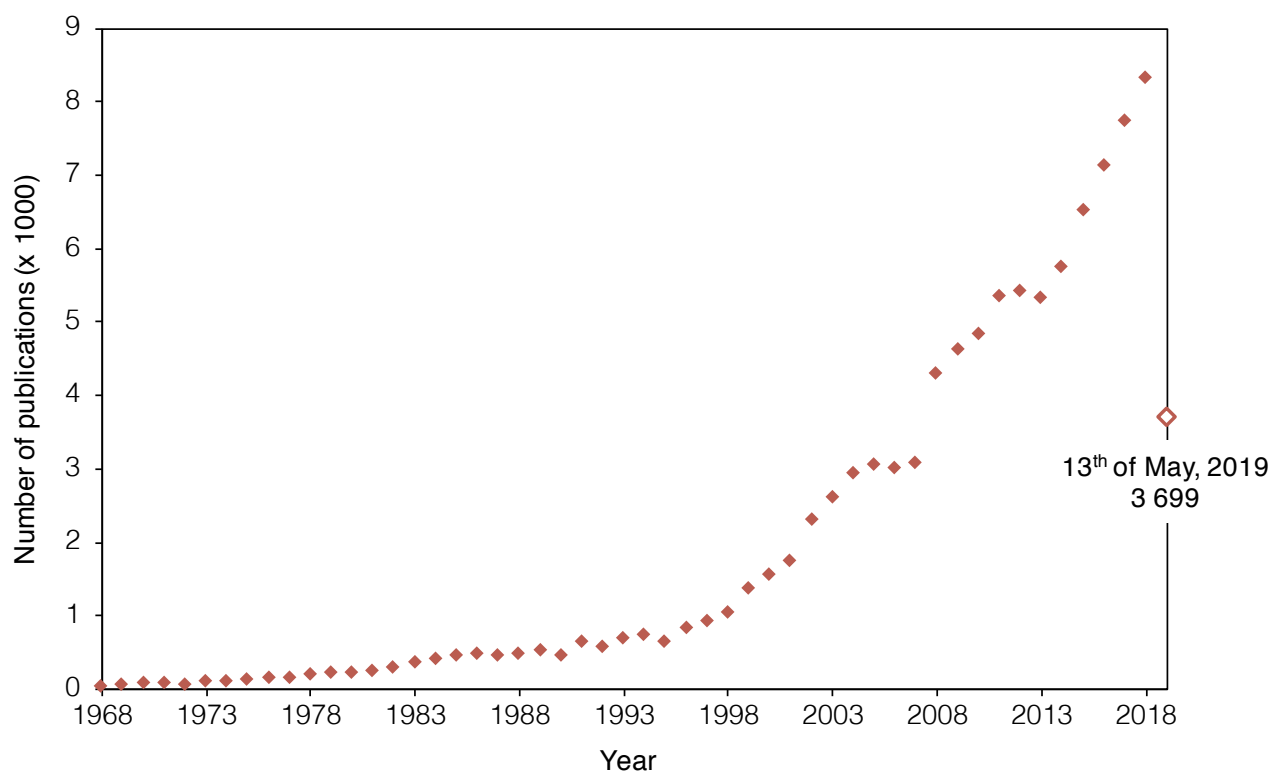


Figure 1.1 The increased number of publications on the topic of organocatalysis from 1968 to 2018. Data were obtained by a search in Scopus website in May 2019 for the keywords “organocatalyst”, “organic catalyst”, “organocatalysis” and “organic catalysis”.

The polymer field is no exception to this movement and substantial efforts have been made on developing metal-free alternatives to supplant the well-established metal-based syntheses,¹⁻⁴ especially to catalyse ring-opening polymerisation reactions.⁵⁻⁸ One of the main drawbacks of organometallics compared to organocatalysis involves the remaining of metal impurities in the

polymer, which can make impossible its use for high performance materials for microelectronic or medical applications for example and is complicating the recycling of the material in general. However, not only organocatalysts are “green” substitutes to classical organometallic chemistry – green being a questionable concept, organic molecules being sometimes as toxic or dangerous as organometallics^{9,10} – but some of them can promote the formation of innovative and attractive molecules.

Although organic catalysts are currently widely investigated for various polymerisation techniques,^{11–13} much less examples of the same catalysts exist for depolymerisations. However, the efficiency of organocatalysed procedures for transesterification reactions opens the way to a bench of chemical degradation of oxygen-containing polymers involving polycarbonates, polyethers, polyesters, polyamides or polyurethanes.

However, organocatalysts usually degrade at relatively low temperatures, thus making them impractical for high temperature reactions such as bulk depolymerisations. As such, we focussed our efforts on acid-base complexes, which have already demonstrated efficiency and good stability for (aza)Michael addition,¹⁴ epoxy curing,¹⁵ ring-opening polymerisation of lactide¹⁶ and even high temperature polymerisation reactions such as lactones copolymerisations^{17,18}. Their controllable reactivity and high stability make them suitable candidates for depolymerisation at high temperatures.

The only reported example of acid-base mixtures for catalysing chemical recycling explored the performances of DBU-based salts, including complexes formed by different ratio of DBU and benzoic acid or phenol for the depolymerisation of PET using ethylene glycol as reagent.¹⁹ (**Fig. 1.2**) The glycolysis was slightly slower compared to DBU alone but the organic salts – especially DBU:BA (1:1) – had the advantage of not aging when exposed to air, facilitating the depolymerisation procedure.

In this chapter the catalytic ability of acid-base mixtures synthesised from commercial acids and bases were explored for the depolymerisation of commodity plastics such as PET and BPA-PC. The thermal behaviour of these

mixtures was investigated through TGA while DFT methodology brought insight into their unique thermal stability.

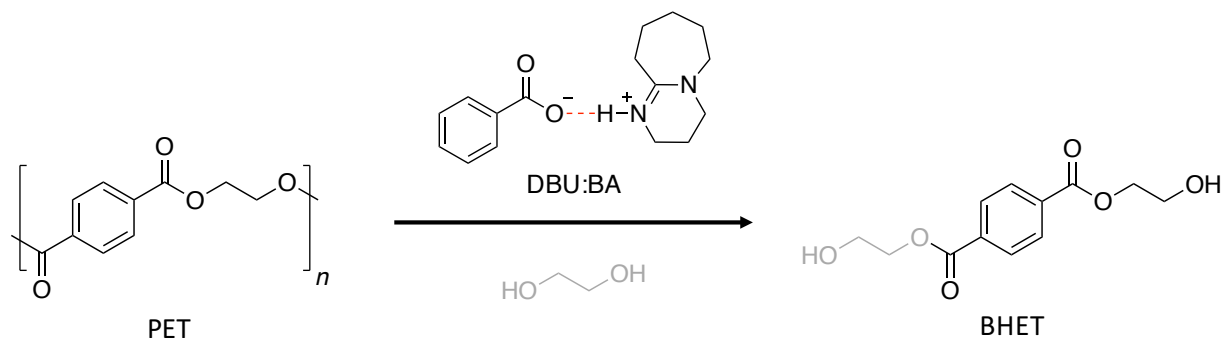


Figure 1.2. Glycolysis of PET using DBU:BA protic ionic salt.

1 Acid-base mixtures

Inspired by the good results obtained for depolymerisation while using strong organic bases¹⁹⁻²¹ and the excellent thermal properties of acid-base mixtures already used for polymerisation reactions,^{22,23} we have selected a strong acid, MSA, and a strong base, TBD, to form acid-base mixtures eventually suitable for depolymerisation.

1.1 Synthesis & characterisation

By mixing a common organic acid, MSA, with a common organic base, TBD, in equimolar ratio at 60 °C, a protic ionic salt, TBD:MSA (1:1), was synthesised. (Figs. 1.3A & 1.3B) In order to confirm the formation of the complex, the resulting mixture was characterised by ¹H NMR spectroscopy in DMSO-*d*₆. The recorded spectra for individual TBD and MSA showed the characteristic N-H proton signal of TBD as a weak, broad resonance at $\delta = 5.81$ ppm and the O-H signal of MSA as a sharp signal at $\delta = 14.16$ ppm. In contrast, for the (1:1) mixture, these two signals disappeared and a new one integrating for 2 protons appears at $\delta = 7.71$ ppm, which demonstrates the formation of the protic ionic salt by a proton transfer from MSA to TBD. (Fig. 1.3C)

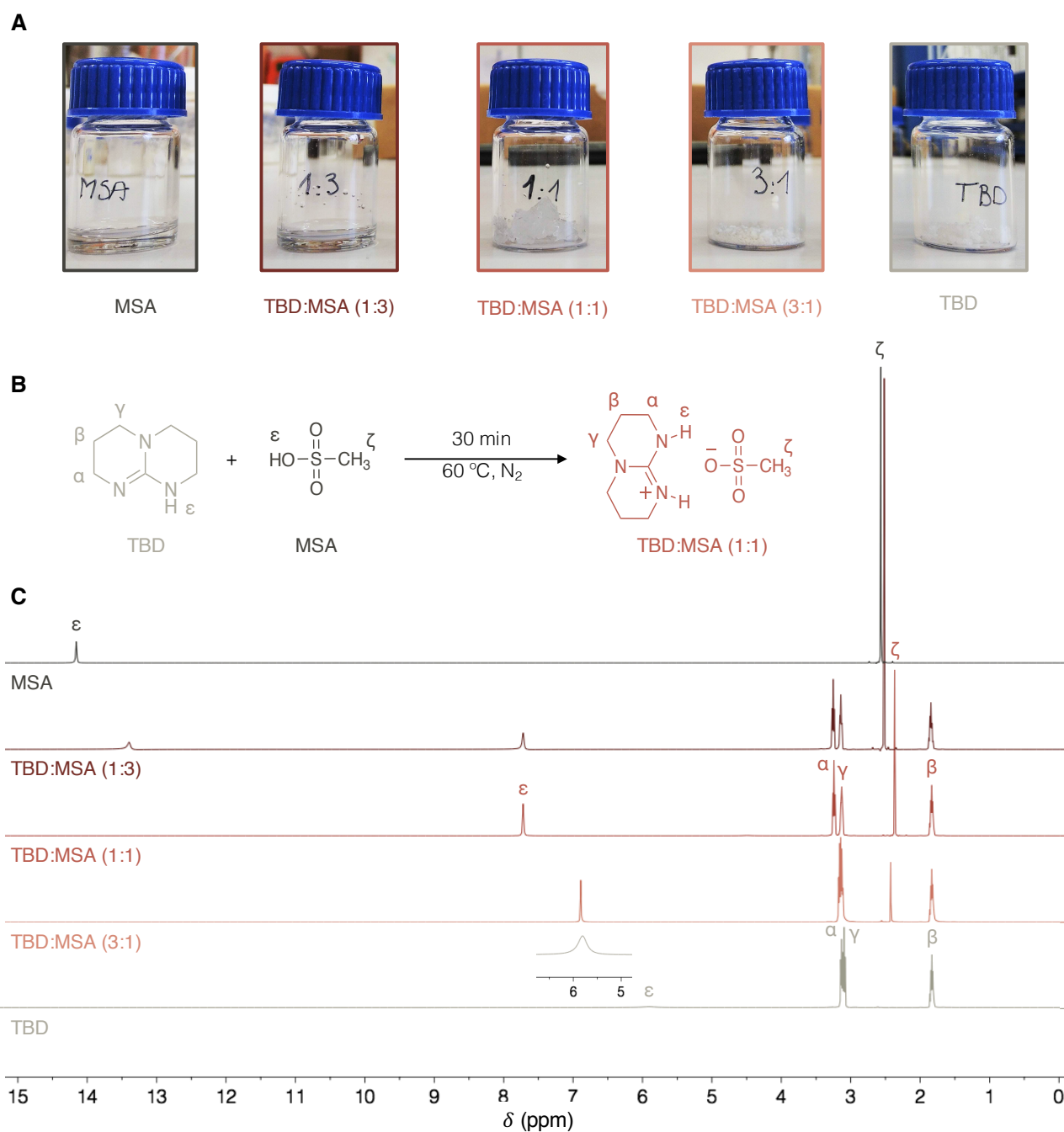


Figure 1.3. (A) Pictures, (B) synthesis and (C) stacked ^1H NMR spectra of TBD:MSA mixtures (400 MHz, $\text{DMSO-}d_6$, 298 K) – Figs. S1.2 to S1.4.

For comparison, two non-equimolar mixtures have been prepared using the same acid and base, TBD:MSA (1:3), with excess MSA and TBD:MSA (3:1) with excess TBD, following the same procedure. After cooling down from 60 °C, while TBD:MSA (3:1) is also a salt, the mixture with excess MSA is a clear transparent solution. (Fig. 1.3A) The ^1H NMR analysis of TBD:MSA (1:3) presents the same characteristic signals than (1:1) mixture with an additional signal at 13.4 ppm, corresponding to the acidic protons of the excess of MSA.

On the contrary, the (3:1) mixture demonstrates similar spectra than TBD alone together with the characteristic signal of MSA methyl group at 2.38 ppm and a new signal at 6.85 ppm integrating for 4 protons, the two protons of N-H-O and two N-H protons of the additional TBD.

1.2 Thermal stability

In order to confirm the resistance of the catalyst to temperature, the thermal stability of each mixture was determined by TGA. (**Fig. 1.4A**) MSA and TBD both degrade at relatively low temperature with 50 % of the mass lost before 180 °C for both molecules ($T_{50\%} = 170$ °C for TBD and $T_{50\%} = 174$ °C for MSA). In contrast, the isolated salt TBD:MSA (1:1) reveals an extraordinary high thermal stability ($T_{50\%} = 438$ °C). In order to gain insight into this remarkable stability, the molecular structure of the TBD:MSA (1:1) has been further investigated by DFT using ω B97XD functional²⁴ in conjunction with the 6-31+G(d,p) basis set for geometry optimisation and frequency calculation while electronic energy was then refined by single-point energy calculations at the ω B97XD/6-311++G(2df,2p) level of theory. Through these calculations, the acidic proton of MSA is observed to completely transfer to the basic nitrogen of TBD, thus creating an ionic pair of the protonated cation [TBDH]⁺ and the anion MSA⁻. Additionally, a hydrogen bond is formed between the N-H moiety of TBD and one of the oxygens of the sulfonyl group of MSA.

This observation supports the ¹H NMR spectra in which the two protons corresponding to the N-H of the TBD:MSA salt are equivalent. These two cooperative interactions lead to a calculated dissociation energy of 37.4 kcal.mol⁻¹. Such a high energetic barrier explains the high decomposition temperature and hence the high stability of the TBD:MSA (1:1) salt. (**Fig. 1.4B**) In comparison, (3:1) and (1:3) mixtures demonstrate thermal profile with two different degradation events. They both have a second decomposition temperature similar to (1:1), over 400 °C, corresponding to 48% weight loss for (1:3) and 44% weight loss for (3:1) but they have a different first decomposition temperature, with TBD:MSA (1:3) losing 44% weight

01. Organocatalysis

between 200 and 350 °C and TBD:MSA (3:1) losing 52% weight between 130 and 190 °C.

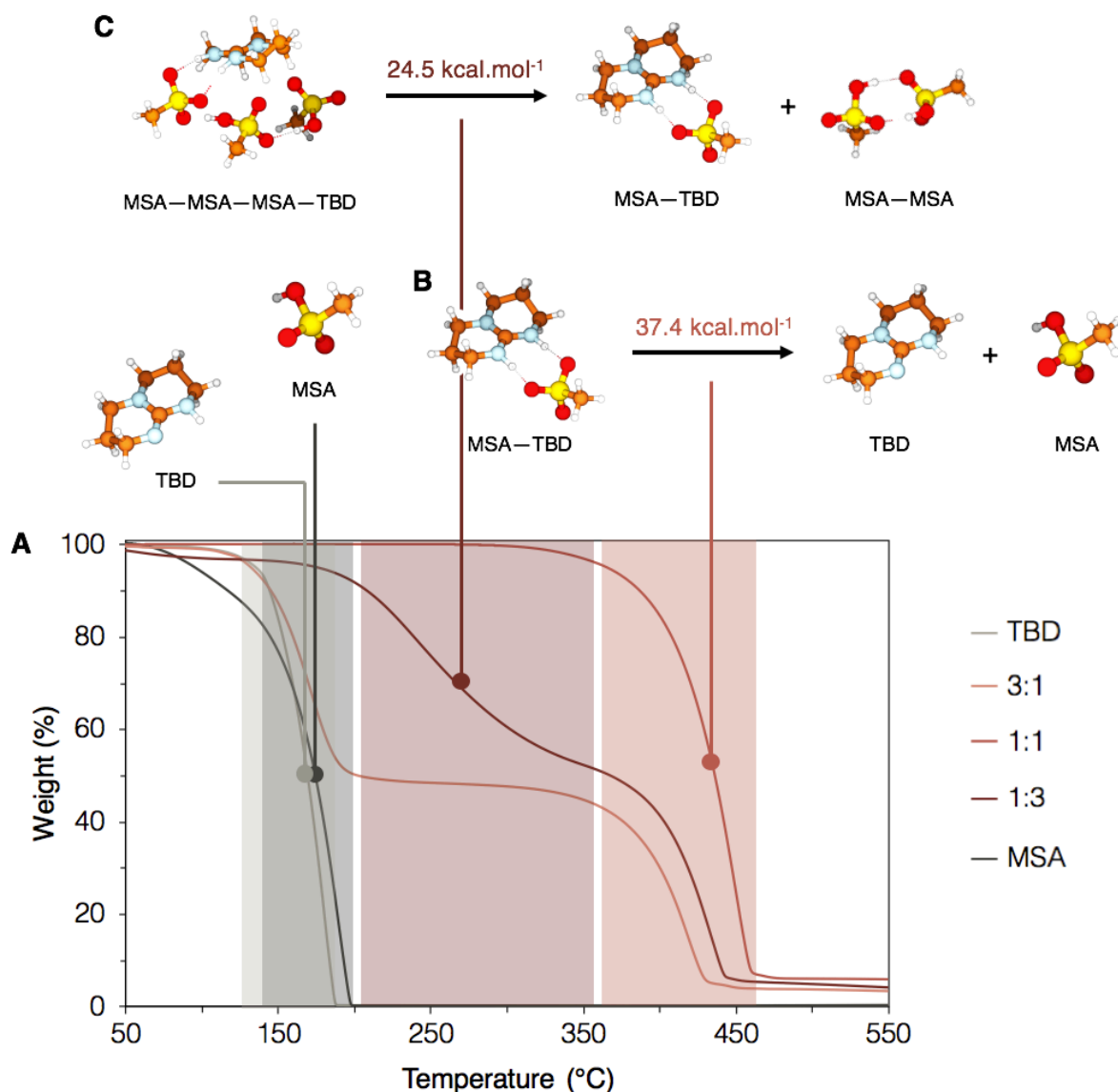


Figure 1.4. (A) TGA of TBD (light grey), MSA (dark grey) and TBD:MSA mixtures (light to dark orange) under nitrogen atmosphere and degradation pathway calculated with DFT for (B) TBD:MSA (1:1) and (C) TBD:MSA (1:3) complexes.

With excess acid – TBD:MSA (1:3) – a stable structure formed by one molecule of TBD and three molecules of MSA was optimised using DFT which, similarly to TBD:MSA (1:1), demonstrates a complete relocation of the acidic proton of MSA on the basic nitrogen of TBD unitedly with the creation of a hydrogen bond between one oxygen of MSA and the N-H moiety of TBD. Additionally, the three molecules of MSA are linked to each other through hydrogen bonds linking the acidic moiety of one MSA to one sulfonyl group of another. The loss of 44% weight observed for the first degradation event on the TGA

corresponds to the loss of two molecules of MSA (theoretical loss = 45%). Thus, it can be postulated that the first degradation event corresponds to the decomposition of the TBD:MSA (1:3) complex into two molecules of MSA plus the TBD:MSA (1:1) complex. The corresponding calculated dissociation energy raised $24.5 \text{ kcal.mol}^{-1}$, a relatively high energetic barrier justifying the stability of the catalyst compare to MSA and TBD separately. (Fig. 1.4C) On the contrary, with excess base – TBD:MSA (3:1) – the first degradation event between $130 \text{ }^{\circ}\text{C}$ and $190 \text{ }^{\circ}\text{C}$ corresponds to the degradation of the excess base as 52% weight loss corresponds to the loss of two molecules of TBD (theoretical loss = 54%). Additionally, no stable complex involving three molecules of TBD and one molecule of MSA could be obtained with DFT. Therefore, it can be hypothesised that TBD:MSA (3:1) is not forming a stable salt but is a mixture between TBD and TBD:MSA (1:1) protic ionic salt.

To further confirm the feasibility of using the TBD:MSA (1:1) salt for catalytic process at the usual high temperatures employed for depolymerisation reactions over extended time period, its thermal stability was studied at $180 \text{ }^{\circ}\text{C}$ by an isothermal TGA experiment for 18 h. (Fig. 1.5)

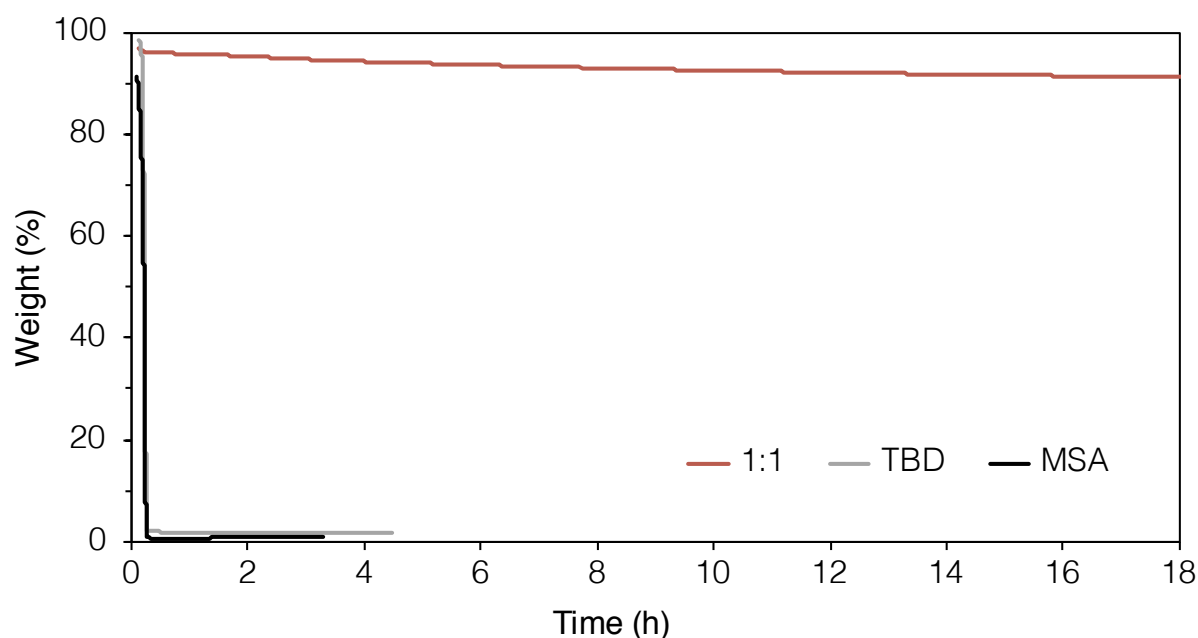


Figure 1.5. Isotherms of TBD:MSA (1:1) (orange line), TBD (light grey line) and MSA (dark grey line) at reaction temperature, $180 \text{ }^{\circ}\text{C}$, for 18 h.

At this temperature, the weight loss of TBD:MSA (1:1) was negligible (less than 3 wt %) while both TBD and MSA suffered a complete decomposition in less than 30 min. This result confirms the excellent thermal stability of TBD:MSA (1:1) protic ionic salt, in particular at the high temperature usually required for commodity polymers depolymerisation, and hence demonstrates its potential utility for chemical recycling.

2 Catalytic activity for PET depolymerisation

The catalytic activity of the acid-base mixtures has been first tested with a well-known commodity polymer: PET. This polymer has been chosen because it is the most studied for recycling at both academic and industrial levels, thus, it was the best starting point to compare the abilities of the catalysts synthesised in this chapter with reported procedures. Additionally, if depolymerisation reactions required high temperatures in general, PET depolymerisation in particular demands even harsher conditions as a consequence of the high chemical stability of this polymer. Thus, PET is indeed an excellent candidate to endure the stability of the present organocatalysts.

2.1 TBD:MSA mixtures

The catalytic activities of TBD, MSA and the different TBD:MSA mixtures were evaluated as catalyst for the glycolysis of PET. (**Fig. 1.6A**) The transesterification of ethylene glycol on PET produces BHET, a diol that can be then employed as monomer for the re-polymerisation of PET.^{25,26}

All experiments were conducted using discarded colourless PET bottle pellets (0.5 g, 2.60 mmol, 1 eq.), in the presence of excess ethylene glycol (2.42 g, 39 mmol, 15 eq.) with 0.25 eq. of each catalyst, at 180 °C, for 4 h and under nitrogen atmosphere. At the end of each reaction, the crude product was analysed by ¹H NMR spectroscopy using DMF as internal standard for performances comparison while eventual residual PET pellets were filtered, washed and dried before weighted. (**Fig. 1.6B**)

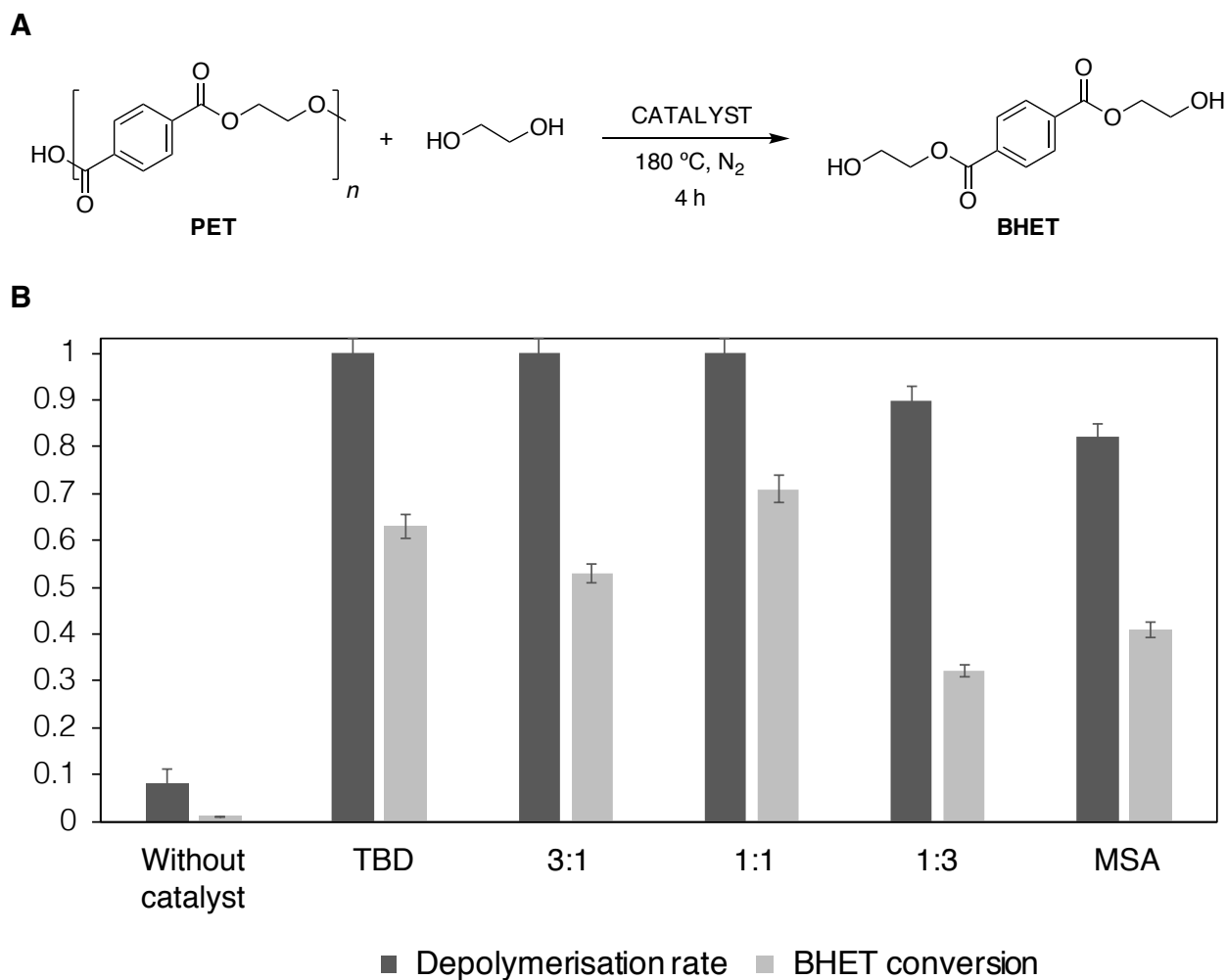


Figure 1.6. (A) Depolymerisation of PET using ethylene glycol and (B) effect of the catalyst on the depolymerisation rate (dark grey) and BHET conversion (light grey). Conversion into BHET was determined by ^1H NMR spectroscopy in $\text{DMSO-}d_6$ from the crude product using DMF as internal standard (signals at $\delta = 2.72$ and 2.88 ppm) and characteristic signals of BHET at $\delta = 4.32$ and 3.72 ppm. Reaction conditions: PET (0.5 g, 2.60 mmol, 1 eq.), ethylene glycol (2.42 g, 39 mmol, 15 eq.), catalyst (0.65 mmol, 0.25 eq.), $180\text{ }^\circ\text{C}$, 4 h.

Each of catalyst system tested demonstrated rapid depolymerisation of PET compared to the reaction without catalyst which demonstrated less than 10% of the PET pellets depolymerised and less than 2% of BHET produced after, 4 h. Analysis of the final crude products by ^1H NMR spectroscopy revealed that reactions with MSA alone or excess MSA depolymerisation were not completed after 4 h and the resultant monomer yield was not quantitative – 32% with TBD:MSA (1:3) and 41% with MSA. (Fig. 1.7) Furthermore, additional resonances can be observed in the ^1H NMR spectra of the products from these reactions in the region between $\delta = 3.5$ and 4.5 ppm which confirms the

formation of products other than the desired monomer, most likely oligomers, which is consistent with the low BHET yield.

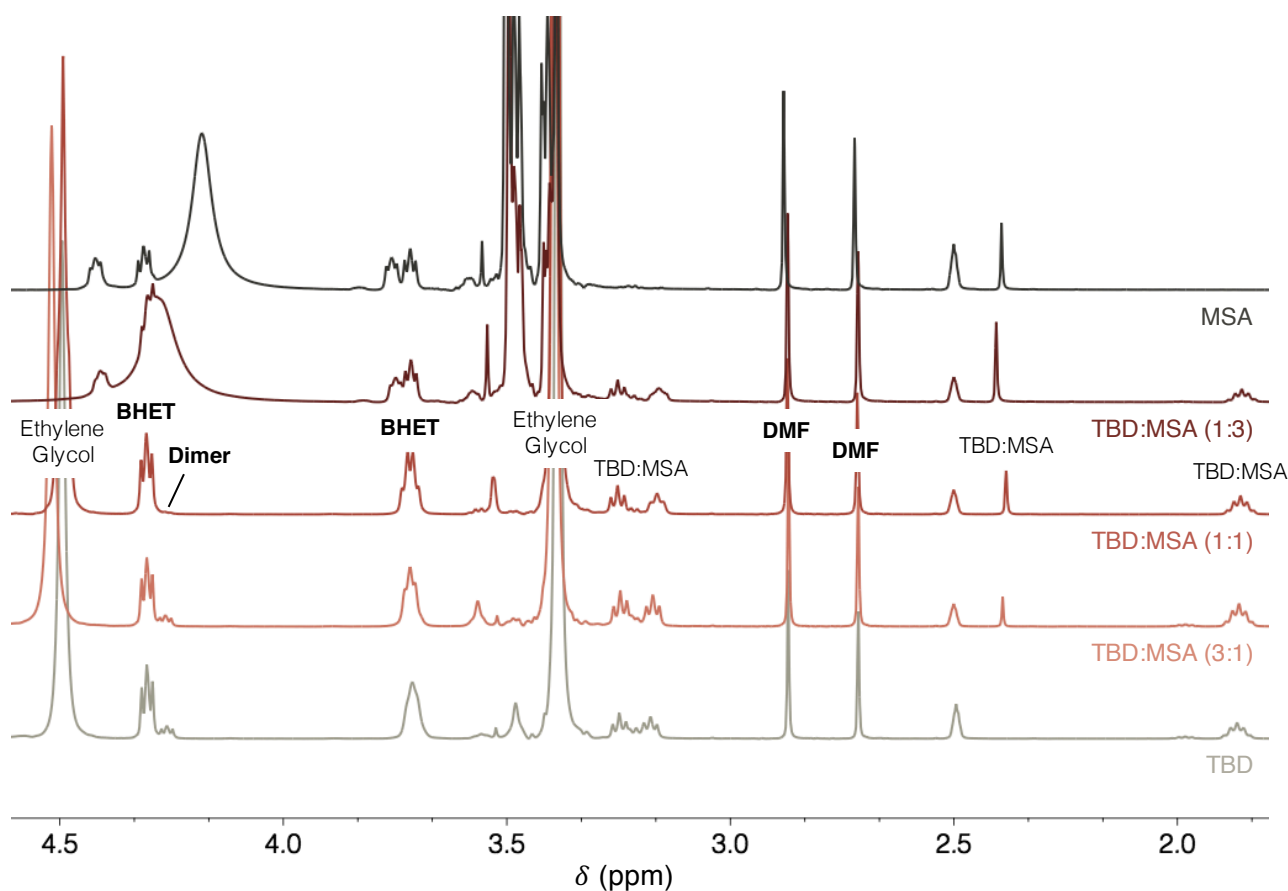


Figure 1.7. Stacked ^1H NMR spectra of the crude products for the depolymerisation of PET using different catalysts (400 MHz, $\text{DMSO-}d_6$, 298 K). Reaction conditions: PET (0.5 g, 2.60 mmol, 1 eq.), ethylene glycol (2.42 g, 39 mmol, 15 eq.), catalyst (0.65 mmol, 0.25 eq.) 180 °C, 4 h.

Reactions with TBD and the mixture with excess TBD (3:1) showed better efficiency (63% and 53% of BHET, respectively) with depolymerisation reactions being complete within 4 h – for the reaction catalysed by TBD, the reaction was completed in less than 1 h. Also here, additional signals in the spectra, especially a triplet resonance at $\delta = 4.27$ ppm, should be noticed. This additional molecule corresponds to the dimer of BHET known to be in equilibrium with BHET during such reaction.²⁷ Finally, the highest BHET conversion was achieved with TBD:MSA (1:1), the depolymerisation reaching completion after 2 h and yielding 71 % of BHET.

Furthermore, it could be noticed that for the reaction using MSA, the mixture very rapidly turned brown to end totally dark after 4 h, the crude products of the reactions with TBD:MSA (3:1), TBD:MSA (1:3) and TBD were yellow to

brownish while the reaction involving TBD:MSA (1:1) stayed almost transparent. (Fig. 1.8) This can also be correlated to the exceptional thermal stability of the TBD:MSA (1:1) complex, able to endure the high depolymerisation temperature of 180 °C.

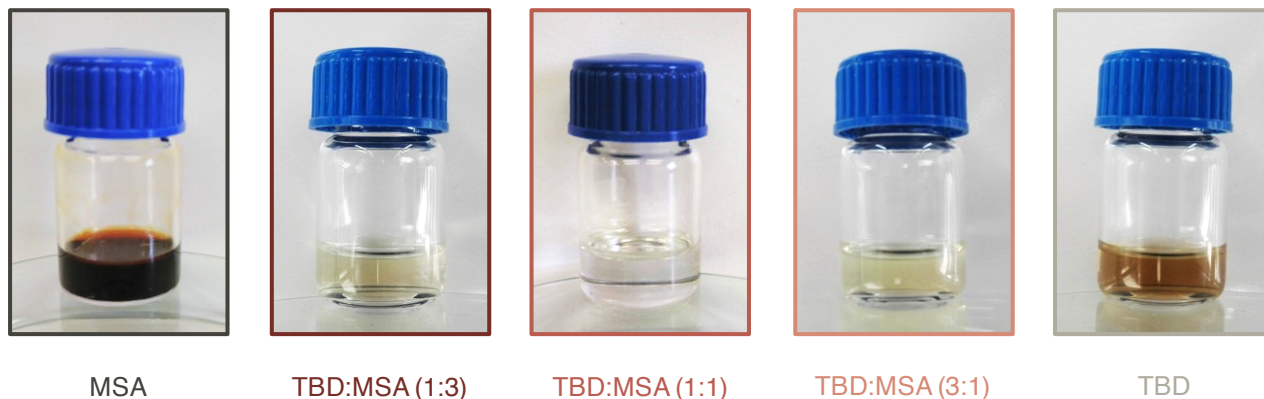


Figure 1.8. Pictures of the crude products for the reactions with the different TBD:MSA mixtures after 4 h of PET depolymerisation at 180 °C.

2.2 Comparison with other acid-base mixtures

Other acid-base mixtures have been synthesised for comparing their catalytic activity to TBD:MSA (1:1). Another base, DBU, was mixed with another acid, BA, to form DBU:BA (1:1), a salt already reported for the glycolysis of PET under different conditions.¹⁹ DBU was also mixed with MSA and TBD with BA for comparison. (Fig. S1.5 to S1.7) The depolymerisation was performed following the same procedure, in bulk, using 15 eq. of ethylene glycol but with 0.5 eq. of catalyst. DBU:BA (1:1) and TBD:BA (1:1) catalysed the reaction in one hour reaching a fair but lower yield of BHET than TBD:MSA (1:1) – 84% and 75%, respectively, versus 91% for TBD:MSA (1:1). (Fig. 1.9A) DBU:MSA (1:1) reached a poorest BHET conversion of 54% after an extended period of 5 h. Although DBU:BA (1:1) and TBD:BA (1:1) demonstrated reasonable conversions into BHET, it can be noticed that their thermal stability is much lower compared to the mixtures containing MSA. While $T_{50\%}$ raises 438°C for TBD:MSA (1:1) or 408 °C for DBU:MSA (1:1), $T_{50\%} = 250$ °C for TBD:BA (1:1) and $T_{50\%} = 240$ °C for DBU:BA (1:1). (Fig. 1.9B) It was macroscopically verified as glycolysis catalysed by mixtures with BA turned brownish while depolymerisations involving TBD:MSA (1:1) and DBU:MSA (1:1) stayed

01. Organocatalysis

transparent until reaction's end. Thus, in the aim of recycling several time the catalyst for further depolymerisations, the poorest resistance to temperature of DBU:BA and TBD:BA could be problematic.

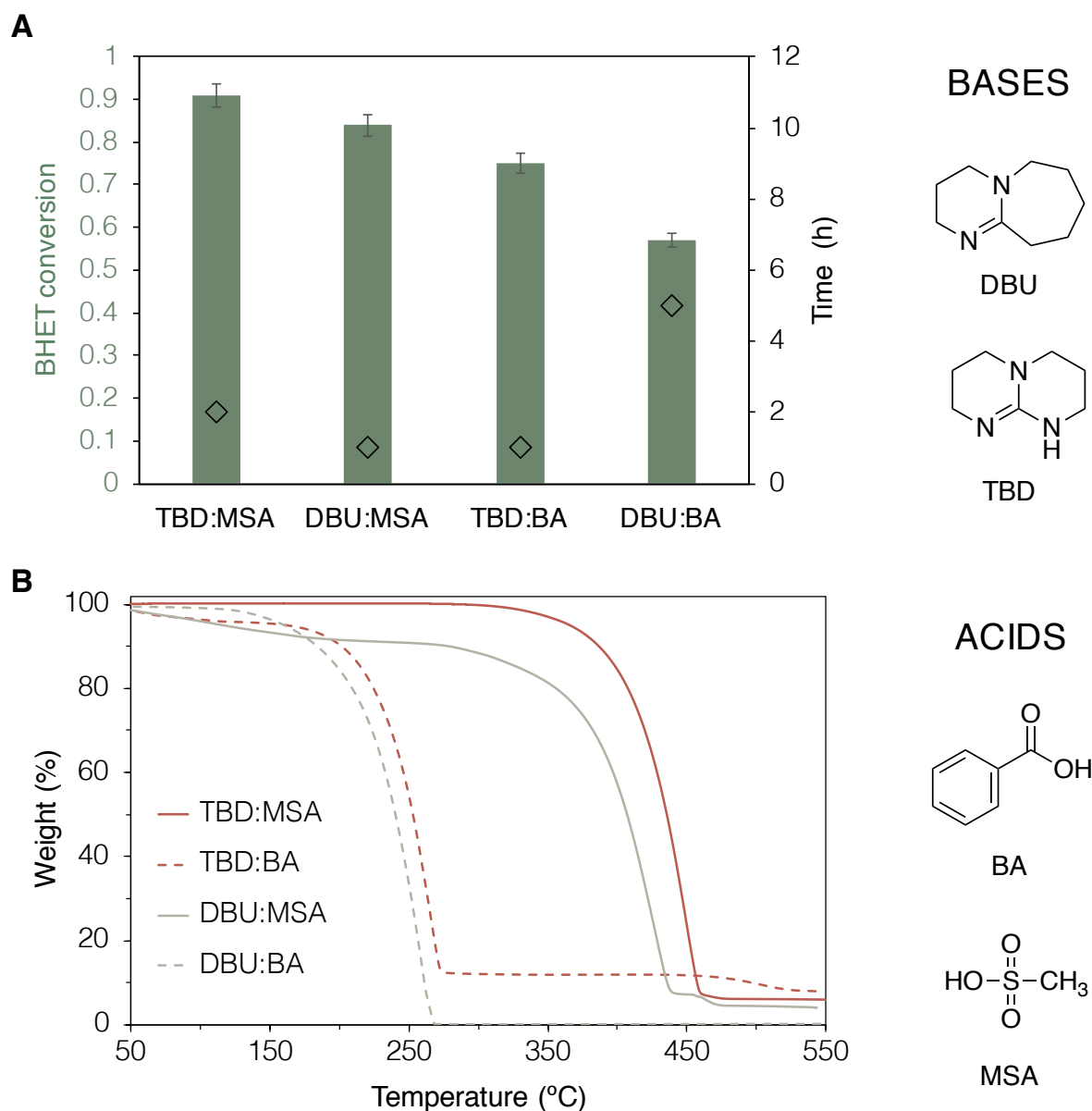


Figure 1.9. (A) Effect of the nature of the catalyst (0.5 eq.) on the degradation time of PET (black diamonds) and BHET conversion (green bars). Conversion of BHET was determined by ^1H NMR spectroscopy in $\text{DMSO-}d_6$ from the crude product using catalyst as internal standard (signals at $\delta = 1.87$ ppm for TBD mixtures and 1.91 ppm for DBU mixtures) and characteristic signals of BHET at $\delta = 4.32$ and 3.72 ppm – Fig. S1.13. Reactions conditions: PET (0.5 g, 2.60 mmol, 1 eq.), ethylene glycol (2.42 g, 39 mmol, 15 eq.), 180 °C. (B) TGA of the different equimolar acid-base mixtures investigated.

These results are explained by the difference of $\text{p}K_a$ between the acid and the base. Indeed, it has been demonstrated that a higher $\Delta\text{p}K_a$ between the acid and the base in these mixtures would lead to better resistance to

temperature.^{28,29} Using mixtures synthesised from DBU and a large library of acids, they postulated that for $\Delta pK_a > 15 - pK_a$ calculated in water – the corresponding mixture demonstrates extraordinary temperature resistance, with $T_{50\%} > 440$ °C. Here, MSA is a strong acid compared to benzoic acid – 2.0 versus 4.2, in water, respectively – which can explain the superior thermal stability for mixtures synthesised from MSA. Similarly, TBD is a slightly stronger base than DBU – 26.0 versus 24.3, in acetonitrile, respectively – which gives the final relative thermal stability for the equimolar mixtures: TBD:MSA > DBU:MSA >> TBD:BA > DBU:MSA.

3 Catalytic activity for BPA-PC depolymerisation

Inspired by the good results obtained with PET, it was decided to also apply TBD:MSA (1:1) catalyst to the depolymerisation of another commonly used thermoplastic: BPA-PC.

The depolymerisation of BPA-PC via the transesterification of an alcohol leads to its starting monomer, BPA, and a carbonate. (**Fig. 1.10A**) The catalytic activity of TBD:MSA (1:1) was compared with TBD and K_2CO_3 . The latter being a common catalyst for BPA-PC depolymerisation,^{30,31} the former being one of the only organocatalyst³² (with DBU and some protic ionic liquids) recently employed for this reaction. The depolymerisation was performed with commercial BPA-PC pellets in a round-bottom flask under N_2 atmosphere, using 1,2-propanediol as reagent. The reaction was performed at 130 °C in bulk, for 48 h, using 6 eq. of reagent. Mimicking the procedure applied to the depolymerisation of PET, after the reaction, the eventual remaining polymer pellets were filtered, dried and weighted to evaluate the depolymerisation rate. Conversions into monomers were determined through 1H NMR spectroscopy analysis. Ethylene glycol could also have been used for this reaction, likewise with PET, but the signal corresponding to the resulting ethylene carbonate in the 1H NMR spectra is overlapped by the hydroxyl groups of the diol, thus, making difficult the quantitative comparison between the different catalysts.

01. Organocatalysis

The control reaction without catalyst demonstrated negligible recycling rate. After 24 h, less than 2% of BPA-PC were depolymerised yielding 1% of BPA and no propylene carbonate. (Fig. 1.10B) On the contrary, the reactions involving TBD and TBD:MSA (1:1) were finished largely before 48 h, as complete disappearance of the BPA-PC pellets was observed after 3.5 h for TBD and 3 h for TBD:MSA (1:1). On the contrary, the reaction performed with potassium carbonate was not completed even after 48 h, the conversion of the reaction was evaluated to 95%.

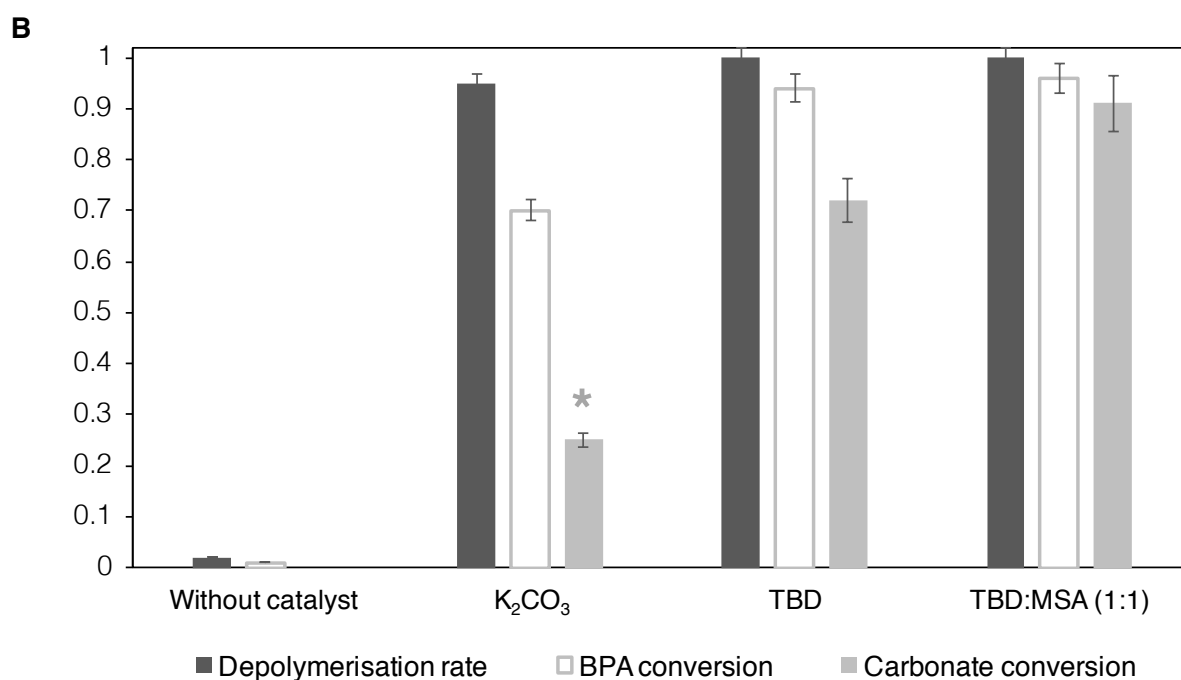
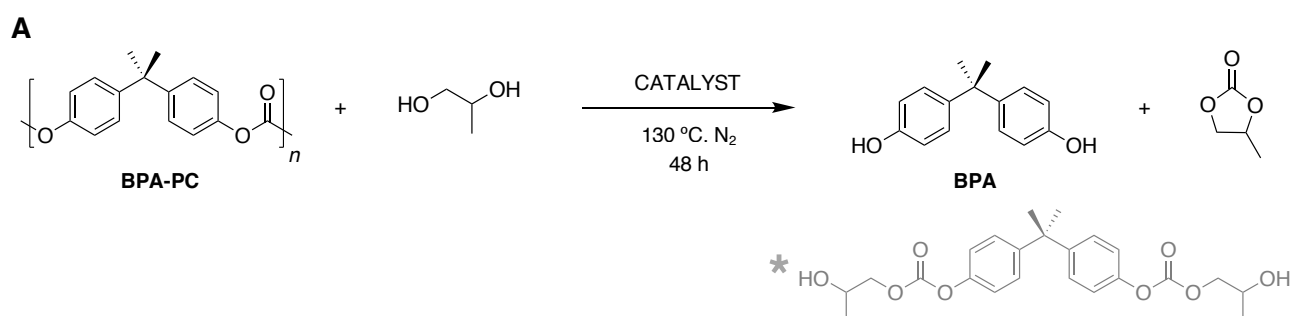


Figure 1.10. Depolymerisation of BPA-PC using 1,2-propanediol with different catalysts (0.15 eq.) for 48 h. Conversions into BPA and carbonate were determined by ¹H NMR spectroscopy in DMSO-*d*₆ from the crude product using the catalyst as internal standard ($\delta = 1.87$ ppm) and characteristic signals, BPA at $\delta = 6.63$ ppm, propylene carbonate at $\delta = 1.36$ ppm and the corresponding linear carbonate at $\delta = 1.12$ ppm. Reactions conditions: BPA-PC (2 g, 7.8 mmol, 1 eq.), 1,2-propanediol (3.56 g, 46.8 mmol, 6 eq.), 130 °C, 48 h.

For reactions with TBD and TBD:MSA (1:1), BPA conversion is really close to the depolymerisation rate with 90 and 96%, respectively, while BPA

conversion only raised 70% for K_2CO_3 . Additionally, the conversion into propylene carbonate is higher for TBD:MSA (1:1) compared to TBD alone, 91% versus 72%, which demonstrates the better ability of TBD:MSA (1:1) to ring-close the resulting intermediate to yield propylene carbonate.

The reaction with K_2CO_3 did not lead at all to the formation of propylene carbonate but to a linear derivative of BPA (in grey in Fig. 1.10A). Indeed, characteristic signals of propylene carbonate at $\delta = 4.89, 4.57, 4.07$ and 1.36 ppm are missing while multiplets at $\delta = 3.90, 3.76 - 3.71$ ppm and doublets at $\delta = 1.12$ ppm together with the additional aromatic signals at $\delta = 7.06$ and 6.80 ppm (grey asterisks) indicates the presence of around 25% of this linear di-carbonate BPA derivative. (Fig. 1.11)

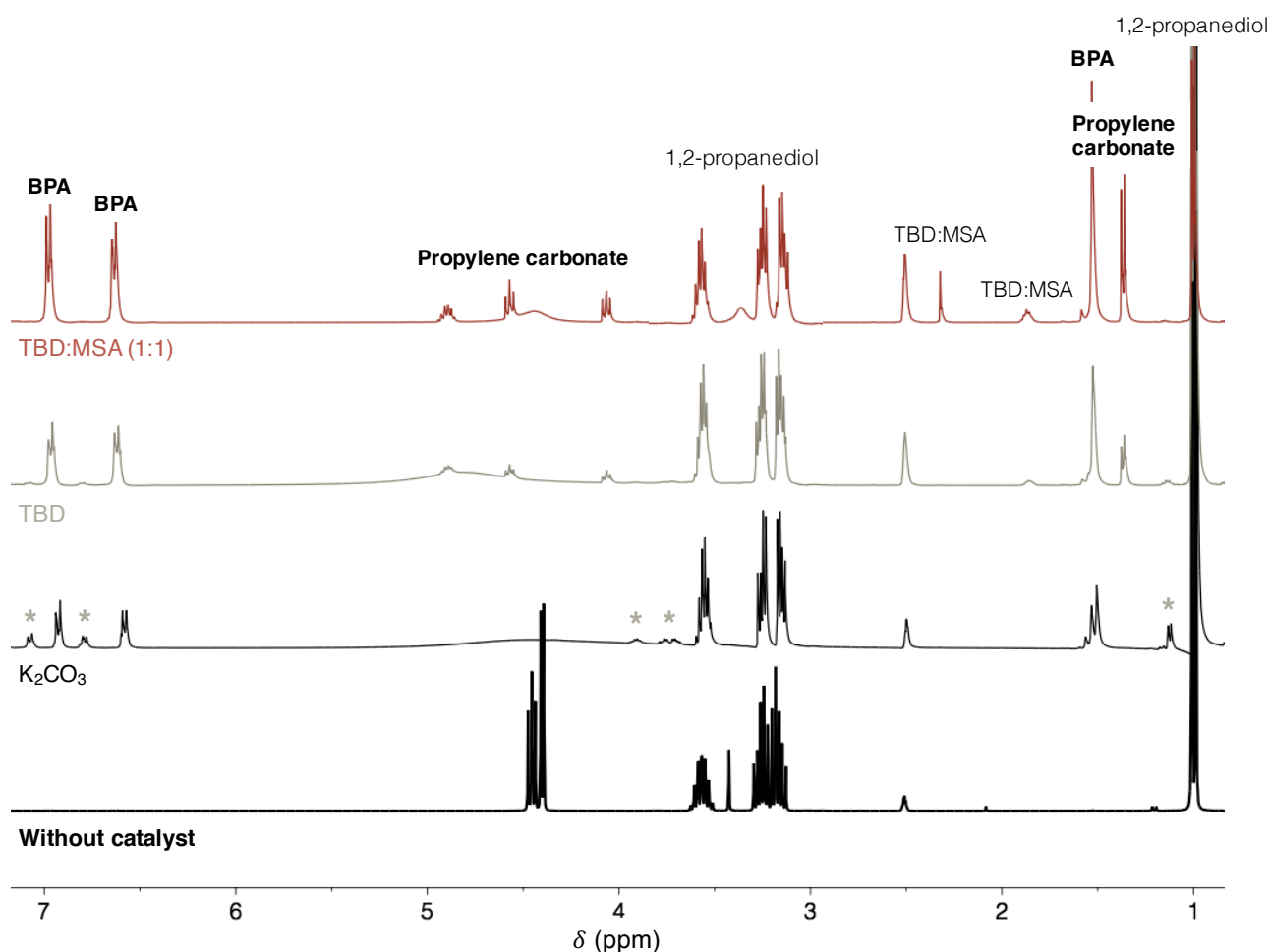


Figure 1.11. Stacked 1H NMR spectra of the crude products for the depolymerisation of BPA-PC using different catalysts (400 MHz, $DMSO-d_6$, 298 K). Reaction conditions: BPA-PC (2 g, 7.8 mmol, 1 eq.), TBD:MSA (1:1) (0.256 g, 1.17 mmol, 0.15 eq.), 1,2-propanediol (3.56 g, 46.8 mmol, 6 eq.), $130^\circ C$, 48 h.

For BPA-PC also TBD:MSA (1:1) seems to be the best candidate for efficient depolymerisation as it promotes a fast reaction yielding very good conversions into both the starting material, BPA, and propylene carbonate, eventually suitable for high added value applications, as it will be explored in Chapter 3.

Conclusion

Mixtures of acids and bases have demonstrated excellent thermal stability, a tremendous advantage for catalysing high temperature depolymerisations. (Fig. 1.12) Avoiding the partial or full degradation of the catalyst prevents from colouration of the final products and undesirable side-reactions with the reagent, which could open the way to recycling and re-use of the catalyst for further reactions. Notably, the stoichiometric mixture of TBD and MSA has led to a protic ionic salt – TBD:MSA (1:1) – which manifests an exceptional thermal resistance and very good ability to catalyse the depolymerisations of both PET and BPA-PC.

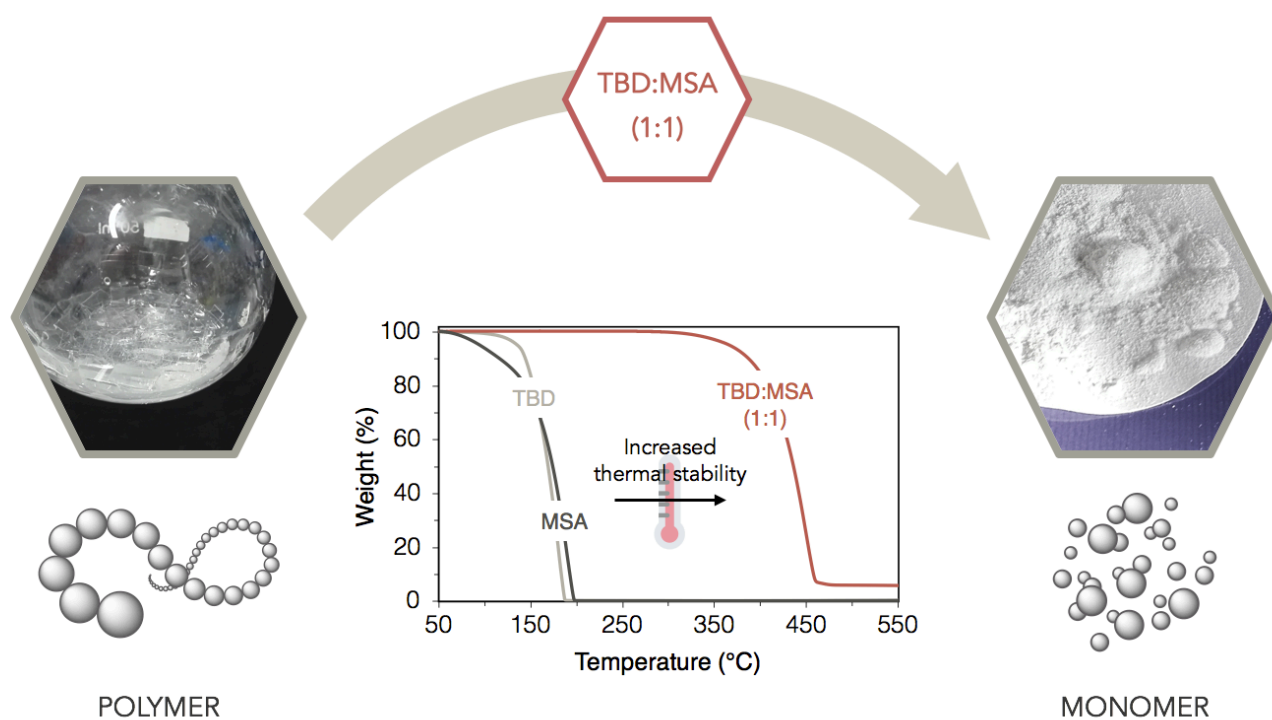


Figure 1.12. General scheme for the depolymerisation of commodity polymers using TBD:MSA (1:1) crystal as catalyst.

It has to be noticed also that PET depolymerisation catalysed by TBD:MSA (1:1) required more time to be completed compared to the depolymerisation with TBD alone. However, the final conversion into BHET is higher for the protic ionic salt, which demonstrates a better control of the reaction.

In a solvent-free procedure, TBD:MSA (1:1) catalyst revealed very good abilities for the depolymerisation of commodity polymers in a closed monomer-polymer-monomer loop.

References

- 1 A. P. Dove, H. Sardon and S. Naumann, *Organic Catalysis for Polymerisation*, Royal society of Chemistry, 2018.
- 2 X. Zhang, M. Fevre, G. O. Jones and R. M. Waymouth, *Chem. Rev.*, 2018, **118**, 839–885.
- 3 H. Sardon, A. Pascual, D. Mecerreyes, D. Taton, H. Cramail and J. L. Hedrick, *Macromolecules*, 2015, **48**, 3153–3165.
- 4 A. Bossion, K. V. Heifferon, L. Meabe, N. Zivic, D. Taton, J. L. Hedrick, T. E. Long and H. Sardon, *Prog. Polym. Sci.*, 2019, **90**, 164–210.
- 5 L. Mezzasalma, A. P. Dove and O. Coulembier, *Eur. Polym. J.*, 2017, **95**, 628–634.
- 6 A. P. Dove, *ACS Macro Lett.*, 2012, **1**, 1409–1412.
- 7 S. Naumann, P. B. V. Scholten, J. A. Wilson and A. P. Dove, *J. Am. Chem. Soc.*, 2015, **137**, 14439–14445.
- 8 B. Lin and R. M. Waymouth, *J. Am. Chem. Soc.*, 2017, **139**, 1645–1652.
- 9 A. Nachtergaele, O. Coulembier, P. Dubois, M. Helvenstein, P. Duez, B. Blankert and L. Mespouille, *Biomacromolecules*, 2015, **16**, 507–514.
- 10 Y. Xia, J. Shen, H. Alamri, N. Hadjichristidis, J. Zhao, Y. Wang and G. Zhang, *Biomacromolecules*, 2017, **18**, 3233–3237.
- 11 N. E. Kamber, W. Jeong, R. M. Waymouth, R. C. Pratt, B. G. G. Lohmeijer and J. L. Hedrick, *Chem. Rev.*, 2007, **107**, 5813–5840.
- 12 M. K. Kiesewetter, E. J. Shin, J. L. Hedrick and R. M. Waymouth, *Macromolecules*, 2010, **43**, 2093–2107.
- 13 W. N. Ottou, H. Sardon, D. Mecerreyes, J. Vignolle and D. Taton, *Prog. Polym. Sci.*, 2016, **56**, 64–115.
- 14 A.-G. Ying, L. Liu, G.-F. Wu, G. Chen, X.-Z. Chen and W.-D. Ye, *Tetrahedron Lett.*, 2009, **50**, 1653–1657.
- 15 W. G. Kim, H. G. Yoon and J. Y. Lee, *J. Appl. Polym. Sci.*, 2001, **81**, 2711–2720.
- 16 D. J. Coady, K. Fukushima, H. W. Horn, J. E. Rice and J. L. Hedrick, *Chem. Commun.*, 2011, **47**, 3105–3107.
- 17 A. Sanchez-Sanchez, A. Basterretxea, D. Mantione, A. Etxeberria, C. Elizetxea, A. de la Calle, S. García-Arrieta, H. Sardon and D. Mecerreyes, *J. Polym. Sci. Part A: Polym. Chem.*, 2016, **54**, 2394–2402.

- 18 A. Basterretxea, E. Gabirondo, A. Sanchez-Sanchez, A. Etxeberria, O. Coulembier, D. Mecerreyes and H. Sardon, *Eur. Polym. J.*, 2017, **95**, 650–659.
- 19 K. Fukushima, D. J. Coady, G. O. Jones, H. A. Almegren, A. M. Alabulrahman, F. D. Alsewailem, H. W. Horn, J. E. Rice and J. L. Hedrick, *J. Polym. Sci. Part A: Polym. Chem.*, 2013, **51**, 1606–1611.
- 20 K. Fukushima, O. Coulembier, J. M. Lecuyer, H. A. Almegren, A. M. Alabulrahman, F. D. Alsewailem, M. A. Mcneil, P. Dubois, R. M. Waymouth, H. W. Horn, J. E. Rice and J. L. Hedrick, *J. Polym. Sci. Part A: Polym. Chem.*, 2011, **49**, 1273–1281.
- 21 E. Quaranta, D. Sgherza and G. Tartaro, *Green Chem.*, 2017, **19**, 5422–5434.
- 22 R. L. Vekariya, *J. Mol. Liq.*, 2017, **227**, 44–60.
- 23 S. García-Argüelles, C. García, M. C. Serrano, M. C. Gutiérrez, M. L. Ferrer and F. del Monte, *Green Chem.*, 2015, **17**, 3632–3643.
- 24 J.-D. Chai and M. Head-Gordon, *Phys. Chem. Chem. Phys.*, 2008, **10**, 6615–6620.
- 25 W. A. MacDonald, *Polym. Int.*, 2002, **51**, 923–930.
- 26 F.-A. El-Toufaily, G. Feix and K.-H. Reichert, *J. Polym. Sci. Part A: Polym. Chem.*, 2006, **44**, 1049–1059.
- 27 R. López-Fonseca, I. Duque-Ingunza, B. de Rivas, L. Flores-Giraldo and J. I. Gutiérrez-Ortiz, *Chem. Eng. J.*, 2011, **168**, 312–320.
- 28 M. S. Miran, H. Kinoshita, T. Yasuda, M. A. B. H. Susan and M. Watanabe, *Phys. Chem.*, 2012, **14**, 5178–5186.
- 29 H. Luo, G. A. Baker, J. S. Lee, R. M. Pagni and S. Dai, *J. Phys. Chem. B*, 2009, **113**, 4181–4183.
- 30 C. Gioia, M. Vannini, A. Celli, M. Colonna and A. Minesso, *RSC Adv.*, 2016, **6**, 31462–31469.
- 31 G. O. Jones, A. Yuen, R. J. Wojtecki, J. L. Hedrick and J. M. García, *Proc. Natl. Acad. Sci.*, 2016, **113**, 7722–7726.
- 32 T. Do, E. R. Baral and J. G. Kim, *Polymer*, 2018, **143**, 106–114.

2

PET depolymerisation

From polymer to monomer to polymer



To celebrate its status as the 2015 European Green capital, Bristol built its own symbol with **The Bristol Whale** installed in the Millennium square.

The sculpture is surrounded by more than 70 000 disposed bottles collected from both the Bristol 10k race and the Bath Half Marathon.

With over 15 million bottles sent to landfill every year only for the city of Bristol, organizers hopped that such initiative was "encouraging people to act now to reduce their consumption of single-use plastics and help protect our oceans for future generations".



The Bristol Whale

Introduction

PET is the most commonly used thermoplastic from the polyester family – *i.e.* 13% of the world plastic production in 2017 – and it is used in a large variety of applications, from clothing to food and beverage packaging.^{1,2} It is also the most recycled polymer in the world, with current industrial applications mainly in Europe and USA. According to the EEA4, the rate of recycled PET bottles reached 57% in 2017 in Europe.³ This encouraging number is however clouded by the domination of mechanical repurposing over chemical recycling processes. As previously evoked in the introduction, while the physical recycling of plastics leads to low-quality materials, mainly synthetic fibres for carpet or clothes in the case of PET – around 70% of the current amount of PET recycled^{4,5} – chemical recycling converts plastic wastes into monomers or oligomeric fragments that can then be polymerised to yield rPET or innovative materials with excellent thermal and physical properties.

Chemical recycling of PET can be conducted by the attack of different nucleophiles to the ester bond of PET by alcoholysis,^{6–10} hydrolysis,^{11–13} glycolysis,^{14–18} or aminolysis^{19–23}. (**Fig. 2.1**) As a consequence of the high chemical stability and low solubility of PET in organic solvents, the depolymerisation processes are generally performed under very harsh conditions and in the presence of catalysts. Organometallic catalysts such as zinc, cobalt, lead or manganese acetates, sodium/potassium sulfate, titanium phosphate, etc., have dominated the field due to their high stability and activity. However, their recovery can be challenging because of the laborious separation of the catalyst from the product.^{24–29} The combination of forcing reaction conditions with catalysts such these providing slow reaction rates and/or low selectivity presents significant difficulties in scaling-up to an industrially-relevant process. Several innovative solutions such as nanocatalysts,^{30,31} ionic liquids^{32–34} or DES^{35–37} have been recently considered. Some of these catalysts promote fast depolymerisation and/or good monomer yield. But they still present similar drawbacks: possible presence of

02. PET depolymerisation

metal in the final product, low monomer yields or challenging purification procedure.

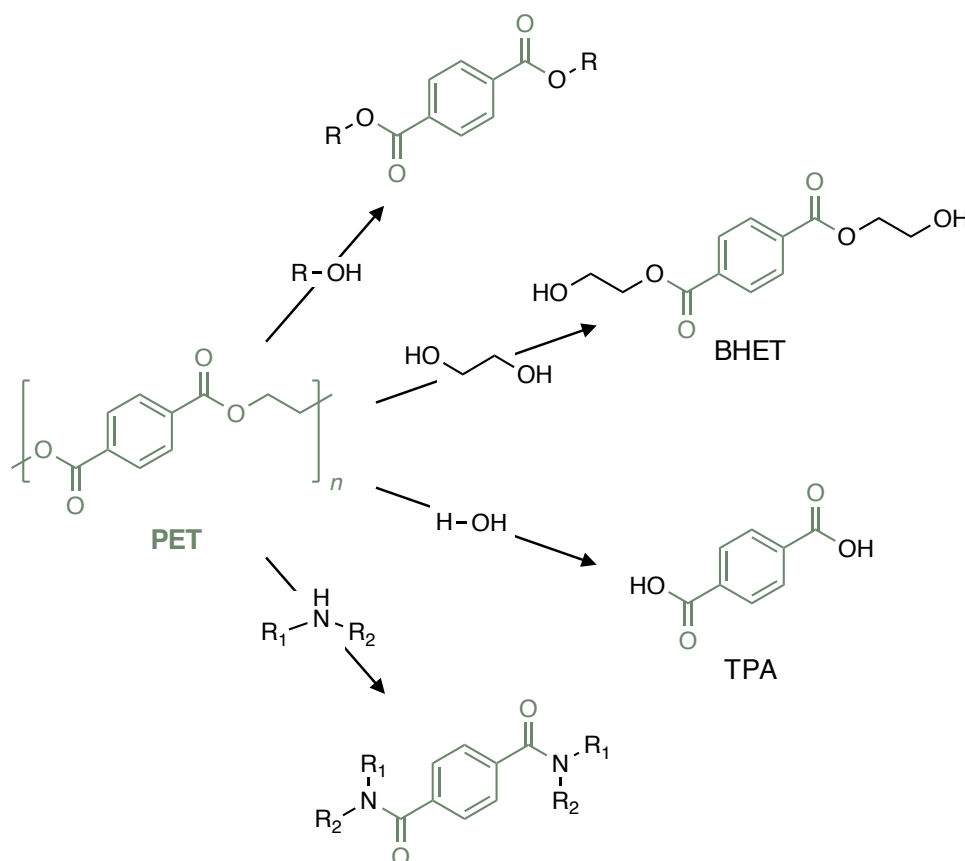


Figure 2.1. Different pathways for the depolymerisation of PET through alcoholysis, glycolysis, hydrolysis or aminolysis.

Organocatalysts are promising “green” substitutes to classic organometallic catalysts.^{38,39} Some organic bases commonly used for transesterification reactions have demonstrated encouraging results on depolymerisation with monomer yields up to 78%.⁴⁰⁻⁴² However, typically such organic compounds show poor thermal resistance to temperature that would be practical for PET recycling and as such, full or partial degradation of the catalyst occurs during the depolymerisation, which hinders the perspective of reusing it for several reactions.⁴³ Key to the advancement of this technology is the attainment not only of PET recycling into monomer at high yields but also the ability to reuse the catalyst towards envisioning a continuous recycling process.

In this chapter, TBD:MSA (1:1) protic ionic salt was employed as catalyst for the high temperature glycolysis of PET and compared with TBD which has been already reported for the depolymerisation of PET. A closed-loop

recycling process has been designed involving the re-polymerisation of the recovered depolymerisation product. The possibility to recycle the catalyst was considered and the mechanism of the reaction has been then investigated using DFT calculations.

1 Glycolysis optimisation

The ability for TBD:MSA (1:1) to catalyse the depolymerisation of PET using ethylene glycol was demonstrated in the previous chapter, reaching 71% conversion in less than 4 h while using 0.25 eq. of the so-called catalyst. Glycolysis has been chosen for the investigations because (1) it is well reported in the literature, (2) the product of this reaction, BHET, can be used as monomer for subsequent polymerisations of PET and (3) the reaction can be performed in bulk, in a large excess of ethylene glycol, preventing the use of organic solvent. However, to enhance the economics of the overall approach, maximising the BHET yield is essential.

1.1 Influence of ethylene glycol and catalyst contents

Parameters influencing the depolymerisation such as the ethylene glycol and catalyst loading were investigated with TBD:MSA (1:1) as catalyst. All experiments were performed using discarded colourless PET bottles pellets (0.5 g, 2.60 mmol, 1 eq.), under nitrogen atmosphere and until the complete disappearance of the polymer pellets in the vial. At the end of the reaction, the crude product was dissolved in water and the insoluble fraction was filtered to obtain a clear aqueous solution. After 24 h at 7 °C, needle-like BHET crystals were collected through filtration before being dried under vacuum and weighted. (**Fig. 2.2A**)

Notably, reducing the equivalents of ethylene glycol below 10 eq., the efficiency of the depolymerisation decreased. (**Fig. 2.2B**) With 5 eq. of ethylene glycol, the time required to complete the reaction exceeded 10 h and the final BHET yield was lower than when higher loadings were used. Using 10 eq. of ethylene glycol, the reaction was completed in just 3 h,

02. PET depolymerisation

however the BHET yield was moderate, 59 %. Indeed, using lower ethylene glycol / PET ratios resulted in a large insoluble fraction to treat during the purification process, because of the presence of PET oligomers which decreases the final BHET content. Increasing the ethylene glycol content up to 15 eq. or above, enabled BHET to yield up to 71% in around 3 h. Above this amount, raising the ethylene glycol content did not provide any significant improvement – 72% while using 20 eq..

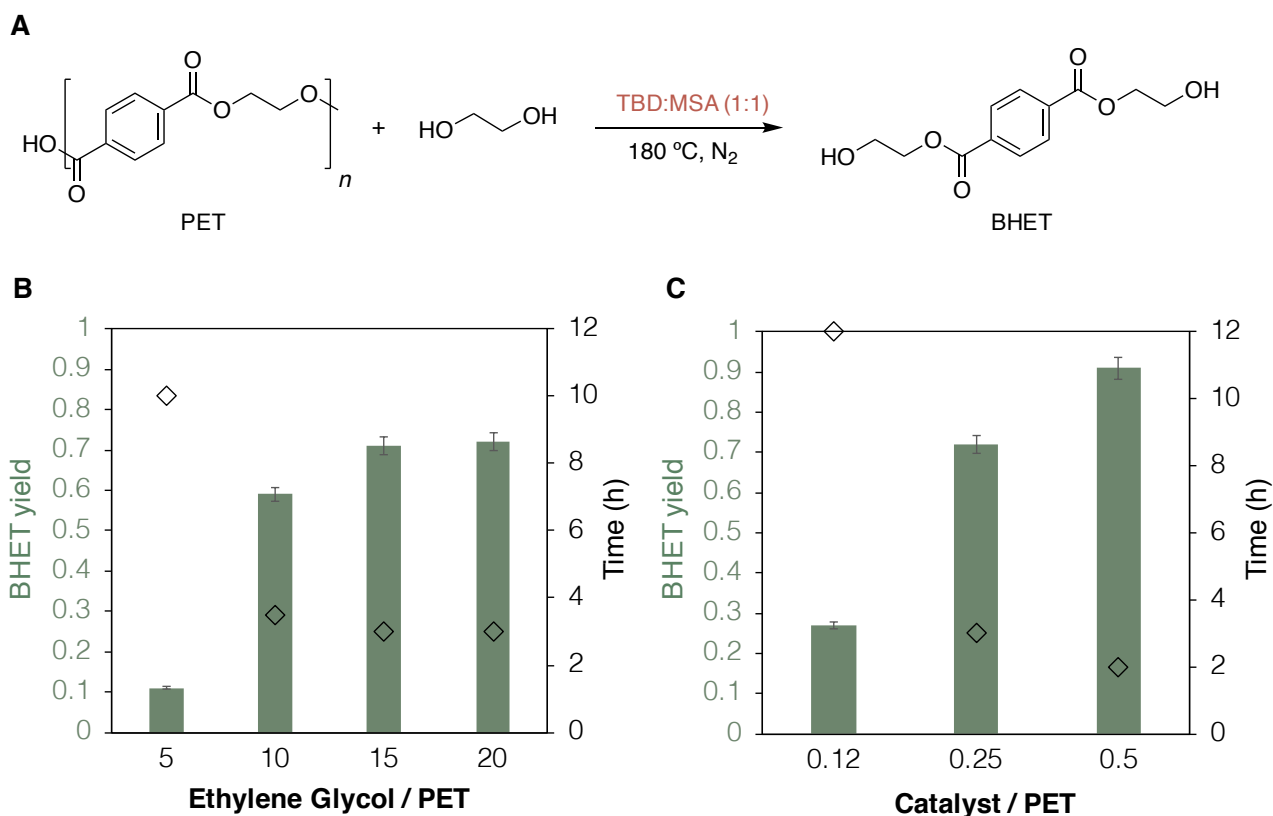


Figure 2.2. (A) PET glycolysis using TBD:MSA (1:1) as catalyst (B) Effect of the amount of ethylene glycol on the depolymerisation time of PET (black diamonds) and BHET yield (green bars). Reactions conditions: PET (0.5 g, 2.60 mmol, 1 eq.), catalyst (153 mg, 0.65 mmol, 0.25 eq.), 180 °C. (C) Effect of the amount of catalyst on the depolymerisation time (black diamonds) and BHET yield (green bars). Reactions conditions: PET (0.5 g, 2.60 mmol, 1 eq.), ethylene glycol (2.42 g, 39 mmol, 15 eq.), 180 °C.

To further optimise BHET yield, the catalyst concentration was also varied (**Fig. 2.2C**). A clear correlation was observed between the amount of catalyst and the reaction performance such that the amount of BHET increased from 27% with 0.12 eq. catalyst to 91% with 0.5 eq.. In addition, the catalyst loading also reduced substantially the depolymerisation time from 10 h to less than 2 h.

Therefore, the optimum conditions for the depolymerisation of PET were found to be 15 eq. of ethylene glycol and 0.5 eq. of catalyst and subsequent reactions will be performed as such.

1.2 Kinetic study

A kinetic study was performed for both TBD:MSA (1:1) and TBD as catalyst for the depolymerisation of PET in order to investigate the superior behaviour of TBD:MSA (1:1) compared to TBD. The BHET conversion was monitored by ^1H NMR spectroscopy in $\text{DMSO-}d_6$ for 48 h using the catalyst as internal standard. (Fig. 2.3)

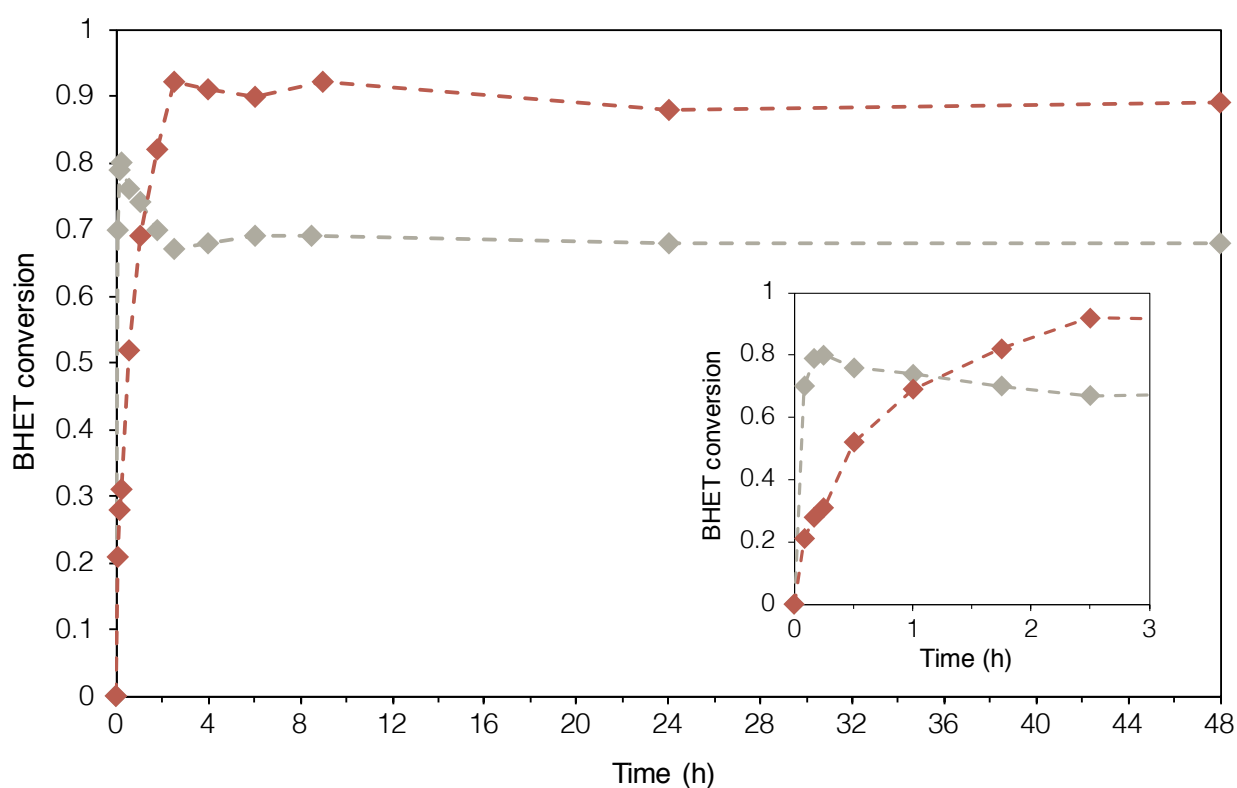
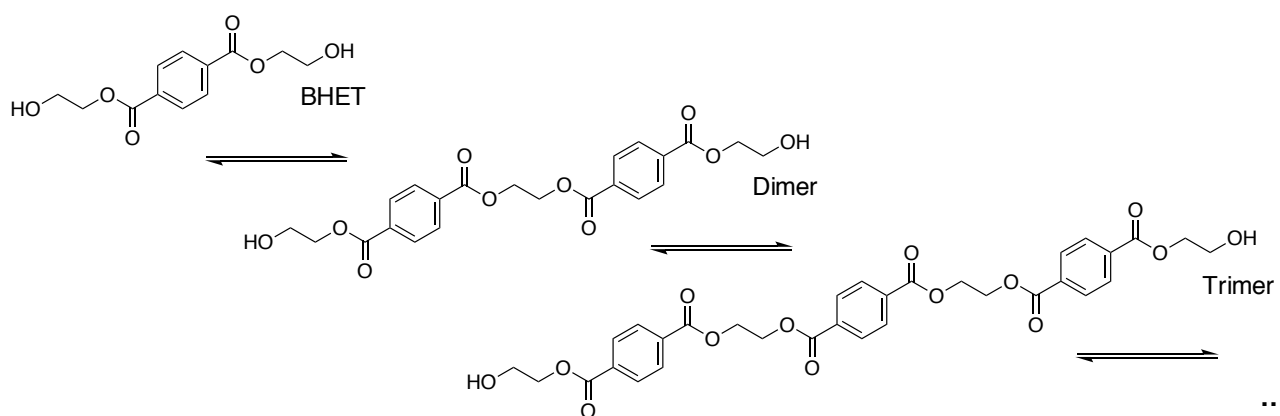


Figure 2.3. Kinetic studies for the depolymerisation of PET using TBD:MSA (1:1) (orange line) and TBD (grey line) as catalyst for 48 h and (internal plot) focus on the 3 first hours. Conversion into BHET was determined by ^1H NMR spectroscopy in $\text{DMSO-}d_6$ from the crude product using the catalyst as internal standard ($\delta = 1.87$ ppm) and characteristic signals of BHET at $\delta = 4.32$ and 3.72 ppm. – Fig. S2.1 & S2.2. Reactions conditions: PET (0.5 g, 2.60 mmol, 1 eq.), catalyst (1.30 mmol, 0.5 eq.), ethylene glycol (2.42 g, 39 mmol, 15 eq.), 180°C .

The reaction involving TBD was faster than with TBD:MSA (1:1), the former depolymerisation was completed in 20 min while the latter required 2.5 h to reach completion. In spite of the longer reaction times, at this time point, the reaction catalysed by TBD:MSA (1:1) raised 92% of BHET and remained

02. PET depolymerisation

constant while the reaction with TBD reached a maximum yield of 81% at 20 min followed by a rapid decrease to reach a plateau at 68% of BHET probably because of undesirable reactions. As it was already noticed in the ^1H NMR spectra of the depolymerisation (Chapter 1), the appearance of other signals and especially a triplet at $\delta = 4.27$ ppm (in addition to the triplet at $\delta = 4.32$ ppm and the quartet at $\delta = 3.73$ ppm from BHET) suggested that other species than BHET were formed. BHET is known to exist in equilibrium with other species, in particular its dimer, in equilibrium with the corresponding trimer, etc.⁴⁴ (Scheme 2.1) If BHET is soluble in water and can be re-crystallised after the reaction, dimer and small oligomers are not, which leads to a water-insoluble fraction filtered right after the end of the depolymerisation.



Scheme 2.1. BHET and the corresponding dimer and trimer structures.

The appearance of those species complicates the reusability of the degradation product for subsequent polymerisation, thus, it is important to minimise their quantity and to eliminate them from the final product to yield pure BHET. At the end of the reactions, after the precipitation and drying of the water insoluble fraction, these by-products reached $m = 162$ mg (32 wt %) for the reaction employing TBD as catalyst versus only $m = 35$ mg (7 wt %) with TBD:MSA (1:1), which is concordant with the lower BHET conversion while using TBD individually.

2 Recycling of the catalyst

Considering the environmental and economical viability of this process, residual reactants and catalyst need to be recycled for further PET

depolymerisations. After filtering the BHET crystals from the aqueous phase, the unreacted ethylene glycol and the catalyst were dried by vacuum evaporation at 60 °C before being stored in a vacuum oven at 60 °C overnight. Then, fresh PET flakes were added to the recycled system [ethylene glycol + catalyst] before repeating the depolymerisation procedure. Five subsequent depolymerisation reactions have been performed for two catalytic systems, TBD:MSA (1:1) and TBD. (Fig. 2.4)

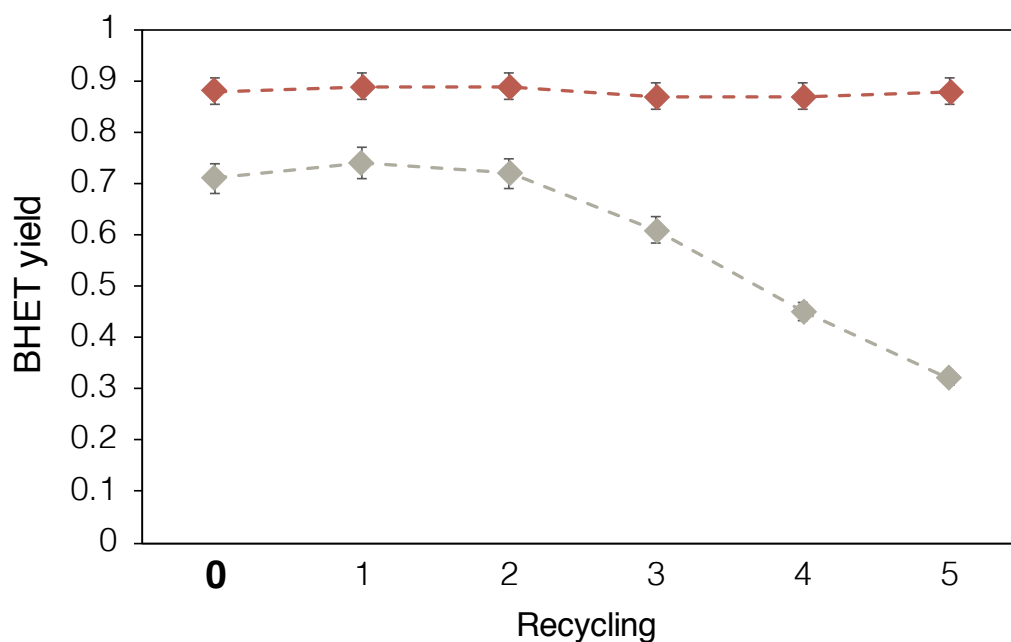


Figure 2.4. Comparison between the recycling of ethylene glycol and catalyst for TBD:MSA (1:1) (orange diamond) and TBD (grey diamond). Reactions conditions: PET (0.5 g, 2.60 mmol, 1 eq.), catalyst (1.30 mmol, 0.5 eq.), ethylene glycol (2.42 g, 39 mmol, 15 eq.), 180 °C.

Using TBD:MSA (1:1) as catalyst, the BHET yield stayed constant with no loss of catalytic activity, even after 5 recycling. In contrast, the TBD-catalysed reaction reached lower yields of BHET starting the second recycling (reaction 3). This difference can be attributed to the exceptional high thermal stability of TBD:MSA (1:1). As it was previously noted, the acid-base mixture is stable at 180 °C for more than 18 h while TBD displays complete degradation in less than 30 minutes. It can be postulated that this stark difference in thermal stability is reflected in the ability of the TBD:MSA (1:1) catalyst to perform at high temperatures over a longer period of time and so, for an increased number of reactions. Moreover, with TBD, the depolymerisation time increased from 20 min for the first reaction to 1.5 h for the second (first

02. PET depolymerisation

recycling) and finally reached more than 8 h at the 5th recycling. On the contrary, the reaction time stays stable – between 2 h 10 min and 3 h – for the depolymerisation using TBD:MSA (1:1).

These results confirmed that the TBD:MSA (1:1) salt is an excellent candidate for the depolymerisation of PET, not only because it can be recycled multiple times, but also because high BHET yields were obtained.

3 Scaling-up and limitations

3.1 Scaling-up the reaction

One of the current limitations of organocatalysis is the need for dry conditions for optimal operation. In order to evaluate the ability of TBD:MSA (1:1) catalyst to work under air, a reaction has been carried out without using inert atmosphere following the same procedure. No significant differences were observed – BHET yields 89 % in 2.5 h – showing the potential of this process to be scaled up. The same experiment was also performed with larger load of PET – 5 g – and either any differences were observed as similar BHET yield was obtained – 88%.

3.2 Reaction with coloured PET

Another common limitation of the PET depolymerisation reactions concerns the recycling of coloured PET bottles.⁴² A previous treatment of coloured bottles by activated carbon and/or ion exchange resin is usually necessary for removing the residual pigments and dyes.⁴⁵ However, we investigated the ability of the present procedure to depolymerise coloured bottles with no preliminary removal of the pigments. Two different PET bottles, one green and another one blue, have been depolymerised using the conditions described in this chapter. (Fig. 2.5)

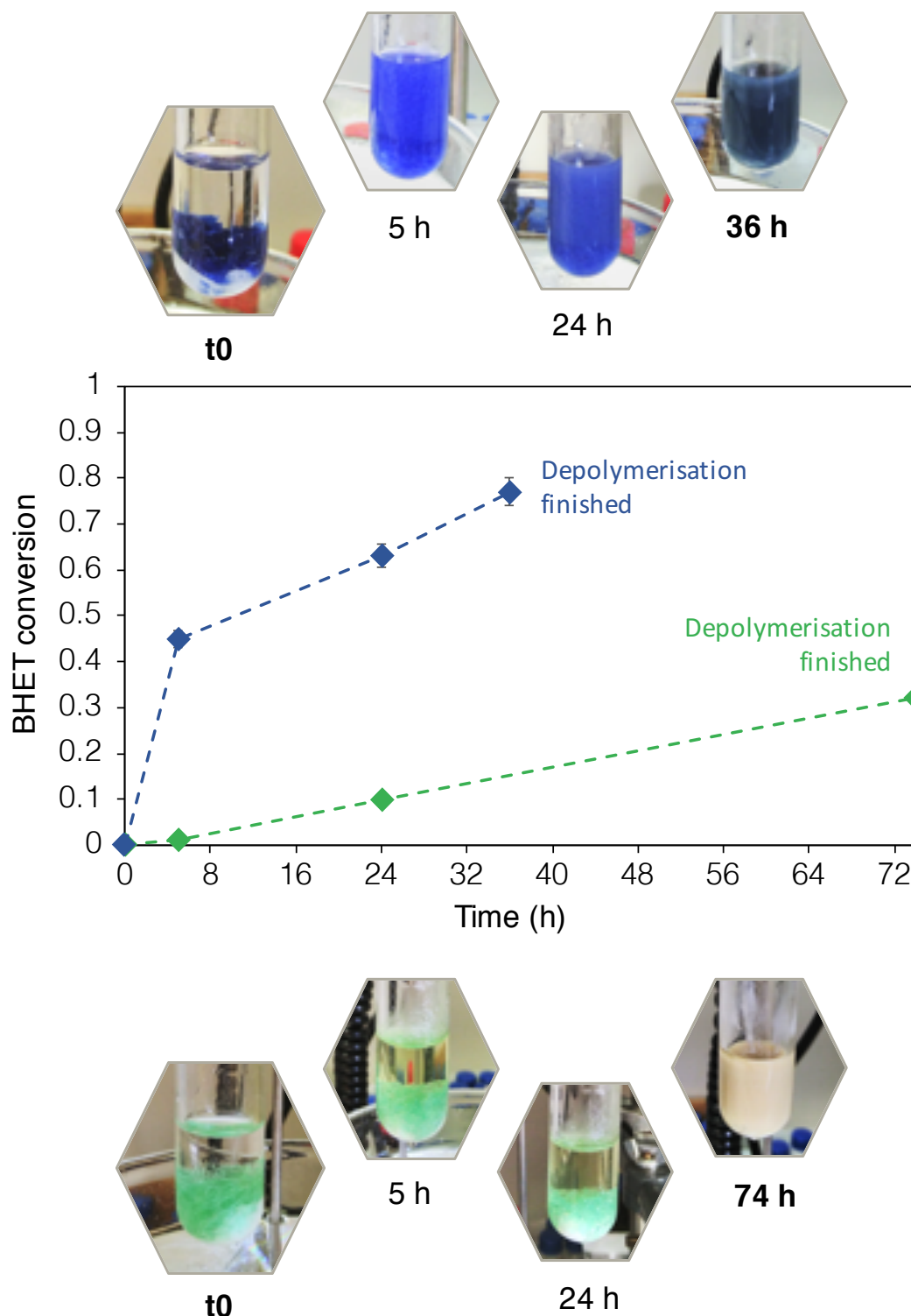


Figure 2.5. Evolution of BHET conversion with time for the depolymerisation of green bottle (in green) and blue bottle (in blue) and pictures of the depolymerisation of both green and blue bottles. Conversion into BHET was determined by ^1H NMR spectroscopy in $\text{DMSO-}d_6$ from the crude product using the catalyst as internal standard ($\delta = 1.87$ ppm) and characteristic signals of BHET at $\delta = 4.32$ and 3.72 ppm – (Fig. S2.3 & S2.4). Reactions conditions: PET (0.5 g, 2.60 mmol, 1 eq.), catalyst (1.30 mmol, 0.5 eq.), ethylene glycol (2.42 g, 39 mmol, 15 eq.), 180°C .

Although reactions ultimately have led to complete disappearance of PET, both required extended reaction times to reach completion. In addition, while

02. PET depolymerisation

the reaction with blue PET pellets reached 77% of BHET after 36 h, green pellets only led to 44% of BHET after 74 h. Most colorants involved in the synthesis of coloured PET bottles are acidic compounds, thus, when depolymerising these additives could lead to catalyst inhibition. This hypothesis is based on the much lower catalytic activity of MSA or TBD:MSA (1:3) in the depolymerisation of PET as acidic media seem to promote longer reaction time and lower BHET conversions. However, applying the same procedure than for reactions with colourless PET pellets (i.e. crystallisation of BHET in water), the isolated BHET (yield = 75% for the blue bottle pellets and 38% for the green bottle pellets) did not show any colouration, confirming the negligible presence of pigments in the final BHET product.

4 Polymerisation of BHET

In order to create a simple process for the chemical recycling of PET, it is of great interest to extend this catalyst's platform from the depolymerisation to the polymerisation *via* typical polyesterification. In order to close the PET-to-PET cycle in a circular economy approach, the polymerisation of BHET was investigated using TBD:MSA (1:1) as catalyst. (Fig. 2.6A)

Considering the high thermal stability of the TBD:MSA (1:1) catalyst, we performed the self-condensation of BHET at 250-270 °C for 1 h under nitrogen atmosphere before applying vacuum for a further 4 h. The final polymer was analysed by ¹H NMR spectroscopy and DSC and compared with a PET obtained in the laboratory with the commonly-used catalyst (titanium butoxide) and monomers (ethylene glycol and DMT). Polymerisation was confirmed with ¹H NMR spectroscopy by evaluating the disappearance of BHET-CH₂ protons at $\delta = 4.7$ ppm and $\delta = 4.3$ ppm and the concomitant appearance of protons assigned to PET at $\delta = 4.8$ ppm. (Fig. 2.6B)

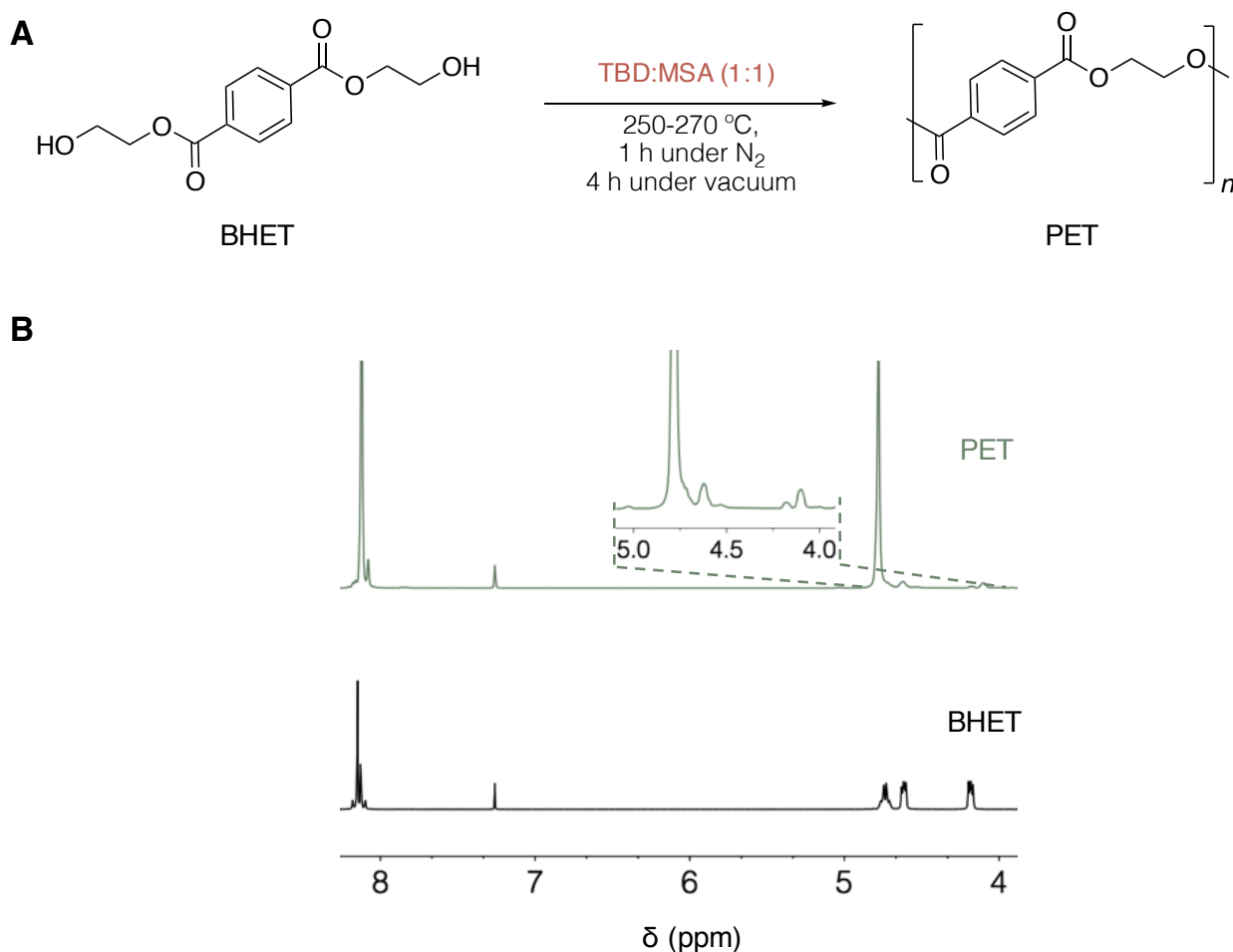


Figure 2.6. (A) Polymerisation of BHET into PET using TBD:MSA (1:1) and (B) stacked ^1H NMR spectra of PET synthesised from recycled BHET (green) and commercial PET (black). (CDCl_3 :TFA (7:1), 400 MHz, 298 K).

To further confirm the formation of PET, the molecular weight was analysed by ^1H NMR spectroscopy using the 2-hydroxyethyl end-group protons at $\delta = 4.62$ and 4.18 ppm.⁴⁶ In both cases M_n values around 12 kDa were obtained. A TGA of the PET synthesised from BHET was performed and compared with the TGA of the commercial PET employed for the depolymerisations described in this chapter. Both thermograms are really similar – $T_{50\%} = 433$ °C for PET from BHET and $T_{50\%} = 438$ °C for commercial PET. This slight difference can be explained by a small weight loss – 3% – occurring at around 260 °C and corresponding to the degradation of residual BHET. (**Fig. 2.7**)

Finally, DSC analysis confirmed that the thermal isotherm of the obtained PET is similar to the virgin-like PET, showing a thermal glass transition at around 60 °C, cold crystallisation at 150 °C, and a melting transition at around 230 °C. With these results, the cycle was closed. Using the same catalyst, but under

02. PET depolymerisation

different conditions, it is possible to polymerise a high quality PET from a monomer obtained from the depolymerisation of PET wastes. (Fig. 2.8)

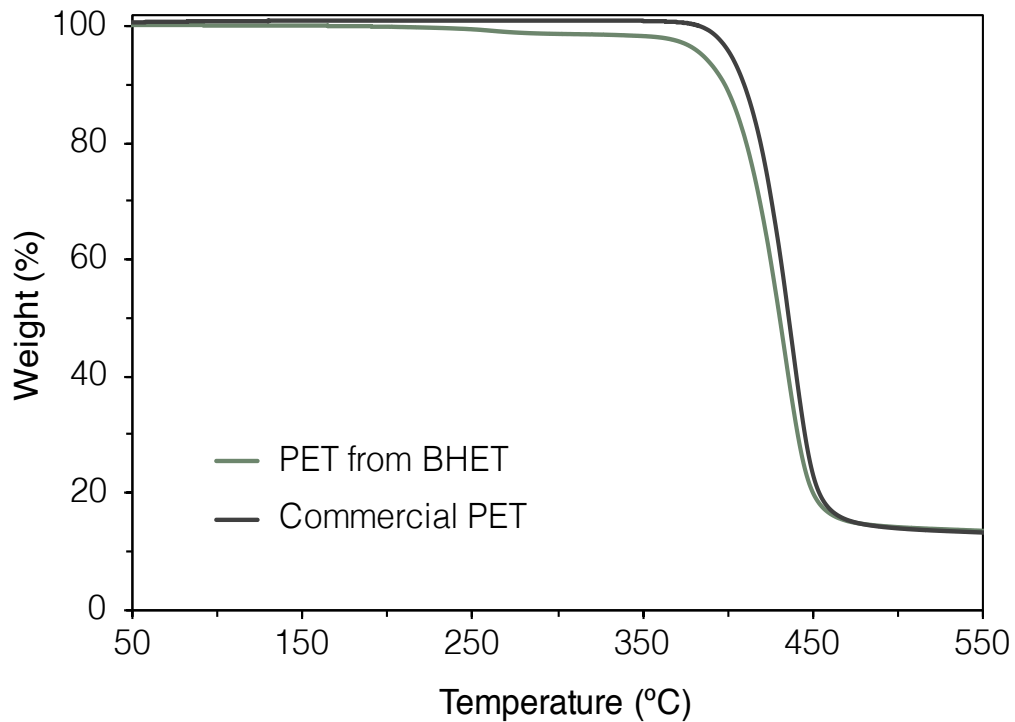


Figure 2.7. TGA analysis of PET synthesised from BHET and commercial PET.

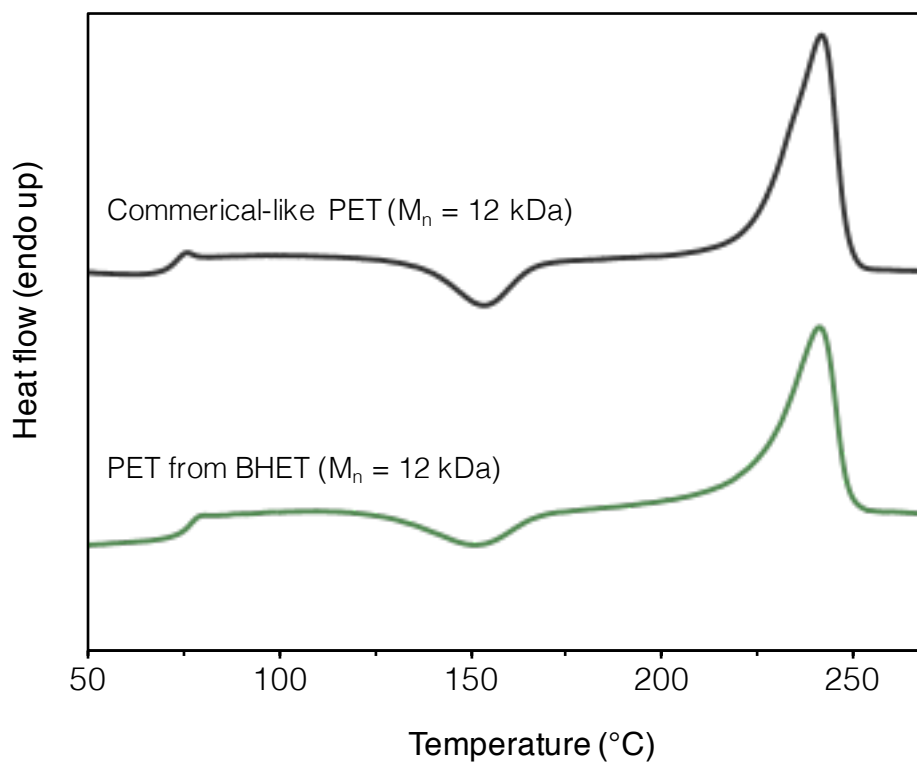


Figure 2.8. DSC of PET synthesised from BHET and comparison with a commercial-like PET of the same molecular weight.

5 Quantum chemical modelling

To gain insight the understanding of the catalytic activity of the TBD:MSA (1:1) protic ionic salt as catalyst, DFT calculations of PET glycolysis were carried out using the Gaussian 16 suite of programs⁴⁷ and using MN12SX functional⁴⁸ in conjunction with the 6-31+G(d,p) basis set for all atoms for geometric optimisation. To confirm that the optimised structures were minima on the potential energy surfaces, frequency calculations were carried out at the same level of theory and then used to evaluate the ZPVE and the thermal vibrational corrections at $T = 298$ K. The electronic energy was then refined by single-point energy calculations at the MN12SX/6-311++ G(2df,2p) level of theory. Methyl benzoate was used as a representative model of PET for the depolymerisation using ethylene glycol as reagent to yield one molecule of 2-hydroxyethyl benzoate and one molecule of methanol. (Fig. 2.9A)

The mechanism has been modelled in gas phase and in ethylene glycol (both geometry optimisation and single-point calculations) using the PCM solvent model⁴⁹⁻⁵¹ with the dielectric constant of ethylene glycol ($\epsilon = 40.245$), as glycolysis in this paper were performed in bulk. The reaction mechanism can be resolved into two transition states, the nucleophilic attack of one hydroxyl group of ethylene glycol on the carbonyl of methyl benzoate (TS 1) followed by the elimination of a molecule of methanol (TS 2). TS 1 is indubitably the rate-determining step with energetic barriers over 30 kcal.mol^{-1} for both pathways – in gas and in ethylene glycol – versus energetic barriers below 20 kcal.mol^{-1} for TS 2. (Fig. 2.9B)

Interestingly, for every TS optimised structures, the catalytic site appears to be located in between the protonated TBD and the deprotonated MSA. (Figs. 2.10A & 2.10B) For TS 1, the protonated TBD activates the carbonyl of methyl benzoate while the proton of one hydroxyl group of the ethylene glycol is abstracted by the deprotonated MSA, thus increasing the nucleophilicity of the ethylene glycol and facilitating the attack to the carbonyl to form a covalent bond between the carbonyl and the ethylene glycol. ($d = 1.62 \text{ \AA}$, Fig. 2.10A)

02. PET depolymerisation

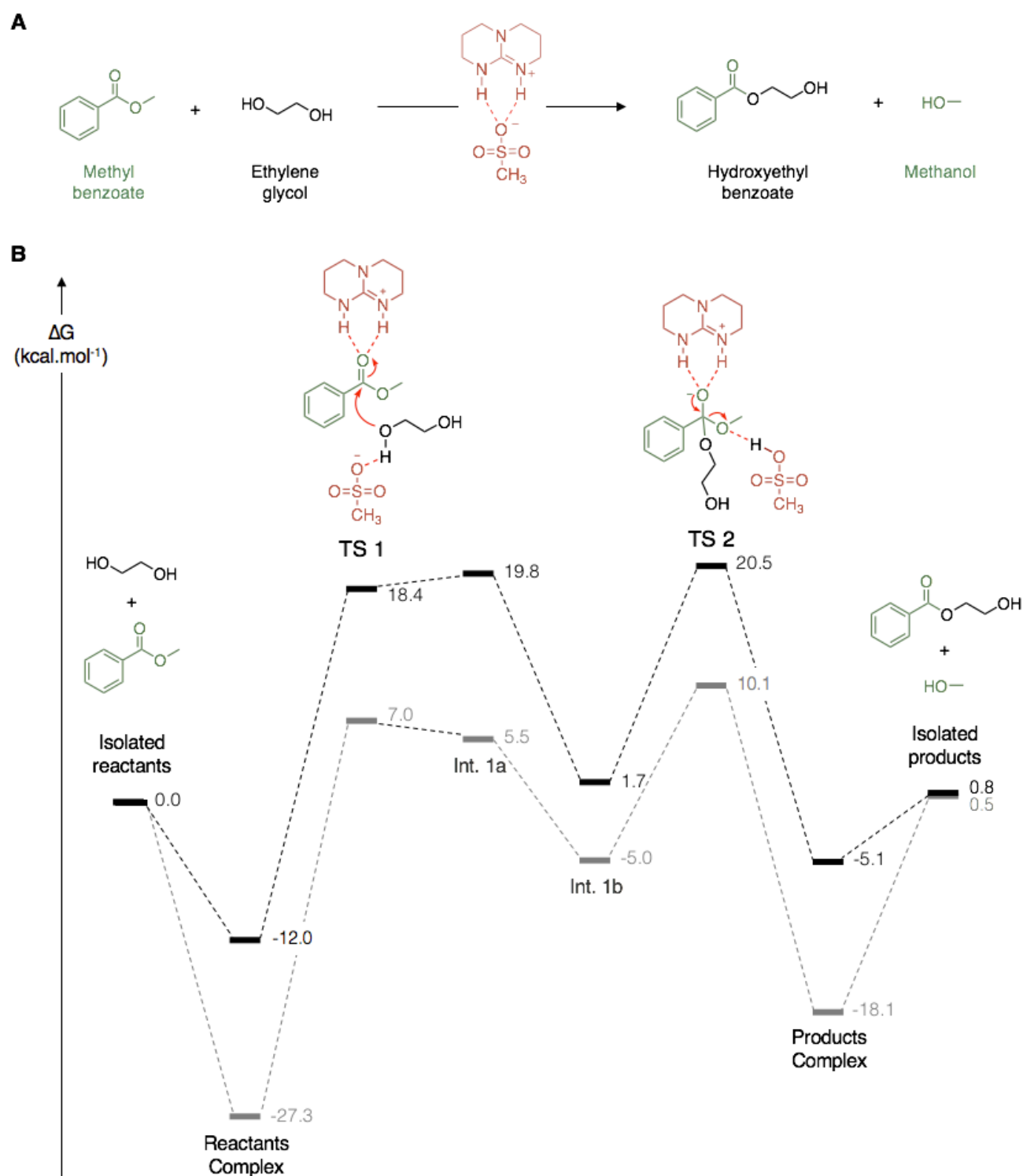


Figure 2.9. (A) Model reaction for the depolymerisation of PET using TBD:MSA (1:1) as catalyst and (B) DFT-computed reaction pathways for the depolymerisation reactions of PET in gas phase (in grey) and in ethylene glycol (in black).

In a very similar conformation, **TS 2** consists in the protonation of the hydroxy-methyl moiety of the methyl benzoate molecule by MSA resulting in the leaving of a molecule of methanol to reach a stable products complex.

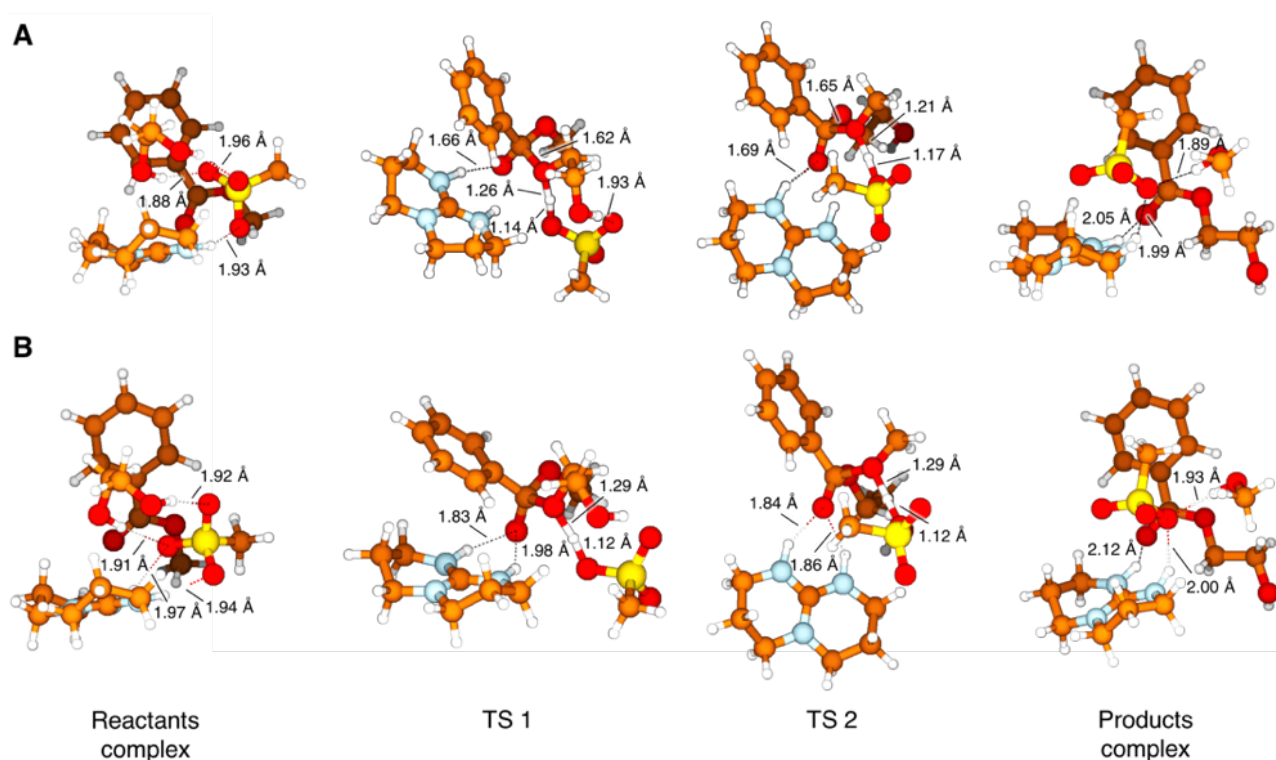


Figure 2.10. DFT-optimised transition states and complex structures for the depolymerisation of PET (A) in gas phase and (B) in ethylene glycol. Color code: orange, carbon; white, hydrogen; red, oxygen; blue, nitrogen; yellow, sulfur.

The overall pathway in gas phase is lower in energy but the energetic barrier for the rate-determining step (TS 1) is slightly higher (30.7 kcal.mol⁻¹ in ethylene glycol against 34.3 kcal.mol⁻¹ in gas). The high energetic barrier observed for the rate-determining step (TS 1) corroborates the experimental data, demonstrating the necessity of high contents of catalyst and high temperatures to complete the depolymerisation of PET and reach high BHET yields in a decent time.

Conclusion

We have demonstrated that the TBD:MSA (1:1) mixture is a very stable protic ionic complex able to catalyse PET glycolysis in less than 2 h. Under optimised conditions, over 90% of BHET were obtained in a solvent-free reaction and easily recovered by crystallisation in water. (Fig. 2.11) Both the reagent, used in excess, and the catalyst are easily recyclable, demonstrating same catalytic activity, even after 6 reactions. In order to close the loop, it was possible to employ this catalyst for the self-condensation of BHET in order to obtain new

02. PET depolymerisation

PET exhibiting good thermal and physical properties, similar to the virgin PET. Owing to the recyclability of the chemicals employed, easy techniques used and sustainability of the protocols, the entire process could be considered for industrial perspectives.

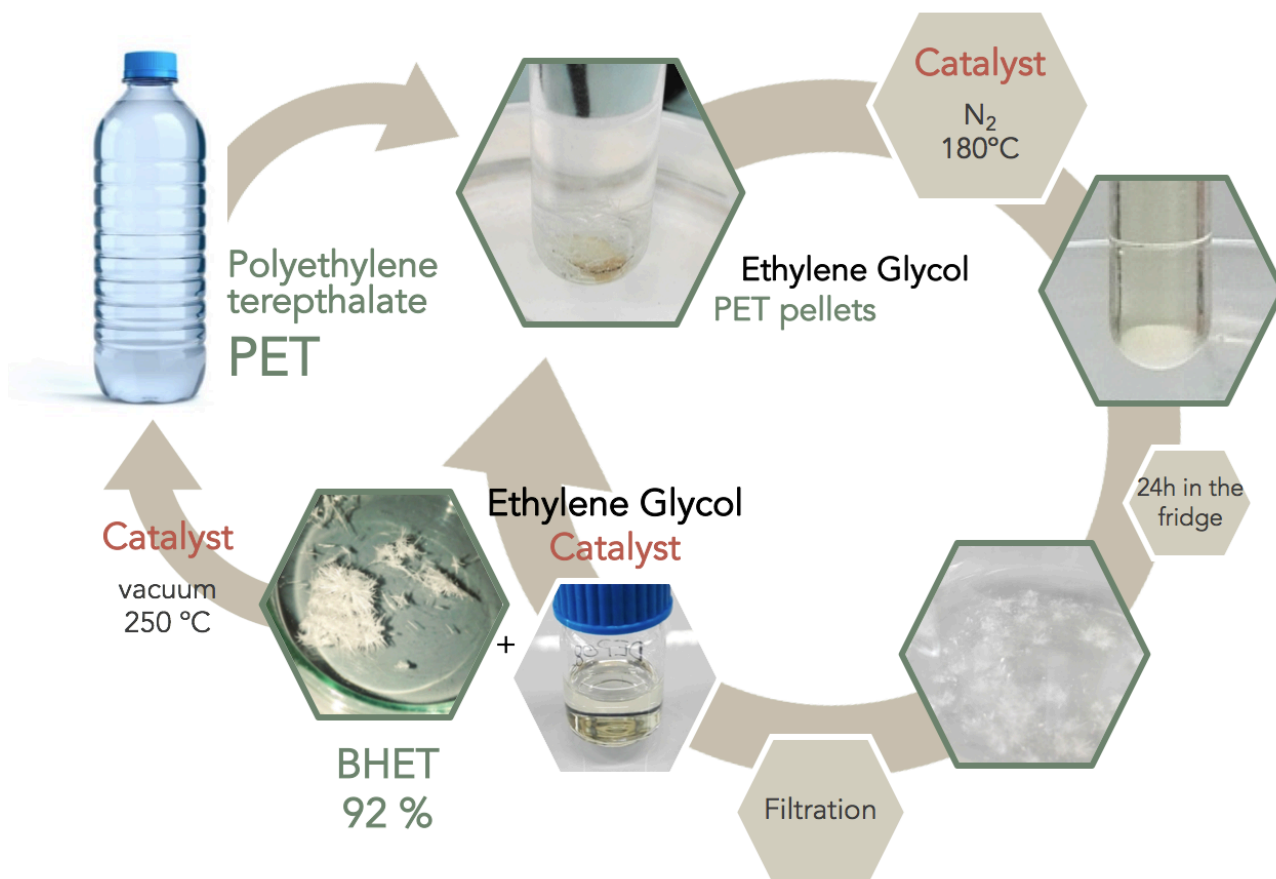


Figure 2.11. Closed-loop recycling of PET in a solvent-free procedure using a recyclable protic ionic salt, TBD:MSA (1:1) as catalyst.

Additionally, because of its large production and better collection system compared to other plastic wastes, PET is one of the most studied polymer for chemical recycling, thus new techniques and in particular the use of organocatalysts have been often tested first on PET before applying them on other type of polymers.⁵²⁻⁵⁴ Hence, designing such sustainable chemical recycling technologies for PET also impact the cyclic production of other polymers as the same procedure could be extended to other commodity polymers families.

References

- 1 W. T. S. Huck, *Nature*, 2011, **472**, 425–426.
- 2 S. M. Al-Salem, P. Lettieri and J. Baeyens, *Waste Manag.*, 2009, **29**, 2625–2643.
- 3 M. D. Schoenmakere, Y. Hoogeveen, J. Gillabel and S. Manshoven, *The circular economy and the bioeconomy - Partners in sustainability*, European Environmental Agency, 2018.
- 4 L. Bartolome, M. Imran, B. G. Cho, W. A. Al-Masry and D. H. Kim, Dr. Dimitris Achilias (Ed.), InTech., 2012.
- 5 *Modern Polyesters: Chemistry and Technology of Polyesters and Copolyesters*, New York, Scheirs, J.; Long, T.E., Eds., 2003.
- 6 H. Kurokawa, M. Ohshima, K. Sugiyama and H. Miura, *Polym. Degrad. Stab.*, 2003, **79**, 529–533.
- 7 F. Pardal and G. Tersac, *Polym. Degrad. Stab.*, 2006, **91**, 2567–2578.
- 8 R. Shamsi and G. M. M. Sadeghi, *RSC Adv.*, 2016, **6**, 38399–38415.
- 9 M. Kathalewar, N. Dhopatkar, B. Pacharane, A. Sabnis, P. Raut and V. Bhave, *Prog. Org. Coat.*, 2013, **76**, 147–156.
- 10 V. Jamdar, M. Kathalewar and A. Sabnis, *J. Coat. Technol. Res.*, 2018, **15**, 259–270.
- 11 T. Yoshioka, T. Sato and A. Okuwaki, *J. Appl. Polym. Sci.*, 1994, **52**, 1353–1355.
- 12 W. P. R. Deleu, I. Stassen, D. Jonckheere, R. Ameloot and D. E. D. Vos, *J. Mater. Chem. A*, 2016, **4**, 9519–9525.
- 13 A. Aguado, L. Martínez, L. Becerra, M. Arieta-araunabeña, S. Arnaiz, A. Asueta and I. Robertson, *J. Mater. Cycles Waste Manag.*, 2013, **16**, 201–210.
- 14 J.-W. Chen and L.-W. Chen, *J. Appl. Polym. Sci.*, 1999, **73**, 35–40.
- 15 G. Xi, M. Lu and C. Sun, *Polym. Degrad. Stab.*, 2005, **87**, 117–120.
- 16 M. Zhu, S. Li, Z. Li, X. Lu and S. Zhang, *Chem. Eng. J.*, 2012, **185–186**, 168–177.
- 17 X. Zhou, X. Lu, Q. Wang, M. Zhu and Z. Li, *Pure Appl. Chem.*, 2012, **84**, 789–801.
- 18 X. Zhou, C. Fang, Q. Yu, R. Yang, L. Xie, Y. Cheng and Y. Li, *Int. J. Adhes. Adhes.*, 2017, **74**, 49–56.

- 19 K. Fukushima, J. M. Lecuyer, D. S. Wei, H. W. Horn, G. O. Jones, H. A. Al-Megren, A. M. Alabdulrahman, F. D. Alsewilem, M. A. McNeil, J. E. Rice and J. L. Hedrick, *Polym. Chem.*, 2013, **4**, 1610–1616.
- 20 E. Bulak and I. Acar, *Polym. Eng. Sci.*, 2014, **54**, 2272–2281.
- 21 R. V. Shah, V. S. Borude and S. R. Shukla, *J. Appl. Polym. Sci.*, 2013, **127**, 323–328.
- 22 M. Teotia, N. Tarannum and R. K. Soni, *J. Appl. Polym. Sci.*, 2017, n/a–n/a.
- 23 J. Natarajan, G. Madras and K. Chatterjee, *ACS Appl. Mater. Interfaces*, 2017, **9**, 28281–28297.
- 24 Y. Chujo, H. Kobayashi and Y. Yamashita, *J. Polym. Sci. Part A: Polym. Chem.*, 1989, **27**, 2007–2014.
- 25 Y. Yang, Y. Lu, H. Xiang, Y. Xu and Y. Li, *Polym. Degrad. Stab.*, 2002, **75**, 185–191.
- 26 C.-H. Chen, C.-Y. Chen, Y.-W. Lo, C.-F. Mao and W.-T. Liao, *J. Appl. Polym. Sci.*, 2001, **80**, 943–948.
- 27 R. López-Fonseca, I. Duque-Ingunza, B. de Rivas, S. Arnaiz and J. I. Gutiérrez-Ortiz, *Polym. Degrad. Stab.*, 2010, **95**, 1022–1028.
- 28 U. R. Vaidya and V. M. Nadkarni, *Ind. Eng. Chem. Res.*, 1987, **26**, 194–198.
- 29 K. Troev, G. Grancharov, R. Tsevi and I. Gitsov, *J. Appl. Polym. Sci.*, 2003, **90**, 1148–1152.
- 30 I. Muhammad, G. L. Kyoung, I. Qasim, K. Bo-kyung, H. Myungwan, G. C. Bong and H. K. Do, *J. Nanosci. Nanotechnol.*, 2011, **11**, 824–828.
- 31 Z. Guo, K. Lindqvist and H. de la Motte, *J. Appl. Polym. Sci.*, 2018, **135**, 46285.
- 32 Q. F. Yue, C. X. Wang, L. N. Zhang, Y. Ni and Y. X. Jin, *Polym. Degrad. Stab.*, 2011, **96**, 399–403.
- 33 A. M. Al-Sabagh, F. Z. Yehia, A.-M. M. F. Eissa, M. E. Moustafa, G. Eshaq, A.-R. M. Rabie and A. E. ElMetwally, *Ind. Eng. Chem. Res.*, 2014, **53**, 18443–18451.
- 34 F. Scé, I. Cano, C. Martin, G. Beobide, Ó. Castillo and I. de Pedro, *New J. Chem.*, 2019, **43**, 3476–3485.
- 35 Q. Wang, X. Yao, Y. Geng, Q. Zhou, X. Lu and S. Zhang, *Green Chem.*, 2015, **17**, 2473–2479.

- 36 L. Zhou, X. Lu, Z. Ju, B. Liu, H. Yao, J. Xu, Q. Zhou, Y. Hu and S. Zhang, *Green Chem.*, 2019, **21**, 897–906.
- 37 B. Liu, W. Fu, X. Lu, Q. Zhou and S. Zhang, *ACS Sustain. Chem. Eng.*, 2019, **7**, 3292–3300.
- 38 Q. Wang, X. Yao, S. Tang, X. Lu, X. Zhang and S. Zhang, *Green Chem.*, 2012, **14**, 2559–2566.
- 39 Y. Hongmei, M. Yongshuai, Z. Weilu and Z. Dong, *Adv. Mater. Res.*, 2012, **550**, 280–283.
- 40 K. Fukushima, D. J. Coady, G. O. Jones, H. A. Almegren, A. M. Alabulrahman, F. D. Alsewailam, H. W. Horn, J. E. Rice and J. L. Hedrick, *J. Polym. Sci. Part A: Polym. Chem.*, 2013, **51**, 1606–1611.
- 41 S. Nica, A. Hanganu, A. Tanase, M. Duldner, S. Iancu, C. Draghici, P. I. Filip and E. Bartha, *Rev. Chim.*, 2015, **66**, 1105.
- 42 K. Fukushima, O. Coulembier, J. M. Lecuyer, H. A. Almegren, A. M. Alabulrahman, F. D. Alsewailam, M. A. Mcneil, P. Dubois, R. M. Waymouth, H. W. Horn, J. E. Rice and J. L. Hedrick, *J. Polym. Sci. Part A: Polym. Chem.*, 2011, **49**, 1273–1281.
- 43 L. Mezzasalma, A. P. Dove and O. Coulembier, *Eur. Polym. J.*, 2017, **95**, 628–634.
- 44 R. López-Fonseca, I. Duque-Ingunza, B. de Rivas, L. Flores-Giraldo and J. I. Gutiérrez-Ortiz, *Chem. Eng. J.*, 2011, **168**, 312–320.
- 45 Asakawa, T. Purification of Bishydroxyalkyl Terephthalate. Japanese patent 2000159729 (A), 2000.
- 46 A. Martínez de Ilarduya and S. Muñoz-Guerra, *Macromol. Chem. Phys.*, 2014, **215**, 2138–2160.
- 47 M. J. Frisch, G. W. Trucks, H. B. Schlegel, G. E. Scuseria, M. A. Robb, J. R. Cheeseman, G. Scalmani, V. Barone, G. A. Petersson, H. Nakatsuji, X. Li, M. Caricato, A. V. Marenich, J. Bloino, B. G. Janesko, R. Gomperts, B. Mennucci, H. P. Hratchian, J. V. Ortiz, A. F. Izmaylov, J. L. Sonnenberg, D. Williams-Young, F. Ding, F. Lipparini, F. Egidi, J. Goings, B. Peng, A. Petrone, T. Henderson, D. Ranasinghe, V. G. Zakrzewski, J. Gao, N. Rega, G. Zheng, W. Liang, M. Hada, M. Ehara, K. Toyota, R. Fukuda, J. Hasegawa, M. Ishida, T. Nakajima, Y. Honda, O. Kitao, H. Nakai, T. Vreven, K. Throssell, J. A. Montgomery, Jr., J. E. Peralta, F. Ogliaro, M. J. Bearpark, J. J. Heyd, E. N. Brothers, K. N. Kudin, V. N. Staroverov, T. A. Keith, R. Kobayashi, J. Normand, K. Raghavachari, A. P. Rendell, J. C. Burant, S. S. Iyengar, J.

02. PET depolymerisation

- Tomasi, M. Cossi, J. M. Millam, M. Klene, C. Adamo, R. Cammi, J. W. Ochterski, R. L. Martin, K. Morokuma, O. Farkas, J. B. Foresman, and D. J. Fox, *Gaussian 16, Revision B.01*, Gaussian, Inc., Wallingford CT, 2016.
- 48 R. Peverati and D. G. Truhlar, *Phys. Chem. Chem. Phys.*, 2012, **14**, 16187–16191.
- 49 M. Cossi, V. Barone, R. Cammi and J. Tomasi, *Chem. Phys. Lett.*, 1996, **255**, 327–335.
- 50 V. Barone, M. Cossi and J. Tomasi, *J. Chem. Phys.*, 1997, **107**, 3210–3221.
- 51 E. Cancès, B. Mennucci and J. Tomasi, *J. Chem. Phys.*, 1997, **107**, 3032–3041.
- 52 V. Sinha, M. R. Patel and J. V. Patel, *J. Polym. Environ.*, 2010, **18**, 8–25.
- 53 B. Geyer, G. Lorenz and A. Kandelbauer, *Express Polym. Lett.*, 2016, **10**, 559–586.
- 54 A. M. Al-Sabagh, F. Z. Yehia, Gh. Eshaq, A. M. Rabie and A. E. El Metwally, *Egypt. J. Pet.*, 2016, **25**, 53–64.

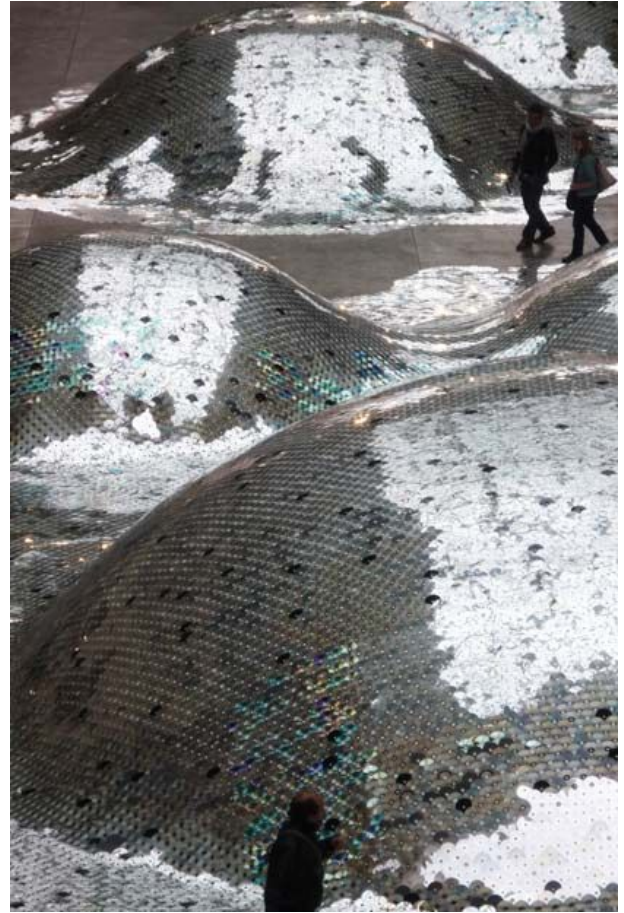
3

BPA-PC depolymerisation

Synthesis of innovative monomers for *upcycling*



Waste Landscape



Waste Landscape is a monumental art work that takes up the "Halle d'Aubervilliers" in Paris, in 2018. It is an artificial undulating landscape covered by 65,000 disposed CDs, which have been sorted and hand-sewn.

This sea of metallic dunes has been designed by an architect, **Clémence Eliard**, and an artist, **Elise Morin** to question the role of art towards alternative consumption modes.

Waste landscape is at the crossroad of contemporary art, landscaping and environmental concerns.

Introduction

Polycarbonates are thermoplastic polymers containing carbonate groups in their main chain. The main advantage of this family of polymers is that their adequate balance of features, such as thermal resistance, excellent mechanical properties, and optical transparency, makes them suitable for both commodity and engineering plastics. BPA-PC is the most widely used polycarbonate with a world production exceeding 5 million tons in 2016.¹ Similar to PET, the chemical depolymerisation of BPA-PC into its starting monomer, BPA, has been performed using different reagents through hydrolysis,²⁻⁷ alcoholysis,⁸⁻¹² aminolysis^{13,14} and even hydrogenolysis.¹⁵ (Recycling – Fig. 3.1) However, the viability of scaling up such processes is complicated by (1) the relatively low economic interest of recycled compared to commercial BPA and (2) the low worldwide production of BPA-PC compared to other commodity polymers that would not make a BPA-PC recycling plant economically viable. But the recycling of BPA-PC also involves the releasing of a carbonyl group that could open the way to *upcycling* procedures.

In opposition to the *downcycling* frequently observed while mechanical recycling is employed for re-processing plastics, leading to poorest quality materials, *upcycling* methods involve the transformation of waste products into high-added value materials. It is an excellent way to inject profit in the recycling economy as discarded items with no other economic value than their possible energetic equivalent if incinerated, can be converted into sellable high-performance materials. Avoiding the loss of the carbonyl group presents a significant advantage towards retention of the value that can be derived from BPA-PC. Very recently, besides the recovery of BPA, the conversion into carbonyl derivatives (carbonates, carbamates, etc.) by means of using BPA-PC as carbonylating agent has been of specific interest. For instance, the methanolysis of BPA-PC allows the recovery of both BPA and DMC, an industrial solvent and methylating reagent.¹⁶⁻¹⁹ Other studies have reported

03. BPA-PC depolymerisation

the possible recovery of organic carbonates, but are mainly focused on low value-added carbonates, precursors or high temperature solvents for example.²⁰⁻²² On the contrary, the synthesis of functionalised 5-membered or even higher added-value 6-membered cyclic carbonates from discarded BPA-PC constitutes an *upcycling* methodology as they can be then polymerised into innovative materials for a large variety of applications that range from biomedicine to electrolytes for energy storage.²³⁻²⁶ (Upcycling – Fig. 3.1) Notably, their current synthesis involves the use of highly toxic reagents, such as phosgene and derivatives or carbon monoxide. More sustainable alternatives for the synthesis of such monomers reported the use of CO₂ coupled with diols or oxetanes, yet these reactions are generally limited by unfavourable equilibria, requiring high-performance catalysts together with high temperature and harsh pressure conditions to obtain average yields (40-60%).²⁷⁻²⁹ (Scheme 3.1) The potential to use discarded plastics as a resource to replace toxic reagents presents an opportunity to create an economically viable method combining cost benefits and waste reduction.

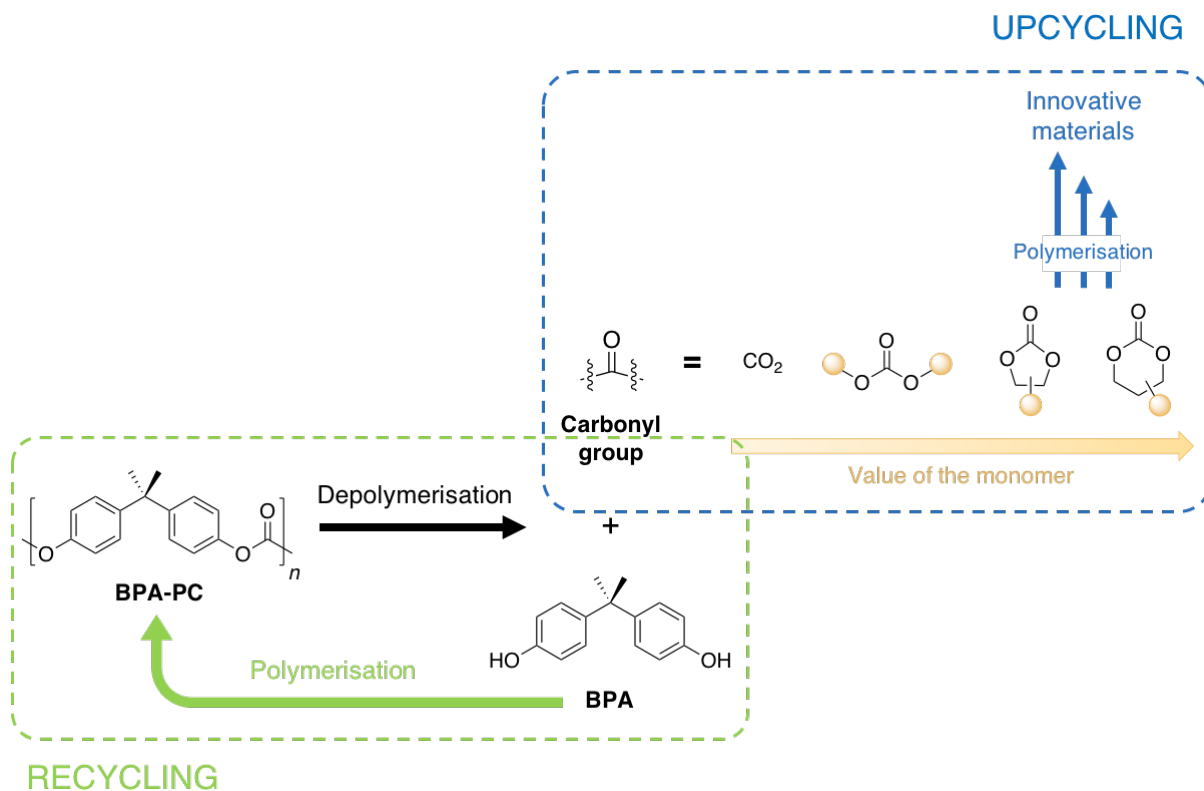
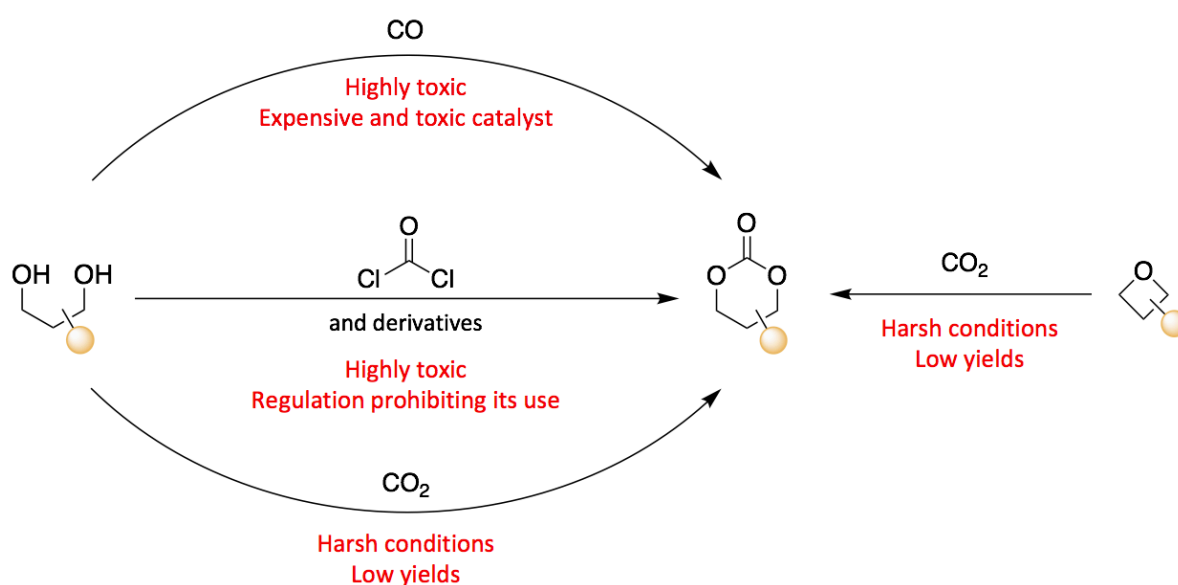


Figure 3.1. Difference between the recycling of BPA from BPA-PC and the *upcycling* of the carbonates obtained from the depolymerisation.

It has to be noticed also that BPA has been recently suspected to be a xenoestrogen.^{30–32} Thus, BPA-PC wastes could cause an additional issue when it is thrown in the environment as uncontrolled hydrolysis of the polymer entails the release of xenoestrogen compounds.

In this chapter the previously established organocatalytic methodology was applied to the depolymerisation of BPA-PC for the synthesis of economically attractive organic molecules. By carefully choosing the nucleophile and tuning the reaction conditions, a library of carbonyl-containing molecules have been synthesised, making BPA-PC an alternative, phosgene-free, source of carbonyl for the synthesis of high added value building blocks: linear ureas, dicyclic carbonates, 5- and 6-membered ring carbonates. DFT calculations have been performed to support the experimental data.



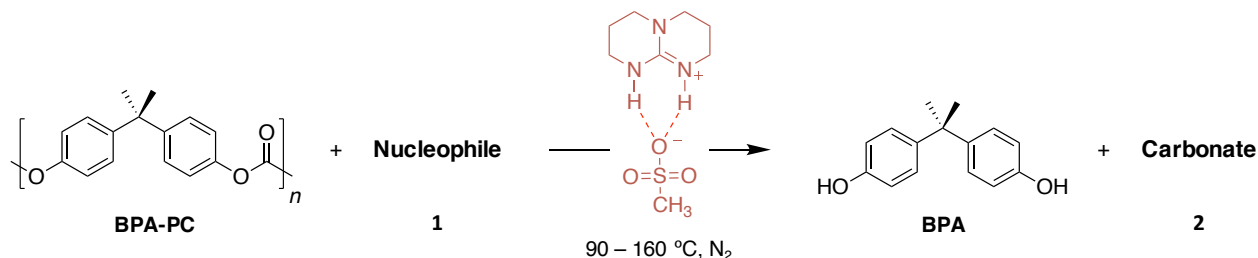
Scheme 3.1. Summary of the different existing pathways for the synthesis of 6-membered cyclic carbonates and their limitations.

1 Comparison between –OH, –NH₂ and –SH groups

To produce valuable monomers from the chemical recycling of commodity polymers, the selection of appropriate reagents is a major challenge. For the depolymerisation of BPA-PC, the transesterification resulting from the nucleophilic attack of a hydroxyl, amine or thiol functional group on the carbonate moiety of the polymer backbone leads to the formation of two

03. BPA-PC depolymerisation

distinct molecules, BPA and a carbonyl-containing molecule (**2**) carrying the same functionality present on the precursor. (Scheme 3.2) Especially, while using short length nucleophiles, the reaction leads to the formation of carbonyl-containing heterocycles.



Scheme 3.2. Depolymerisation of BPA-PC (2 g, 7.8 mmol, 1 eq.), using different nucleophiles with TBD:MSA (1:1) catalyst (0.256 g, 1.17 mmol, 0.15 eq.).

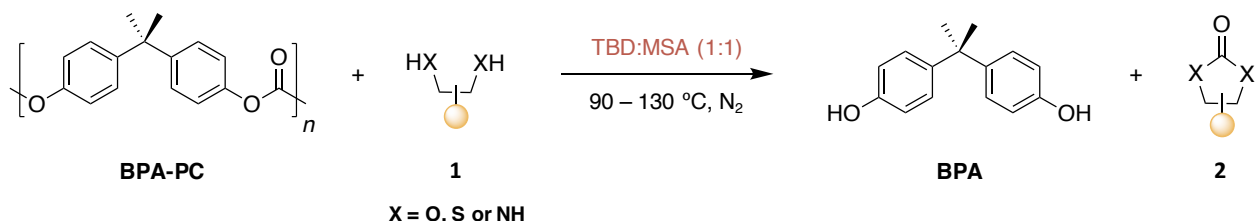
Different nucleophiles (**1**) were evaluated for the depolymerisation of BPA-PC using TBD:MSA (1:1), (0.15 eq.) as catalyst, in a solvent-free process with a temperature range from 90 to 160 °C. All experiments were conducted in bulk, until complete disappearance of residual BPA-PC pellets was observed.

1.1 Reactions with symmetric nucleophiles

In the light of the good results obtained in chapter 1 with 1,2-propanediol (**1a**), nucleophiles of the same length were investigated under the same conditions, employing 6 eq. of nucleophile, at 130 °C. Reactions were performed with ethylene glycol (**1b**), ethylene diamine (**1c**) and ethane-1,2-dithiol (**1d**) to screen the effect of the nucleophile nature on the depolymerisation process (Table 3.1). The depolymerisation of BPA-PC with **1c** was completed in less than five minutes to give BPA and imidazolidin-2-one (**2c**), while the reaction using **1d** was completed in 30 minutes and led to BPA and 1,3-dithiolan-2-one (**2d**). Both reactions were conducted at 90 °C, owing to the low boiling point of **1c** (118 °C) and the instability of **1c** at high temperatures – during preliminary reactions performed at 110 and 130 °C, the crude product rapidly turned dark and the ¹H NMR spectra exhibited a lot of non-assigned signals. When **1b** was used, the reaction proceeded more slowly, as depolymerisation required 5 h to be complete at 130 °C, providing the following order of reactivity: -NH₂ > -SH >> -OH. However, BPA raised

excellent conversion for all reactions (89 to 98%) while heterocyclic carbonates were also obtained with good to excellent conversions (83% for **2b**, 96% and 92% for **2c** and **2d** respectively).

Table 3.1. Depolymerisation of BPA-PC (2 g, 7.8 mmol, 1 eq.), using different nucleophiles (**1**) (46.8 mmol, 6 eq.) with TBD:MSA (1:1) catalyst (0.256 g, 1.17 mmol, 0.15 eq.) to yield 5-membered cyclic carbonyl-containing heterocycles (**2**).

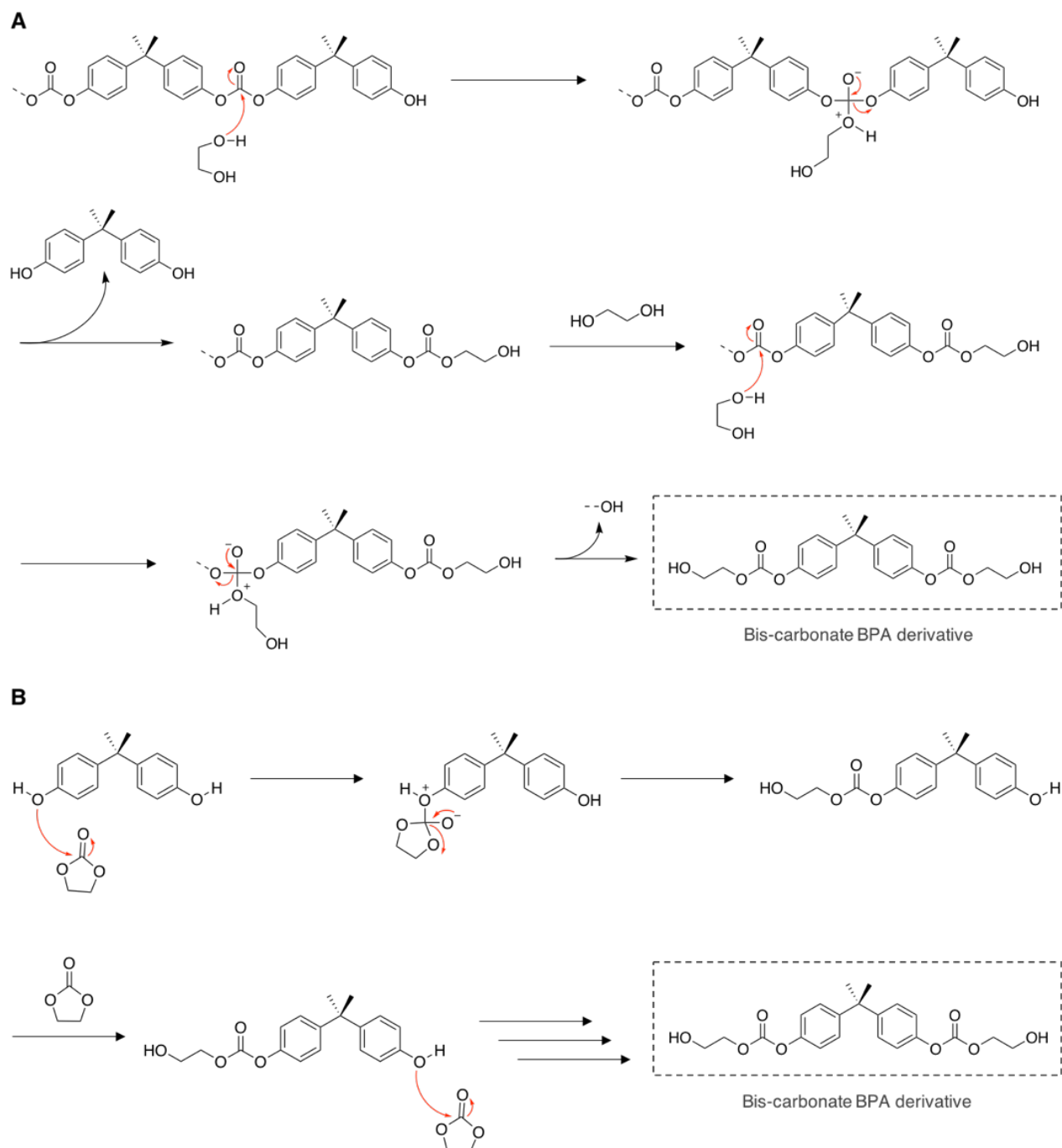


	Nucleophile (1)	Carbonate (2)	Conditions ^a	BPA (%) ^b	2 (%) ^b
a			130 °C 3 h 6 eq.	98 (86)	90 (87)
b			130 °C 5 h 6 eq.	89 (82)	83 (78)
c			90 °C 5 min 6 eq.	90 (86)	96 (92)
d			90 °C 30 min 6 eq.	96 (87)	92 (87)

^a Reaction temperature, depolymerisation duration and amount of reagent used for the depolymerisation. ^b Conversion was determined by ¹H NMR spectroscopy in DMSO-*d*₆ from the crude product using the catalyst as internal standard ($\delta = 1.87$ ppm) and characteristic peaks of BPA and the carbonate. Yields in parenthesis are isolated products. (Fig. S3.1 to S3.16)

Notably, the depolymerisation with ethylene glycol (**1b**) resulted in the observation of additional signals in the ¹H NMR spectrum ($\delta = 6.82 - 7.07$ ppm, ~8%) that correspond to a bis-carbonate derivative of BPA with ethylene glycol attached through a carbonate linkage. This is most likely formed from either the incomplete cyclisation that results in the linear carbonate (**Scheme**

3.3A) or through ring-opening of the *in situ*-formed cyclic carbonate (2b) by BPA (Scheme 3.3B).



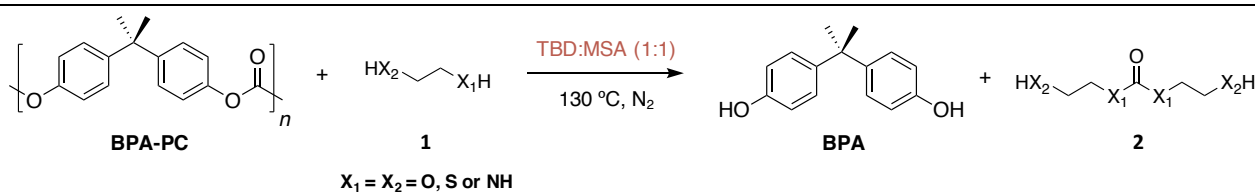
Scheme 3.3. (A) Formation of side-product through non-cyclisation after the nucleophilic attack of ethylene glycol. (B) Formation of side-product through the ring-opening of the formed carbonate by BPA.

1.2 Reactions with asymmetric nucleophiles

Asymmetric nucleophiles involving two different moieties above $-OH$, $-NH_2$ and $-SH$, such as ethanolamine (1e), mercaptoethanol (1f) or cysteamine (1g) were also investigated for the depolymerisation of BPA-PC. Similar to previous

reactions, depolymerisations were performed using 6 eq. of reagent at 130 °C. If all reactions were completed in a reasonable time, reaching a BPA conversion above 94%, products here are not cyclic. Unlike their symmetric analogous, linear carbonyl-containing molecules, **2e**, **2f** and **2g** were synthesised, accordingly to the relative functional group reactivity's previously determined. (Table 3.2)

Table 3.2. Depolymerisation of BPA-PC (2 g, 7.8 mmol, 1 eq.), using different asymmetric nucleophiles (**1**) (46.8 mmol, 6 eq.) with TBD:MSA (1:1) catalyst (0.256 g, 1.17 mmol, 0.15 eq.) to yield linear carbonyl-containing molecules (**2**).



	Nucleophile (1)	Carbonate (2)	Conditions ^a	BPA (%) ^b	2 (%) ^b
e			130 °C 30 min 6 eq.	94 (86)	93 (88)
f			130 °C 2 h 6 eq.	95	23
g			130 °C 5 min 6 eq.	97	57

^a Reaction temperature, depolymerisation duration and amount of reagent used for the depolymerisation. ^b Conversion was determined by ¹H NMR spectroscopy in DMSO-*d*₆ from the crude product using the catalyst as internal standard ($\delta = 1.87$ ppm) and characteristic peaks of BPA and the carbonate, according to literature.³³ Yields in parenthesis are isolated products. (Fig. S3.17 to S3.20)

Indeed, while the reaction provided the urea employing **1e** and **1g** because of the higher reactivity of the amine, the reaction with **1f** preferentially reacts on the thiol functionality to reach **2f**, owing to the higher reactivity of -SH compared to -OH. **1e** has led to the hydroxyl-terminated urea **2e** with excellent conversion (93%) and very good isolated yield (88%) while both **1f**

03. BPA-PC depolymerisation

and **1g** gave lower conversions, 23% and 57%, respectively.³³ Although the reaction using **1f** was completed in a reasonable time, the reaction mixture rapidly turned brown, maybe because of the degradation of the starting material or the product, which could explain the low conversion into **2f**. The depolymerisation of BPA-PC using **1g** reached a reasonable yield of the thio-terminated urea **2g** in less than 5 min.

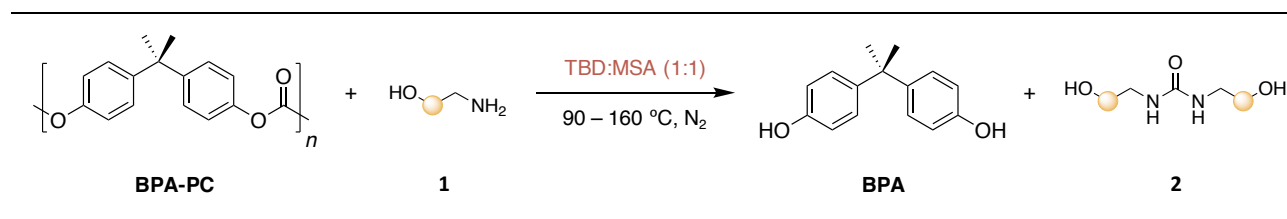
The formation and easy isolation of **2e** specifically is interesting as subsequent polycondensation of such products could result in an easy route to synthesise polyurea. Thus, other amino-alcohols were employed as nucleophile for the depolymerisation of BPA-PC.

1.3 Further investigations on amino-alcohols

Identical to the reaction employing **1e**, the depolymerisations of BPA-PC with other amino-alcohols reached completion in around 30 min. Reactions were also performed using 6 eq. of reagent at 130 °C – the reaction temperature was increased to 160 °C for the reaction with **1i** because of the high viscosity of the reagent. Very good conversion into BPA (91 to 95%) were afforded for the three reactions, employing 3-aminopropan-1-ol (**1h**), 3-aminopropane-1,2-diol (**1i**) and 2-(2-aminoethoxy)ethan-1-ol (**1j**) as well as very good conversions into the corresponding ureas **2h**, **2i** and **2j** – 92, 86 and 88%, respectively. (Table 3.3)

These examples demonstrated the possibilities for the present procedure to convert BPA-PC into linear hydroxyl-terminated ureas.

Table 3.3. Depolymerisation of BPA-PC (2 g, 7.8 mmol, 1 eq.), using different amino-alcohols (**1**) (46.8 mmol, 6 eq.) with TBD:MSA (1:1) catalyst (0.256 g, 1.17 mmol, 0.15 eq.) to yield hydroxyl-terminated ureas (**2**).



	Nucleophile (1)	Carbonate (2)	Conditions ^a	BPA (%) ^b	2 (%) ^b
h			130 °C 30 min 6 eq.	94 (85)	92 (89)
i			160 °C 30 min 6 eq.	95 (86)	86 (81)
j			130 °C 30 min 6 eq.	91	88

^a Reaction temperature, depolymerisation duration and amount of reagent used for the depolymerisation. ^b Conversion was determined by ¹H NMR spectroscopy in DMSO-*d*₆ from the crude product using the catalyst as internal standard ($\delta = 1.87$ ppm) and characteristic peaks of BPA and the carbonate, according to literature.³³ Yields in parenthesis are isolated products. (Fig. S3.21 to S3.25)

2 Renewable feedstock as nucleophiles

2.1 Screening of bio-based feedstocks

Following the goal of synthesising high-added value cyclic carbonates in a sustainable way, different diols – or tetraol – were used as nucleophiles for the depolymerisation of BPA-PC, particularly glycerol (**1h**), meso-erythritol (**1i**) and a derivative of glycerol, α,α' -diglycerol (**1m**), which are all excellent examples of bio-based, sustainable feedstocks. (Table 3.4) On one hand, glycerol is a widely available by-product of the biodiesel and chemical industries^{34–36} and the corresponding cyclic carbonate, glycerol carbonate, is a versatile building block largely investigated for organic chemistry.^{37,38} On the other hand, erythritol is an alternative to sugar for the food industry and is largely available in nature, it can be encountered in fruits, soya and fermented products.^{39–41} The reactions with these three nucleophiles led to full degradation of the BPA-PC pellets into BPA and the corresponding 5-membered cyclic carbonate – or dicyclic dicarbonate. Compared to the reaction using 1,2-propanediol (**1a**), the reaction with **1h** required an increased temperature (2 h at 160 °C) while

03. BPA-PC depolymerisation

the reaction with **1l** required an increased time (8 h at 130 °C) to reach a maximum yield of both BPA and the corresponding carbonates, **2h** and **2l**. Indeed, when the depolymerisation with **1h** was performed at 130 °C, no changes were observed in the reaction medium, even after 48 h. Similarly, the depolymerisation of BPA-PC using a tetraol derived from glycerol, α,α' -diglycerol (**1m**), yielded a dicyclic compound (**2m**) – 3 eq. of **1m** were employed instead of 6 eq. as the reagent is a tetraol, in order to carry out the depolymerisation with the same quantity of hydroxyl functions compared to other reagents. This depolymerisation was also highly temperature dependent, while no depolymerisation was observed at 130 °C for 48 h, the desired product was obtained in very good yield (87%) after 8 h at 160 °C. Further increase of the temperature to 190 °C shortened the depolymerisation to 30 min while slightly increasing the reaction yield (91%).

Table 3.4. Depolymerisation of BPA-PC (2 g, 7.8 mmol, 1 eq.), using different nucleophiles (**1**) (3 or 6 eq.) with TBD:MSA (1:1) catalyst (0.256 g, 1.17 mmol, 0.15 eq.) to yield 5-membered cyclic carbonates (**2**).

BPA-PC + **1** $\xrightarrow[90 - 130\text{ }^\circ\text{C, N}_2]{\text{TBD:MSA (1:1)}}$ **BPA** + **2**

X = O, S or NH

	Nucleophile (1)	Carbonate (2)	Conditions ^a	BPA (%) ^b	2 (%) ^b
k			160 °C 2 h 6 eq.	89 (81)	90 (86)
l			130 °C 8 h 6 eq.	98 (86)	74 (70)
m			160 °C 8 h 3 eq.	87 (83)	87 (84)

^a Reaction temperature, depolymerisation duration and amount of reagent used for the depolymerisation. ^b Conversion was determined by ¹H NMR spectroscopy in DMSO-*d*₆ from the

crude product using the catalyst as internal standard ($\delta = 1.87$ ppm) and characteristic peaks of BPA and the carbonate. Yields in parenthesis are isolated products. (Fig. S3.26 to S3.37)

2.2 Optimisation of the reaction using erythritol (1I)

The reaction employing **1I** yielded 74% of **2I** and additional signals in between 4 and 5.5 ppm in the ^1H NMR spectra reveals the formation of side-products. These side products more likely could be attributed to other cyclic carbonates considering their ^1H NMR handles. Then, in an attempt to increase the yield of the cyclic carbonate **2I**, reaction parameters were modified, particularly the quantity of reagent and the depolymerisation temperature. At 130 °C, using a limited amount of **1I** – 2 eq. – the conversion into carbonate severely decreased to 35%. While doubling the starting quantity of **1I** – from 6 to 12 eq. – the conversion raised 71% in 7 h. Thus, no significant changes were observed compared to the reaction employing 6 eq. (74% in 8 h). (Fig. 3.2A)

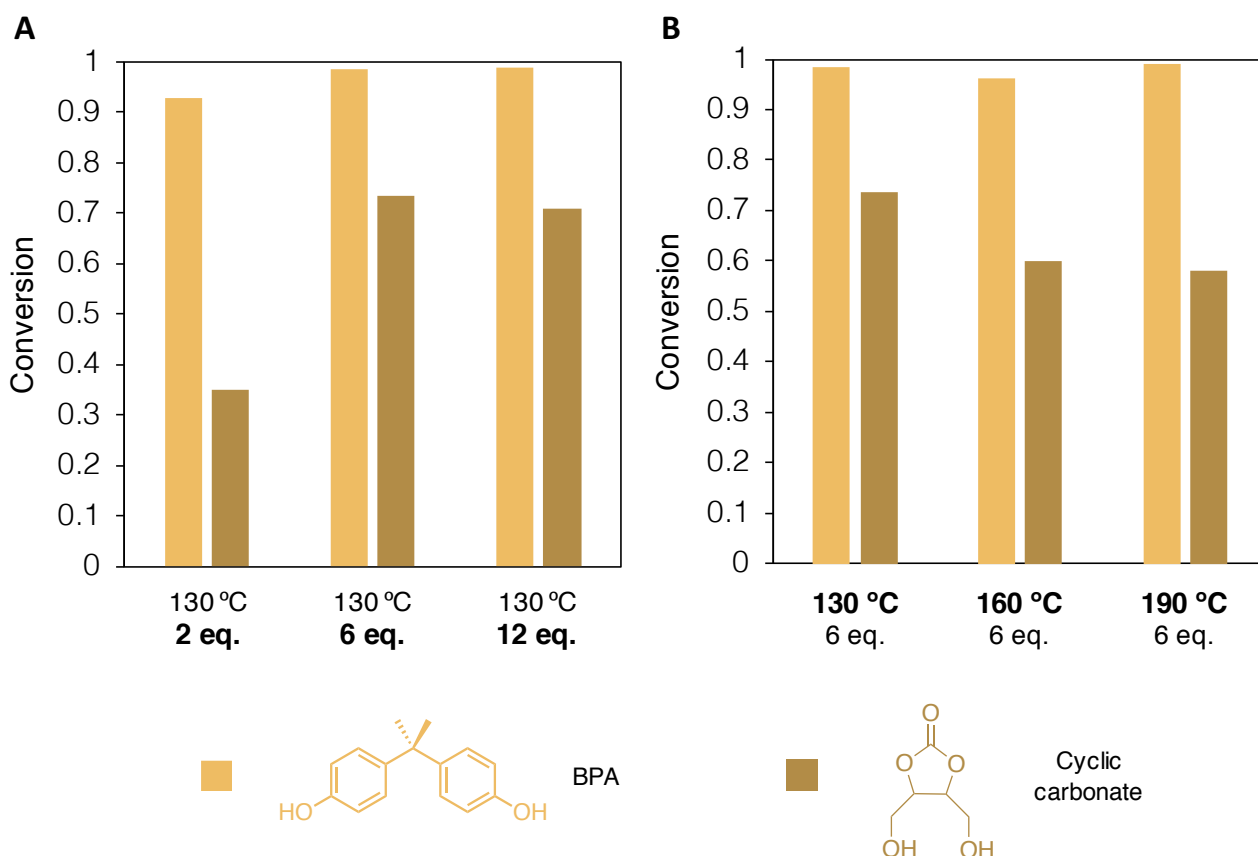


Figure 3.2. (A) using various content of **1I** reagent at 130 °C, (B) using different temperatures using 6 eq. of reagent. Conversion into BPA and carbonate were determined by ^1H NMR spectroscopy in $\text{DMSO}-d_6$ from the crude product using the catalyst as internal standard ($\delta = 1.87$ ppm) and characteristic signals, BPA at $\delta = 6.63$ ppm, **2I** at $\delta = 3.75$ ppm – Fig S3.38 & S3.39. Reactions conditions: BPA-PC (2 g, 7.8 mmol, 1 eq.) and TBD:MSA (1:1) (0.256 g, 1.17 mmol, 0.15 eq.).

03. BPA-PC depolymerisation

Different temperatures were also employed for the same reaction, with 6 eq. of reagent, and, although the depolymerisation time is substantially shortened while employing higher temperature, from 8 h at 130 °C to 45 min at 190 °C, better carbonate yields were achieved using lower temperatures. Thus, the conversion into the cyclic carbonate **2l**, increased while increasing the temperature, from 61% and 56 % at 160 and 190 °C, to 74% at 130°C. (**Fig. 3.2B**) After exploring different conditions, it was concluded that the initial conditions – 130°C and 6 eq. of reagent – were leading to a better overall conversion of **2l**.

2.3 Isolation of the cyclic carbonates

As expressed in the introduction of this chapter, the interest of such reactions is to employ the carbonyl-containing molecules obtained as monomers for the synthesis of high-added value materials. In this aim, the isolation and purification of both the carbonate and BPA is a key step.

2.3.1 General procedure

The isolation of the products from the starting nucleophile was a complicated step of the procedure as classical liquid-liquid extractions were inefficient because of (1) the close structures of starting nucleophile and targeted carbonate and (2) the affinity of BPA with the starting nucleophile. Thus, we decided to apply an original technique by adding subsequent equivalents of BPA-PC until complete consumption of the starting nucleophile, monitored by ¹H NMR spectroscopy, to afford a 100% atom economy procedure, a considerable advantage in terms of cost and sustainability. (**Fig. 3.3**)

This procedure allows the obtaining of only BPA and the carbonyl-containing molecule in the crude product. The separation was facilitated and liquid-liquid extraction or column chromatography were then used, depending on the starting reagent employed to separate the products. Carbonates were obtained highly pure in good to very good yields as well as BPA after crystallisation in hot water.

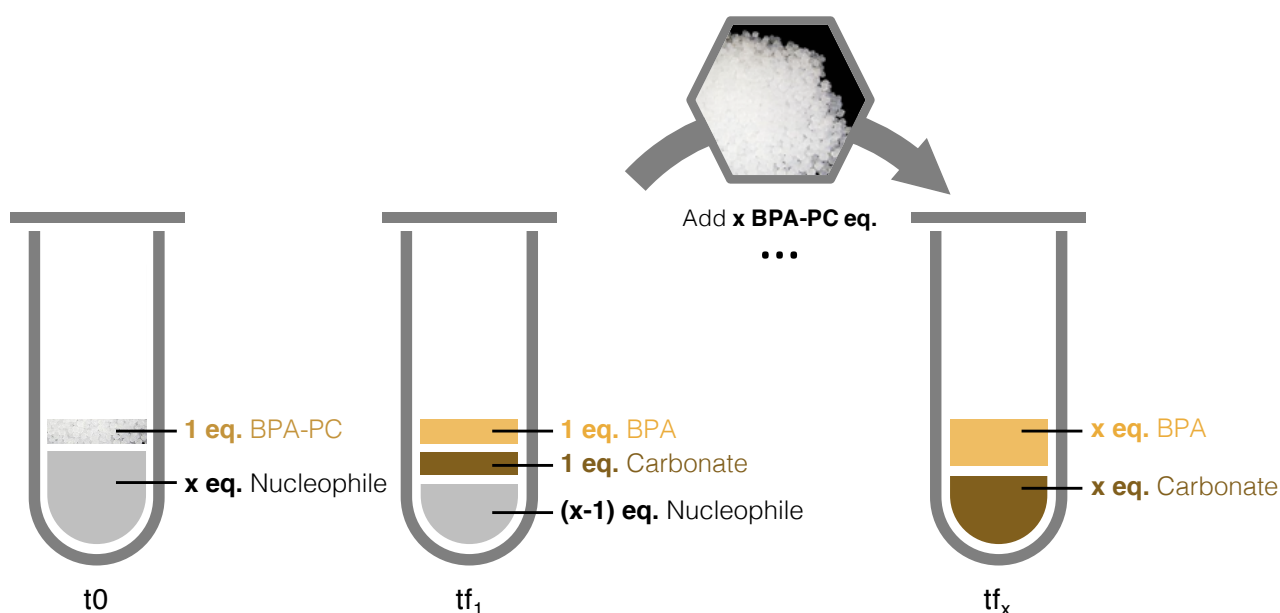


Figure 3.3. General procedure to facilitate the isolation of BPA and carbonate after the depolymerisation of BPA-PC by subsequent adding of polymer pellets.

2.3.2 Example of the diglycerol dicarbonate (**2m**)

In order to obtain the diglycerol dicarbonate **2m** in very good yield, the procedure described previously was applied to the depolymerisation of BPA-PC using **1m**. As previously noticed, performing the reaction at 190 °C instead of 160 °C allows to decrease the reaction time with no significant changes in the final conversion into carbonate. Thus, the reaction was performed at 190°C using 0.15 eq. of TBD:MSA (1:1) as catalyst and 1.5 eq. of the starting reagent α,α' -diglycerol. A ^1H NMR spectrum was performed at the complete disappearance of every BPA-PC eq. added – it should be noticed here that 1 eq. of BPA-PC is depolymerised using only 0.5 eq. of starting reagent as it is a tetraol, thus 3 eq. of BPA-PC needs to be successively added to consume the 1.5 eq. of **1m** initially used.

The first depolymerisation reached conversions into BPA and **2m** of 91 and 92%, respectively, after 30 min. After the addition of the second eq. of BPA-PC, the depolymerisation reached 95 and 87%, respectively, in less than 40 min. Finally, the addition of the last eq. of BPA-PC led to final conversions of 94 and 83%, after 40 min. After isolation through flash column chromatography, **2m** was obtained pure (76%) while re-crystallisation in hot water allowed the recovery of BPA (84%). (Fig. 3.4)

03. BPA-PC depolymerisation

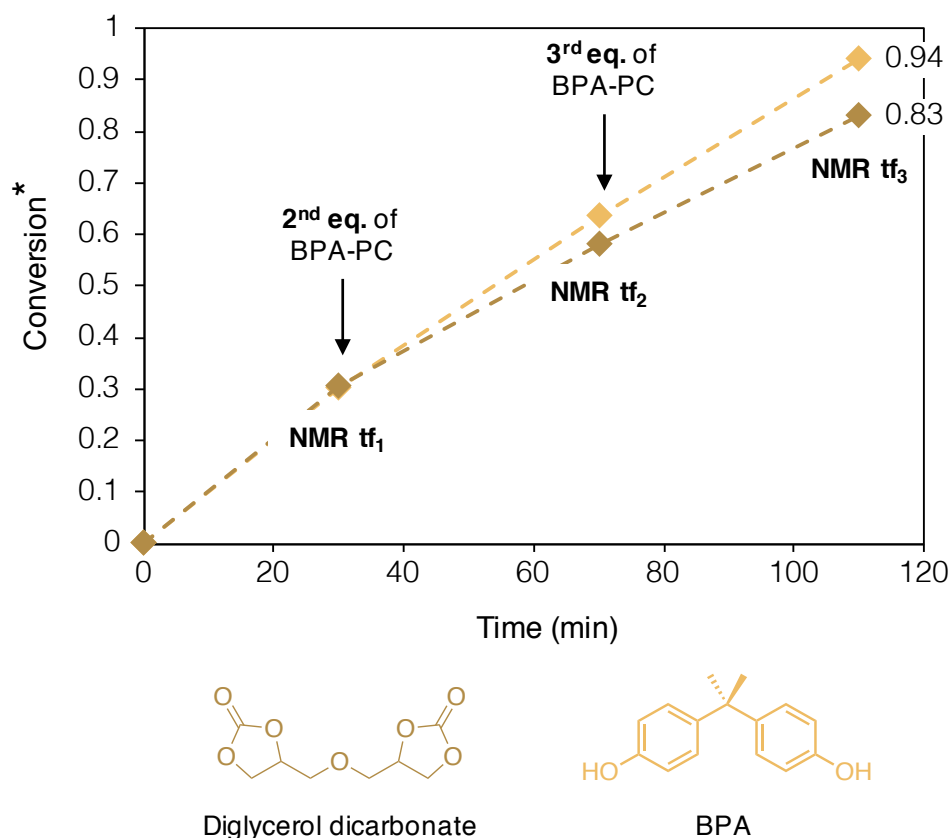


Figure 3.4. Conversion into BPA and diglycerol dicarbonate (**2m**) versus time for the depolymerisation of BPA-PC (2 g, 7.8 mmol, 1 eq. – x3) with **1m** (1.90 g, 11.7 mmol, 1.5 eq.) and TBD:MSA (1:1) (0.256 g, 1.17 mmol, 0.15 eq.). Conversion into BPA and **2m** were determined by ^1H NMR spectroscopy in $\text{DMSO-}d_6$ from the crude product using the catalyst as internal standard ($\delta = 1.87$ ppm) and characteristic signals, BPA at $\delta = 6.65$ ppm and **2m** at $\delta = 4.94$ ppm – Fig. S3.40. *Conversions were calculated regarding the final conversion of products – after addition of 3 eq. of BPA-PC.

The diglycerol dicarbonate (**2m**) has been recently studied for the synthesis of NIPUs, a non-toxic harmless alternative to the current industrial production of PU.^{42–44} But this dicarbonate is difficult to obtain in outstanding yields without the use of phosgene derivatives.^{43–45} Thus, the methodology presented here presents tremendous advantages as it allows the recovery of BPA and the diglycerol dicarbonate in good yields through a 100% atom economy procedure.

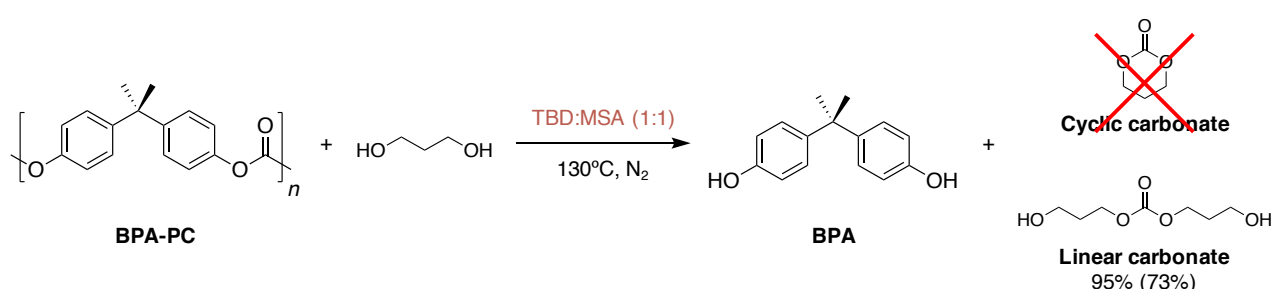
3 Synthesis of valuable 6-membered cyclic carbonates

To further explore the scope of nucleophiles that successfully depolymerise BPA-PC, diols with longer main chains were employed. Although the synthesis of 5-membered cyclic carbonates has been recently studied, the higher

reactivity of 6-membered cyclic carbonates towards ring-opening polymerisation makes them better candidates for the synthesis of materials suitable for high added-value applications such as medical devices or polymer electrolytes.^{46–48} Such monomers are, however, most commonly synthesised using phosgene or its substitutes, therefore greener alternatives such as generating the cyclic carbonate monomers from 1,3-diols and waste BPA-PC are of crucial interest.

3.1 The specific case of 1,3-propanediol

1,3-propanediol was investigated as nucleophile for the depolymerisation of BPA-PC but, notably, the reaction did not lead to the corresponding cyclic carbonate, TMC (**2n**), but to the linear analogous.⁴⁹ The Bis(3-hydroxypropyl) carbonate was indeed obtained with 95% conversion while BPA yields 96%. (Scheme 3.4 – Fig S3.41)



Scheme 3.4. Depolymerisation of BPA-PC using 1,3-propanediol (**1n**) as reagent.

Although it can not be employed for subsequent ring-opening polymerisations, the valorisation of such chemical is possible through polycondensation. The linear bis(3-hydroxypropyl) carbonate could be an excellent candidate for the synthesis of poly(TMC).

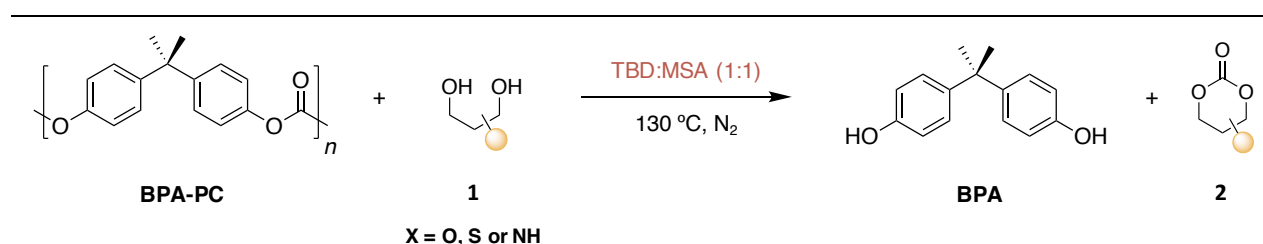
If 1,3-propanediol is not leading to the corresponding cyclic carbonate, similar 1,3-diols bearing different substituents can lead to the formation of the targeted 6-membered cyclic carbonates. In order to evaluate the influence of the diol substituents on the depolymerisation performances, 1,3-propanediol derivatives were employed as reagent for the depolymerisation of BPA-PC.

03. BPA-PC depolymerisation

3.2 Alkyl groups in α position of the hydroxyl groups

First nucleophiles investigated were 1,3-propanediol derivatives bearing alkyl chains in α of the hydroxyl groups. Depolymerisations performed with 3 eq. of 1,3-butanediol (**1o**), 3-methylbutane-1,3-diol (**1p**) and 3-methylpentane-2,4-diol (**1q**) gave the corresponding 6-membered cyclic carbonates in good to excellent yields in 1 to 3 h. (Table 3.5)

Table 3.5. Depolymerisation of BPA-PC (2 g, 7.8 mmol, 1 eq.), using different 1,3-propanediol derivatives bearing substituent(s) in α position (**1**) (23.4 mmol, 3 eq.) with TBD:MSA (1:1) catalyst (0.256 g, 1.17 mmol, 0.15 eq.) to yield 6-membered cyclic carbonates (**2**).



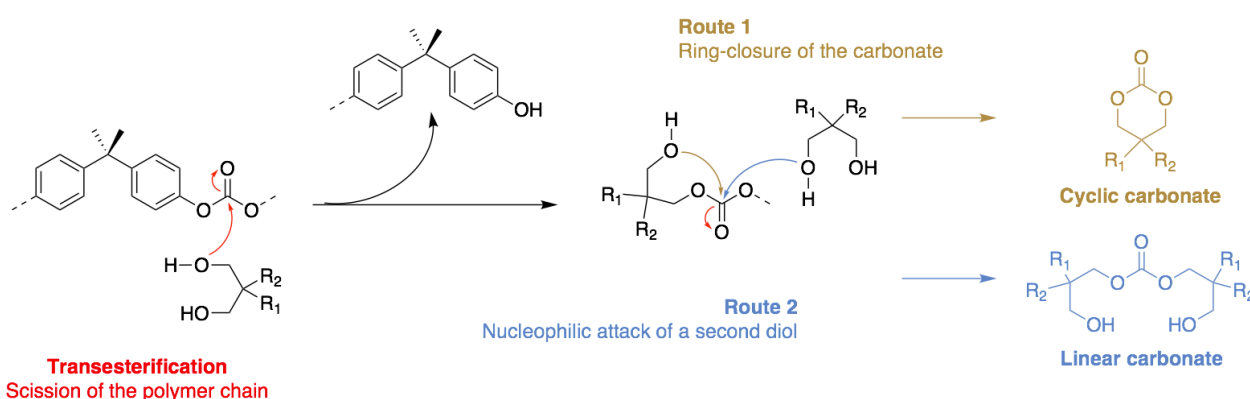
	Nucleophile (1)	Carbonate (2)	Conditions ^a	BPA (%) ^b	2 (%) ^b
n			130 °C 1 h 3 eq.	96	NA
o			130 °C 1 h 3 eq.	97	97
p			130 °C 3 h 3 eq.	98	79
q			130 °C 1 h 3 eq.	85	86

^a Reaction temperature, depolymerisation duration and amount of reagent used for the depolymerisation. ^b Conversion was determined by ¹H NMR spectroscopy in DMSO-*d*₆ from the crude product using the catalyst as internal standard ($\delta = 1.87$ ppm) and characteristic peaks of BPA and the carbonate, according to literature.^{51,52} (Fig. S3.42 to S3.44)

Notably, the reaction employing **1o** led to complete depolymerisation of BPA-PC in 1 h reaching to both BPA and **2o** in quantitatively.⁵⁰ A parallel can be

done with the reaction employing 1,2-propanediol (**1a**). Indeed, the structures of these two diols are similar, varying only by one carbon, hence the difference in the reaction time – **2o** reached 97% conversion after 1 h whereas **2a** reached 90% conversion after 3 h – demonstrated a more facile ring-closure of the 6-membered cyclic carbonates compared to 5-membered. Despite the increased ring strain of the resulting 6-membered over 5-membered cyclic carbonates, the longer chain diols seem to react faster than their 1,2-diol analogues.

The reaction employing **1o** was compared with **1p** and **1q** to estimate the impact of methyl substituents in α position of the hydroxyl groups. Compared to **1o**, the reaction with **1p** is slower (3 h) and even if the depolymerisation reached similar conversion into BPA (98%), the conversion into the cyclic carbonate **2p** is lower (79%). On the ^1H NMR spectrum of the reaction with **1p**, an extra triplet at $\delta = 4.17$ ppm (Fig. S3.43) suggests the presence of another product corresponding to the linear carbonate resulting from the attack of a second molecule of nucleophile on the so-formed carbonate. (Scheme 3.5 – route 2) In this specific case, the difference of reactivity between the primary alcohol and the tertiary alcohol could explain the non-negligible proportion of linear carbonate obtained.



Scheme 3.5. Description of the two possible routes for the depolymerisation of BPA-PC using 1,3-propanediol derivatives, yielding to 6-membered cyclic carbonate (route 1) or linear carbonate as a consequence of a second nucleophilic attack (route 2).

Similarly, the depolymerisation undergone with **1q** also raised a lower conversion into cyclic carbonate compared to the reaction using **1o** (86% versus 97%) but, although the reaction time was identical (1 h), the BPA

03. BPA-PC depolymerisation

conversion was not quantitative and comparable to the cyclic carbonate (85%). The analysis of the ^1H NMR spectrum revealed the presence of additional signals in the aromatic region, at $\delta = 7.26$ ppm ($\sim 12\%$), similar to the side-product that has been observed for the depolymerisation using ethylene glycol (**1b**). (**Scheme 3.3**) These signals are characteristic of the formation of an additional molecule corresponding to the BPA pattern with two nucleophiles attached through a carbonate linkage. Also here, the reactivity difference between the secondary and the tertiary alcohol probably influences the reaction products.

3.3 Alkyl groups in β position of the hydroxyl groups

A range of 1,3-diols bearing different alkyl substituents in β position were also evaluated namely 2,2-dimethylpropane-1,3-diol (**1r**), diethylpropane-1,3-diol (**1s**) and 2-methyl-2-propylpropane-1,3-diol (**1t**). Similar to previous reactions leading to 6-membered cyclic carbonates, depolymerisations performed with 3 eq. of reagent and 0.15 eq. of catalyst were completed in short time, 2.5 h for **1r** and 1.5 h for **1s** and **1t**, reaching high conversions of BPA ($> 95\%$). (Fig S3.45 to S3.47) Interestingly, the reactions generated a mixture of the corresponding cyclic and linear carbonates with a majority of the latter one for **1r** – bearing shorter alkyl chains – compared to **1s** and **1t**, majorly leading to the cyclic carbonates **2s** and **2t**. Indeed, using 3 eq. of **1r** the depolymerisation has led to only 23% of cyclic carbonate while reactions with **1s** and **1t** reached 57 and 58%, respectively.

For these reagents, it was decided to investigate further the different parameters influencing the reaction to aim a maximum conversion into cyclic carbonate. Different experiments have been performed using diethylpropane-1,3-diol (**1s**) before applying the best depolymerisation conditions to **1r** and **1t**.

3.3.1 Kinetic of the reaction with **1s**

In order to better understand the depolymerisation, a kinetic study was performed for the reaction employing 3 eq. of **1s** and 0.15 eq. of catalyst at

130 °C. (Fig. 3.5) The analysis of the ^1H NMR spectra along the reaction revealed that linear and cyclic carbonates are first formed simultaneously before reaching a plateau for the linear carbonate while the cyclic carbonate continuously increased until the end of the reaction, at 3 h. Indeed, after 1 h and 15 min, the amount of both cyclic and linear carbonates are similar – 33 and 32%, respectively – but after this time point, the amount of linear carbonate remains unchanged while the conversion into cyclic carbonate continues to increase to reach 61%. After 6 h, the amount of BPA, cyclic and linear carbonates remained constant – 99, 61 and 32 %, respectively. Thus, no disappearance of one product to the profit of another seems to occur. While the conversion into BPA and the cyclic carbonate continuously increases, the amount of linear carbonate reaches a plateau at around 1 h to finally give a ratio cyclic to linear carbonate of 2/1. In order to change this ratio by increasing the content of cyclic carbonate, parameters such as the temperature, the catalyst loading or the reagent quantity were optimised.

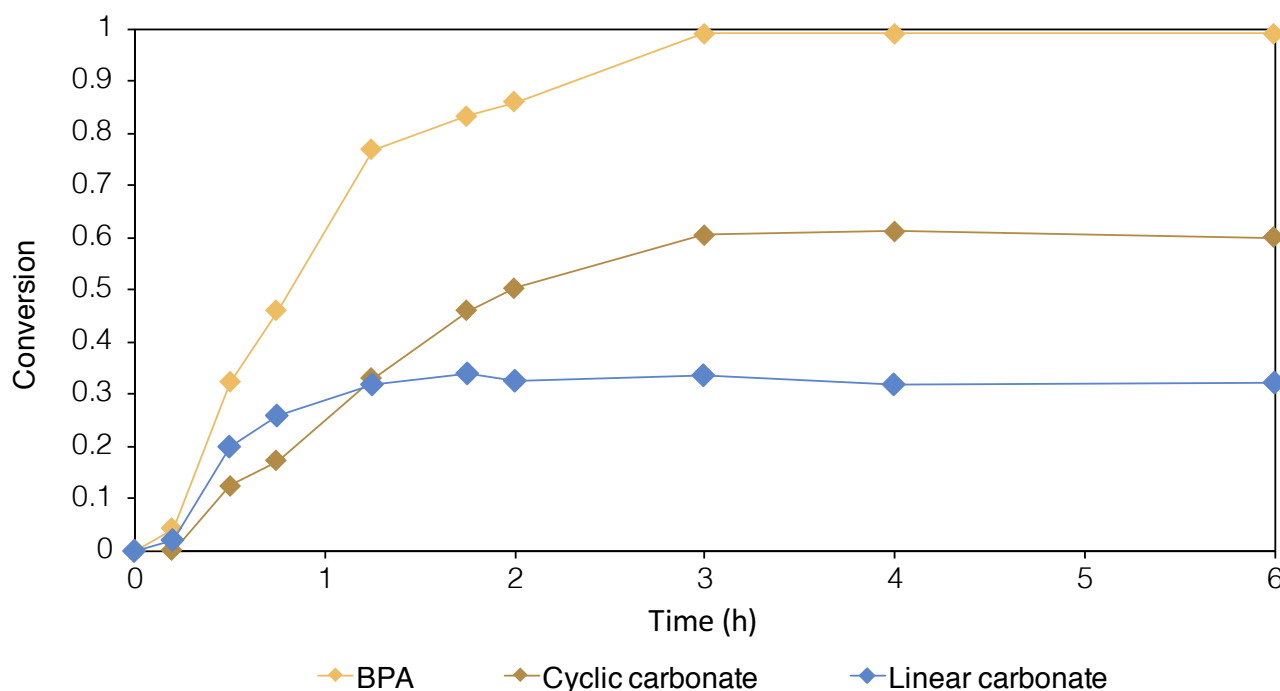


Figure 3.5. Kinetic plot for the depolymerisation of BPA-PC (2 g, 7.80 mmol, 1 eq.) using **1s** as reagent (3.10 g, 23.4 mmol, 3 eq.) and TBD:MSA (1:1) as catalyst (0.277 g, 1.18 mmol, 0.15 eq.) at 130 °C. The conversions were followed by ^1H NMR spectroscopy in $\text{DMSO-}d_6$ using the catalyst signals as internal standard ($\delta = 1.87$ ppm, 4H), and the characteristic signals of BPA ($\delta = 6.66$ ppm, 4H), cyclic carbonate **2s** ($\delta = 4.16$ ppm, 4H) and linear carbonate ($\delta = 3.90$ ppm, 4H) – Fig. S3.48.

03. BPA-PC depolymerisation

3.3.2 Temperature and catalyst loading

It was demonstrated previously that the temperature can influence the depolymerisation by fastening the reaction and possibly avoid side-reactions to occur. Depolymerisations were performed at 110 °C, 130 °C and 160 °C and a clear difference could be observed in the reaction time, 18 h at 110 °C versus only 2 h 20 min and 2 h 10 min at 130 and 160 °C, respectively. The same correlation can be done for the cyclic carbonate conversions, only 34% at 110 °C against 59 and 58% for the reactions at 130 and 160 °C, respectively. (Fig. 3.6A)

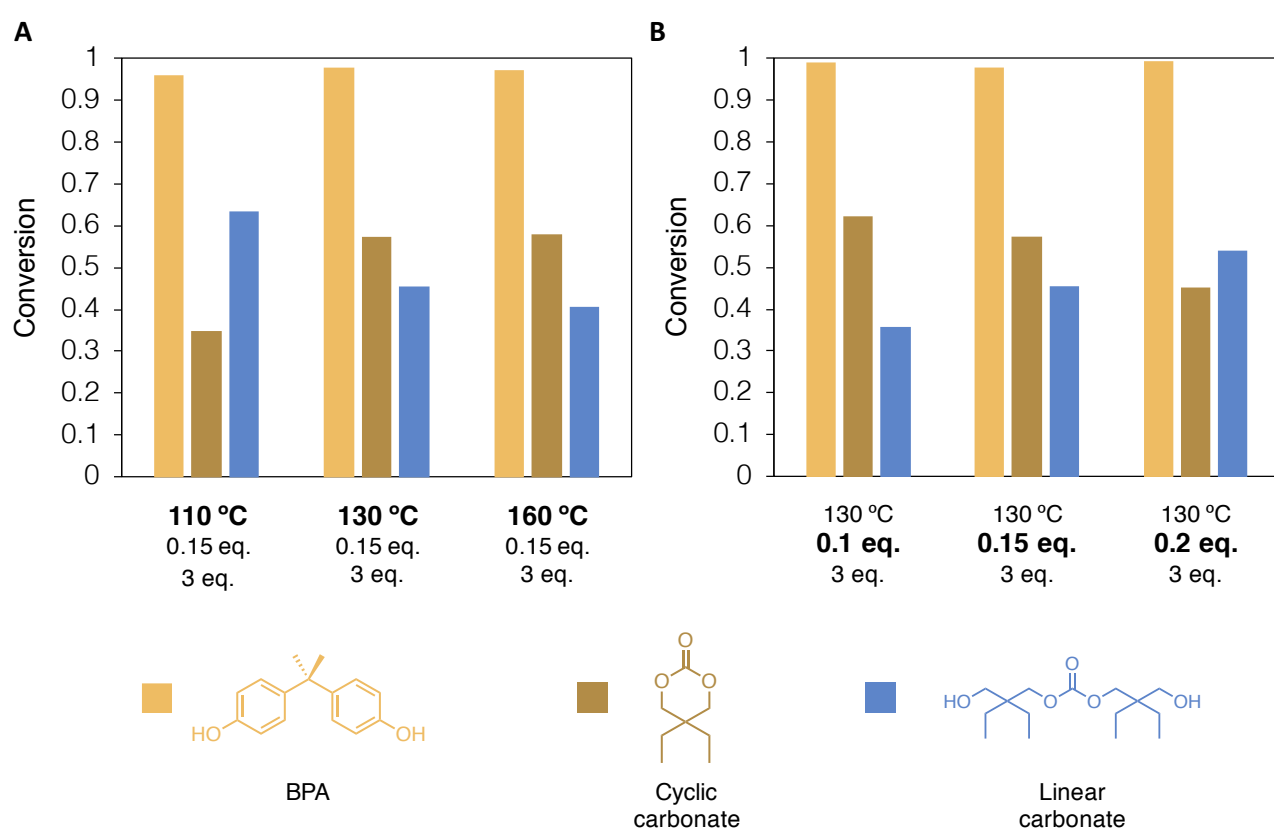


Figure 3.6. Depolymerisation of BPA-PC using (A) different reaction temperatures, (B) different catalyst contents. Conversion of BPA and both cyclic and linear carbonates were determined by ¹H NMR spectroscopy in DMSO-*d*₆ from the crude product using the catalyst as internal standard ($\delta = 1.87$ ppm) and characteristic signals, BPA at $\delta = 6.65$ ppm, **2s** at $\delta = 4.11$ ppm and the corresponding linear carbonate at $\delta = 3.89$ ppm – Fig. S3.49 & S3.50. Reactions conditions: BPA-PC (2 g, 7.8 mmol, 1 eq.), **2s** (3.1 g, 23.4 mmol, 3 eq.).

Thus, increasing the temperature further 130 °C seems to do not provide significant improvement either in the depolymerisation time or yields. On the contrary, diminishing the amount of catalyst led to better conversions of cyclic carbonate. Indeed, while using 0.2 eq. of TBD:MSA (1:1), the

depolymerisation provided 45% of **2s** for 54% of the linear analogous, with 0.1 eq. the main product is the cyclic compound with 62% conversion versus 36% for the linear carbonate. (Fig. 3.6B) However, although with 0.15 eq. and 0.2 eq. the reaction is completed in a reasonable time – 3 h and 1 h, respectively – while the content of catalyst was decreased down to 0.1 eq., the reaction was extended to 22 h.

3.3.3 Amount of reagent

Finally, different amounts of reactant have been employed for the depolymerisation and it appeared that the lower the amount of nucleophile employed, the better the conversion into cyclic carbonate. From 41% of cyclic carbonate while using 6 eq. of the diol, the conversion reached 77% with 1.5 eq.. (Fig. 3.7)

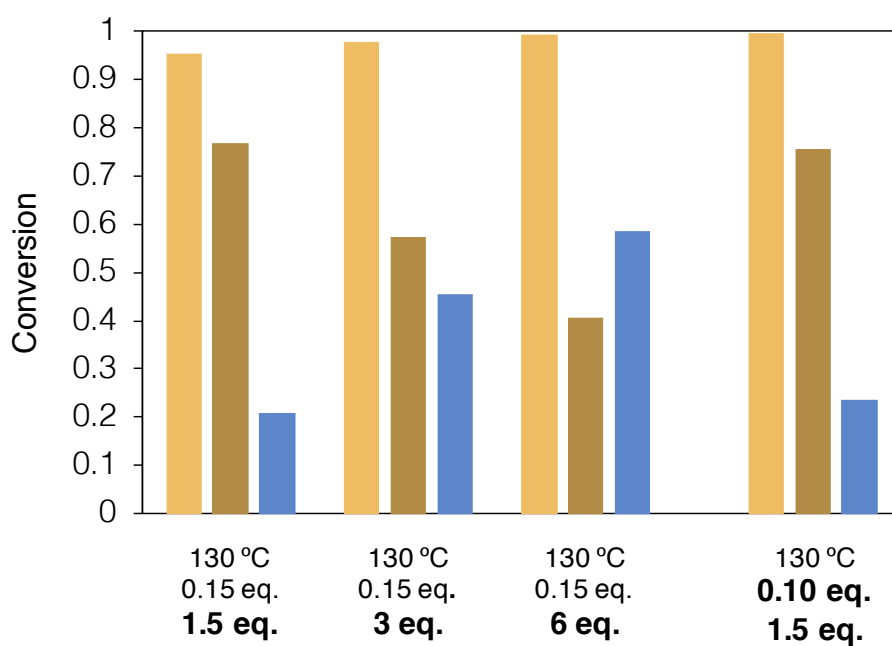


Figure 3.7. Depolymerisation of BPA-PC using different content of nucleophile **2s**. Conversion of BPA and both cyclic and linear carbonates were determined by ^1H NMR spectroscopy in $\text{DMSO-}d_6$ from the crude product using the catalyst as internal standard ($\delta = 1.87$ ppm) and characteristic signals, BPA at $\delta = 6.65$ ppm, **2s** at $\delta = 4.11$ ppm and the corresponding linear carbonate at $\delta = 3.89$ ppm – Fig. S3.51. Reactions conditions: BPA-PC (2 g, 7.8 mmol, 1 eq.), **2s** (3.1 g, 23.4 mmol, 3 eq.).

The depolymerisation time was only slightly extended while using a minimal amount of reagent, from 3 h using 6 or 3 eq. to 5 h with 1.5 eq.. The quantity of nucleophile seems to be the critical parameter to reach higher conversion into cyclic carbonate. Thus, lowering further this amount could improve the

03. BPA-PC depolymerisation

conversion into cyclic carbonate but the depolymerisation being performed in bulk, a lower quantity of the diol would have been practically difficult.

As it was previously noticed that decreasing the catalyst loading resulted in an increased content of cyclic carbonates, the reaction was repeated with an optimal amount of reagent – 1.5 eq. – and a lower catalyst loading – 0.10 eq.. However, the final conversions were not demonstrating any significant improvement compared to the reaction performed with 0.15 eq. of catalyst while the reaction time was considerably increased (24 h). According to previous results, the best conditions for affording a maximum conversion into cyclic carbonate in a reasonable time for the depolymerisation employing **1s** are the following: 1.5 eq. of reagent and 0.15 eq. of catalyst at 130 °C.

3.3.4 Optimised conditions

These conditions were applied to the depolymerisation of BPA-PC using **1r** and **1t** in an attempt to increase the content of cyclic carbonate for these reactions also. (Fig. 3.8)

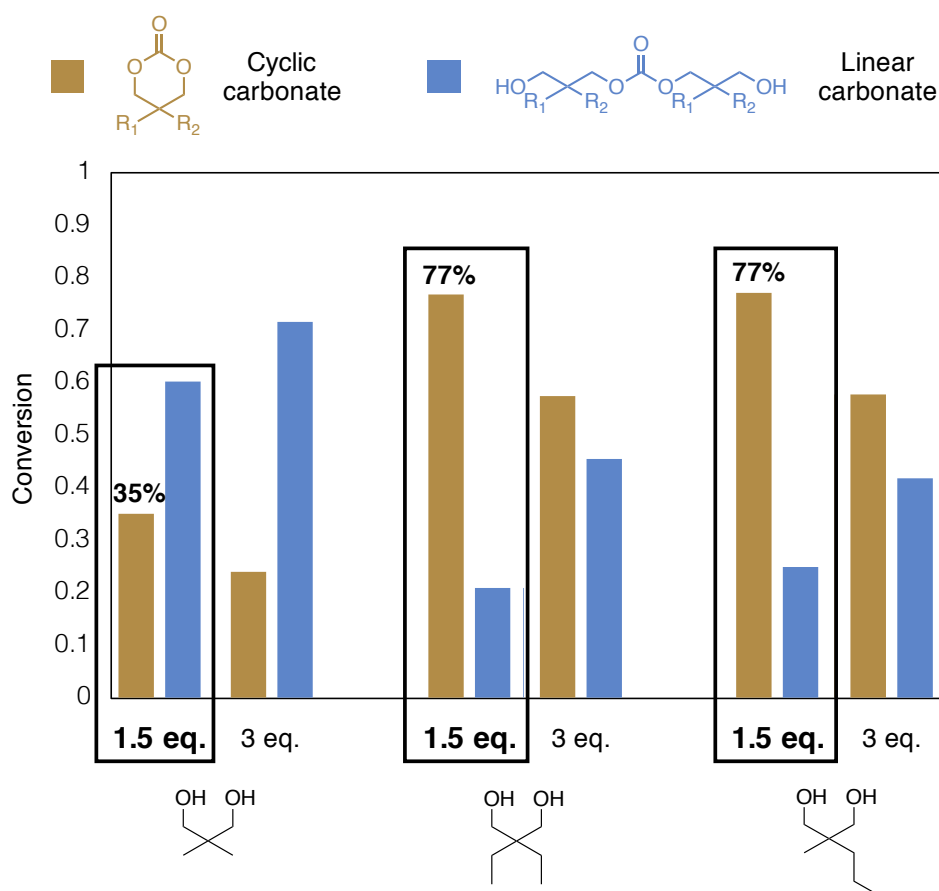


Figure 3.8. Depolymerisation of BPA-PC using 1.5 or 3 eq. of **1r**, **1s** and **1t** as reagent. Conversion into BPA and carbonates were determined by ^1H NMR spectroscopy in $\text{DMSO-}d_6$ from the crude

product using the catalyst as internal standard ($\delta = 1.87$ ppm) and characteristic signals, BPA at $\delta = 6.63$ ppm, **2r**, **2s** and **2t** at $\delta = 4.10$ ppm, and the corresponding linear carbonates at $\delta = 3.87$, respectively – Fig. S3.52. Reactions conditions: BPA-PC (2 g, 7.8 mmol, 1 eq.), TBD:MSA (1:1) (0.256 g, 1.17 mmol, 0.15 eq.), 130 °C.

Employing 1.5 eq. of **1r**, the depolymerisation reached 35% conversion into **2r** while the reaction with 1.5 eq. of **1t** reached 77% of **2t** in 4 and 2 h, respectively. (Table 3.6)

Table 3.6. Depolymerisation of BPA-PC (2 g, 7.8 mmol, 1 eq.), using different 1,3-propanediol derivatives bearing substituent(s) in β position (**1**) (11.7 mmol, 1.5 eq.) with TBD:MSA (1:1) catalyst (0.256 g, 1.17 mmol, 0.15 eq.) to yield 6-membered cyclic carbonates (**2**).

Nucleophile (1)	Carbonate (2)	Conditions ^a	BPA (%) ^b	2 (%) ^b
		130 °C 1 h 3 eq.	NA	96
		130 °C 4 h 1.5 eq	35	94
		130 °C 2 h 1.5 eq	77	96
		130 °C 2 h 1.5 eq	77	98

^a Reaction temperature, depolymerisation duration and amount of reagent used for the depolymerisation. ^b Conversion was determined by ¹H NMR spectroscopy in DMSO-*d*₆ from the crude product using the catalyst as internal standard ($\delta = 1.87$ ppm) and characteristic peaks of BPA and the carbonate, according to literature.⁵³ (Fig. S3.45 to S3.47)

03. BPA-PC depolymerisation

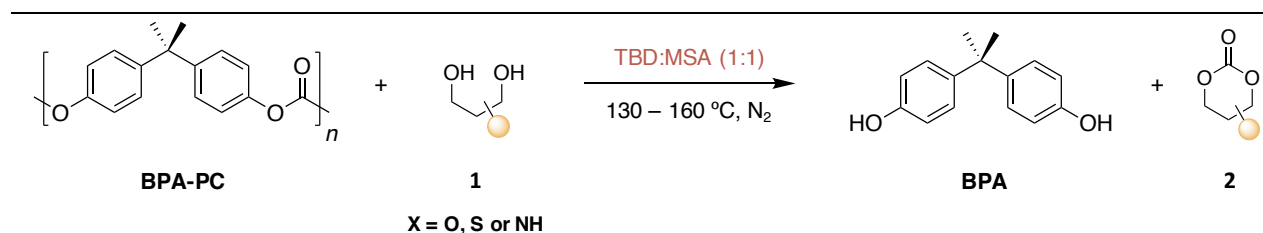
Similar to the reaction with **1s**, lowering the content of nucleophile results in an increased conversion into cyclic carbonate. (**Fig. 3.8**)

This confirmed the influence of the starting product content on the ability to ring-close the carbonate, a smaller amount of the nucleophile leading to a constrained environment and so, to higher rates of 6-membered cyclic carbonate.

3.4 Functional groups in β position of the hydroxyl groups

Derivatives of 1,3-propanediol bearing functionalised substituents in β position have also been employed for the depolymerisation of BPA-PC. (**Table 3.7**)

Table 3.7. Depolymerisation of BPA-PC (2 g, 7.8 mmol, 1 eq.), using different functionalised 1,3-propanediol derivatives bearing substituents in β position (**1**) (23.4 mmol, 3 eq.) with TBD:MSA (1:1) catalyst (0.256 g, 1.17 mmol, 0.15 eq.) to yield functionalised 6-membered cyclic carbonates (**2**).



	Nucleophile (1)	Carbonate (2)	Conditions ^a	BPA (%) ^b	2 (%) ^b
u			130 °C 22 h 3 eq.	98	72
v			630 °C 1 h 3 eq.	96	97
w			130 °C 1 h 3 eq.	97(82)	93 (88)

^a Reaction temperature, depolymerisation duration and amount of reagent used for the depolymerisation. ^b Conversion was determined by ¹H NMR spectroscopy in DMSO-*d*₆ from the crude product using the catalyst as internal standard ($\delta = 1.87$ ppm) and characteristic peaks of BPA and the carbonate, according to literature.^{54,55} Yields in parenthesis are isolated products. (Fig. S3.53 to S3.58)

Similar to previous results, the reaction with 1,1,1-Tris(hydroxymethyl)propane (**1u**) also led to a mixture of linear and cyclic carbonates with the cyclic compound **2u** as major product. Using 3 eq. of the triol at 130 °C, the reaction required 22 h to be completed. Similar to what it was already observed with the glycerol (**1h**) or the *meso*-erythritol (**1i**) for example, the high viscosity of the reaction mixture was slowing the reaction which was nevertheless reaching 98% of BPA and 72% of cyclic carbonate, an improved conversion compared to reactions using 3 eq. of **1s** or **1t**.

Reactions with nucleophiles **1v** and **1w** yielded BPA and the corresponding 6-membered cyclic carbonate (**2v** and **2w**) with conversions above 95%. ¹H NMR spectroscopic analysis confirmed the preservation of the functional side groups, the ester for **2v** and the alkene in the case of **2w**. (Fig. S54 & S55)

The method used herein is chemoselective and therefore functional monomers could be obtained, leading to high value monomers for the synthesis of high-performance polymeric materials. In particular, the ester moiety of **2v** is broadly used to produce polycarbonates that are suitable for drug delivery or antimicrobial purposes.⁵⁶⁻⁵⁸ Similarly, the allyl moiety in **2w** can be used for post-polymerisation modifications, opening the way to a variety of materials for applications in energy storage or drug delivery.^{59,60}

Thus, the isolation of such chemicals is of major interest for their subsequent use for ring-opening polymerisation. Using the isolation technique previously described for the diglycerol dicarbonate **2m**, the cyclic carbonate **2w** was obtained pure after 3 successive additions of 1 eq. of BPA-PC to the depolymerisation crude. The ¹H NMR spectra at the end of the first reaction (tf₁), after the first addition (tf₂) and the second addition (tf₃) highlights the increase of the characteristic signals of the cyclic carbonate ($\delta = 4.23$ ppm) simultaneously to the decrease of the diol signal ($\delta = 3.90$ ppm). (Fig. 3.9)

03. BPA-PC depolymerisation

After a flash column chromatography in pure acetone, **2w** was obtained pure. (yield = 82%) This procedure consists in a sustainable 100% atom economy methodology for the recovery of high-added value cyclic carbonates as all the reagent employed for the reaction is transformed in the product, with no use of organic solvent.

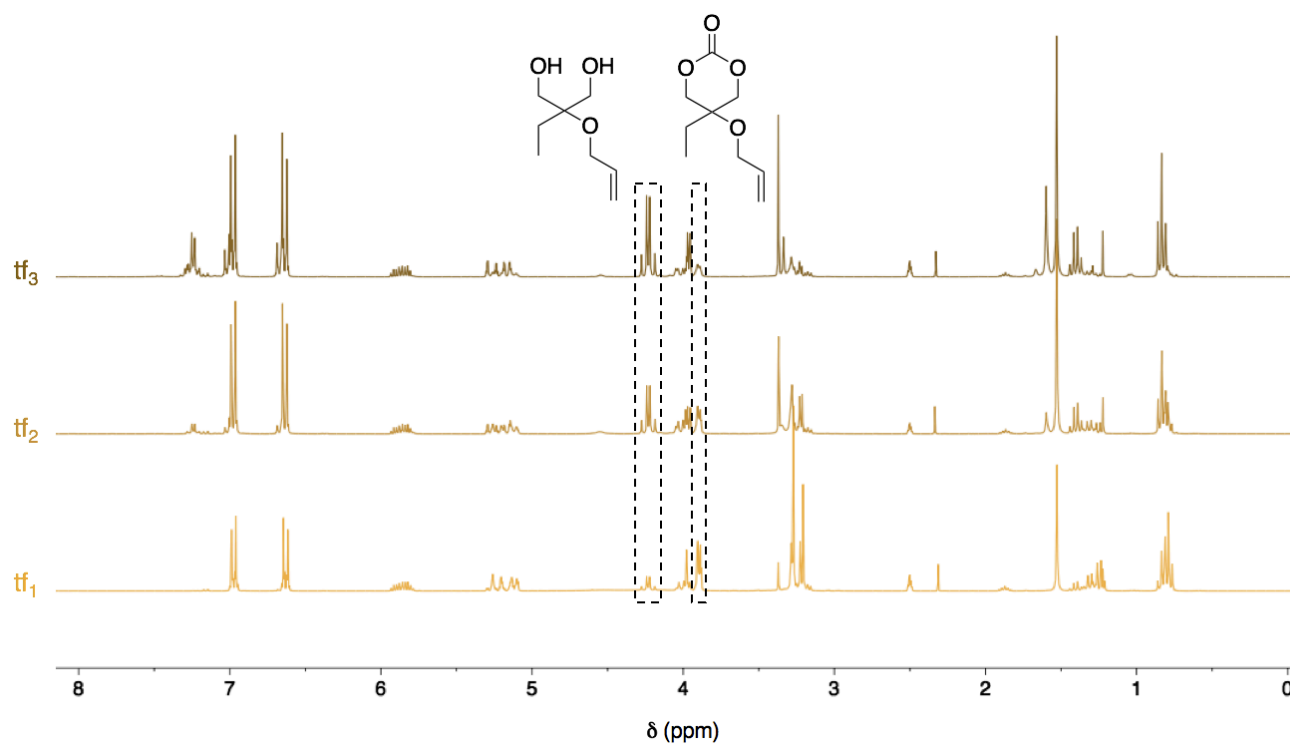


Figure 3.9. Stacked ¹H NMR spectra of the crude product containing **2w** (DMSO-*d*₆, 400 MHz, 298 K) after each adding of 1 eq. of BPA-PC.

3.5 Influence of the substituent bulkiness on the ring-closure of the carbonate

Noticeably, the higher the steric bulkiness of the substituents in β position, the higher the conversion into cyclic carbonate. (Fig. 3.10) The relationship between the ring substituent and their ability to polymerise has been previously correlated through a thermodynamic study⁵³. Indeed, the increase in stability of the 6-membered cyclic carbonate with increasing substituent steric bulk is consistent with the Thorpe-Ingold effect⁶¹ and has been previously related to the polymerisability of cyclic carbonate monomers.⁵³ It was found that increasing the bulkiness of substituents on the 6-membered cyclic carbonate decreases their ability to ring-open as a consequence of the polymer chain torsion rather than the cyclic monomer conformation. Applied

to the depolymerisation of BPA-PC, the conformational distortion of the initial diol could lead to more favoured ring-closing in the presence of bulky substituents.

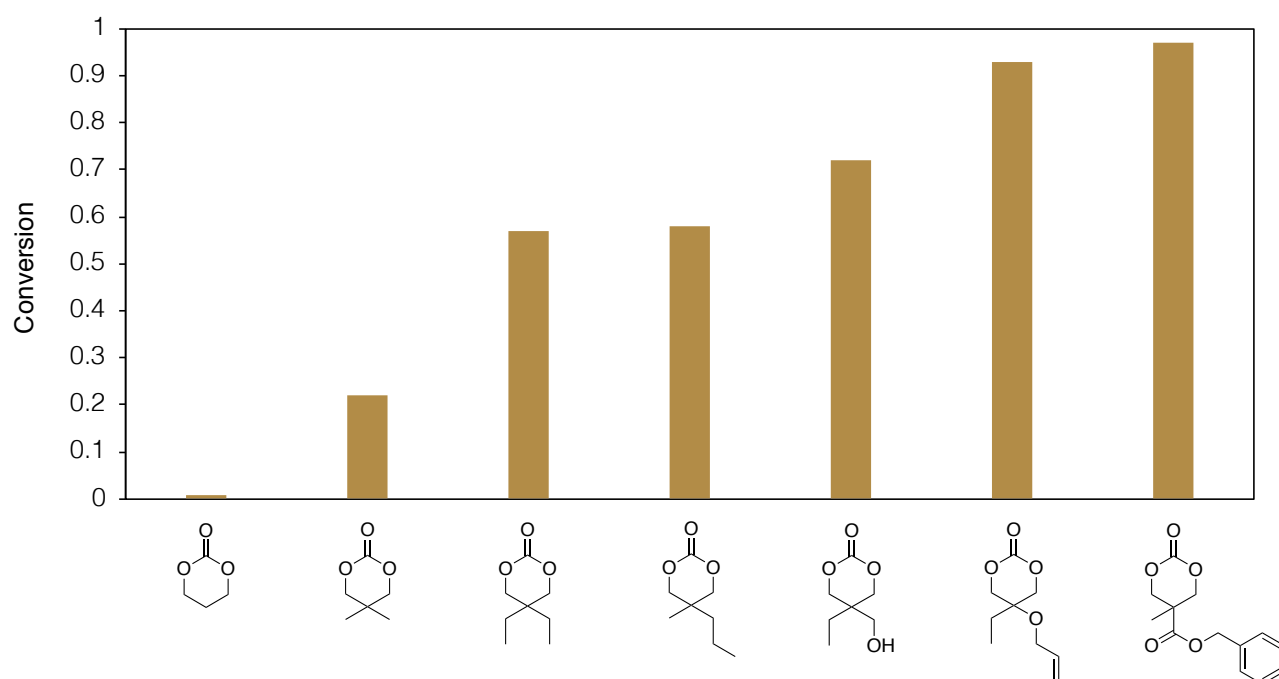


Figure 3.10. Conversion into cyclic carbonate for the depolymerisation of BPA-PC using 1,3-propanediols bearing substituents in β position of the hydroxyl groups (3 eq.).

4 Quantum chemical modelling

4.1 Model reaction with ethylene glycol

DFT calculations were performed to gain mechanistic insights into the glycolysis of BPA-PC using the Gaussian 16 suite of programs⁶² with MN12SX functional⁶³ in conjunction with the 6-31+G(d,p) basis set for geometry optimisation. To confirm that the optimised structures were minima on the potential energy surfaces, frequency calculations were carried out at the same level of theory and then used to evaluate the ZPVE and the thermal vibrational corrections at $T = 298$ K. The electronic energy was then refined by single-point energy calculations at the MN12SX/6-311++G(2df,2p) level of theory. In order to obtain a representative and realistic model using small molecules, the polymer was replaced by diphenyl carbonate, the reaction with ethylene glycol releasing two molecules of phenol and ethylene carbonate (Fig. 3.11A).

03. BPA-PC depolymerisation

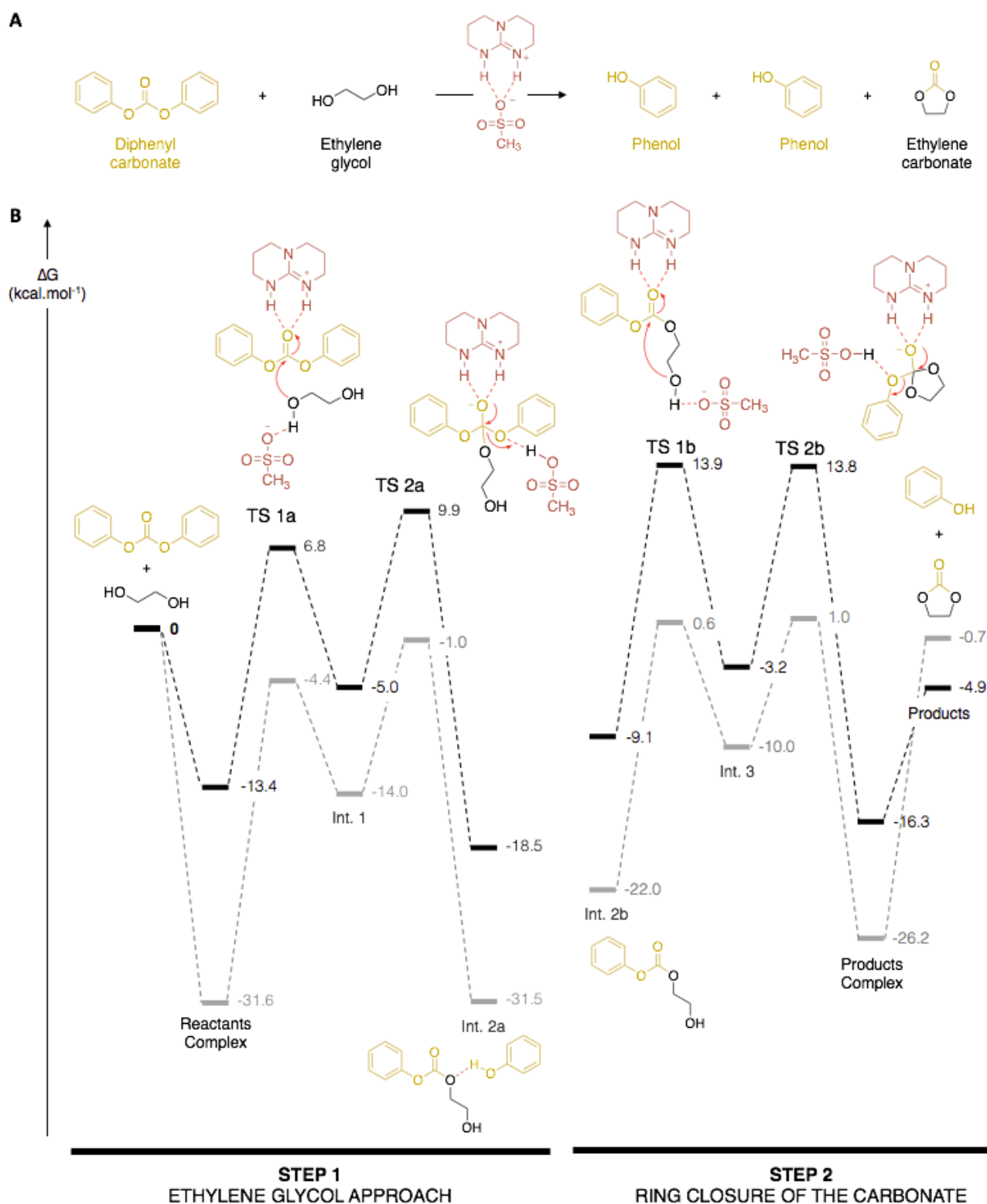


Figure 3.11. (A) Model reaction for the depolymerisation of BPA-PC using TBD:MSA (1:1) as catalyst and (B). DFT-computed reaction pathways for the depolymerisation reactions of BPA-PC in gas phase (in grey) and in ethylene glycol (in black) divided in two steps: the nucleophilic attack of one hydroxyl group of the ethylene glycol (step1) and the ring-closure of the carbonate (step 2).

The mechanism has been modelled in gas phase and in ethylene glycol (both geometry optimisation and single-point calculations) using the PCM solvent

model^{64–66} with the dielectric constant of ethylene glycol ($\epsilon = 40.245$), as glycolysis in this chapter were performed in bulk.

The transesterification leading to the degradation of the polymer involves two different steps: the nucleophilic attack of one hydroxyl group of ethylene glycol on the carbonyl of the polymer (**step 1**) and the ring closure via a second nucleophilic attack of the second hydroxyl group of the diol (**step 2**). (Fig. 3.11B) Every step is divided into two transition states: the nucleophilic attack of the hydroxyl (TS 1a and TS 1b) and the subsequent elimination of one molecule of phenol (TS 2a and TS 2b). For every transition state the protonated TBD stabilised the carbonyl of the polymer while the MSA anion enables a proton transfer. Similar to PET depolymerisation described in the last chapter, the catalytic site is localised between the TBD^+ and MSA^- . (Figs. 3.12 & 3.13)

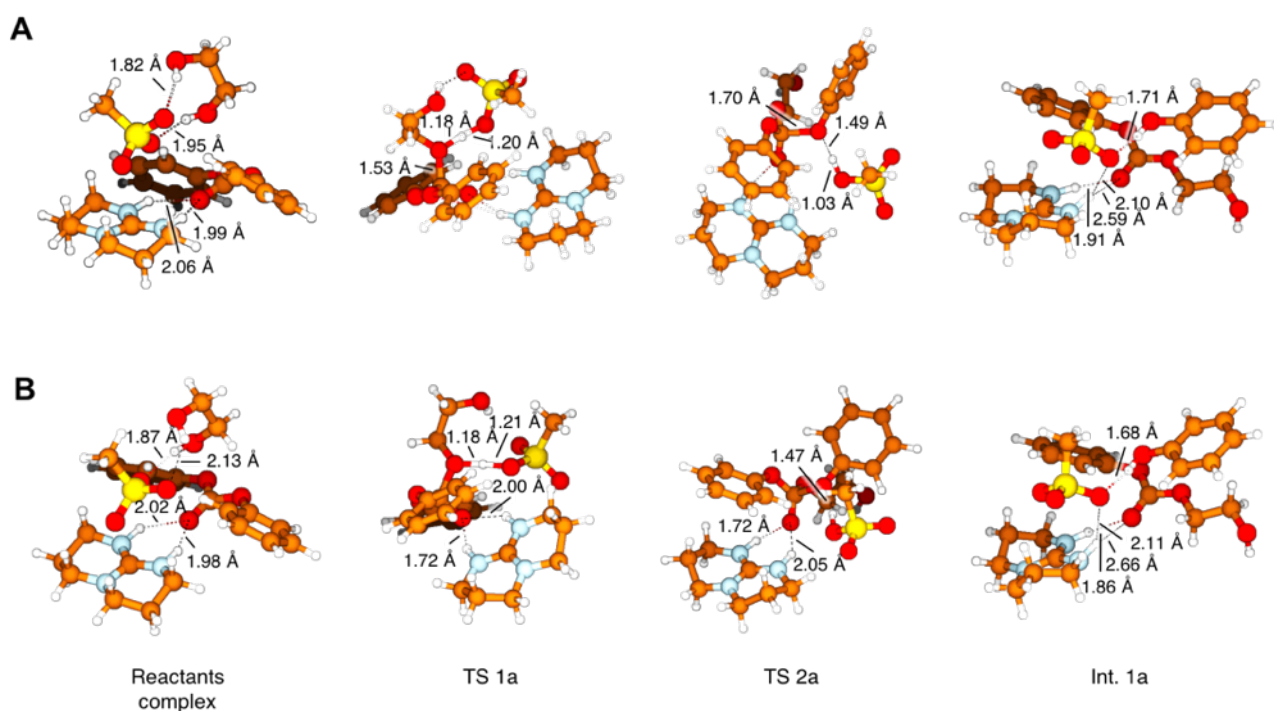


Figure 3.12. DFT-optimised complexes and transition states for the nucleophilic attack of one hydroxyl group of the ethylene glycol (**step1**) of the glycolysis of BPA-PC (A) in gas phase and (B) in ethylene glycol. Color code: orange, carbon; white, hydrogen; red, oxygen; blue, nitrogen; yellow, sulfur.

Considering the pathway calculated with the ethylene glycol parameter (black), both steps have very similar profiles, with the first transition state being rate-determining. The energy was calculated as $20.2 \text{ kcal}\cdot\text{mol}^{-1}$ for the first

03. BPA-PC depolymerisation

transition state in step 1 (**TS 1a**) and 23 kcal·mol⁻¹ for the first transition state in step 2 (**TS 1b**). Although the carbonate ring closure (**TS 1b**, 23 kcal·mol⁻¹) has a higher energetic barrier than the nucleophilic attack from ethylene glycol (**TS 1a**, 20.2 kcal·mol⁻¹), these values remain very close, hence it indicates that both transition states greatly influence the reaction rate. In each step, the first transition state has larger barrier – higher – than the second transition state, the latter representing the subsequent release of a phenol molecule *via* the MSA⁻ proton transfer, which requires 14.9 and 17.0 kcal·mol⁻¹ for **TS 2a** and **TS 2b**, respectively. The overall mechanistic pathways are similar in gas phase and using PCM with ethylene glycol. All stationary points are lower in energy in gas phase but the energetic barriers are very similar for **TS 2a** (14.9 in ethylene glycol versus 13 kcal·mol⁻¹ in gas phase) and **TS 1b** (23.0 in ethylene glycol versus 22.6 kcal·mol⁻¹ in gas phase). However, the energetic barrier for **TS 1a** is lower for the pathway in ethylene glycol (20.2 kcal·mol⁻¹ against 27.2 in gas).

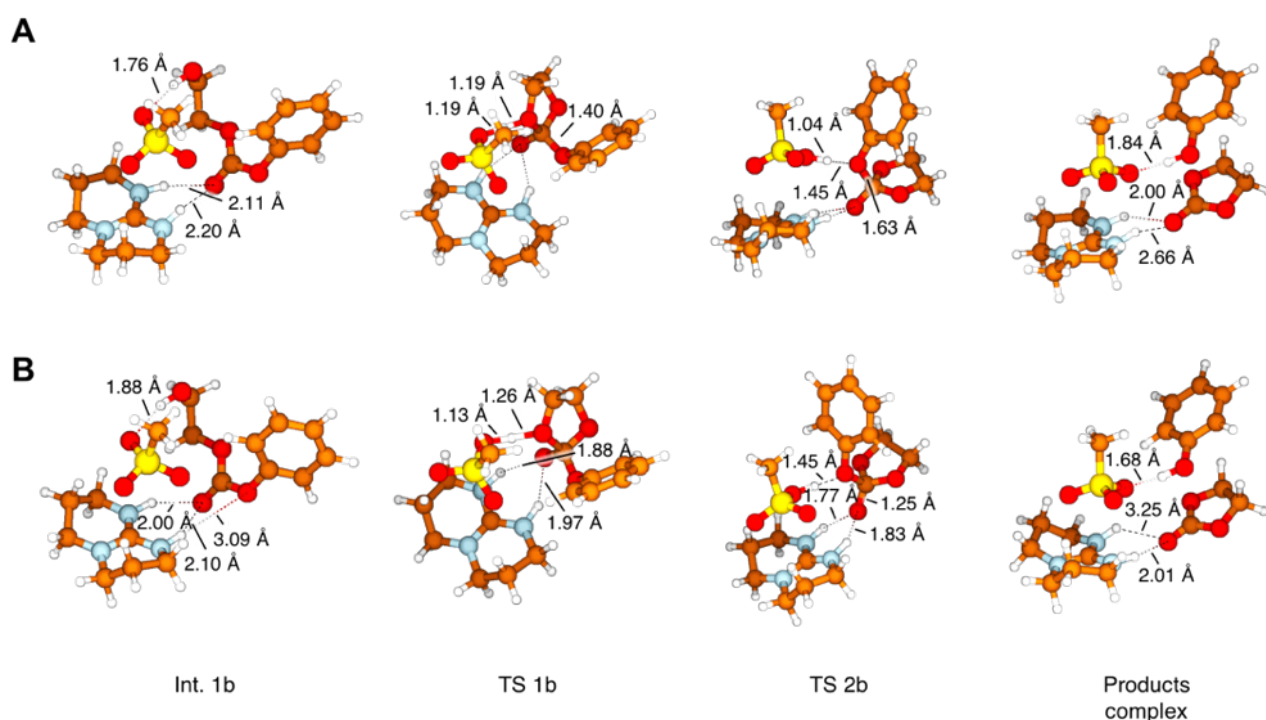


Figure 3.13. Complexes and transitions states for the ring-closure of the carbonate (step 2) of the glycolysis of BPA-PC (A) in gas phase and (B) in ethylene glycol. Color code: orange, carbon; white, hydrogen; red, oxygen; blue, nitrogen; yellow, sulfur.

On the contrary, the energetic barrier for the elimination of the second phenol (**TS 2b**) is lower while computed in gas phase (9 kcal·mol⁻¹ against 17 using

ethylene glycol dielectric constant). It results that first transition state for the transesterification of the ethylene glycol on diphenyl carbonate (**TS 1a**, 27.2 kcal.mol⁻¹) is the rate-determining step in gas phase while the carbonate ring-closure (**TS 1b**, 23.0 kcal.mol⁻¹) is the rate-determining step using ethylene glycol as solvent. As it was noticed before, these values are in the same range and both transition states are influencing the reaction in any case, but the higher stability of complexes and intermediates while computed in gas phase leads to these slight differences of energetic barriers.

4.2 Comparison between 5- and 6-membered cyclic carbonate

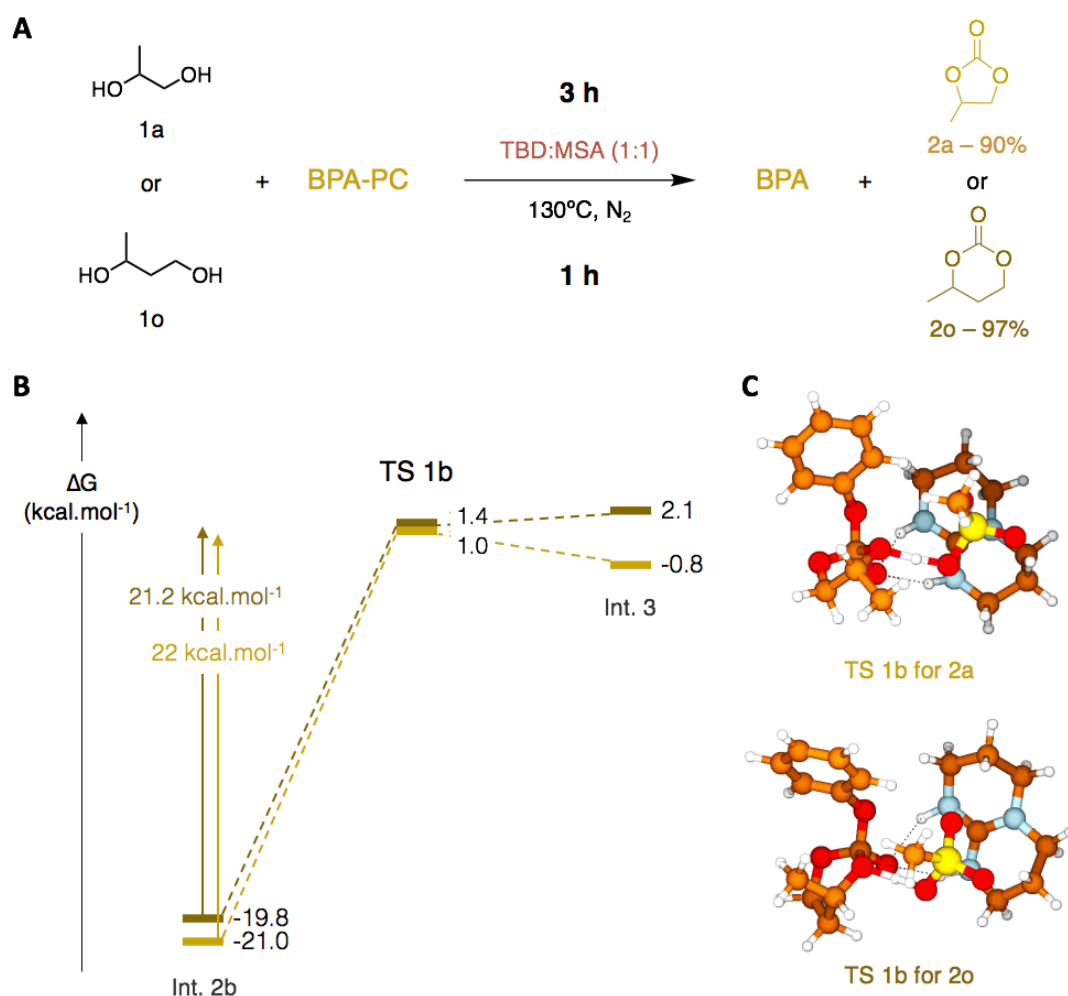
Reaction pathways in this section have been performed at the MN12SX/6-311+G(d,p) level of theory, in ethylene glycol using the PCM solvent model⁶⁴⁻⁶⁶ with the dielectric constant of ethylene glycol ($\epsilon = 40.245$).

4.2.1 Comparing reaction time

The experimental results have demonstrated that the depolymerisations involving the ring closure of the 6-membered cyclic carbonates were faster than for the 5-membered – the reaction with **1a** giving **2a** in 3 h while the reaction with **1o** gave **2o** in 1 h. (**Fig 3.14A**)

In order to understand these kinetical differences, the transition state corresponding to the ring closing of **int. 2b** (**TS 1b**) was modelled for the two reactions. No significant differences were observed between the energetic barriers calculated for **TS 1b** describing the ring-closing of the nucleophile (22 kcal.mol⁻¹ for **1a** and 21.2 kcal.mol⁻¹ for **1i**) which confirmed that reaching 5- or 6- membered cyclic carbonates from BPA-PC is energetically similar, considering equivalent substituents. (**Fig. 3.14B**) The 3D image of the corresponding transition states illustrates the identical action of the catalyst on the structure and the similar conformations taken after **int. 2b**. (**Fig. 3.14C**) However, it could have been expected to observe a difference of stability for the stationary points on the energetic diagram, but the reaction involving 1,2-propanediol did not demonstrate lower levels of energy than with 1,3-butanediol for the overall pathway.

03. BPA-PC depolymerisation



4.2.2 Comparing ability to ring-close

The ring-closing of the intermediate formed after the leaving of one molecule of phenol (**TS 1b**) has been also calculated for 1,3-propanediol and compared with the pathway for ethylene glycol. In parallel, another transition state corresponding to the attack of a second molecule of nucleophile to form the linear analogous (for both ethylene glycol and 1,3-propanediol) has been modeled. (**Fig. 3.15**) Indeed, experimental results demonstrated that the depolymerisation employing ethylene glycol majorly led to the cyclic carbonate while the reaction with 1,3-propanediol only gave a linear carbonate formed through the successive transesterifications of two molecules of nucleophile. Comparing the pathways leading to the cyclic or the linear carbonates for both diols, it was expected to obtain a higher

energetic barrier for the linear pathway in the case of ethylene glycol and a higher energetic barrier for the obtaining of the cyclic carbonate in the case of 1,3-propanediol. However, no significant differences were observed in between the four pathways as energetic barriers for **TS 1b** are very close, all comprised between 22.2 and 23.7 kcal.mol⁻¹.

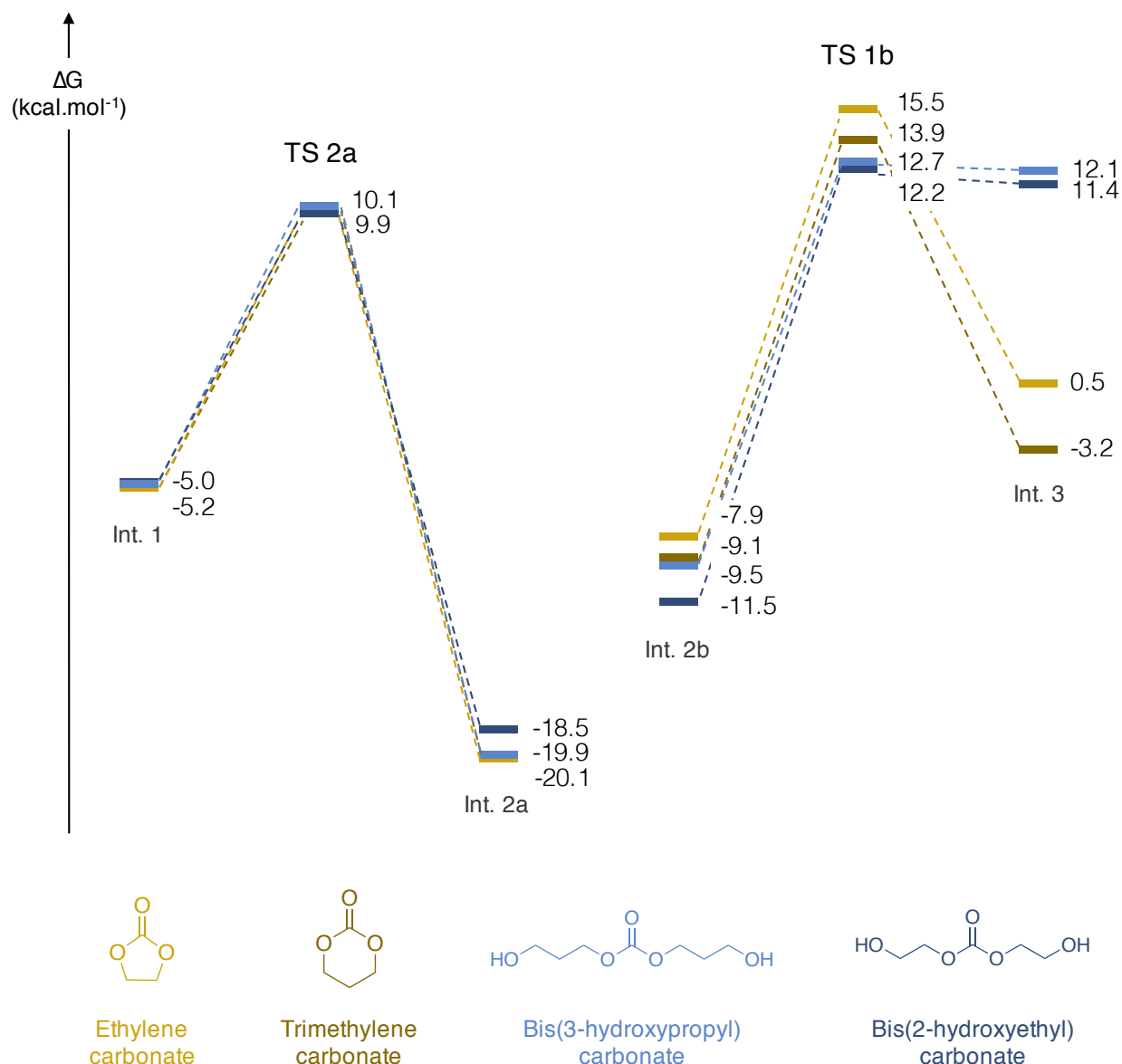


Figure 3.15. DFT-computed reaction pathway for the leaving of phenol (TS 2a), the ring closure of cyclic carbonate (TS 1b) for the obtaining of ethylene carbonate (yellow), trimethylene carbonate (brown), and the attack of a second nucleophile (TS 1b) for the obtaining of bis(3-hydroxypropyl) carbonate (light blue) and bis(2-hydroxyethyl) carbonate (dark blue) at MN12SX/6-311+G(d,p) level of theory.

It is required to be critical here and to take into account that a lot of parameters influencing the reaction are not considered in the calculations. Firstly, the polymeric nature of the reagent, if the model reaction involves

03. BPA-PC depolymerisation

small molecules, the reaction is performed with a polymer which is not melted at the reaction temperature, as previously evoked, all reactions are in a solid-liquid state – which surely influences the mechanism – and the surface interactions are not taken into account by the DFT methodology. Secondly, the reaction is performed in bulk and the reagents employed are hydroxyl-rich. Experimental results have demonstrated that employing different starting amount of reagent (from 1.5 eq to 12 eq.) can greatly influence the product(s) nature and conversion(s), decreasing the reagent loading generally favouring the ring-closing into cyclic carbonates. Thus, the hydrogen-bond network surrounding the reaction site has to be considered to model the difference between two reagents, which is not the case with the present calculations.

Conclusion

The depolymerisation of waste plastics to yield high added-value cyclic carbonates presents a significant advance for chemical recycling methodologies. By a careful choice of nucleophile, a library of carbonyl-containing heterocycles can be obtained via a simple solvent-free depolymerisation using TBD:MSA (1:1) as catalyst. Not only can it enable a polymer-monomer-polymer cycle with the recovery of BPA but, achieving high atom efficiency by retaining the carbonyl group, it can also deliver valuable monomers for a range of high performance materials. **(Fig. 3.16)**

It has to be noticed that the characteristics of the nucleophiles used (viscosity, melting and boiling points, ability to create hydrogen bonds network, ...) and the parameters of the reaction (temperature, catalyst load, reagent quantities) can greatly influence the depolymerisation. The aim of the current chapter was a large screening of different nucleophiles for the depolymerisation of BPA-PC in order to understand the mechanism and obtain a library of carbonyl-containing heterocycles. In the perspective of scaling-up one of these reactions, further optimisations of the reaction parameters should certainly be undergone to reach maximum efficiency.

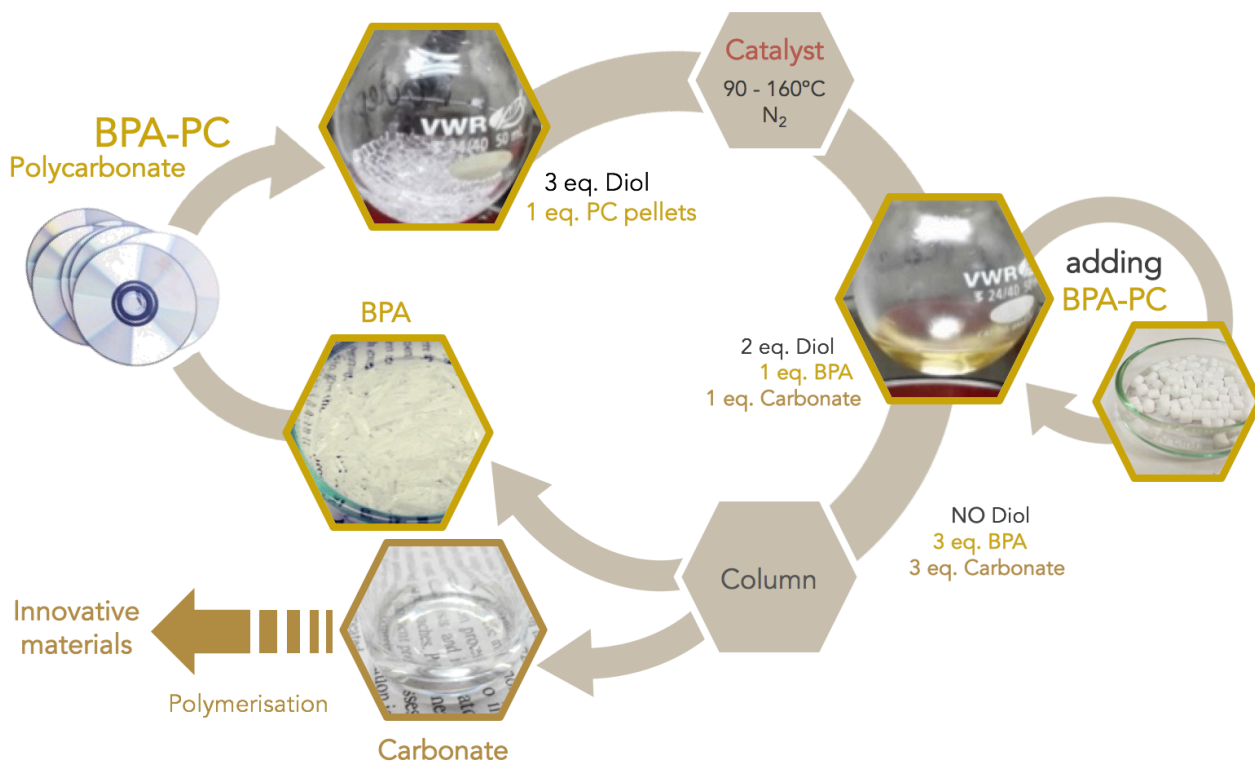


Figure 3.16. Closed-loop recycling of BPA-PC in a solvent-free procedure using TBD:MSA (1:1) as catalyst and *upcycling* through the polymerisation of carbonates for innovative materials.

References

- 1 Plastic Insights, Plastics Insight - Market Intelligence Portal for Plastics Industry, <https://www.plasticsinsight.com/>, (accessed August 22, 2018).
- 2 D. J. Brunelle and T. G. Shannon, *Macromolecules*, 1991, **24**, 3035–3044.
- 3 H. Tagaya, K. Katoh, J. Kadokawa and K. Chiba, *Polym. Degrad. Stab.*, 1999, **64**, 289–292.
- 4 G. Grause, N. Tsukada, W. J. Hall, T. Kameda, P. T. Williams and T. Yoshioka, *Polym. J.*, 2010, **42**, 438–442.
- 5 L. Li, F. Liu, Z. Li, X. Song, S. Yu and S. Liu, *Fibers Polym.*, 2013, **14**, 365–368.
- 6 M. M. A. Nikje and M. Askarzadeh, *Polímeros*, 2013, **23**, 29–31.
- 7 E. Quaranta, *Appl. Catal. B Environ.*, 2017, **206**, 233–241.
- 8 L.-C. Hu, A. Oku and E. Yamada, *Polymer*, 1998, **39**, 3841–3845.
- 9 R. Piñero, J. García and M. J. Cocero, *Green Chem.*, 2005, **7**, 380–387.
- 10 C.-H. Lin, H.-Y. Lin, W.-Z. Liao and S. A. Dai, *Green Chem.*, 2007, **9**, 38–43.
- 11 D. Kim, B. Kim, Y. Cho, M. Han and B.-S. Kim, *Ind. Eng. Chem. Res.*, 2009, **48**, 685–691.
- 12 E. Quaranta, D. Sgherza and G. Tartaro, *Green Chem.*, 2017, **19**, 5422–5434.
- 13 S. Hata, H. Goto, E. Yamada and A. Oku, *Polymer*, 2002, **43**, 2109–2116.
- 14 S. Hata, H. Goto, S. Tanaka and A. Oku, *J. Appl. Polym. Sci.*, 2003, **90**, 2959–2968.
- 15 S. Westhues, J. Idel and J. Klankermayer, *Sci. Adv.*, 2018, **4**, eaat9669.
- 16 H.-Z. Tan, Z.-Q. Wang, Z.-N. Xu, J. Sun, Y.-P. Xu, Q.-S. Chen, Y. Chen and G.-C. Guo, *Catal. Today*, 2018, **316**, 2–12.
- 17 S.-H. Pyo, J. H. Park, T.-S. Chang and R. Hatti-Kaul, *Curr. Opin. Green Sustain. Chem.*, 2017, **5**, 61–66.
- 18 B. A. V. Santos, V. M. T. M. Silva, J. M. Loureiro and A. E. Rodrigues, *ChemBioEng Rev.*, 2014, **1**, 214–229.
- 19 M. A. Pacheco and C. L. Marshall, *Energy Fuels*, 1997, **11**, 2–29.
- 20 T. Do, E. R. Baral and J. G. Kim, *Polymer*, 2018, **143**, 106–114.

- 21 E. Quaranta, C. C. Minischetti and G. Tartaro, *ACS Omega*, 2018, **3**, 7261–7268.
- 22 F. Iannone, M. Casiello, A. Monopoli, P. Cotugno, M. C. Sportelli, R. A. Picca, N. Cioffi, M. M. Dell'Anna and A. Nacci, *J. Mol. Catal. Chem.*, 2017, **426, Part A**, 107–116.
- 23 N. Yanagihara, N. Abe, H. Takama, Y. Shimamura and M. Yoshida, *Chem. Lett.*, 2007, **36**, 1128–1129.
- 24 X.-B. Lu and D. J. Darensbourg, *Chem. Soc. Rev.*, 2012, **41**, 1462–1484.
- 25 H. Zhang and M. W. Grinstaff, *J. Am. Chem. Soc.*, 2013, **135**, 6806–6809.
- 26 J. Kalhoff, D. Bresser, M. Bolloli, F. Alloin, J.-Y. Sanchez and S. Passerini, *ChemSusChem*, 2014, **7**, 2939–2946.
- 27 X. Zhang, M. Fevre, G. O. Jones and R. M. Waymouth, *Chem. Rev.*, 2018, **118**, 839–885.
- 28 C. Martín, G. Fiorani and A. W. Kleij, *ACS Catal.*, 2015, **5**, 1353–1370.
- 29 S.-H. Pyo and R. Hatti-Kaul, *Adv. Synth. Catal.*, 2016, **358**, 834–839.
- 30 P. Palanza, L. Gioiosa, F. S. vom Saal and S. Parmigiani, *Environ. Res.*, 2008, **108**, 150–157.
- 31 S. Biedermann, P. Tschudin and K. Grob, *Anal. Bioanal. Chem.*, 2010, **398**, 571–576.
- 32 Tucker Deirdre K., Hayes Bouknight Schantel, Brar Sukhdev S., Kissling Grace E. and Fenton Suzanne E., *Environ. Health Perspect.*, 2018, **126**, 087003.
- 33 M. Leung, J.-L. Lai, K.-H. Lau, H. Yu and H.-J. Hsiao, *J. Org. Chem.*, 1996, **61**, 4175–4179.
- 34 H. Röper and J. Goossens, *Starch - Stärke*, 1993, **45**, 400–405.
- 35 M. Besson, P. Gallezot and C. Pinel, *Chem. Rev.*, 2014, **114**, 1827–1870.
- 36 A. M. Mirończuk, J. Furgała, M. Rakicka and W. Rymowicz, *J. Ind. Microbiol. Biotechnol.*, 2014, **41**, 57–64.
- 37 J. R. Ochoa-Gómez, O. Gómez-Jiménez-Aberasturi, C. Ramírez-López and M. Belsué, *Org. Process Res. Dev.*, 2012, **16**, 389–399.
- 38 M. O. Sonnati, S. Amigoni, E. P. T. de Givenchy, T. Darmanin, O. Choulet and F. Guittard, *Green Chem.*, 2013, **15**, 283–306.
- 39 A. Corma, S. Iborra and A. Velty, *Chem. Rev.*, 2007, **107**, 2411–2502.

- 40 A. Behr, J. Eilting, K. Irawadi, J. Leschinski and F. Lindner, *Green Chem.*, 2008, **10**, 13–30.
- 41 B. Schöffner, F. Schöffner, S. P. Verevkin and A. Börner, *Chem. Rev.*, 2010, **110**, 4554–4581.
- 42 M. Tryznowski, A. Świdorska, Z. Żołek-Tryznowska, T. Gołofit and P. G. Parzuchowski, *Polymer*, 2015, **80**, 228–236.
- 43 A. Bossion, R. H. Aguirresarobe, L. Irusta, D. Taton, H. Cramail, E. Grau, D. Mecerreyes, C. Su, G. Liu, A. J. Müller and H. Sardon, *Macromolecules*, 2018, **51**, 5556–5566.
- 44 V. Schimpf, J. B. Max, B. Stolz, B. Heck and R. Mülhaupt, *Macromolecules*, 2019, **52**, 320–331.
- 45 M. Aresta, A. Dibenedetto and L. di Bitonto, *RSC Adv.*, 2015, **5**, 64433–64443.
- 46 M. Alves, B. Grignard, A. Boyaval, R. Méreau, J. De Winter, P. Gerbaux, C. Detrembleur, T. Tassaing and C. Jérôme, *ChemSusChem*, 2017, **10**, 1128–1138.
- 47 P. Goodrich, H. Q. N. Gunaratne, J. Jacquemin, L. Jin, Y. Lei and K. R. Seddon, *ACS Sustain. Chem. Eng.*, 2017, **5**, 5635–5641.
- 48 F. Suriano, O. Coulembier, J. L. Hedrick and P. Dubois, *Polym. Chem.*, 2011, **2**, 528–533.
- 49 B. Ochiai, H. Amemiya, H. Yamazaki and T. Endo, *J. Polym. Sci. Part Polym. Chem.*, 2006, **44**, 2802–2808.
- 50 M. Fujiwara, A. Baba and H. Matsuda, *J. Heterocycl. Chem.*, 1989, **26**, 1659–1663.
- 51 V. Zubar, Y. Lebedev, L. M. Azofra, L. Cavallo, O. El-Sepelgy and M. Rueping, *Angew. Chem. Int. Ed.*, 2018, **57**, 13439–13443.
- 52 M. Selva, A. Caretto, M. Noè and A. Perosa, *Org. Biomol. Chem.*, 2014, **12**, 4143–4155.
- 53 J. Matsuo, K. Aoki, F. Sanda and T. Endo, *Macromolecules*, 1998, **31**, 4432–4438.
- 54 K. J. Wright, V. D. Badwaik, S. Samaddar, S.-H. Hyun, K. Glauning, T. Eom and D. H. Thompson, *Macromolecules*, 2018, **51**, 670–678.
- 55 H. Matsukizono and T. Endo, *J. Mater. Sci. Res.*, 2016, **5**, p11.
- 56 A. P. Goodwin, S. S. Lam and J. M. J. Fréchet, *J. Am. Chem. Soc.*, 2007, **129**, 6994–6995.

- 57 F. Nederberg, Y. Zhang, J. P. K. Tan, K. Xu, H. Wang, C. Yang, S. Gao, X. D. Guo, K. Fukushima, L. Li, J. L. Hedrick and Y.-Y. Yang, *Nat. Chem.*, 2011, **3**, 409–414.
- 58 F. Suriano, R. Pratt, J. P. K. Tan, N. Wiradharma, A. Nelson, Y.-Y. Yang, P. Dubois and J. L. Hedrick, *Biomaterials*, 2010, **31**, 2637–2645.
- 59 A. W. Thomas, P. K. Kuroishi, M. M. Pérez-Madrigal, A. K. Whittaker and A. P. Dove, *Polym. Chem.*, 2017, **8**, 5082–5090.
- 60 J. Mindemark, L. Imholt, J. Montero and D. Brandell, *J. Polym. Sci. Part Polym. Chem.*, 2016, **54**, 2128–2135.
- 61 R. M. Beesley, C. K. Ingold and J. F. Thorpe, *J. Chem. Soc. Trans.*, 1915, **107**, 1080–1106.
- 62 M. J. Frisch, G. W. Trucks, H. B. Schlegel, G. E. Scuseria, M. A. Robb, J. R. Cheeseman, G. Scalmani, V. Barone, G. A. Petersson, H. Nakatsuji, X. Li, M. Caricato, A. V. Marenich, J. Bloino, B. G. Janesko, R. Gomperts, B. Mennucci, H. P. Hratchian, J. V. Ortiz, A. F. Izmaylov, J. L. Sonnenberg, D. Williams-Young, F. Ding, F. Lipparini, F. Egidi, J. Goings, B. Peng, A. Petrone, T. Henderson, D. Ranasinghe, V. G. Zakrzewski, J. Gao, N. Rega, G. Zheng, W. Liang, M. Hada, M. Ehara, K. Toyota, R. Fukuda, J. Hasegawa, M. Ishida, T. Nakajima, Y. Honda, O. Kitao, H. Nakai, T. Vreven, K. Throssell, J. A. Montgomery, Jr., J. E. Peralta, F. Ogliaro, M. J. Bearpark, J. J. Heyd, E. N. Brothers, K. N. Kudin, V. N. Staroverov, T. A. Keith, R. Kobayashi, J. Normand, K. Raghavachari, A. P. Rendell, J. C. Burant, S. S. Iyengar, J. Tomasi, M. Cossi, J. M. Millam, M. Klene, C. Adamo, R. Cammi, J. W. Ochterski, R. L. Martin, K. Morokuma, O. Farkas, J. B. Foresman, and D. J. Fox, *Gaussian 16, Revision B.01*, Gaussian, Inc., Wallingford CT, 2016.
- 63 R. Peverati and D. G. Truhlar, *Phys. Chem. Chem. Phys.*, 2012, **14**, 16187–16191.
- 64 M. Cossi, V. Barone, R. Cammi and J. Tomasi, *Chem. Phys. Lett.*, 1996, **255**, 327–335.
- 65 V. Barone, M. Cossi and J. Tomasi, *J. Chem. Phys.*, 1997, **107**, 3210–3221.
- 66 E. Cancès, B. Mennucci and J. Tomasi, *J. Chem. Phys.*, 1997, **107**, 3032–3041.

4

Selective depolymerisation

Selective recycling from plastic wastes stream



In 2014, Gregg Segal photographed people of all ages and backgrounds in different settings – water, beach and forest – surrounded by a week's worth of their rubbish, in Altadena, CA. The subjects were asked to collect and store their rubbish for a week.

With *7 Days of Garbage*, "I call attention to the problem of waste by personalizing it" Segal said.

7 Days of Garbage

Introduction

Even though it was demonstrated in the previous chapters that both the depolymerisations of PET and BPA-PC efficiently occurred using TBD:MSA (1:1) as catalyst, realistically these procedures imply the need for pre-emptive re-organisation of plastic wastes at the point of collection in order to only depolymerise the desired polymer. Thus, another challenge for plastic recycling is the design of depolymerisation processes that can selectively degrade one polymer without introducing contamination products from other plastics or other wastes (organic, glass, metals, ...) in general.

On this regard, different sorting techniques exist and are already employed in recycling plants. Manual sorting is feasible when plastic components are present in large amount but it is a laborious intensive work. Floating techniques involve the sorting of plastics regarding their density in different solvents, while less dense materials float, the heavier ones sink. Apart the low sustainability of this method as it involves the use of large quantities of solvent, polymers with similar densities, typically PVC and PET, cannot be separated using such technique. Finally, the most efficient instrumentation for sorting nowadays available is IR spectroscopy, especially near-IR, but they are still very expensive and not suitable for dark coloured plastics.¹ Other separation techniques exist at minor scales such as air sorting, X-ray or electrostatic sorting techniques but their expensiveness and the similarities in between commodity polymer structures regarding these technologies make them anecdotic.²⁻⁴ Even though the continuous development of sorting technologies can facilitate the plastic recycling in an economically efficient way, contamination may still be present. Therefore, it is important to find ways to selectively depolymerise one polymer from mixed plastics waste by control of process conditions. Ideally, the depolymerisation of a targeted polymer in between mixed plastics could be achieved by a careful tuning of the different reaction parameters such as temperature, catalyst loading, reaction time, etc. Despite the importance of demonstrating the depolymerisation in the

04. Selective depolymerisation

presence of waste streams, few studies are reporting this problem. For instance, in a recent study PLA and PET were selectively depolymerised using a commercial zinc catalyst. Authors were able to depolymerise both polymers in ethanol and methanol at high temperatures. Because of the large difference of reactivity between the two polymers, PLA methanolysis yielded lactate esters (65%) in 15 h at the boiling point of methanol, while PET remained unchanged. Then a simple filtration leads to the recovery of PET plastic pieces that can be then chemically recycled by conventional method.⁵ (Fig. 4.1A)

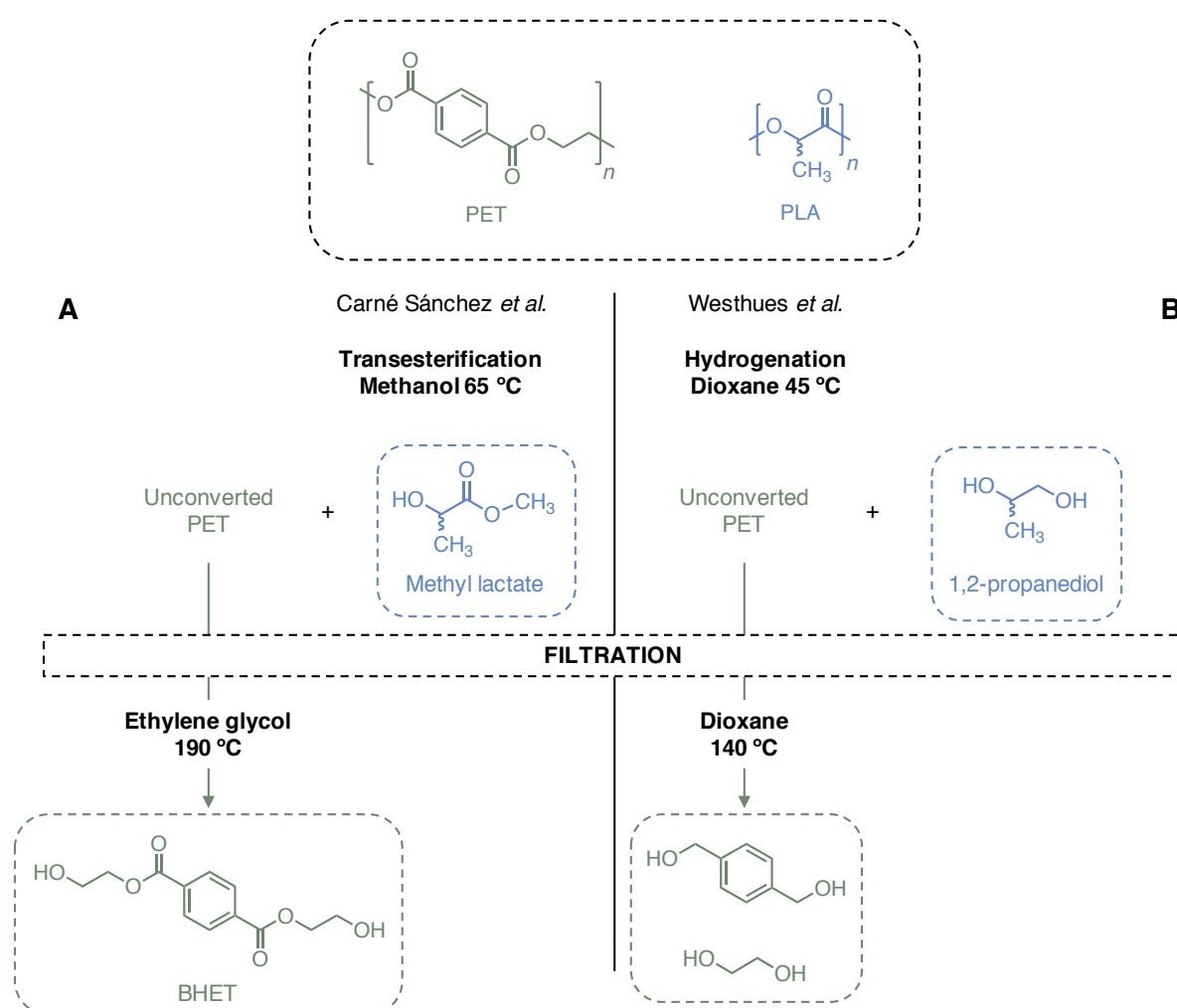


Figure 4.1. Selective depolymerisation of PET and PLA using two different reported procedures.

More recently, Westhues *et al.* have demonstrated the ability for a hydrogenolysis procedure involving the use of a ruthenium catalyst to selectively depolymerise PLA in the presence of PET. At 140 °C in 1,2-propanediol or 45 °C in dioxane, PLA is being completely hydrogenalised into 1,2-propanediol while PET remained unchanged. Its non-solubility in these solvents made easy the recovery of PET pellets for subsequent hydrogenolysis

at 120-140 °C in dioxane.⁶ (Fig. 4.1B) The same reaction was used for an entire half-litter bottle together with cap and label of PP and PE, respectively. The depolymerisation reached completion using 0.2 mol% of catalyst with polyolefins molten but unconverted. Similarly, a CD of BPA-PC was hydrogenolysed into BPA and methanol using 0.5 mol% of catalyst while, again, residue from coating stayed unconverted, demonstrating the tolerance of the procedure to other additives. One of the main drawbacks of this study was related with the use of ruthenium-based catalyst which is not only expensive but also moisture sensitive. In spite of the limitations of this organometallic catalysts, this study should be considered a precursor for future works in the depolymerisation field. Indeed, the tolerance of a system towards other polymers and metallic residue is a key challenge for the development of efficient chemical recycling techniques.

In a similar fashion, in this chapter the selective depolymerisations of BPA-PC and PET were performed. Inspired by the difference in reactivity predicted by the DFT calculations, the simultaneous depolymerisations of BPA-PC and PET were investigated with the aim of selectively degrade the two materials. By tuning the depolymerisation temperature and catalyst loading the selective depolymerisation of BPA-PC was fully achieved without depolymerising PET. Moreover, the selective depolymerisation was further extended to other nucleophiles with the aim of obtaining high added value material from BPA-PC in the presence of PET. Finally, the selective depolymerisation of BPA-PC and PET in the presence of PP was conducted to evaluate the effect of the possible contamination of polyolefins and to better model a mixed plastic waste stream.

1 PET vs BPA-PC reaction pathways

Interestingly, the comparison of the mechanisms and reaction conditions revealed that there may be a sufficient thermodynamic difference to enable the selective depolymerisation of BPA-PC in the presence of PET. Given the challenging nature of mechanical separation of BPA-PC from PET and other

04. Selective depolymerisation

waste plastics, this could present a useful technology to recover value from mixed plastic wastes. The comparison between the energy profiles of BPA-PC and PET depolymerisations – pathways presented here are computed using PCM⁷⁻⁹ with the dielectric constant of ethylene glycol ($\epsilon = 40.245$) – highlighted large energetic differences for both transition steps. (Fig. 4.2)

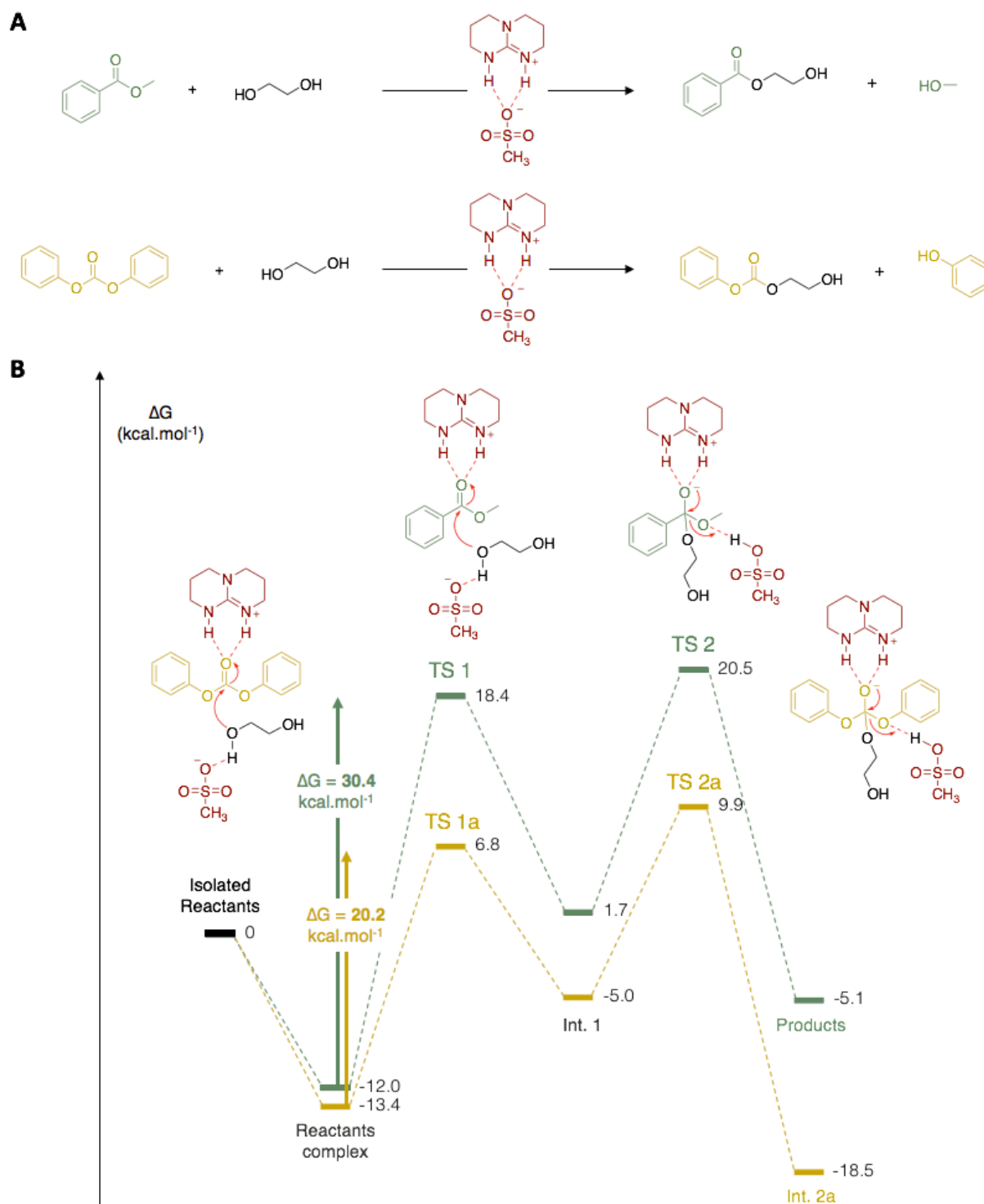


Figure 4.2. Comparison of the DFT-computed reaction pathways for the depolymerisations of BPA-PC (in yellow) and PET (in green) with ethylene glycol at the MN12SX/6-311++G(2df,2p) //

MN12SX/6-31+G(d,p) level of theory using PCM with the dielectric constant of ethylene glycol ($\epsilon = 40.245$).

2 Depolymerisation of BPA-PC and PET in ethylene glycol

2.1 Preliminary trial

Inspired by the difference in reactivity predicted by the DFT calculations, the concurrent depolymerisations of BPA-PC and PET was investigated with the aim of selectively degrade the two materials. The conditions for the depolymerisation of PET, optimised in chapter 2, were used, both polymer pellets were mixed in the same vial with the reagent in large excess and under nitrogen, using TBD:MSA (1:1) (0.5 eq.) as catalyst, at 180 °C. As expected, BPA-PC depolymerised first and an aliquot was taken at this time point to determine by ^1H NMR spectroscopy (DMSO- d_6 , 300 MHz, 298 K), the conversion into each molecule. While PET depolymerisation was completed, with no residual pellets of polymer in the vial, another ^1H NMR was performed to determine the final conversions. (Fig. 4.3A)

The depolymerisation of BPA-PC was completed in 20 min, raising 93% of BPA and 84% of ethylene carbonate. (Fig. 4.3B) These conversions were similar to the ones obtained when BPA-PC was solely depolymerised (89% of BPA and 83% of ethylene carbonate). At the same time point, BHET conversion reached less than 1%, confirming that BPA-PC can be fully depolymerised before PET. PET depolymerisation was completed after 10 h, yielding similar ratio of BHET than while PET was depolymerised alone (89%). However, the depolymerisation was 4 times longer in the present case. Probably, the presence of BPA and ethylene carbonate in the system disturbed the depolymerisation of PET that required extended time to be completed.

Moreover, the conversion of BPA diminished with time in the same proportion that the bis-carbonate BPA derivative – side product previously identified in chapter 3 – increased to yield 65% of BPA after 10h. In the same time, the signal corresponding to the ethylene carbonate seems to have disappeared

04. Selective depolymerisation

in the ^1H NMR spectra, which suggests the re-opening of the pre-formed cyclic carbonate. Thus, to avoid the degradation of BPA-PC depolymerisation products, a good option could be the subsequent degradation of the two polymers. Because of its insolubility in most of the solvent, PET could be very easily filtered off the reaction crude product and depolymerised in a second vial using the procedure tuned in chapter 2.

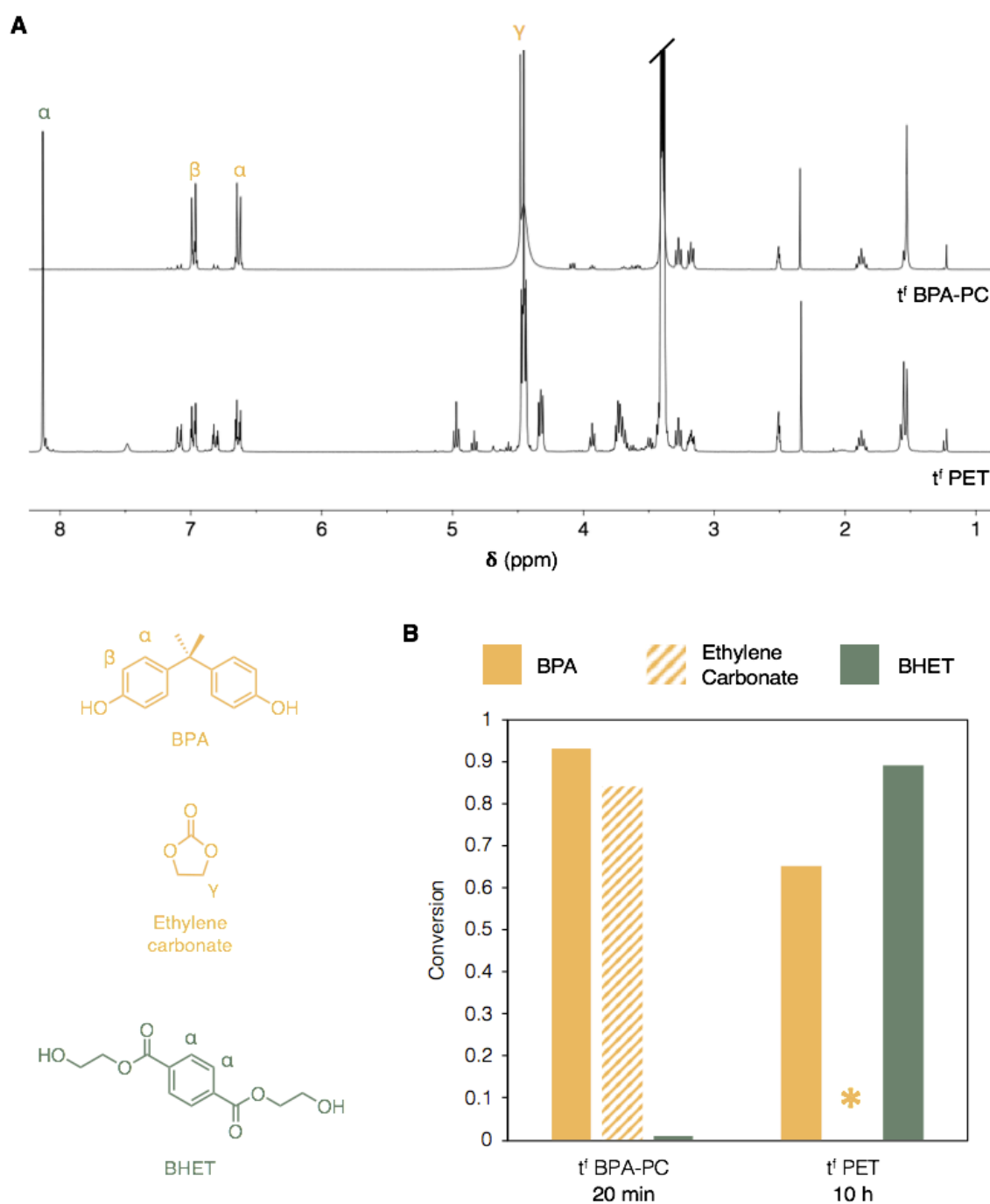


Figure 4.3. (A) Stacked ^1H NMR spectra at t^f BPA-PC and t^f PET for the selective depolymerisation of PET and BPA-PC using ethylene glycol as reagent and (B) corresponding conversion into each monomer. Conversions were determined by ^1H NMR spectroscopy in $\text{DMSO-}d_6$ from the crude product using the catalyst as internal standard ($\delta = 1.87$ ppm) and characteristic signals, BPA at $\delta =$

6.64 ppm, ethylene carbonate at $\delta = 4.48$ ppm and BHET at $\delta = 8.13$ ppm. Reaction conditions: BPA-PC (2 g, 7.8 mmol, 1 eq.), PET (1.5 g, 7.8 mmol, 1 eq.), TBD:MSA (1:1) (0.916 g, 3.9 mmol, 0.5 eq.), ethylene glycol (7.74 g, 124.8 mmol, 16 eq.), 180 °C.

2.2 Kinetic study using ethylene glycol as reagent

In order to gain insight of the behaviour of these successive depolymerisations, kinetic studies were conducted using different conditions including the temperatures and catalyst loading previously employed for the individual BPA-PC and PET depolymerisations – 130 and 180 °C, 0.15 eq and 0.5 eq, respectively.

First, the kinetic was followed using the milder conditions – the procedure conditions used for the depolymerisation of BPA-PC – heating at 130 °C and using 0.15 eq. of catalyst, but with an extended amount of ethylene glycol (16 eq.). (**Fig. 4.4A**) The conversions into BPA, BHET, and potential side-product resulting from BPA-PC depolymerisation were monitored by ^1H NMR spectroscopy in $\text{DMSO-}d_6$ for 48 h using the characteristic signals of each molecule. (**Fig. 4.4B**) As expected, BPA-PC depolymerised first yielding 95% of BPA after 10 h. At the same time point the amount of BHET obtained from PET depolymerisation did not exceed 2%. It should be noticed however, that after reaching a maximum, the BPA yield slightly decreased to 79% while the BPA-biscarbonate side-product described previously increased in the same proportion, from 8% at BPA-PC depolymerisation completion to 22% after 48 h. In the same time, PET only slightly depolymerised, reaching a 7% yield of BHET. Importantly, the depolymerisation of BPA-PC is not significantly affected by the presence of PET; under identical conditions, the depolymerisation of BPA-PC alone reached 94% conversion to BPA after 11 h. (**Fig. S4.1**)

Further kinetic studies under different conditions were performed in an attempt to fully depolymerise PET in the same reaction without affecting the selectivity of the process. When the reaction was conducted at 180 °C using 0.15 eq. of catalyst, full depolymerisation of BPA-PC was observed after 45 min, yielding 96% BPA (**Fig. 4.5**). As expected, the increase in temperature allowed for PET depolymerisation to occur after increased reaction times to

04. Selective depolymerisation

yield 88% of BHET after 31 h. However, similar to the reaction at 130 °C, the BPA yield decreased after completion of BPA-PC depolymerisation.

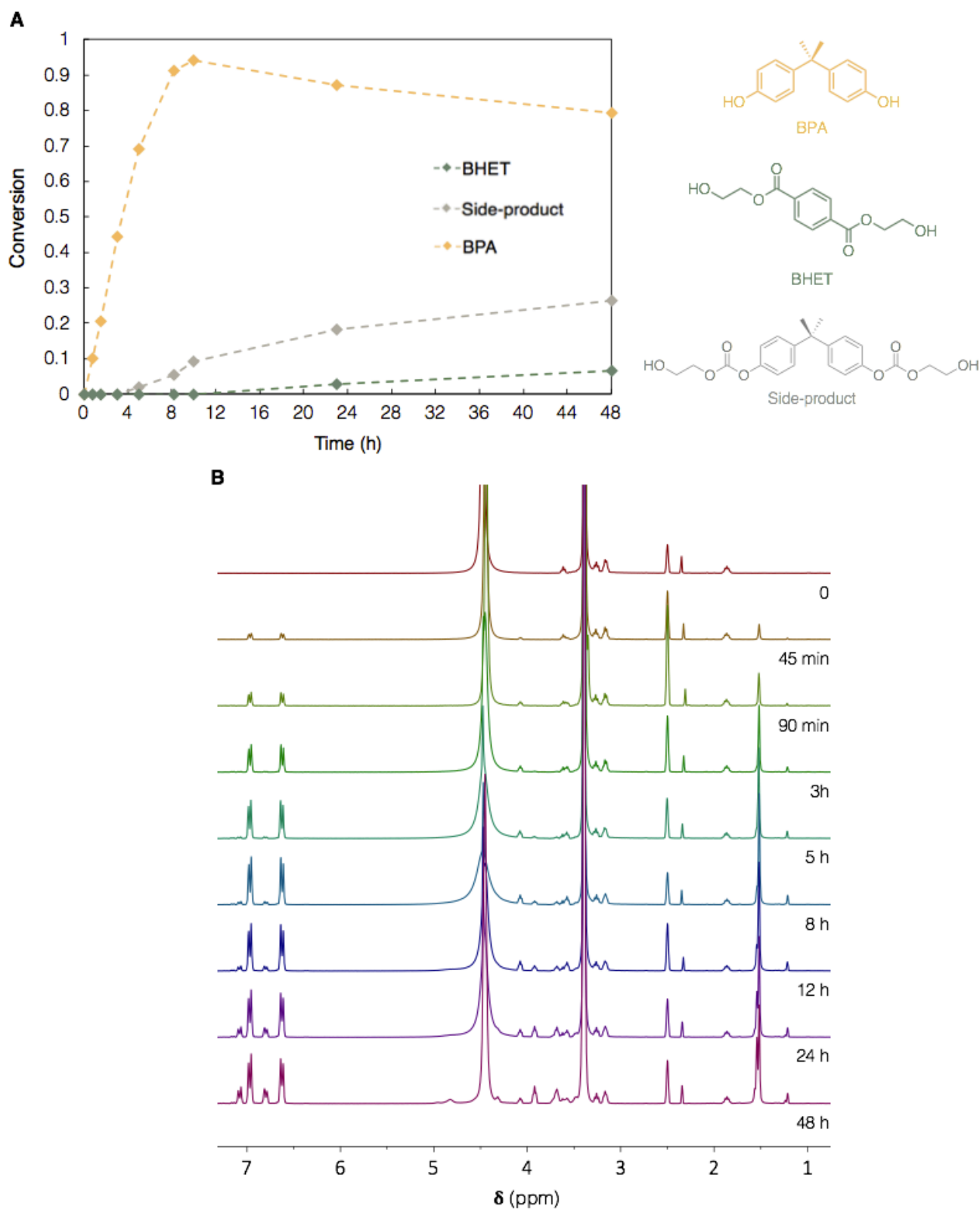


Figure 4.4. (A) Kinetic plot for the selective depolymerisation of BPA-PC (2 g, 7.80 mmol, 1 eq.) and PET (1.5 g, 7.80 mmol 1 eq.) using 0.15 eq. of TBD:MSA (1:1) as catalyst (0.277 g, 1.18 mmol) at 130 °C. The kinetic was followed by ¹H NMR spectroscopy in DMSO-*d*₆ using the catalyst signals as internal standard ($\delta = 1.87$ ppm), and the characteristic signals of BPA ($\delta = 6.66$ ppm), side-product

($\delta = 6.81$ ppm, 4H) and BHET ($\delta = 8.12$ ppm) and (B) corresponding stacked ^1H NMR spectra (DMSO- d_6 , 300 MHz, 298 K).

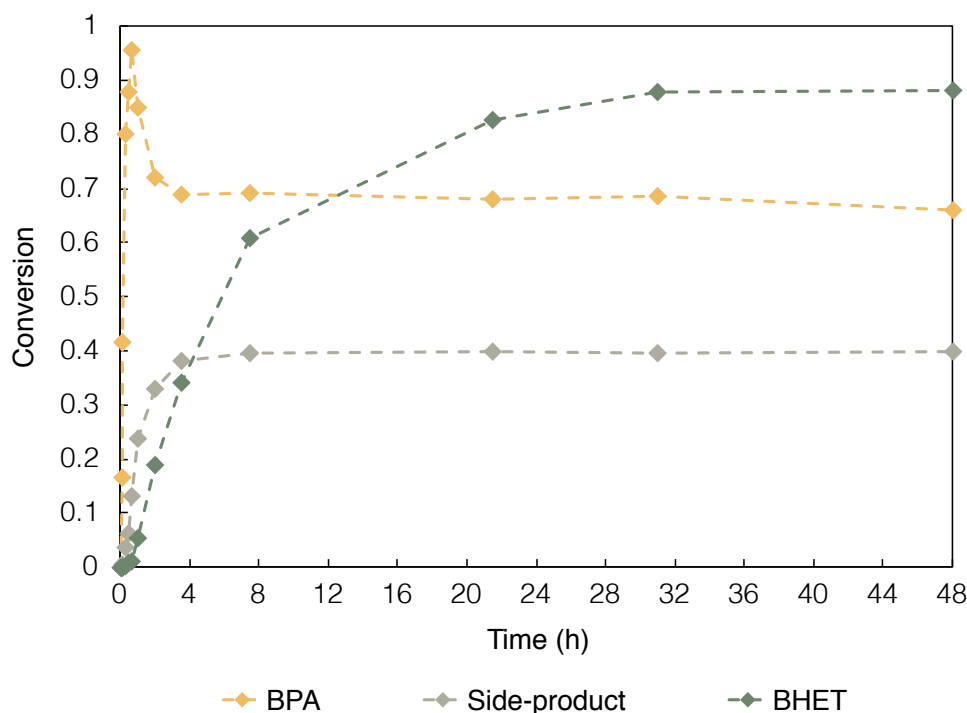


Figure 4.5. Kinetic plot for the selective depolymerisation of BPA-PC (2 g, 7.80 mmol, 1eq.) and PET (1.5 g, 7.80 mmol 1 eq.) using 0.15 eq. of TBD:MSA (1:1) as catalyst (0.277 g, 1.18 mmol) at 180 °C. The kinetic was followed by ^1H NMR spectroscopy in DMSO- d_6 using the catalyst signals as internal standard ($\delta = 1.87$ ppm), and the characteristic signals of BPA ($\delta = 6.66$ ppm), side-product ($\delta = 6.81$ ppm, 4H) and BHET ($\delta = 8.12$ ppm) – Fig. S4.2.

Additional experiments were conducted employing a higher amount of catalyst (0.5 eq.) to increase the rate and potentially reduce the side-product formation.

At 130 °C, reaction is faster using 0.5 eq. of catalyst, being completed in 3 h, but BPA only yields 85 % before suffering drop down to 78% in the same time that the increasing of the side-product yields 23%. (Fig. 4.6A) These conversions then stay constant, from 10 h of reaction until the end of the measurements. In the same time, PET degrades slowly, only attaining 51% of BHET after 48 h.

Finally, at 180 °C, the behaviour for BPA-PC depolymerisation is very similar than while using 0.15 eq. of catalyst, full depolymerisation occurs after 20 min to yield 96% of BPA. (Fig. 4.6B) Similar to previous reactions, BPA yield reduces after completion of BPA-PC depolymerisation to reach a plateau while side-product yields increase in the same proportions. However, if using

04. Selective depolymerisation

0.5 eq. of catalyst, BPA yield rapidly drops down to 64% (after 3 h), with 0.15 eq. of catalyst, the yield of BPA stabilises at 78% after 8 h.

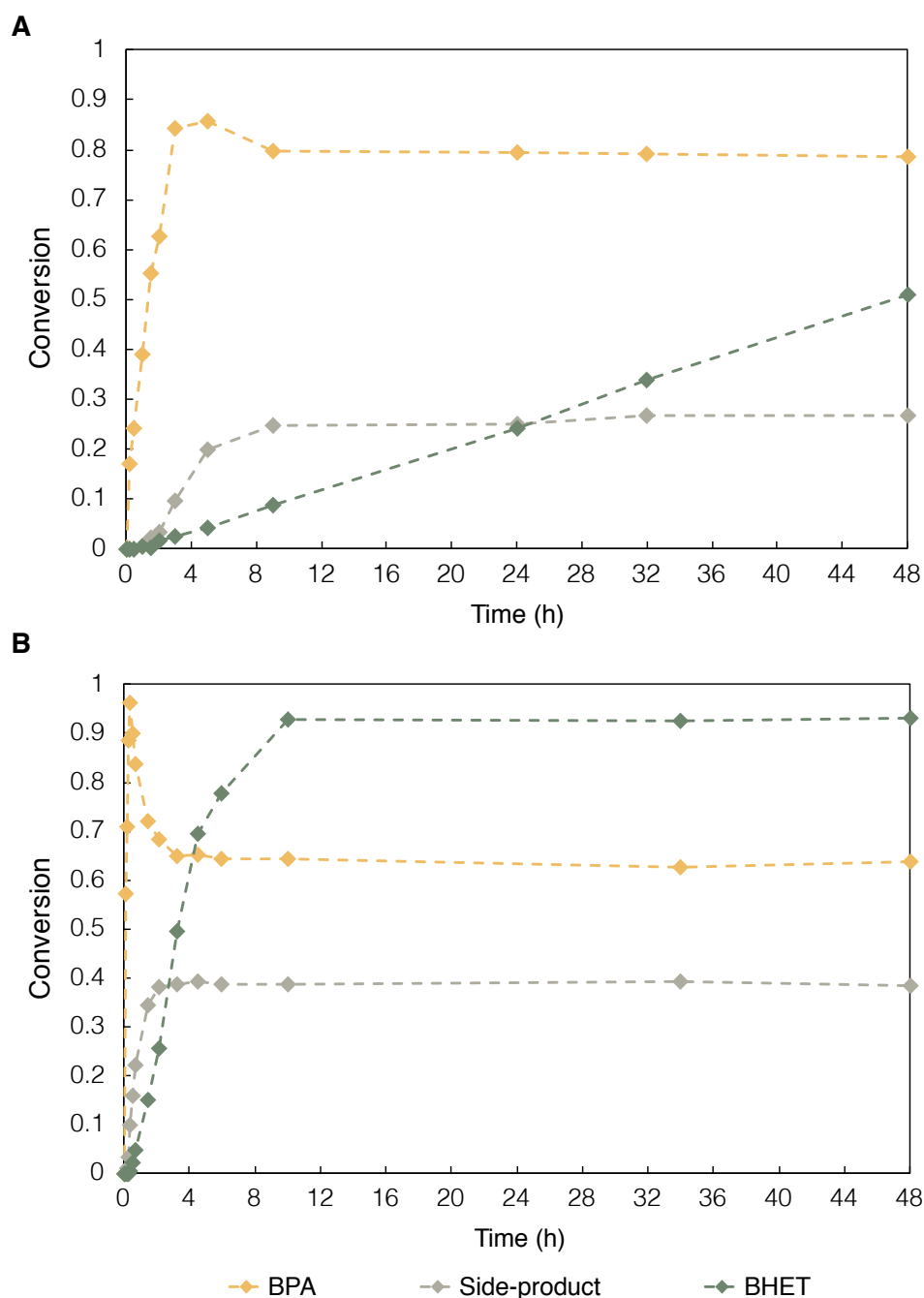


Figure 4.6. Kinetic plot for the selective depolymerisation of BPA-PC (2 g, 7.80 mmol, 1 eq.) and PET (1.5 g, 7.80 mmol 1 eq.) using 0.5 eq. of TBD:MSA (1:1) as catalyst (0.917 g, 3.90 mmol) in ethylene glycol (7.74 g, 124.8 mmol, 16 eq.) at (A) 130 °C and (B) 180 °C. The kinetic was followed by ^1H NMR spectroscopy in $\text{DMSO-}d_6$ using the catalyst signals as internal standard ($\delta = 1.87$ ppm, 4H), and the characteristic signals of BPA ($\delta = 6.66$ ppm), side-product ($\delta = 6.81$ ppm) and BHET ($\delta = 8.12$ ppm) – Fig. S4.3 & S4.4.

Thus, increasing the catalyst content from 0.15 eq. to 0.5 eq. was fastening the reactions but also favouring the rapid formation of the undesired BPA-biscarbonate side-product (from 22 to 39% at 130 °C and from 26 to 38% at 180 °C).

3 Depolymerisation of BPA-PC and PET in other reagents

3.1 Ethylene diamine and ethanolamine

Two other reagents were employed for the depolymerisation reaction, ethylene diamine and ethanolamine. Similar to the reaction employing ethylene glycol, both polymer pellets were mixed in the same vial with the reagent and the catalyst, under nitrogen. An aliquot was kept for ^1H NMR spectroscopy analysis (DMSO- d_6 , 300 MHz, 298 K), while each depolymerisation was completed to determine the conversion into each monomer. Both reagents were successfully used in chapter 3 for the depolymerisation of BPA-PC and gave the corresponding cyclic urea, **imidazolidin-2-one** for the reaction with ethylene diamine and the corresponding linear urea, **BHEU**, for the reaction with ethanolamine. Both reagents have been also reported for the depolymerisation of PET, yielding to the corresponding terephthalamides, **BAETA** and **BHETA** while employing ethylene diamine and ethanolamine, respectively.¹¹ (Figs. 4.7 & 4.8) Following the procedure for PET depolymerisation – using TBD as catalyst – encountered in literature, reactions were conducted at 110 °C using 8 eq. of reagent and 0.2 eq. of catalyst. Similar to glycolysis, depolymerisation of BPA-PC occurred first, almost instantaneously for ethylene diamine, in less than a minute, and in 5 min with ethanolamine. (Figs. 4.7A & 4.8A) Both reactions yielded BPA in outstanding yields (99% for ethylene diamine and 97% for ethanolamine) while **imidazolidin-2-one** reached 95% and **BHEU** 91%. At this time point the BHET conversion raised 4% and less than 9% while employing ethylene diamine and ethanolamine, respectively. (Figs. 4.7B & 4.8B)

04. Selective depolymerisation

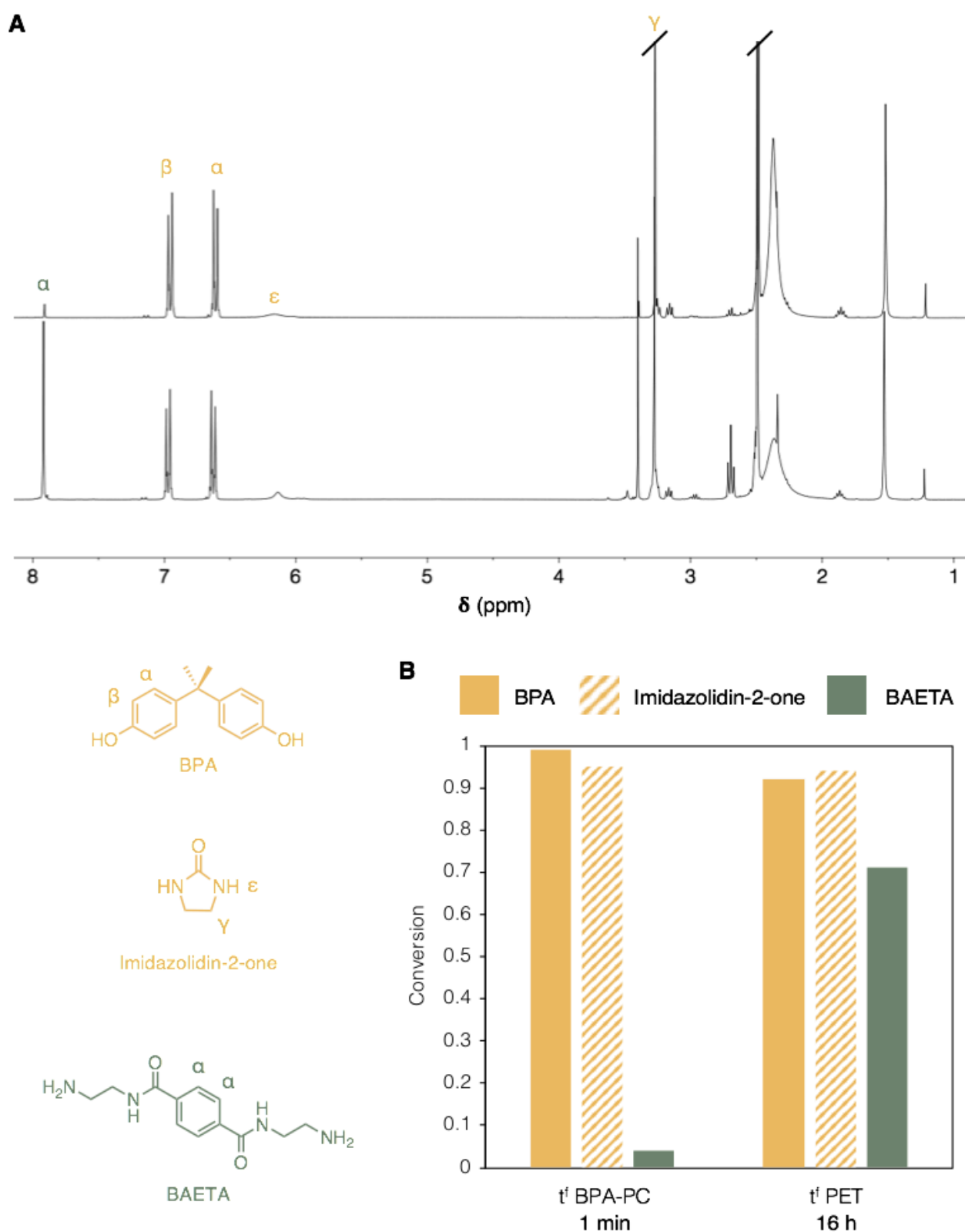


Figure 4.7. (A) Stacked ^1H NMR spectra at t^f BPA-PC and t^f PET for the selective depolymerisation of PET and BPA-PC using ethylene diamine as reagent and (B) corresponding conversion into each monomer. Conversions were determined by ^1H NMR spectroscopy in $\text{DMSO-}d_6$ from the crude product using the catalyst as internal standard ($\delta = 1.87$ ppm) and characteristic signals, BPA at $\delta = 6.64$ ppm, imidazolidin-2-one at $\delta = 3.27$ ppm and BAETA at $\delta = 7.92$ ppm. Reaction conditions: BPA-PC (2 g, 7.8 mmol, 1 eq.), PET (1.5 g, 7.8 mmol, 1 eq.), TBD:MSA (1:1) (0.367 g, 1.56 mmol, 0.2 eq.), ethylene diamine (3.75 g, 62.4 mmol, 8 eq.), 110 °C.

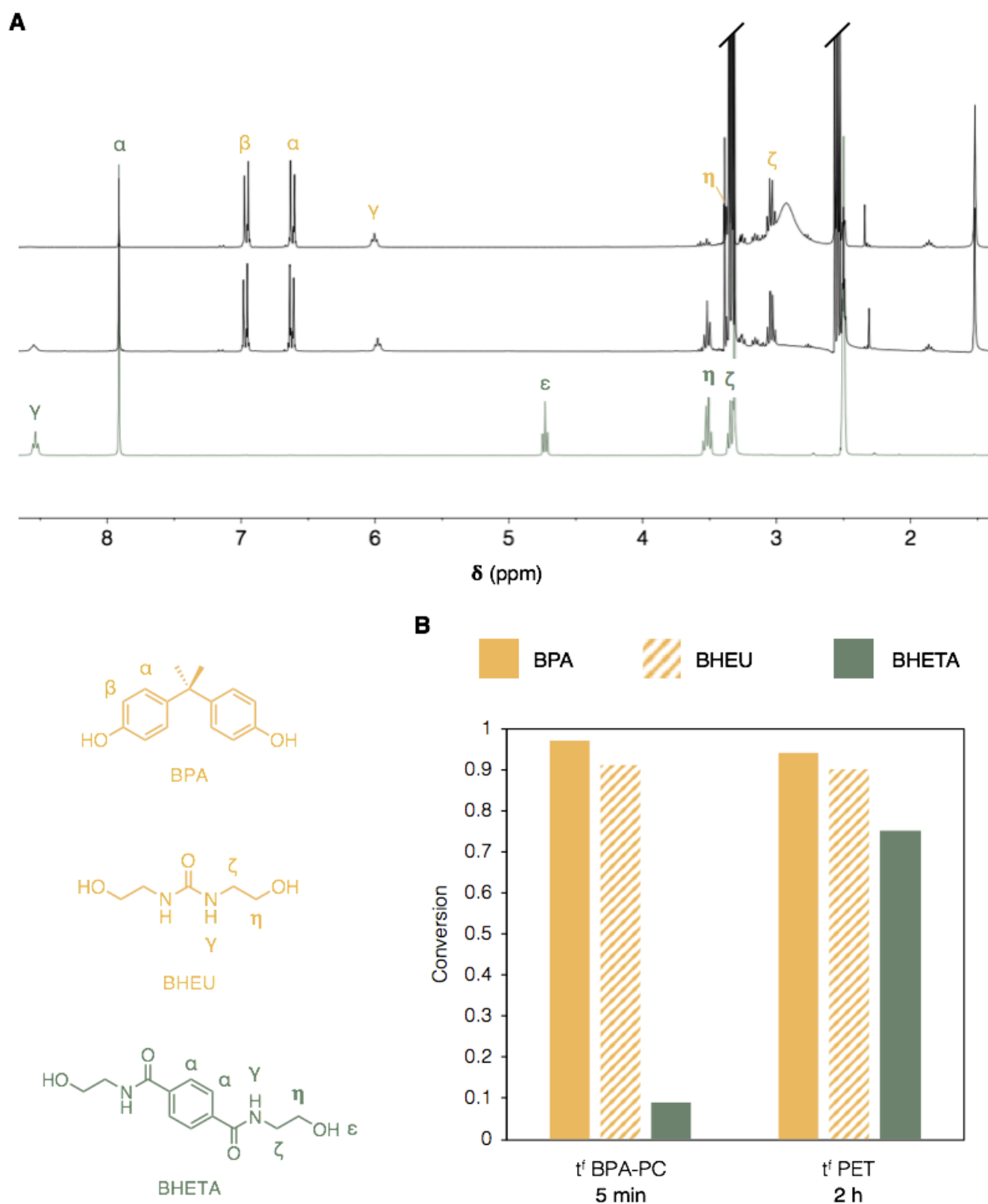


Figure 4.8. (A) Stacked ^1H NMR spectra at t^f BPA-PC and t^f PET for the selective depolymerisation of PET and BPA-PC using ethanolamine as reagent and (B) corresponding conversion into each monomer. Conversions were determined by ^1H NMR spectroscopy in $\text{DMSO-}d_6$ from the crude product using the catalyst as internal standard ($\delta = 1.87$ ppm) and characteristic signals, BPA at $\delta = 6.64$ ppm, BHEU at $\delta = 3.05$ ppm and BHETA at $\delta = 7.91$ ppm. Reaction conditions: BPA-PC (2 g, 7.8 mmol, 1 eq.), PET (1.5 g, 7.8 mmol, 1 eq.), TBD:MSA (1:1) (0.367 g, 1.56 mmol, 0.2 eq.), ethanolamine (3.81 g, 62.4 mmol, 8 eq.), 110 °C.

04. Selective depolymerisation

After 2 h in the case of ethanolamine, the PET depolymerisation was also completed, which is in good agreement with literature as they reported the same reaction time at 120 °C while using TBD as catalyst. At this time point, conversion into both BPA and **BHEU** remained almost unchanged (94% and 90%, respectively) while conversion of **BHETA** yielded 75%. It is a good but probably underestimated conversion as the signals used as reference to calculate the conversion here are the aromatic signals (other signals being overlapped by the reagent signals).

On the contrary, the reaction with ethylene diamine was completed after 16 h, a largely extended time compared to the 1 h at 110 °C reported in literature. It was visible that the stirring was difficult because of the high viscosity of the mixture. It is possible that BPA and/or the **imidazolin-2-one** obtained was/were not completely soluble with the reagent and complicated the reaction stirring as well as the catalytic abilities of TBD:MSA (1:1). However, the conversions into both BPA and **imidazolidin-2-one** were very similar after 16 h (92% and 94%, respectively) while **BAETA** ratio reached 71%. For this reaction also and for the same reason than while using ethylene diamine, **BAETA** conversion is probably underestimated.

Additionally, for the reaction with ethanolamine, **BHETA** precipitated while cooling down the reaction at t^f PET. After mixing the crude product with a minimal amount of acetone, a white solid was recovered by filtration (76%). This yield is superior to the conversion obtained while using the aromatic protons for calculating the reaction rate (71%). This confirms that the conversion into the corresponding monomer was underestimated for the depolymerisation of PET.

3.2 Glycerol and allyl ether

In the objective of recovering high added value monomers from BPA-PC depolymerisation from plastic wastes stream, the selective depolymerisation was performed in the presence of PET using diols with higher functionalisation. To this end, an equimolar mixture of BPA-PC and PET was treated with 6 eq. of (1) glycerol (**1h**) and (2) the functionalised diol **1w** using

the temperatures and catalyst loading described in chapter 3. (Fig. 4.9) Both crude products were then analysed through ^1H NMR spectroscopy ($\text{DMSO-}d_6$, 300 MHz, 298 K) to determine the conversions into each molecule.

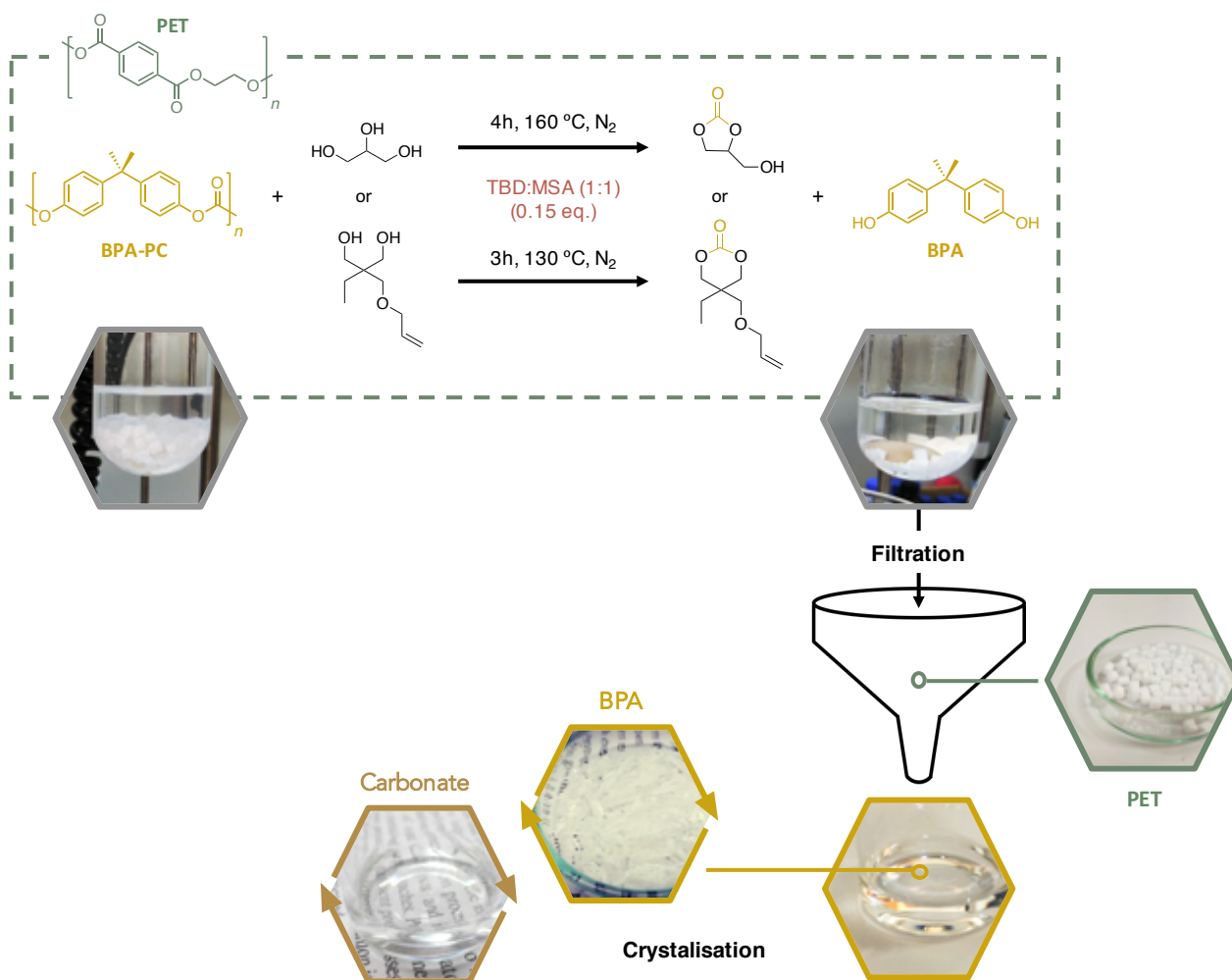


Figure 4.9. Selective depolymerisation of BPA-PC in the presence of PET using **1h** or **1w** (23.4 mmol, 6 eq.) as nucleophile. Reaction conditions: BPA-PC (2 g, 7.8 mmol, 1 eq.), PET (1.5 g, 7.8 mmol, 1 eq.), TBD:MSA (0.277 g, 1.17 mmol, 0.15 eq.).

Even in the presence of PET pellets, the depolymerisation with **1h**, performed at $160\text{ }^\circ\text{C}$, using 0.15 eq. of TBD:MSA (1:1) catalyst, was completed in 4 h reaching 98% of BPA and 94% of cyclic carbonate. Even though the reaction time is slightly extended, no difference in the final conversion of BPA or the cyclic carbonate (**2h**) could be noticed compared to the depolymerisation performed without PET (99% for BPA and 94% for carbonate). In the same time, no BHET signals were observed in the ^1H NMR spectra of the final crude products. (Fig. S4.5)

04. Selective depolymerisation

Finally, the equimolar mixture of BPA-PC and PET was treated with the functionalised diol **1w** (6 eq.) with 0.15 eq. of TBD:MSA (1:1) catalyst at 130 °C. After stirring for 3 h, the depolymerisation was completed yielding 96% conversion for BPA and 98% for the cyclic carbonate **2w**. (Fig. S4.6) Using the simple filtration of the residual PET pellets (in quantitative yield) enabled the isolation of BPA and the 6-membered cyclic carbonate, **2w**, in excellent yields 83% and 81%, respectively. Notably, no signals attributable to BHET were observed in the ¹H NMR spectra of the crude carbonate/BPA product mixture. The PET pellets could then be sequentially depolymerised at higher temperature and catalyst loading.

4 Reactions in the presence of other polymers

4.1 Depolymerisation in the presence of PP

The selective depolymerisation of BPA-PC and PET in the presence of PP was conducted to evaluate the effect of the possible contamination of polyolefins and to better model a mixed plastic wastes stream. In order to obtain both BPA and BHET in a reasonable time and in good yields while avoiding the formation of side-product, the reaction was performed at 180 °C with 0.15 eq. of catalyst. (Fig. 4.10)

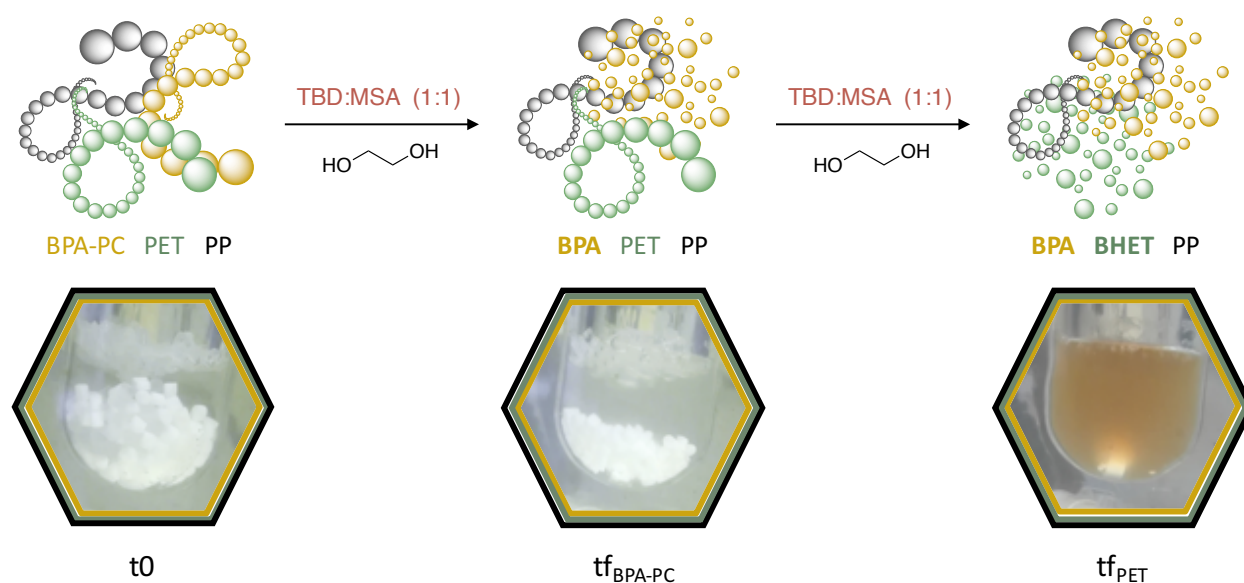


Figure 4.10. Successive depolymerisations of BPA-PC and PET using ethylene glycol in the presence of PP. Reaction conditions: BPA-PC (2 g, 7.80 mmol, 1eq.), PET (1.5 g, 7.80 mmol 1 eq.), PP (0.98 g,

23.4 mmol, 3 eq.), ethylene glycol (7.74 g, 124.8 mmol, 16 eq.) and TBD:MSA (1:1) as catalyst (0.275 g, 1.17 mmol, 0.15 eq), 180 °C.

The reaction times and ¹H NMR spectroscopic characterisation of the crude product after disappearance of BPA-PC (40 min.) and PET (30 h) pellets respectively demonstrated little to no interference from PP. (Fig. S4.7 & S4.8) The conversion to monomers were similar, with 70% of BPA and 88% of BHET obtained when both depolymerisations were completed. GPC analysis of the recovered PP demonstrated that no degradation was observed under these conditions (Fig. S4.11).

4.2 Depolymerisation in the presence of PVC

The same procedure has been applied to the selective depolymerisation of BPA-PC and PET in the presence of PVC – 0.15 eq. of catalyst at 180 °C – but after 96 h, either the depolymerisation of BPA-PC or PET were completed with PVC pellets in the mixture – conversions reach 2% for BPA-PC and 10% for PET. (Fig. S4.9) The reaction has been also performed with 0.5 eq. of catalyst but even though conversions into BPA and BHET are better, the analysis of the crude product still demonstrates poor performances after 4 days – 24% and 32% for BPA and BHET, respectively. (Fig. S4.10) Notably, here BPA-PC did not depolymerise before PET, and the conversion was higher for BHET than BPA. Additionally, the reaction mixture in both cases very rapidly turned brown to end completely black after 96 h.

It was previously pointed out that PET and PVC are incompatible for recycling as even a small amount of one can contaminate the depolymerisation of the other. Quantities as low as 0.001% of PVC in a PET batch can severely degrade the polymer because of the releasing of hydrochloric acid gas at the high temperature required to melt and reprocess PET.¹²⁻¹⁴ Thus, the selective depolymerisation of PC or PET in the presence of PVC was not investigated further.

Conclusion

It was demonstrated in this part that the procedure developed in the last chapters also allows the depolymerisation of several polymers in a mixed batch. Indeed, the difference of reactivity between polymers such as PET and BPA-PC leads to their possible subsequent depolymerisations and recovery of the obtained molecules in one-pot.

Through the different reactions presented in this chapter, it has been proven the possibility to (1) depolymerise successively BPA-PC and PET using different reagents to reach similar yields of products than while individually recycled, (2) selectively depolymerise BPA-PC to yield high added value cyclic carbonates and BPA with no disruption of PET present in the vial and (3) afford the same depolymerisation performances in the presence of another commodity plastic – *i.e.* PP – with no changes in the reaction time or yields of molecules obtained. (Fig. 4.11)

Nevertheless, the kinetic studies revealed that, in the case of ethylene glycol, the cyclic carbonate resulting in the BPA-PC depolymerisation can be degraded during the extended time required to complete PET depolymerisation. Thus, a preferable method in this case would involve the filtration of PET pellets at the time point of the BPA-PC depolymerisation completion for, from one side, recovering the BPA and cycling carbonate and, from another side, recovering the PET pellets that could be subsequently depolymerised using conventional methods such as the one described in chapter 2.

These experiments reveal the great adaptability of the procedure described in the last chapters.

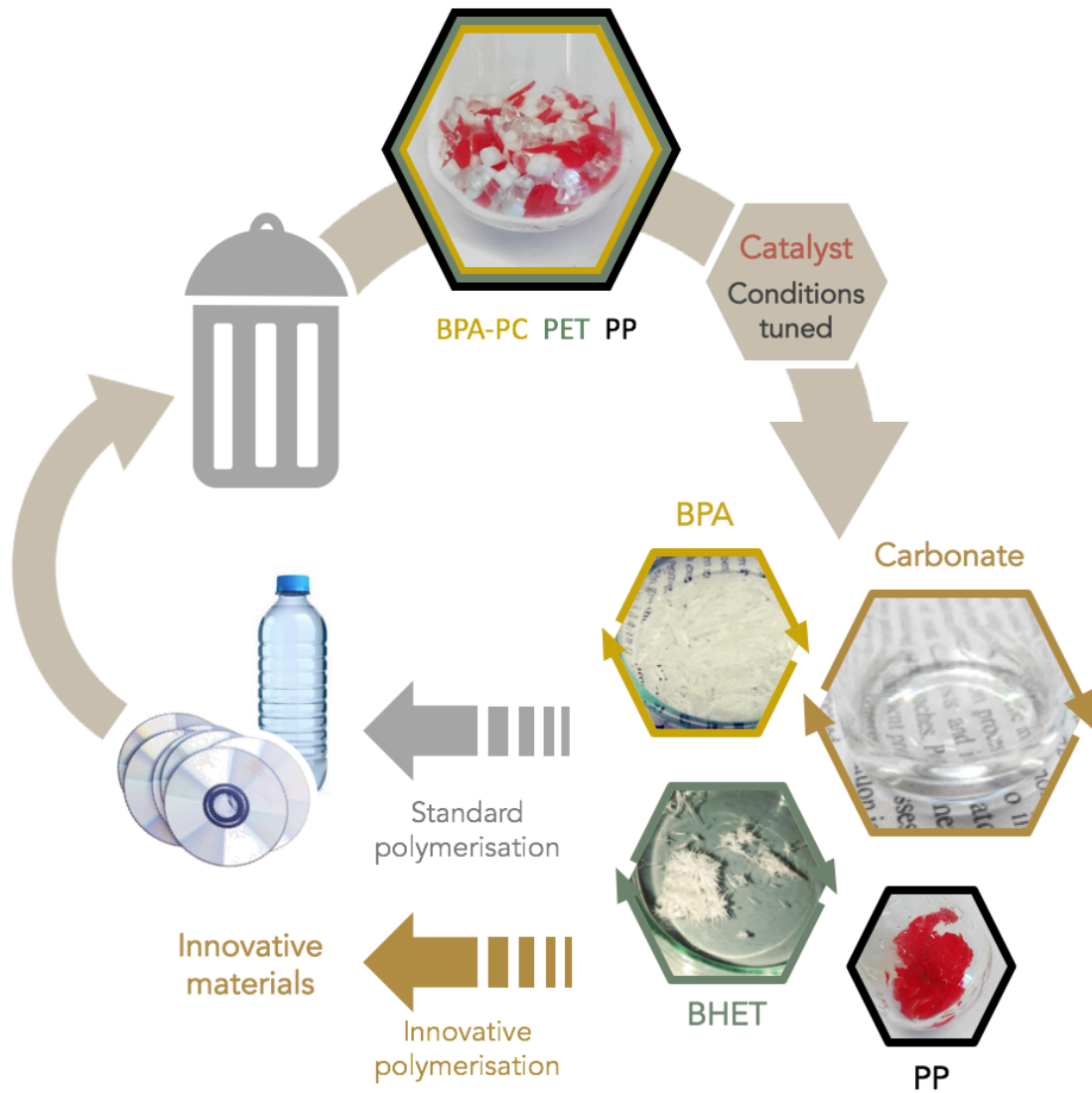


Figure 4.11. The selective depolymerisation of BPA-PC and PET from mixed plastic wastes following the procedure employed in chapter 4.

References

- 1 A. Turner, *Environ. Int.*, 2018, **117**, 308–318.
- 2 B. Ruj, V. Pandey, P. Jash and V. K. Srivastava, *Int J. Appl. Sci. Eng. Res.*, 2015, **4**, 564–571.
- 3 R. Geyer, J. R. Jambeck and K. L. Law, *Sci. Adv.*, 2017, **3**, e1700782.
- 4 I. A. Ignatyev, W. Thielemans and B. Vander Beke, *ChemSusChem*, 2014, **7**, 1579–1593.
- 5 A. Carné Sánchez and S. R. Collinson, *Eur. Polym. J.*, 2011, **47**, 1970–1976.
- 6 S. Westhues, J. Idel and J. Klankermayer, *Sci. Adv.*, 2018, **4**, eaat9669.
- 7 M. Cossi, V. Barone, R. Cammi and J. Tomasi, *Chem. Phys. Lett.*, 1996, **255**, 327–335.
- 8 V. Barone, M. Cossi and J. Tomasi, *J. Chem. Phys.*, 1997, **107**, 3210–3221.
- 9 E. Cancès, B. Mennucci and J. Tomasi, *J. Chem. Phys.*, 1997, **107**, 3032–3041.
- 10 C. Jehanno, I. Flores, A. P. Dove, A. J. Müller, F. Ruipérez and H. Sardon, *Green Chem.*, 2018, **20**, 1205–1212.
- 11 K. Fukushima, J. M. Lecuyer, D. S. Wei, H. W. Horn, G. O. Jones, H. A. Al-Megren, A. M. Alabdulrahman, F. D. Alsewailem, M. A. McNeil, J. E. Rice and J. L. Hedrick, *Polym. Chem.*, 2013, **4**, 1610–1616.
- 12 J. Hopewell, R. Dvorak and E. Kosior, *Philos. Trans. R. Soc. B Biol. Sci.*, 2009, **364**, 2115–2126.
- 13 K. Hamad, M. Kaseem and F. Deri, *Polym. Degrad. Stab.*, 2013, **98**, 2801–2812.
- 14 *The new plastics economy - Catalysing action*, 2017.

5

Conclusions & Perspectives

In this thesis different ways of chemically recycle commodity polymers were explored and, on this purpose, a cheap and thermoresistant innovative organocatalyst has been synthesised from the equimolar mixture of a common base, TBD, and a common acid, MSA. The exceptional thermal stability, up to 400 °C, of the so-formed protic ionic salt made it a preferential candidate for high temperature depolymerisation reactions.

The depolymerisation of commonly used plastics was considered, starting with the most recycled polymer, PET. The glycolysis of this polymer in a solvent-free procedure has led to very high yields of the corresponding monomer, BHET, up to 92%. The catalyst was recycled up to 5 times with no loss of catalytic activity and the subsequent polymerisation of BHET was also catalysed by TBD:MSA (1:1) to obtain virgin-like rPET, closing the polymer to monomer to polymer loop.

The same procedure was applied to the depolymerisation of BPA-PC using various nucleophiles to yield excellent conversion into BPA, its industrial monomer, and carbonyl-containing molecules. By wisely choosing the reagent and tuning the reaction conditions, 5- and 6- membered cyclic carbonates were obtained in reasonable to excellent yields, constituting a phosgene-free, 100% atom economy procedure for the ring-closing of valuable carbonates widely reported for the synthesis of high performance materials. Similarly, innovative linear carbonates and ureas were obtained.

DFT methodology was employed for determining the mechanisms involved for both reactions – with PET and with BPA-PC. The obtained pathways exhibited similar chemical interactions but with a large energetic difference, inspiring the possibility for these two polymers to be recycled in the same batch. Using the different reagents and different reaction conditions investigated in the previous chapters, the simultaneous depolymerisations of BPA-PC and PET were explored. Several conclusions have been made, (1) BPA-PC can be depolymerised into the corresponding monomers with no depolymerisation of PET, (2) PET can be then depolymerise in the same batch to recover all monomers at the end of the reaction or, PET pellets can be

05. Conclusions & Perspectives

filtered after the completion of BPA-PC depolymerisation to be depolymerised apart, and, (3) both polymers can be recycled in the presence of commodity polyolefins with no disturbance of the reaction.

Thus, using an innovative recyclable organocatalyst in a solvent-free procedure, PET has been depolymerised in a circular economy approach, the upcycling of BPA-PC has led to the formation of valuable building blocks for subsequent polymerisations, and the selective depolymerisation of both polymers has demonstrated the ability of this process to be performed in a mixed plastic wastes stream. These results open the way to new perspectives for the efficient chemical recycling of commodity polymers and, based in the current findings, future works can be envisaged. (Fig. 5.1)

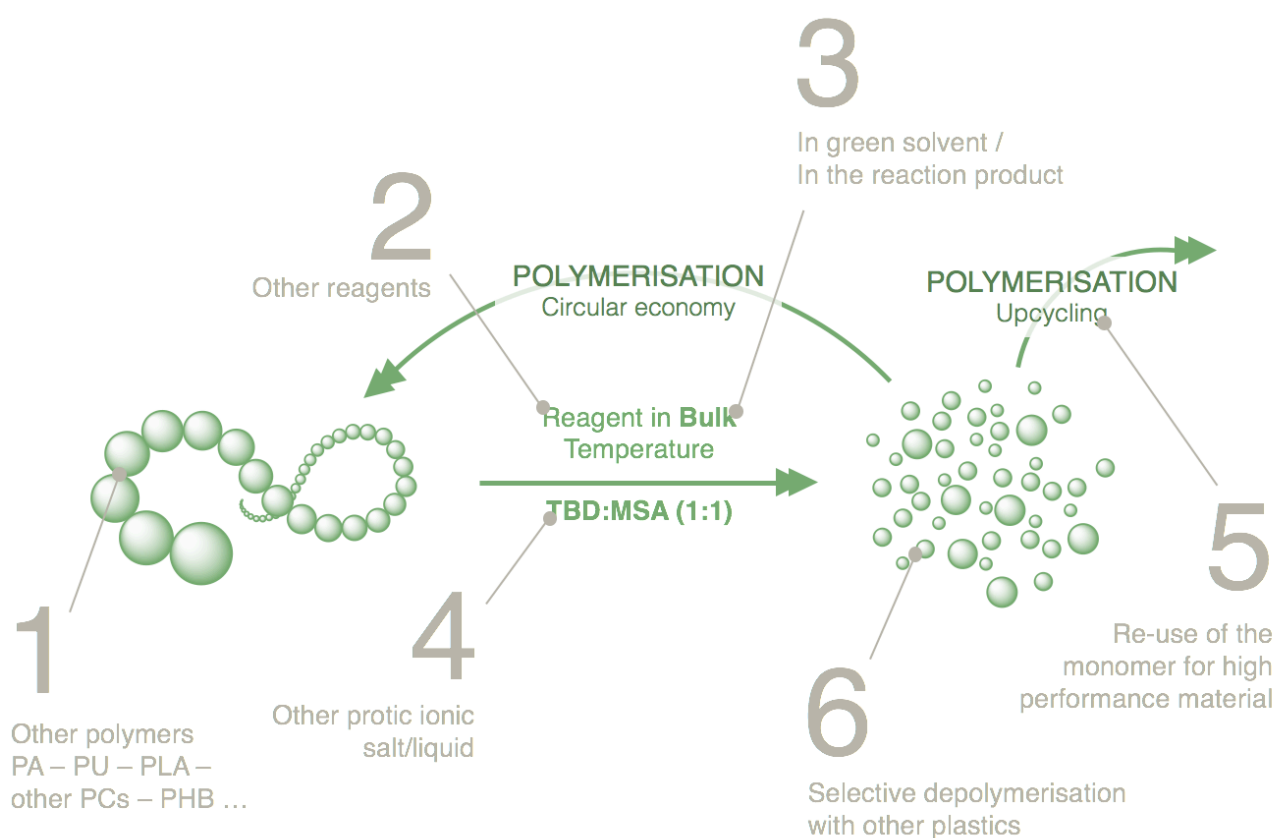


Figure 5.1. Future works based on the findings detailed in this thesis

1. Other commodity polymers and in particular other oxygen-containing polymers could be depolymerised using the same catalyst and procedure. PA, PLA or PU could be for example degraded through the same transesterification reaction. Indeed, while depolymerisation of PLA is currently under investigation using the same kind of procedure, PU

flexible foam has already been successfully depolymerised using TBD:MSA (1:1). The characterisation of the obtained product is more complex compared to the present study with PET or BPA-PC as the depolymerisation of flexible foam practically requires a huge amount of reagent to be performed in bulk, which renders the analysis of the crude product difficult, but investigations are on-going.

2. Although a large bench of nucleophiles has been tested in the present work, in particular for the depolymerisation of BPA-PC, infinite possibilities exist for the synthesis of new compounds. Here, reagents have been chosen because they were commercially available, non-CMR and cheap – except cysteamine, 3-aminopropane-1,2-diol, 1,1,1-Tris(hydroxymethyl)propane that raise around 1 200 euros per kilo, none of the reagents overtake 500 euros per kilo. However, easy-to-prepare or easy-to-extract – bio-sourced for example – nucleophiles could be also considered.
3. In a solvent-free and greener perspective, reactions have been all performed in bulk, which has complicated sometimes the reaction (high viscosity, low boiling point, high melting point, low degradation temperature, ...) and the purification of the products. Using green solvent or directly performing the reaction in the product (in the case of ethylene or propylene carbonate for example) could be another approach, in particular to obtain cyclic carbonates from the depolymerisation of BPA-PC, as decreasing the quantity of starting reagent can constrain the reaction to the formation of cyclic carbonates instead of their linear analogues.
4. If TBD:MSA (1:1) has performed remarkably for the reactions presented here, this is only one example of the acid-base mixtures possibly catalysing depolymerisation reactions. Once again, if acid-base mixtures have been already tested for common polymerisation reactions, the same catalysts for depolymerisation stayed anecdotic in literature. The DFT calculations presented in this study demonstrated the importance

of the dual activation in the transesterification mechanism occurring for those depolymerisations. Thus, other acid-base mixtures, synthesised from other organic acids or bases and/or in different ratios, could be suitable for different depolymerisation reactions.

5. Only few examples were pointed out herein about the reported re-use of the depolymerisation products for subsequent syntheses of innovative materials. But all the molecules obtained could potentially be then employed as monomers, cyclic carbonates for ring opening polymerisation, linear ureas or carbonates for poly-condensation of innovative materials.
6. Finally, the selective depolymerisation of BPA-PC and PET in one pot could be extrapolate to a larger variety of polymers. Other polymers such as PU, PLA or other PCs could be depolymerised *via* the same or a similar method as well as the depolymerisation of more than two polymers could be undergone subsequently.

Nowadays, politicians, industrials and scientists are realising the environmental emergency we are facing but, even more important, citizens, and especially young generations are more and more conscious of the challenges regarding climate change, depletion of finite resources or wastes accumulation in the environment, consequently, important citizen moves are raising all over the world. **(Fig. 5.2A)** If environmentalist associations or ONG were already considering the climate change as a major problem and taking actions since decades, the catastrophic impact of the millions of tons of plastic wastes encountered in the ocean is now a growing topic for these organisations. **(Fig. 5.2B)** In the same time, governments and interstate institutions are slowly but constantly legislating in the way of limiting the use of plastics, in particular single-use plastic items. In April 2015, the European parliament adopted a directive (2015/720) for banning plastic bags for all member states. Similarly, discussions are currently on the table for a ban in a near future of other single-use items such as plastic cotton buds, cutlery, plates, straws or drink stirrers while others will be use with limitations including

food containers and drink cups. (Fig 5.2C) In parallel, start-ups are emerging with innovative solutions for solving the daily problems people are facing to reduce their use of plastics by launching new kind of products on the market. (Fig. 5.2D)

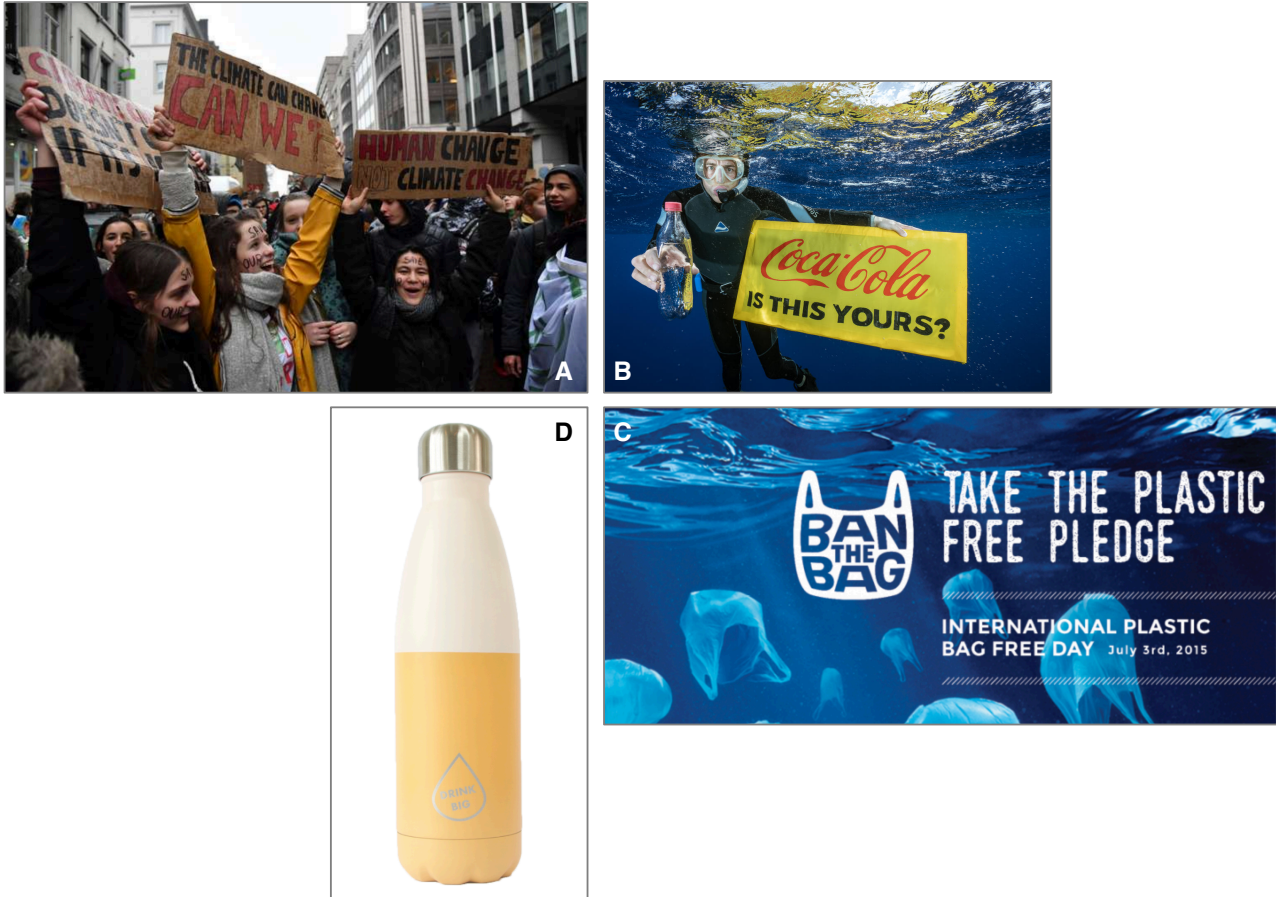


Figure 5.2. (A) Mobilisation of 13 000 young people standing against the climate change in Brussels in 2018, (B) Green peace campaign “Coca-Cola is flooding our oceans with plastic”, (C) campaign for the banning of plastic bags in Europe, in 2015, (D) reusable bottle from the company “Drink big”.

Problems are multiple: accumulation of plastics in the oceans lead to depletion of corals, moving of micro-organisms from one part of the globe to another, releasing of toxic compounds in the environment, micro-plastics eaten by fishes and oceanic mammals. And so also solutions are multiple, polymers recycling obviously but also reuse of plastic products, produce less single-use items, replace some polymers by organic materials, glass, paper or metal for commodity applications, synthesise bio-degradable plastics or infinitely recyclable polymers designed in a cradle-to-cradle perspective.

Thus, plenty of questions come to mind while speaking of a sustainable plastic economy. Should next plastics generation last or is it preferable them to self-degrade rapidly? Should researches be focused on the recycling of the existing polymers or on the synthesis of new materials designed to be easily recyclable? The use of renewable sources-based monomers are they all more sustainable than petroleum-based ones while considering purification, energy demanded or water used? How innovative polymers can be economically competitive compared to commonly used polyolefins industrially produced since decades? Who should be responsible for the collecting, sorting and recycling of plastics, governments, industries or citizens? Etc. The answers to these questions depend on a lot of factors and are different regarding the application considered. If compostable materials could be recommended for single or short-term -use items (food and beverage, packaging, cosmetics) or season-use products (agriculture), innovative materials with re-processability or recyclability built-in are most likely an option for the high-performance materials required for automotive or energy storage applications for instance. While the treatment of the millions of tons of commodity plastics produced since decades are mandatory to obstruct the ecological disaster already observable, some new materials should replace in a near future the current plastics which are too costly to recycle. When institutions and governments should regulate and legislate about collecting and recycling, companies and citizens surely have to take their part while choosing, the materials they process for the former, the products they buy for the latter.

Points of view can be commented or criticised but the increase of actions taken by all entities since a decade are definitely demonstrated how important is and will be the topic of recycling plastics.

Methods

Instrumentation

^1H NMR and ^{13}C NMR spectroscopic measurements were carried out in deuterated dimethyl sulfoxide (DMSO- d_6) on a Bruker Advance 400 (400 MHz) spectrometer at ambient temperature (298 K) for crude product reaction characterisation and isolated products characterisations. Data are recorded as follows: chemical shift (ppm), multiplicity (s, singlet; d, doublet; t, triplet; q, quartet; m, multiplet – splitting patterns that could not be interpreted or easily visualised were designated as multiplet), integration, referenced to the residual solvent peak of DMSO- d_6 ($\delta = 2.50$ ppm).

The thermal stability was analysed by a TGA Q500 (TA instrument) under nitrogen atmosphere. Samples of 5 - 10 mg were heated from 40 to 600 °C at a rate of 10 °C.min $^{-1}$.

The weight loss for a degradation event was calculated as following:

$$\text{Weight lost} = \frac{M_w^{\text{molecule loss}}}{M_w^{\text{complex}}} \times 100$$

FT-IR spectra were recorded using Nicolet 6700 FT-IR spectrophotometer (Thermo Scientific Inc., USA) using the ATR technique (Golden Gate, spectra Tech). Spectra were recorded between 4000 and 525 cm^{-1} and all spectra were averaged over 10 scans.

DSC measurements were performed using a DSC8500 (PerkinElmer). The instrument was calibrated with indium and tin standards. The DSC scans were performed with 4.5 - 5.5 mg samples at heating and cooling rates of 20 °C/min from -20 to 270 °C under a nitrogen flow of 20 mL/min. The data reported in the results section are the second heating scans.

GPC analysis for PP was performed by ITS Testing Services UK limited, Intertek Wilton, Redcar, UK.

GPC analysis for molar mass distributions of other polymers in the thesis were measured by a set up consisting of a pump (LC-20A, Shimadzu), an autosampler (Waters 717), a differential refractometer (Waters 2410) and three

Methods

columns in series (Styragel HR2, HR4 and HR6 with pore sizes ranging from 10^2 to 10^6 Å). Samples were diluted in THF (GPC grade) to a concentration of approximately 5 g.L^{-1} and filtered through a 0.45 mm nylon filter prior to injection.

Materials

PET beverage bottles (transparent, blue and green) employed in Chapter 2 were washed with water and dried before being shredded to 4 mm squares prior to use, PET pellets employed in Chapter 4 were purchased from Merck, BPA-PC pellets were purchased from Idemitsu Chemical Europe (TARFLON IV1900R), PP pellets were obtained from the grinding of PP pipette tips, PVC powder was purchased from Merck.

All commercial chemicals were used without further treatment from Merck, TCI, Acros, Alfa Aesar or Fisher. Flash column chromatography was carried out on silica gel purchased from Merck (High purity grade, 0.035 – 0.070 mm, 60 Å), using reagent grade solvent purchased from Scharlau or Fisher Scientific. Water was distilled and deionised.

Experimental part

Preparation of the catalyst mixtures

Different dual catalysts were prepared by mixing TBD and MSA at molar ratios of base to acid from (3:1) to (1:3) at 60 °C for 30 minutes until obtaining a transparent and homogeneous solution. Similarly, TBD or DBU and MSA or BA in equimolar ratios at 60 °C for 30 minutes. ^1H NMR characterisations demonstrated the formation of the salts. (Fig. S1.1 to S1.7)

TBD:MSA (1:1)

^1H NMR (400 MHz, $\text{DMSO-}d_6$) δ (ppm) 7.76, (s, 2H, N-H-O), 3.28 (t, 4H, CH_2), 3.17 (t, 4H, CH_2), 2.41 (s, 3H, CH_3). 1.88 (q, 4H, CH_2). ^{13}C NMR δ (ppm) 150.58 (s, 1C, N-C-N), 46.24 (2C, $\text{CH}_2\text{-CH}_2\text{-NH}$), 39.74 (2C, S- CH_3), 37.55 (2C, $\text{CH}_2\text{-CH}_2\text{-N}$), 20.26 (2C, $\text{CH}_2\text{-CH}_2\text{-CH}_2$).

TBD:MSA (3:1)

^1H NMR (400MHz, DMSO- d_6) δ (ppm) 6.85, (s, 2H, N-H-O) & (s, 2H, NH), 3.12 (t, 12H, CH₂, TBD), 3.09 (t, 12H, CH₂, TBD), 2.52 (s, 3H, CH₃, MSA). 1.85 (q, 12H, CH₂, TBD).

TBD:MSA (1:3)

^1H NMR (400MHz, DMSO- d_6 , 298 K) δ (ppm) 13.14, (s, 2H, OH), 7.72, (s, 2H, N-H-O), 3.25 (t, 4H, CH₂), 3.14 (t, 4H, CH₂), 2.52 (s, 9H, CH₃), 1.85 (q, 4H, CH₂).

TBD:BA (1:1)

^1H NMR (400 MHz, DMSO- d_6) δ (ppm) 10.80, (s, 2H, N-H-O), 7.88 (d, 2H, C-CH-CH₂), 7.33 (m, 3H, C-CH-CH₂) 3.27 (t, 4H, CH₂), 3.21 (t, 4H, CH₂), 1.90 (q, 4H, CH₂).

DBU:MSA (1:1)

^1H NMR (400 MHz, DMSO- d_6) δ (ppm) 10.80, (s, 2H, N-H-O), 7.88 (d, 2H, C-CH-CH₂), 7.33 (d, 2H, C-CH-CH₂) 3.27 (t, 4H, CH₂), 3.21 (t, 4H, CH₂), 1.90 (q, 4H, CH₂).

DBU:BA (1:1)

^1H NMR (400 MHz, DMSO- d_6) δ (ppm) 11.91, (s, 1H, N-H-O), 7.82 (d, 2H, C-CH-CH), 7.28 (m, 3H, CH-CH-CH) 3.52 (d, 2H, N-CH₂-CH₂), 3.47 (t, 2H, N-CH₂-CH₂), 3.29 (t, 2H, N-CH₂-CH₂), 2.78 (d, 2H, C-CH₂-CH₂), 1.91 (q, 2H, CH₂-CH₂-CH₂), 1.65 (m, 6H, CH₂-CH₂-CH₂).

Re-crystallisation of TBD:MSA (1:1)

In a flame dried round bottom flask, an equimolar quantity of TBD (2 g, 14.3 mmol) and MSA (1.38 g, 14.3 mmol) were added and dissolved completely in dry acetone (60 mL). The mixture was heated until it became clear before being left to cool to ambient temperature. The solution was subsequently cooled to 6-8 °C for 24 h to yield long, platelet crystals. (3.12 g, 13.2 mmol, 92%). NMR spectral characterisation corresponds to data before re-crystallisation, FT-IR spectrum, X-ray analysis of the single crystal and elemental analysis confirmed the formation of the salt highly pure. (Fig. S1.8 & S1.9 – Tables S1.1 & S1.2)

PET depolymerisation

In each experiment, 0.5 g of PET flakes were degraded using ethylene glycol with 0.25 eq. of catalyst. A 10 mL Schlenck flask equipped with a magnetic stirrer was used for all the reactions. The depolymerisations were carried out under atmospheric pressure at 180 °C for a determined amount of time or until complete disappearance of residual PET pellets. Reagents and catalysts were loaded in the glovebox, under nitrogen atmosphere, before sealing the flask and immersion in an oil bath. When the reaction was completed, the crude product was cooled to room temperature and a large excess of distilled water was added. The resulting solution was vigorously stirred and filtered to separate ethylene glycol, catalyst and main product from oligomers and bottle additives, insoluble in water. The aqueous transparent filtrate was stored in a refrigerator at 4 °C overnight. White needle-like crystals were formed in the solution, which were then recovered by filtration before drying. FT-IR, ¹H NMR and ¹³C NMR spectroscopic characterisations revealed the crystals to be highly pure (BHET) monomer (See Fig. S1.10 to S1.12) with characterising data in accordance with commercially-supplied BHET. ¹H NMR (400 MHz, DMSO-*d*₆, 298 K) δ (ppm) 8.12, (s, 4H, CH), 4.97 (t, 2H, OH), 4.32 (t, 4H, O-CH₂), 3.73 (q, 4H, CH₂-OH). ¹³C NMR δ (ppm) 165.14 (2C, C=O), 133.73 (2C, -C-C=O) 129.50 (4C, CH), 67.01 (2C, O-CH₂), 58.96 (2C, CH₂-OH).

The selectivity of BHET is calculated by the following equation:

$$\text{BHET yield} = \frac{\text{moles of BHET}}{\text{moles of depolymerised PET units}}$$

BPA-PC depolymerisation

In a typical experiment, BPA-PC pellets (2g, 7.87 mmol, 1 eq.), catalyst (0.277 g, 1.18 mmol, 0.15 eq.) and a determined amount of nucleophile were charged in a 25 mL glass flask equipped with a magnetic stirrer and nitrogen inlet. Each depolymerisation was carried out at a determined temperature under nitrogen at atmospheric pressure for a determined amount of time or until complete disappearance of any residual BPA-PC. Once the reaction was complete, the crude product was cooled to room temperature and an aliquot

was kept for ^1H NMR spectroscopic analysis to determine the conversion to products, using the catalyst signals as an internal standard (δ 1.87, 4H). If isolated, BPA (Fig S1.14 to S1.15) and carbonates were purified as specified for each compound.

Characterising data for isolated BPA were in accordance with commercially-supplied material: ^1H NMR (DMSO- d_6 , 400 MHz, 298 K), δ 9.12 (s, 2H), 6.96 (d, 4H), 6.65 (d, 4H), 1.53 (s, 3H); ^{13}C NMR (DMSO- d_6 , 400 MHz, 298 K), δ 154.85, 141.02, 127.25, 114.51, 40.33, 30.85.

Polymerisation of recycled BHET

Synthesis of PET was accomplished by bulk polymerisation of BHET in the presence of 5 mol % of TBD:MSA (1:1) catalyst following a two-step self-polycondensation of BHET in the melt. BHET (2 g, 7.9 mmol) was introduced together with the catalyst into a Schlenk flask equipped with a magnetic stirrer. The reaction mixture was heated at 250-270 °C for 1 hour before vacuum was applied (10^{-2} bar) for 4 h at the same temperature. After completion, PET was dissolved in a mixture of chloroform and trifluoroacetic acid (8:1) and precipitated in excess of methanol to remove impurities. Finally, the polymer was collected by centrifugation and dried under vacuum. ^1H NMR (400 MHz, DMSO- d_6 , 298 K) δ (ppm) 8.12, (s, 4H, CH), 4.78 (s, 4H, CH₂). Yield 92%

Isolation of carbonates

Propylene carbonate (2a)

After complete consumption of the BPA-PC pellets, the vial was charged with another equivalent of BPA-PC pellets (2 g, 1 eq., 7.80 mmol). The vial was resealed under nitrogen and immersed in an oil bath at 130 °C. This step was repeated until disappearance of the characteristic signals of propane-1,2-diol in the ^1H NMR spectrum of the crude product. The reaction was then cooled to room temperature before being dissolved in diethyl ether (20 mL) and water (20 mL). The organic phase was washed 3 times with water before drying the organic phase with MgSO_4 before evaporation of the solvent to yield a

Methods

white solid that was crystallised from hot water to yield BPA (4.61 g, 20.2 mmol, 86%). The combined aqueous phase was evaporated to recover the heterocycle and catalyst. **Propylene carbonate (2a)** was purified by flash column chromatography using acetone as the eluent (2.08 g, 20.4 mmol, 87%) Characterising data was consistent with that reported previously (Figs. S3.2 to S3.4)

FT-IR ν (cm⁻¹) 2987, 1778, 1387, 1352, 1173, 1117, 1041; **¹H NMR** (DMSO-*d*₆, 400 MHz, 298 K), δ 4.89 (m, 1H), 4.58 (t, 1H), 4.07 (t, 1H), 1.39 (t, 3H); **¹³C NMR** (DMSO-*d*₆, 400 MHz, 298 K), δ 154.92, 73.77, 70.48, 18.74.

Ethylene carbonate (2b)

After complete consumption of the BPA-PC pellets, the vial was charged with another equivalent of BPA-PC pellets (2 g, 1 eq., 7.80 mmol). The vial was resealed under nitrogen and immersed in an oil bath at 130 °C. This step was repeated until disappearance of the characteristic signals of ethylene carbonate in the ¹H NMR spectrum of the crude product. The reaction was then cooled to room temperature before being dissolved in diethyl ether (30 mL) and water (30 mL). The organic phase was washed 3 time with water before drying the organic phase with MgSO₄ before evaporation of the solvent to yield a white solid that was crystallised from hot water to yield BPA (8.64 g, 38.4 mmol, 82%). The combined aqueous phase was evaporated to recover the heterocycle and catalyst. **Ethylene carbonate (2b)** was purified by flash column chromatography using acetone as the eluent (3.21 g, 36,5 mmol, 79%). Characterising data was consistent with that reported previously. (Figs. S3.6 to S3.8)

FT-IR ν (cm⁻¹) 2997, 1790, 1770, 1471, 1390, 1216, 1059; **¹H NMR** (DMSO-*d*₆, 400 MHz, 298 K), δ 4.49 (s, 4H); **¹³C NMR** (DMSO-*d*₆, 400 MHz, 298 K), δ 165.59, 65.00.

Imidazolidin-2-one (2c)

After complete consumption of the BPA-PC pellets, the vial was charged with another equivalent of BPA-PC pellets (2 g, 1 eq., 7.80 mmol). The vial was resealed under nitrogen and immersed in an oil bath at 90 °C. This step was

repeated until disappearance of the characteristic signals of ethane-1,2-diamine in the ^1H NMR spectrum of the crude product. The reaction was then cooled to room temperature before being dissolved in diethyl ether (20 mL) and water (20 mL). The organic phase was washed 3 times with water before drying the organic phase with MgSO_4 before evaporation of the solvent to yield a white solid that was crystallised from hot water to yield BPA (9.18 g, 40.3 mmol, 86%). The combined aqueous phase was evaporated to recover the heterocycle and catalyst. **Imidazolidin-2-one (2c)** was purified by flash column chromatography using acetone as the eluent (3.71 g, 43.1 mmol, 92%). Characterising data was consistent with that reported previously. (Figs. S3.10 to S3.12)

FT-IR ν (cm^{-1}) 3292, 2958, 2900, 1645, 1506, 1446, 1267, 1105, 1038; **^1H NMR** ($\text{DMSO-}d_6$, 400 MHz, 298 K), δ 6.11 (s, 1H), 3.27 (s, 4H); **^{13}C NMR** ($\text{DMSO-}d_6$, 400 MHz, 298 K), δ 163.69, 39.50.

1,3-Dithiolan-2-one (2d)

After complete consumption of the BPA-PC pellets, the vial was charged with another equivalent of BPA-PC pellets (2 g, 1 eq., 7.80 mmol). The vial was resealed under nitrogen and immersed in an oil bath at 90 °C. This step was repeated until disappearance of the characteristic signals of ethane-1,2-dithiol. The reaction was then cooled down to room temperature before a column chromatography in hexane:acetone (20:80) was performed to recover a first phase containing **1,3-dithiolan-2-one (2d)**, obtained pure after drying under vacuum overnight (2.44 g, 20.4 mmol, 87%), and a second phase containing BPA obtained pure after crystallisation from hot water. (6.75 g, 29.6 mmol, 79%). Characterising data was consistent with that reported previously. (Figs. S3.14 to S3.16).

FT-IR ν (cm^{-1}) 2927, 1670, 1629, 1153, 939, 885, 823; **^1H NMR** ($\text{DMSO-}d_6$, 400 MHz, 298 K), δ 3.81 (s, 4H); **^{13}C NMR** ($\text{DMSO-}d_6$, 400 MHz, 298 K), δ 199.39, 36.42.

1,3-bis(2-hydroxyethyl)urea (2e)

After complete consumption of the BPA-PC pellets, the vial was charged with another equivalent of BPA-PC pellets (2 g, 1 eq., 7.80 mmol). The vial was resealed under nitrogen and immersed in an oil bath at 130 °C. This step was repeated until disappearance of the characteristic signals of ethanolamine (**1aa**). The reaction was then cooled down to room temperature before a column chromatography in hexane:acetone (80:20) was performed to recover a first phase containing **1,3-bis(2-hydroxyethyl)urea (2e)**, obtained pure after drying under vacuum overnight (3.08 g, 20.8 mmol, 89%), and a second phase containing BPA obtained pure after crystallisation from hot water (4.59 g, 20.2 mmol, 86%). Characterising data was consistent with that reported previously. (Fig. S3.18).

¹H NMR (DMSO-*d*₆, 400 MHz, 298 K), δ 5.98 (t, 2H, NH), 4.64 (t, 2H, OH), 3.35 (t, 4H, NH-CH₂-CH₂-OH), 3.05 (q, 4H, NH-CH₂-CH₂-OH).

1,3-bis(3-hydroxypropyl)urea (2h)

After complete consumption of the BPA-PC pellets, the vial was charged with another equivalent of BPA-PC pellets (2 g, 1 eq., 7.80 mmol). The vial was resealed under nitrogen and immersed in an oil bath at 130 °C. This step was repeated until disappearance of the characteristic signals of employing 3-aminopropan-1-ol (**1h**). The reaction was then cooled down to room temperature before a column chromatography in hexane:acetone (70:30) was performed to recover a first phase containing **1,3-bis(3-hydroxypropyl)urea (2h)**, obtained pure after drying under vacuum overnight (3.63 g, 20.6 mmol, 88%), and a second phase containing BPA obtained pure after crystallisation from hot water. (4.54 g, 19.9 mmol, 85%). Characterising data was consistent with that reported previously. (Fig. S3.22)

¹H NMR (DMSO-*d*₆, 400 MHz, 298 K) δ 5.83 (t, 2H, NH), 4.45 (t, 2H, OH), 3.41 – 3.39 (t, 4H, CH₂-CH₂-OH), 3.02 (t, 4H, NH-CH₂-CH₂), 1.50 (t, 4H, NH-CH₂-CH₂).

1,3-bis(2-(2-hydroxyethoxy)ethyl) urea (2i)

After complete consumption of the BPA-PC pellets, the vial was charged with another equivalent of BPA-PC pellets (2 g, 1 eq., 7.80 mmol). The vial was resealed under nitrogen and immersed in an oil bath at 130 °C. This step was repeated until disappearance of the characteristic signals of 3-aminopropane-1,2-diol (**1i**). The reaction was then cooled down to room temperature before a column chromatography in hexane:acetone (60:40) was performed to recover a first phase containing **1,3-bis(2-(2-hydroxyethoxy)ethyl) urea (2i)**, obtained pure after drying under vacuum overnight (3.97g, 18.9 mmol, 81%), and a second phase containing BPA obtained pure after crystallisation from hot water (4.59 g, 20.2 mmol, 86%). Characterising data was consistent with that reported previously. (Fig. S3.24)

¹H NMR (DMSO-*d*₆, 400 MHz, 298 K) δ 6.08 (t, 2H, NH), 4.77 (m, 2H, CH-OH), 4.55 (m, 2H, CH₂-OH), 3.41 (m, 2H, CH₂-CH-CH₂), 3.27 (m, 4H, CH-CH₂-OH), 3.16 – 2.94 (t, 4H, CH₂-NH).

4-(Hydroxymethyl)-1,3-dioxolan-2-one (2k)

After complete consumption of the BPA-PC pellets, the vial was charged with another equivalent of BPA-PC pellets (2 g, 1 eq., 7.80 mmol). The vial was resealed under nitrogen and immersed in an oil bath at 130 °C. This step was repeated until disappearance of the characteristic signals of glycerol in the ¹H NMR spectrum of the crude product. The reaction was then cooled to room temperature before being dissolved in diethyl ether (20 mL) and water (20 mL). The organic phase was washed 3 time with water before drying the organic phase with MgSO₄ before evaporation of the solvent to yield a white solid that was crystallised from hot water to yield BPA (4.3 g, 18.9 mmol, 81%). The combined aqueous phase was evaporated to recover the heterocycle and catalyst. **4-(hydroxymethyl)-1,3-dioxolan-2-one (2k)** was purified by flash column chromatography using acetone as the eluent (2.37 g, 20.1 mmol, 86%). (Figs. S3.27 to S3.29)

FT-IR ν (cm⁻¹) 3386, 2935, 1763, 1400, 1173, 1047; ¹H NMR (DMSO-*d*₆, 400 MHz, 298 K), δ 5.25 (t, 1H), 4.80 (m, 1H), 4.50 (t, 1H), 4.31 (t, 1H), 3.71 - 3.64

Methods

(m, 1H), 3.55 -3.48 (m, 1H); ^{13}C NMR (DMSO- d_6 , 400 MHz, 298 K), δ 155.26, 77.09, 65.93, 60.66.

4,5-Bis(hydroxymethyl)-1,3-dioxolan-2-one (2l)

After complete consumption of the BPA-PC pellets, the vial was charged with another equivalent of BPA-PC pellets (2 g, 1 eq., 7.80 mmol). The vial was resealed under nitrogen and immersed in an oil bath at 130 °C. This step was repeated until disappearance of the characteristic signals of *meso*-erythritol in the ^1H NMR spectrum of the crude product. The reaction was then cooled to room temperature before being dissolved in diethyl ether (20 mL) and water (20 mL). The organic phase was washed 3 times with water before drying the organic phase with MgSO_4 before evaporation of the solvent to yield a white solid that was crystallised from hot water to yield BPA (4.61 g, 20.2 mmol, 86%). The combined aqueous phase was evaporated to recover the heterocycle and catalyst. **4,5-Bis(hydroxymethyl)-1,3-dioxolan-2-one (2l)** was purified by flash column chromatography using acetone as the eluent (2.56 g, 17.3 mmol, 74%). Characterising data was consistent with that reported previously. (Figs. S3.31 to S3.33)

FT-IR ν (cm^{-1}) 3351, 2952, 2877, 1645, 1655, 1122, 1052, 900; ^1H NMR (DMSO- d_6 , 400 MHz, 298 K), δ 4.72 (s, 2H), 3.99 (s, 2H), 3.75 (s, 2H), 3.46 (s, 2H); ^{13}C NMR (DMSO- d_6 , 400 MHz, 298 K), δ 155.32, 71.82, 70.59.

Diglycerol Carbonate (2m)

After complete consumption of the BPA-PC pellets, the vial was charged with another equivalent of BPA-PC pellets (2 g, 1 eq., 7.80 mmol). The vial was resealed under nitrogen and immersed in an oil bath at 160 °C. This step was repeated until disappearance of the characteristic signals of α,α' -diglycerol. The reaction was then cooled down to room temperature before a column chromatography in hexane:acetone (20:80) was performed to recover a first phase containing **Diglycerol Carbonate (2m)**, obtained pure after drying under vacuum overnight (4.23 g, 19.7 mmol, 84%), and a second phase containing BPA obtained pure after crystallisation from hot water. (4.43 g, 19.4 mmol,

83%). Characterising data was consistent with that reported previously. (Figs. S3.35 to S3.37)

FT-IR ν (cm^{-1}) 2925, 1770, 1479, 1392, 1169, 1031; **^1H NMR** ($\text{DMSO-}d_6$, 400 MHz, 298 K), δ 5.25 (t, 1H), 4.80 (m, 1H), 4.50 (t, 1H), 4.31 (t, 1H), 3.71 - 3.64 (m, 1H), 3.55 - 3.48 (m, 1H); **^{13}C NMR** ($\text{DMSO-}d_6$, 400 MHz, 298 K), δ 154.81, 75.40, 70.39, 65.87.

5-((Allyloxy)methyl)-5-ethyl-1,3-dioxan-2-one (2w)

After complete consumption of the BPA-PC pellets, the vial was charged with another equivalent of BPA-PC pellets (2 g, 1 eq., 7.80 mmol). The vial was resealed under nitrogen and immersed in an oil bath at 130 °C. This step was repeated until disappearance of the characteristic signals of 5-((allyloxy)methyl)-2-ethyl-1,3-propanediol. The reaction was then cooled down to room temperature before a column chromatography in hexane:acetone (10:90) was performed to recover a first phase containing **5-((Allyloxy)methyl)-5-ethyl-1,3-dioxan-2-one (2w)**, obtained pure after drying under vacuum overnight (4.12 g, 20.6 mmol, 88%), and a second phase containing BPA obtained pure after crystallisation from hot water. (4.38 g, 19.2 mmol, 82%). Characterising data was consistent with that reported previously. (Figs. S3.56 to S3.58)

FT-IR ν (cm^{-1}) 2971, 1745, 1471, 1405, 1172, 1108, 1091, 765 cm^{-1} ; **^1H NMR** ($\text{DMSO-}d_6$, 400 MHz, 298 K), δ 5.94 - 5.82 (m, 1H), 5.30 - 5.16 (m, 2H), 4.25 (q, 4H), 3.97 (d, 2H), 3.38 (s, 2H), 1.40 (q, 2H), 0.85 (t, 3H); **^{13}C NMR** ($\text{DMSO-}d_6$, 400 MHz, 298 K), δ 147.83, 134.70, 116.68, 72.22, 71.48, 68.06, 34.69, 22.53, 7.12.

Selective depolymerisation procedures

Successive depolymerisations of BPA-PC and PET

In a typical experiment, BPA-PC pellets (2.0 g, 7.80 mmol, 1 eq.), PET pellets (1.5 g, 7.80 mmol, 1 eq.), the nucleophile (15 eq.) – ethylene glycol, ethanolamine or ethylene diamine – and a determined amount of catalyst – 0.15 eq. or 0.5 eq. – were charged in a 50 mL glass round-bottomed flask

Methods

equipped with a magnetic stirrer. Each depolymerisation was carried out at a determined temperature under nitrogen and at atmospheric pressure until complete disappearance of the polymer pellets or for 48 h.

While kinetics were recorded, they were followed by ^1H NMR spectroscopy in $\text{DMSO-}d_6$ using the catalyst signals as internal standard ($\delta = 1.87$ ppm, 4H). (Fig. S4.2 to S4.4)

Selective depolymerisation of BPA-PC using 1h

BPA-PC pellets (2.0 g, 7.80 mmol, 1 eq.), PET pellets (1.5 g, 7.80 mmol, 1 eq.), 1h (4.3 g, 46.8 mmol, 6 eq.) and TBD:MSA (1:1) catalyst (0.28 g, 1.18 mmol, 0.15 eq.) were charged in a 50 mL glass flask equipped with a magnetic stirrer. The reaction was heated to 160 °C under N_2 and atmospheric pressure until complete disappearance of BPA-PC pellets.

Conversions were determined by ^1H NMR spectroscopic analysis of the crude product. (Fig. S4.5)

Selective depolymerisation of BPA-PC using 1w

BPA-PC pellets (2.0 g, 7.80 mmol, 1 eq.), PET pellets (1.5 g, 7.80 mmol, 1 eq.), 1w (8.2 g, 46.8 mmol, 6 eq.) and TBD:MSA (1:1) catalyst (0.28 g, 1.18 mmol, 0.15 eq.) were charged in a 50 mL glass flask equipped with a magnetic stirrer. The reaction was heated to 130 °C under N_2 and atmospheric pressure until complete disappearance of BPA-PC pellets.

Conversions were determined by ^1H NMR spectroscopic analysis of the crude product. (Fig. S4.6)

Selective depolymerisation in the presence of PP pellets

BPA-PC pellets (2.0g, 7.80 mmol, 1 eq.), PET pellets (1.5 g, 7.80 mmol, 1 eq.), PP pellets (0.98 g, 23.4 mmol, 3 eq.), ethylene glycol (7.8 g, 125 mmol, 16 eq.) and TBD:MSA (1:1) catalyst (0.28 g, 1.18 mmol, 0.15 eq.) were charged in a 50 mL glass flask equipped with a magnetic stirrer. The reaction was carried out at 180 °C under N_2 and atmospheric pressure until complete disappearance of both BPA-PC and PET pellets.

Conversions were determined by ^1H NMR spectroscopic analysis of the crude product at points that correspond to the disappearance of BPA-PC pellets ($t_{\text{BPA-PC}}^f$) and the disappearance of PET pellets (t_{PET}^f). (Fig. S4.7 & S4.8)

Selective depolymerisation in the presence of PVC powder

BPA-PC pellets (2.0g, 7.80 mmol, 1 eq.), PET pellets (1.5 g, 7.80 mmol, 1 eq.), PVC pellets (1.45g, 23.4 mmol, 3 eq.), ethylene glycol (7.8 g, 125 mmol, 16 eq.) and a determined amount of catalyst – 0.15 eq. or 0.5 eq. – were charged in a 50 mL glass flask equipped with a magnetic stirrer. The reaction was carried out at 180 °C under N_2 and atmospheric pressure during 96 h.

Conversions were determined by ^1H NMR spectroscopic analysis of the crude product at points that correspond to the disappearance of BPA-PC pellets ($t_{\text{BPA-PC}}^f$) and the disappearance of PET pellets (t_{PET}^f). (Fig. S4.9 & S4.10)

Computational methodology

Introduction to Quantum Chemistry

Computational chemistry makes use of quantum mechanical methods in order to calculate different properties of a chemical system. It can be used to determine properties that are inaccessible experimentally or to interpret experimental data.

The Schrödinger equation

The time-dependent Schrödinger equation,² is a partial differential equation of the total energy operator, the Hamiltonian \hat{H} .

$$i\hbar \frac{\partial \Psi}{\partial t} = \hat{H}\Psi$$

For a closed system, the conservation of energy makes possible the separation of time and spatial coordinates. The time-independent Schrödinger equation can be formulated as an eigenvalue equation,

$$\hat{H}(\mathbf{r}, \mathbf{R})\Psi(\mathbf{r}, \mathbf{R}) = E\Psi(\mathbf{r}, \mathbf{R})$$

For a system with N electrons and M nuclei, the non-relativistic Hamiltonian includes the kinetic energy of both nuclei (\hat{T}_n) and electrons (\hat{T}_e), the electron-

nucleus attraction (\hat{V}_{ne}) as well as the repulsion between electrons (\hat{V}_{ee}) and nuclei (\hat{V}_{nn}):

$$\hat{H} = \hat{T}_e + \hat{T}_n + \hat{V}_{ne} + \hat{V}_{ee} + \hat{V}_{nn}$$

$$\hat{H} = \sum_{i=1}^N \left[\frac{-\nabla_i^2}{2} + \sum_{A=1}^M \frac{-Z_A}{|\vec{r}_i - \vec{R}_A|} \right] + \sum_{i>j}^N \frac{1}{|\vec{r}_i - \vec{r}_j|} + \sum_{A=1}^M \frac{-\nabla_A^2}{2m_A} + \sum_{A>B}^M \frac{Z_A Z_B}{|\vec{R}_A - \vec{R}_B|}$$

where i and j stand for electrons, and A and B for nuclei. This complex equation can only be solved exactly for a one-electron system (e.g. the hydrogen atom), due to the electron-electron interaction term ($|\vec{r}_i - \vec{r}_j|$, second summation in previous Equation) and approximations must be done.

The Born-Oppenheimer approximation

The Born-Oppenheimer approximation³ is based on the large difference in mass and velocity between electrons and nuclei, which allows the exact wavefunction, $\Psi(\mathbf{r}, \mathbf{R})$, to be approximated as a product of an electron and a nuclear part: $\Psi(\mathbf{r}, \mathbf{R}) = \psi_{el}(\mathbf{r})\psi_{nuc}(\mathbf{R})$.

Thus, the motion of the electrons is several orders of magnitude faster than that of the nuclei, that is, on the time scale of the electron motion, nuclei can be considered as stationary objects. Similarly, electrons are assumed to respond instantaneously to any change in the nuclear configuration and, therefore, the nuclei are considered to move in the mean field generated by the electrons. In consequence, this allows the nuclear and electronic parts of the Schrödinger equation to be treated separately. In other words, for the electronic motion, the nuclear kinetic energy term (\hat{T}_n) is neglected and the nuclear repulsion term (\hat{V}_{nn}) is a constant, while the interaction between nuclei and electrons (\hat{V}_{ne}) depends parametrically on the coordinates of the fixed nuclei.

As a result, the molecular Schrödinger equation is transformed into the electronic Schrödinger equation, where the wavefunction, $\psi_{el}(\mathbf{r})$, depends explicitly only on the electronic coordinates. In this thesis, only the electronic Hamiltonian will be considered.

Basis sets

Another fundamental approximation in quantum chemistry is the introduction of a basis set, which expands an unknown function, such as an atomic orbital, in a set of known functions. Thus, an atomic orbital (AO) can be described as a combination of gaussian and spherical harmonic functions: $\phi(\mathbf{r}) = R(\mathbf{r})e^{-\alpha r^2}Y_{lm_l}(\theta, \varphi)$. A linear combination of AOs (LCAO)⁴ can be used to represent a molecular orbital (MO).

A minimal basis set that only contains one basis function for each occupied atomic orbital is defined as a basis set of *single- ζ* quality. This minimal LCAO description of the molecular orbital is inadequate and needs to be improved. The basis can be *split* and, if all basis functions are doubled, i.e. two basis functions per atomic orbital, the basis set has a *double- ζ* quality. Similarly, the *triple-* and *quadruple- ζ* types consist of further splittings.

Further improvement of the basis set can be done by adding polarisation functions, that consist of higher angular momentum functions. Polarisation functions are essential to describe the electron correlation. For molecules where the charge distribution is more diffuse, such as anions, diffuse functions are needed for a better description of the electron distribution.

The accuracy of a quantum chemical calculation depends not only on the level of theory but also on the quality of the basis set. The greater the number of basis functions, the better the resulting MOs and, thus, the wavefunction.

Quantum chemical methods

In quantum chemistry, two main groups of methods exist for the calculation of properties of a chemical system: (i) wavefunction-based methods (WF) and (ii) density functional theory-based (DFT) methods. In the former, the methods provide a direct (but approximate) solution to the Schrödinger equation. In the latter category, the energy is a functional of the electron density.

Wavefunction theory. The Hartree-Fock method

A wavefunction-based method derives the electronic structure and the corresponding energy for a system with N electrons, by solving the

Schrödinger equation. The expectation value of the electronic Hamiltonian can be written as:

$$E_{el} = \frac{\langle \Psi | H | \Psi \rangle}{\langle \Psi | \Psi \rangle}$$

and the lowest possible energy for a system is obtained by varying E_{el} with respect to the orbitals using, for example, the Lagrange's method of undetermined multipliers. Thus, using the variational principle, we ensure that the obtained wavefunction is the best one, that is, that yields the lowest energy of the system. If a Slater determinant is used as a trial wavefunction, the *Hartree-Fock* equations^{5,6} are derived:

$$\hat{F}\Psi = \varepsilon\Psi$$

At the Hartree-Fock level of theory, the Hamiltonian includes the one-electron operator, \hat{h}_i , describing the kinetic energy of electron i in the field of the nuclei, and the two-electron operator describing the electron-electron repulsion. The contribution from the term $1/r_{ij} = 1/|\vec{r}_i - \vec{r}_j|$ is the Coulomb interaction (\hat{J}_{ij}) and the exchange interaction (\hat{K}_{ij}), where the former describes the classical repulsion between electrons.

The *Self-Consistent Field (SCF)* approach is an iterative process where an approximate Hamiltonian is constructed to solve the Schrödinger equation and to obtain a set of molecular orbitals that are used to construct another Hamiltonian and obtain a new more accurate set of molecular orbitals until the process reaches convergence. The SCF procedure leads to the molecular orbitals that minimise the energy. Thus, the Hartree-Fock energy can be written as:

$$E_{HF} = \sum_{i=1}^N \hat{h}_{ii} + \frac{1}{2} \sum_{i=1}^N \sum_{j=1}^N (\hat{J}_{ij} - \hat{K}_{ij})$$

The Hartree-Fock method leads to an important class of quantum chemical models, the molecular orbital models, and also provides the foundation for both simpler and more complex models. Hartree-Fock models provide reasonably good description of equilibrium geometries and conformations, except when transition metals are involved. However, they behave poorly in

accounting for the thermochemistry of reactions involving explicit bond breaking and forming. The failures can be traced back to the incomplete description of electron correlation, that is, the way in which the motion of one electron affects the motions of all the other electrons. In order to allow for electron correlation, several quantum chemical methods have been developed. Among them, three fundamental approaches must be underlined: (i) configuration interaction (CI),⁷ Møller-Plesset perturbation theory (MP)⁸ and (iii) coupled-cluster approaches (CC),⁹ which extend the flexibility of the HF method by mixing ground-state and excited-state wavefunctions, that is, using several Slater determinants obtained from a permutation of electron occupancies among all the molecular orbitals available. These approaches are significantly costlier than HF but provide excellent descriptions of thermochemistry.

Density Functional Theory

A conceptually different methodology to include electron correlation is DFT, which is based on the electron density (ρ), as opposed to the many-electron wave function, Ψ . This is the main difference that makes DFT to be more cost-efficient: the simplest wave function depends on $3N$ spatial coordinates, whereas the probability distribution of electrons in space depends only on three coordinates.

The two fundamental theorems in DFT are the Hohenberg-Kohn theorems¹⁰:

- i) Any observable of a stationary non-degenerate ground state can be calculated, exactly in theory, from the electron density of the ground state. In other words, any observable can be written as a functional of the electron density of the ground state.
- ii) The electron density of a non-degenerate ground state can be calculated, exactly in theory, determining the density that minimises the energy of the ground state.

The first theorem is considered the foundations of DFT, as states that the energy, as all the other properties of a system, are uniquely defined by the electronic density (ρ):

$$E_0[\rho] = T[\rho] + E_{ee}[\rho] + E_{Ne}[\rho]$$

$$E_0[\rho] = F_{HK}[\rho] + E_{Ne}[\rho]$$

In this equation, the ground state energy $E_0[\rho]$ is defined as the sum of the kinetic energy ($T[\rho]$), the electron-electron repulsion ($E_{ee}[\rho]$) and the nucleus-electron attraction ($E_{Ne}[\rho]$). As $T[\rho]$ and $E_{ee}[\rho]$ are unknown, they are gathered in the so-called Hohenberg and Kohn functional $F_{HK}[\rho]$. The second theorem provides the variational principle for $E(\rho)$, that is, allows to obtain ρ variationally.

Nevertheless, the Hohenberg-Kohn theorems are not enough to obtain information about the energy or other properties as none of them provide an explicit formula to perform the calculation of ρ . However, Kohn and Sham suggested a route to find the electronic density in the ground state using a non-interacting reference system.¹¹ In that manner, a Hamiltonian of a non-interacting system could be defined as follows, in which the first term is the kinetic energy and the second is an effective local potential.

$$\hat{H}_S = -\frac{1}{2} \sum_i^N \nabla_i^2 + \sum_i^N V_S(\mathbf{r}_i)$$

Since this Hamiltonian does not contain any electron-electron interaction term, the ground state wave function ψ can be expressed in terms of spin orbitals (φ_i), in analogy to the HF method, that are eigenfunctions of the so-called Kohn-Sham operator (\hat{h}^{KS}):

$$\hat{h}^{KS}(i)\varphi(i) = \varepsilon_i\varphi(i)$$

$$\hat{h}^{KS}(i) = -\frac{1}{2}\nabla_i^2 - V_S(i)$$

To define the energy of a real (interacting) system, Kohn and Sham reformulated the Hohenberg-Kohn functional as:

$$F_{HK}[\rho] = T_S[\rho] + E_{ee}[\rho] = T_S[\rho] + J[\rho] + E_{XC}[\rho]$$

Following the previous equation, the electron-electron repulsion term is split into the classical Coulomb part ($J[\rho]$) and an unknown term called exchange-correlation energy ($E_{XC}[\rho]$), that basically contains the residual part of the true

kinetic energy ($T[\rho] - T_S[\rho]$) and the non-classical electrostatic contributions ($E_{ee}[\rho] - J[\rho]$).

Finally, the potential due the exchange-correlation energy ($V_{xc}[\rho]$), which is also unknown, is defined as the derivative of $E_{xc}[\rho]$ with respect to ρ :

$$V_{xc}[\rho] = \frac{\delta E_{xc}[\rho]}{\delta \rho}$$

Exchange-correlation functionals

A lot of effort has been done on the development of an expression for the exchange-correlation term. This term can be viewed as the energy resulting from the inter-electronic repulsion interaction, and can be decomposed into an exchange and a correlation part:

$$E_{xc} = E_x + E_c$$

The first approximation for the exchange-correlation energy was the local density approximation (LDA) method, where the density is considered as a homogeneous gas, so each single position of the space is assigned to have the same constant value for the density. Binding energies of molecules obtained at the LDA level are often overestimated and the bond lengths underestimated.

LDA might be suitable for systems where the electron density can be considered as slowly varying, but for most chemical systems this description is not sufficient. An improvement of the exchange-correlation energy can be found with gradient-corrected functionals, within the generalised gradient approximation (GGA):

$$E_{xc}^{GGA}[\rho] = \int \rho \epsilon_{xc}^{GGA}(\rho, \nabla \rho) dr$$

One example of a GGA functional is the B88 exchange functional suggested by Becke,¹² including one parameter determined by fitting the exact exchange energies of the He, Ne, Ar, Kr and Xe atoms. Lee, Yang and Parr suggested a correction, the LYP correlation functional,¹³ that includes four parameters fitted so that the result for the He atom is correct. The combination of B88 and LYP gives the commonly used BLYP functional.¹⁴ Other examples are the

PBE functional¹⁵ and the BP86 functional, a combination including the B88 exchange functional and correlation corrections suggested by Perdew.¹⁶

The GGA methods can be further improved by introducing the laplacian of the electron density or the local kinetic energy density, denominated as meta-GGA methods. A different approach to improve the exchange-correlation energy is the combination of GGA functionals with explicit Hartree-Fock exchange to generate the so-called hybrid functionals. One of the most commonly used hybrid functional is B3LYP:^{12,13,17}

$$E_{XC}^{B3LYP} = (1 - a)E_X^{LSDA} + aE_X^{HF} + b\Delta E_X^B + (1 - c)E_C^{LSDA} + cE_C^{LYP}$$

The parameters $a = 0.20$, $b = 0.72$ and $c = 0.81$ were originally determined by a fit to the set of atomisation energies, ionisation potentials, proton affinities and total atomic energies from systems of the so-called G1 set.¹⁸ Another example is the B3PW91 functional,¹⁹⁻²¹ that combines the Becke three-parameter functional and the PW91 correlation as shown in the formula:

$$E_{XC}^{B3PW91} = (1 - a)E_X^{LSDA} + aE_X^{HF} + b\Delta E_X^B + E_C^{LSDA} + c\Delta E_C^{PW91}$$

In both cases, the parameter that multiplies the E_X^{HF} is 0.2, so the percentage of HF used is 20%. However, these parameters may be optimised for each functional and it may suffer strong variations from one to another functional. For instance, in the M06-2X functional developed by Truhlar and Zhao,²² the percentage of HF exchange is enhanced to a 51%, following the next expression:

$$E_{XC}^{M06-2X} = (1 - a)E_X^{M06} + aE_X^{HF} + E_C^{M06}$$

The exchange-correlation functionals have been represented by using only local quantities at a reference point, such as the electron density. It is, therefore, presumed that those functionals overestimate local contributions and underestimate non-local contributions. The most significant non-local contribution may be the long-range electron-electron exchange interaction because it may be impossible to represent this interaction as a functional of a one-electron quantity.

In 1996, Savin suggested a long-range exchange correction scheme for LDA functionals.²³ In this scheme, the two-electron operator, $1/r_{ij}$, is separated

into the short-range and long-range parts by using the standard error function (*erf*):

$$\frac{1}{r_{ij}} = \frac{1 - \text{erf}(\mu r_{ij})}{r_{ij}} + \frac{\text{erf}(\mu r_{ij})}{r_{ij}}$$

where μ is a parameter that determines the ratio of these two parts. However, Savin's scheme is inapplicable to conventional GGA functionals. In 2001, Iikura, Tsuneda, Yanai and Hirao²⁴ solved this problem in such a way that the new expression reproduces the original GGA exchange functional for $\mu = 0$. This scheme is defined as the long range correction (LC) scheme. Examples of these functionals are CAM-B3LYP²⁵ and ω B97X.²⁶

Besides the long-range problem, nowadays, it is clear that all semilocal density functionals and conventional hybrid functionals asymptotically cannot reproduce correctly the $-C_6/R^6$ dependence of the dispersion interaction energy on the interatomic distance R . This dispersion is of particular importance for the equilibrium structure of many van der Waals complexes and for thermodynamic properties of larger molecules. The failure of standard functionals may be understood by considering the "true" wavefunction-based origin of the dispersion energy. For example, in second-order Møller-Plesset perturbation theory,⁸ it is given by the Coulomb and exchange interactions of single-electron transition densities centered on interacting fragments A and B:

$$E_{disp}^{(2)} = - \sum_{ia} \sum_{jb} \frac{(ia|jb)[(ia|jb) - (ib|ja)]}{\epsilon_a + \epsilon_b - \epsilon_i - \epsilon_j}$$

where the sum is over all possible single-particle hole excitations between orbitals $i \rightarrow a$ (localised on A) and $j \rightarrow b$ (on B), $(ia|jb)$ is a two-electron integral and ϵ are the corresponding orbital energies.

Most of the current dispersion-corrected DFT approaches include empirical corrections in several ways. The basic reason is the fact that the dispersion is a special kind of electron correlation operating on long-range scales. At short electron-electron distances, the standard functionals describe well the corresponding effects. Thus, any dispersion-including approach is faced with

Methods

the problem to merge in a smooth way the short- and long-range asymptotic regions that are fairly well understood separately. Examples of this kind of functionals are X3LYP,²⁷ TPSS²⁸ or ω B97XD²⁹.

References

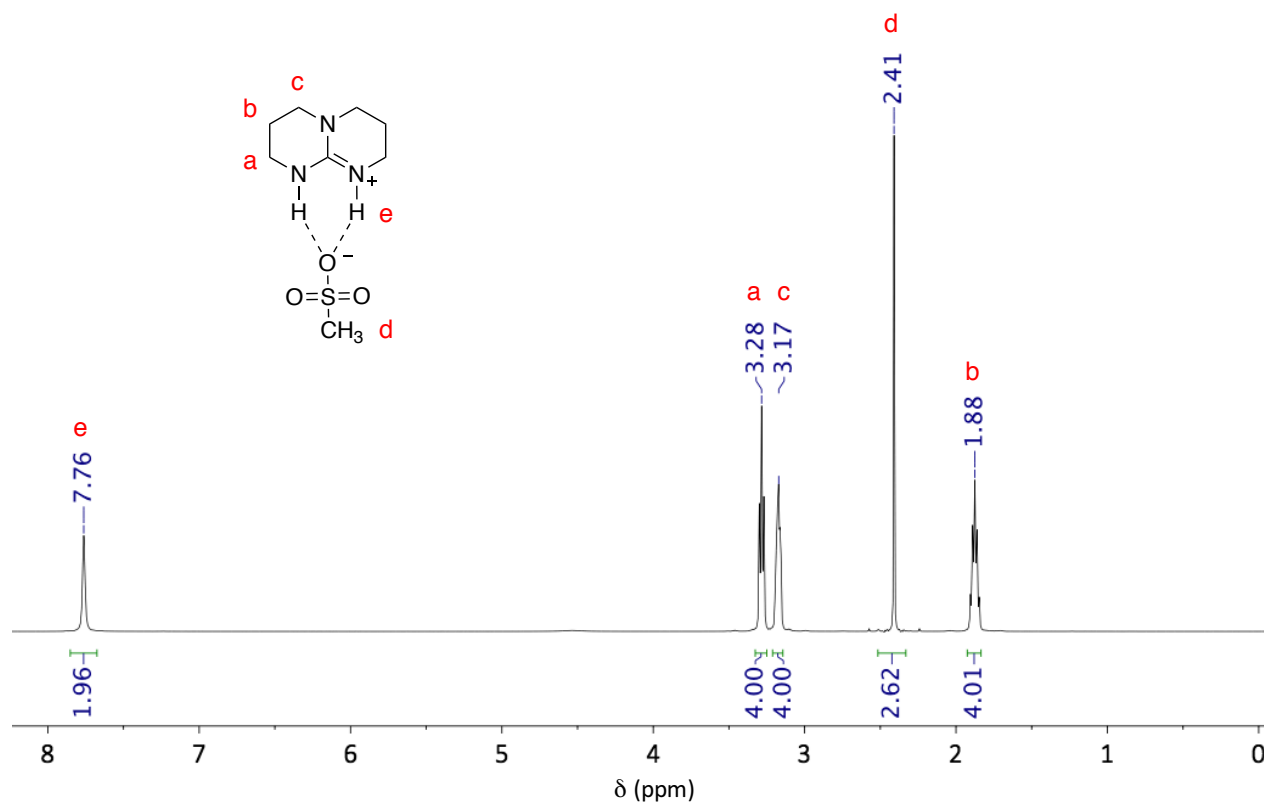
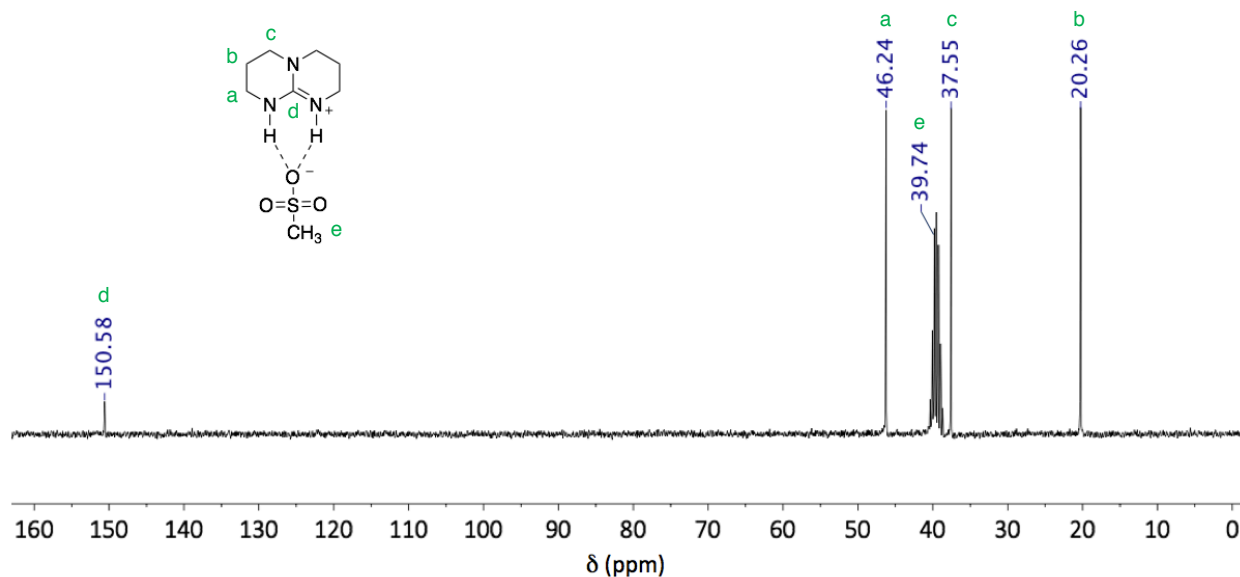
- 1 J. Sun and D. Kuckling, *Polym. Chem.*, 2016, **7**, 1642–1649.
- 2 E. Schrödinger, *Ann. Phys.*, 1926, **81**, 109.
- 3 M. Born and R. Oppenheimer, *Ann. Phys.*, 1927, **389**, 457–484.
- 4 H. Eschrig, *Optimized LCAO Method and the Electronic Structure of Extended Systems*, 1989.
- 5 D. R. Hartree, *Math. Proc. Camb. Philos. Soc.*, 1928, **24**, 89–110.
- 6 V. Fock, *Z. Für Phys.*, 1930, **61**, 126–148.
- 7 W. Kutzelnigg, *J. Mol. Struct. THEOCHEM*, 1988, **181**, 33–54.
- 8 Chr. Møller and M. S. Plesset, *Phys. Rev.*, 1934, **46**, 618–622.
- 9 J. Bartlett Rodney, *Recent Advances In Coupled-cluster Methods*, World Scientific, Bartlett Rodney J., 1997.
- 10 P. Hohenberg and W. Kohn, *Phys. Rev.*, 1964, **136**, B864–B871.
- 11 W. Kohn and L. J. Sham, *Phys. Rev.*, 1965, **140**, A1133–A1138.
- 12 A. D. Becke, *Phys. Rev. A*, 1988, **38**, 3098–3100.
- 13 C. Lee, W. Yang and R. G. Parr, *Phys. Rev. B*, 1988, **37**, 785–789.
- 14 B. Miehlich, A. Savin, H. Stoll and H. Preuss, *Chem. Phys. Lett.*, 1989, **157**, 200–206.
- 15 J. P. Perdew, K. Burke and M. Ernzerhof, *Phys. Rev. Lett.*, 1996, **77**, 3865–3868.
- 16 J. P. Perdew, *Phys. Rev. B*, 1986, **33**, 8822–8824.
- 17 S. H. Vosko, L. Wilk and M. Nusair, *Can. J. Phys.*, 1980, **58**, 1200–1211.
- 18 J. A. Pople, M. Head-Gordon, D. J. Fox, K. Raghavachari and L. A. Curtiss, *J. Chem. Phys.*, 1989, **90**, 5622–5629.
- 19 A. D. Becke, *J. Chem. Phys.*, 1993, **98**, 5648–5652.
- 20 J. F. Dobson, G. Vignale and M. P. Das, Eds., *Electronic Density Functional Theory: Recent Progress and New Directions*, Springer, New York, 1998 edition., 1998.
- 21 J. P. Perdew, *Electronic structure of solids*, Akademie Verlag, Berlin, 1st ed., 1991.
- 22 Y. Zhao and D. G. Truhlar, *Theor. Chem. Acc.*, 2008, **120**, 215–241.
- 23 J. M. Seminario, *Recent Developments and Applications of Modern Density Functional Theory*, Elsevier, 1996.

Methods

- 24 H. Iikura, T. Tsuneda, T. Yanai and K. Hirao, *J. Chem. Phys.*, 2001, **115**, 3540–3544.
- 25 T. Yanai, D. P. Tew and N. C. Handy, *Chem. Phys. Lett.*, 2004, **393**, 51–57.
- 26 J.-D. Chai and M. Head-Gordon, *J. Chem. Phys.*, 2008, **128**, 084106.
- 27 X. Xu and W. A. Goddard, *Proc. Natl. Acad. Sci.*, 2004, **101**, 2673–2677.
- 28 V. N. Staroverov, G. E. Scuseria, J. Tao and J. P. Perdew, *J. Chem. Phys.*, 2003, **119**, 12129–12137.
- 29 J.-D. Chai and M. Head-Gordon, *Phys. Chem. Chem. Phys.*, 2008, **10**, 6615–6620.

Appendix

Appendix Chapter 1

Figure S1.1. ^1H NMR spectrum of TBD:MSA (1:1) ($\text{DMSO}-d_6$, 400 MHz, 298 K).Figure S1.2. ^{13}C NMR spectrum of TBD:MSA (1:1) ($\text{DMSO}-d_6$, 400 MHz, 298 K).

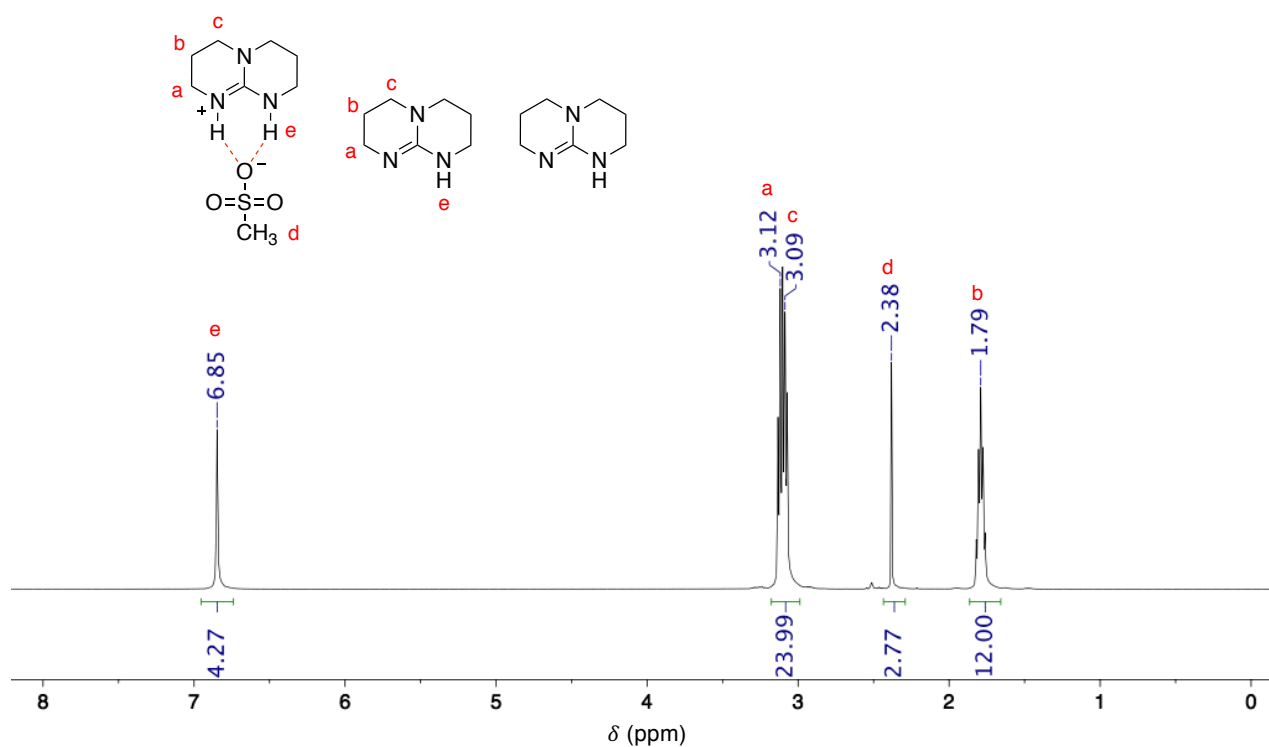


Figure S1.3. ^1H NMR spectrum of TBD:MSA (3:1) ($\text{DMSO-}d_6$, 400 MHz, 298 K).

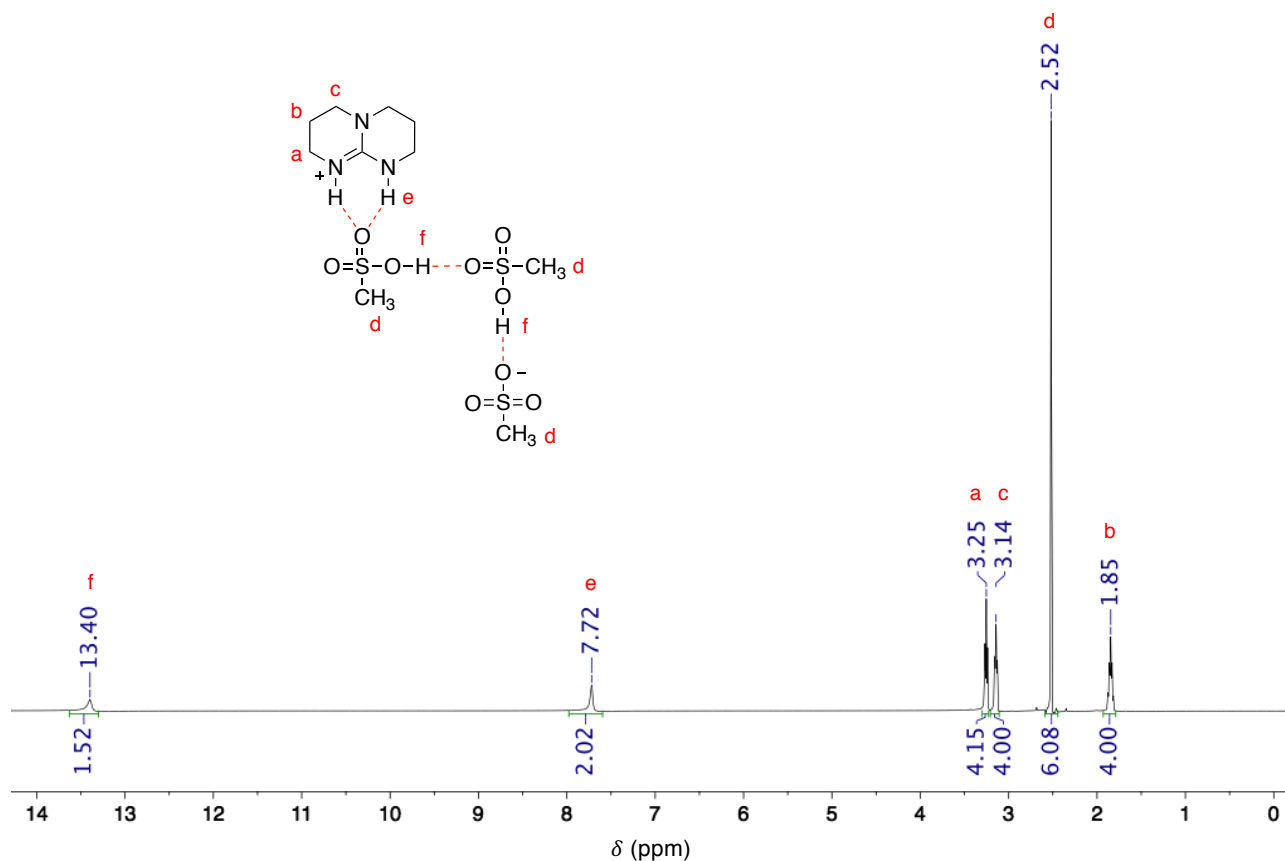


Figure S1.4. ^1H NMR spectrum of TBD:MSA (1:3) ($\text{DMSO-}d_6$, 400 MHz, 298 K).

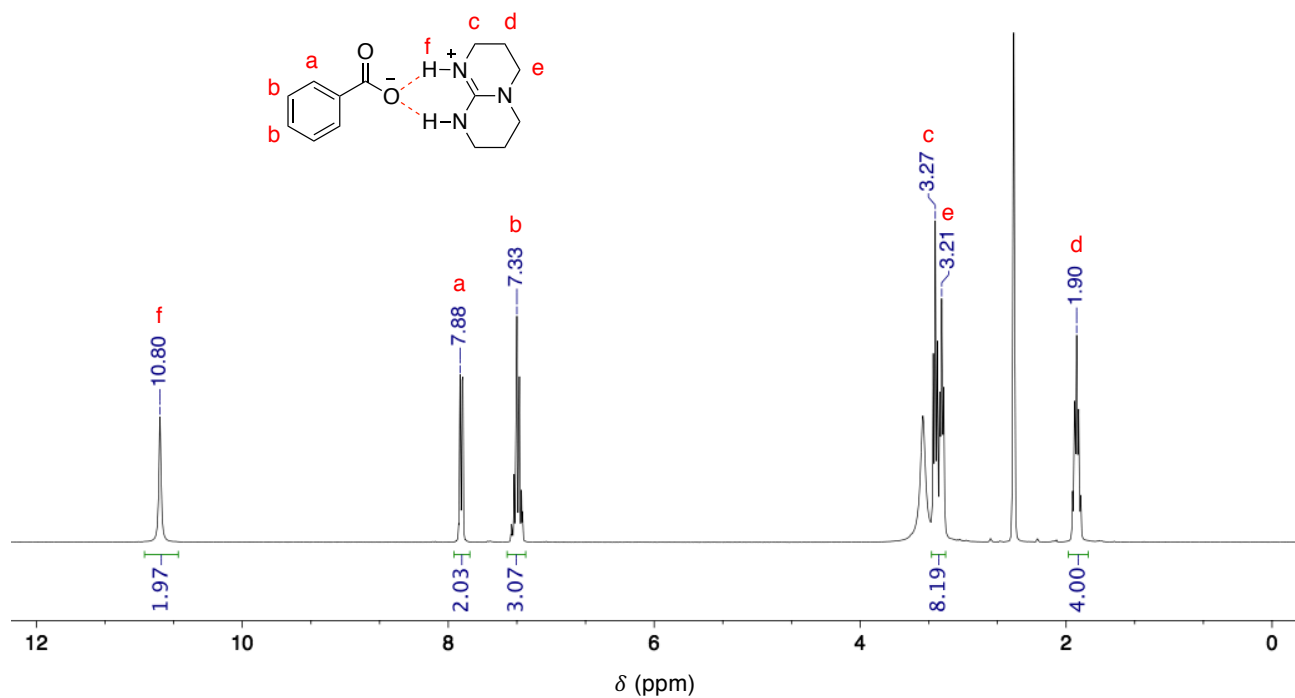


Figure S1.5. ^1H NMR spectrum of TBD:BA ($\text{DMSO-}d_6$, 400 MHz, 298 K).

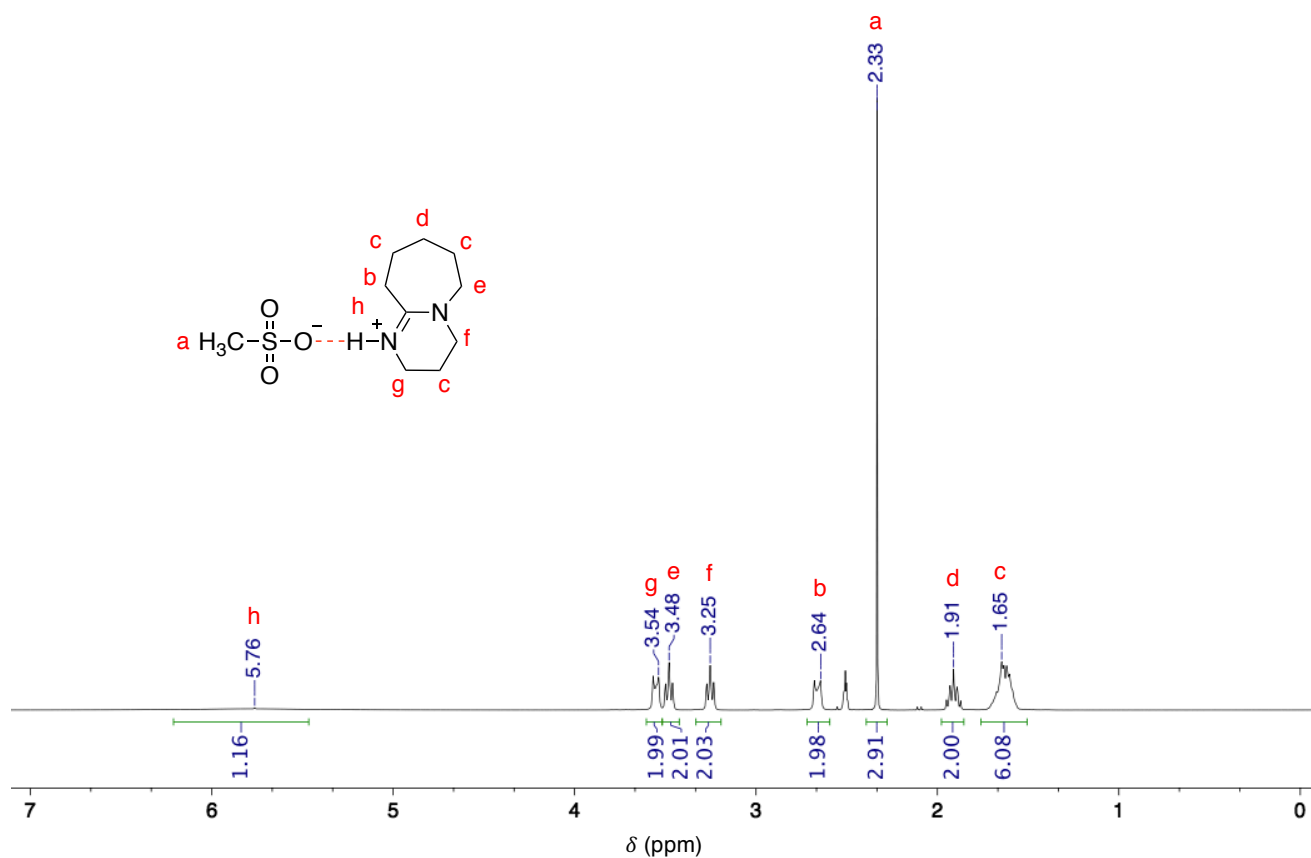


Figure S1.6. ^1H NMR spectrum of DBU:MSA ($\text{DMSO-}d_6$, 400 MHz, 298 K).

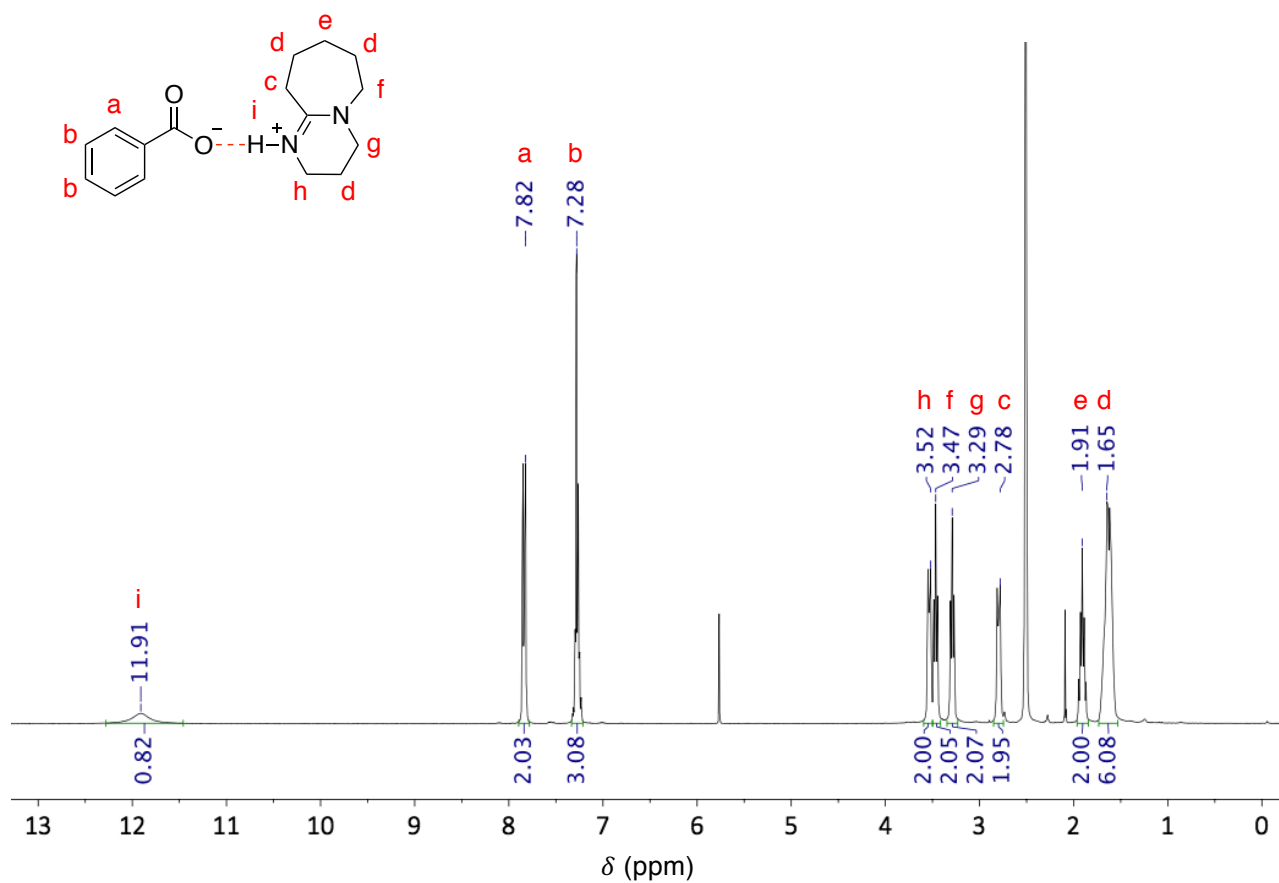


Figure S1.7. ¹H NMR spectrum of DBU:BA (DMSO-*d*₆, 400 MHz, 298 K).

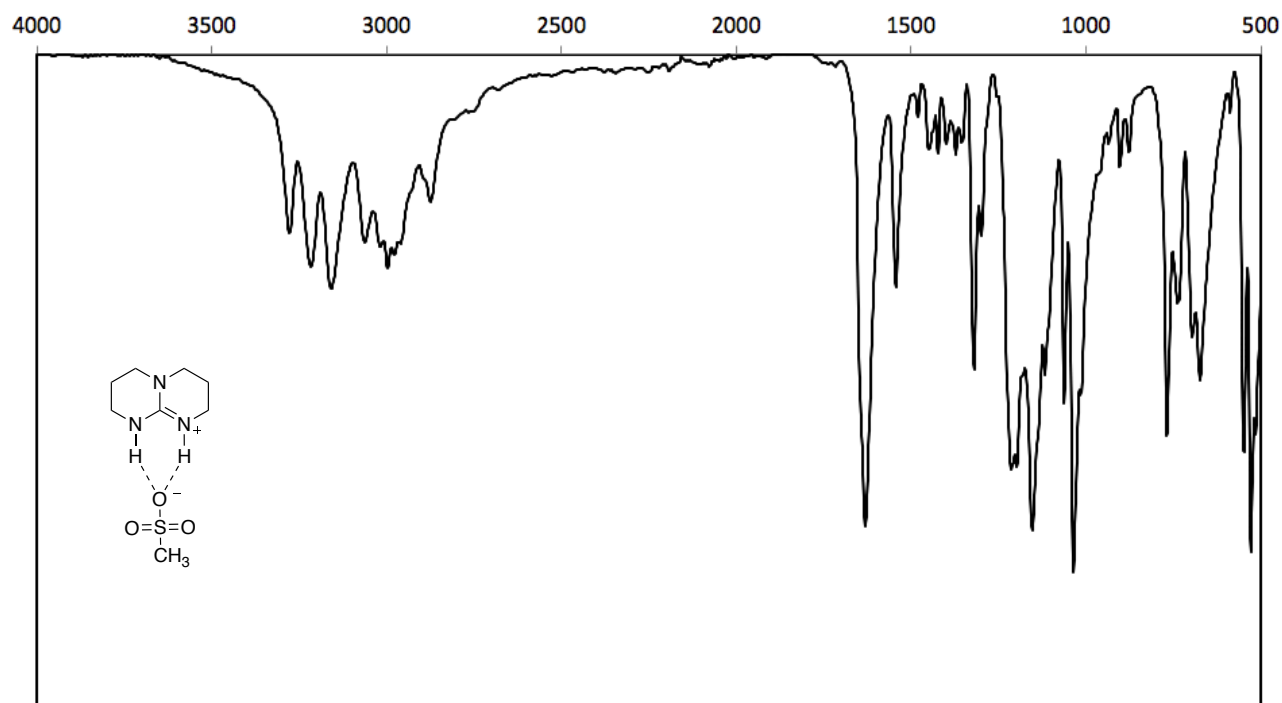


Figure S1.8. FT-IR spectrum of TBD:MSA (1:1)

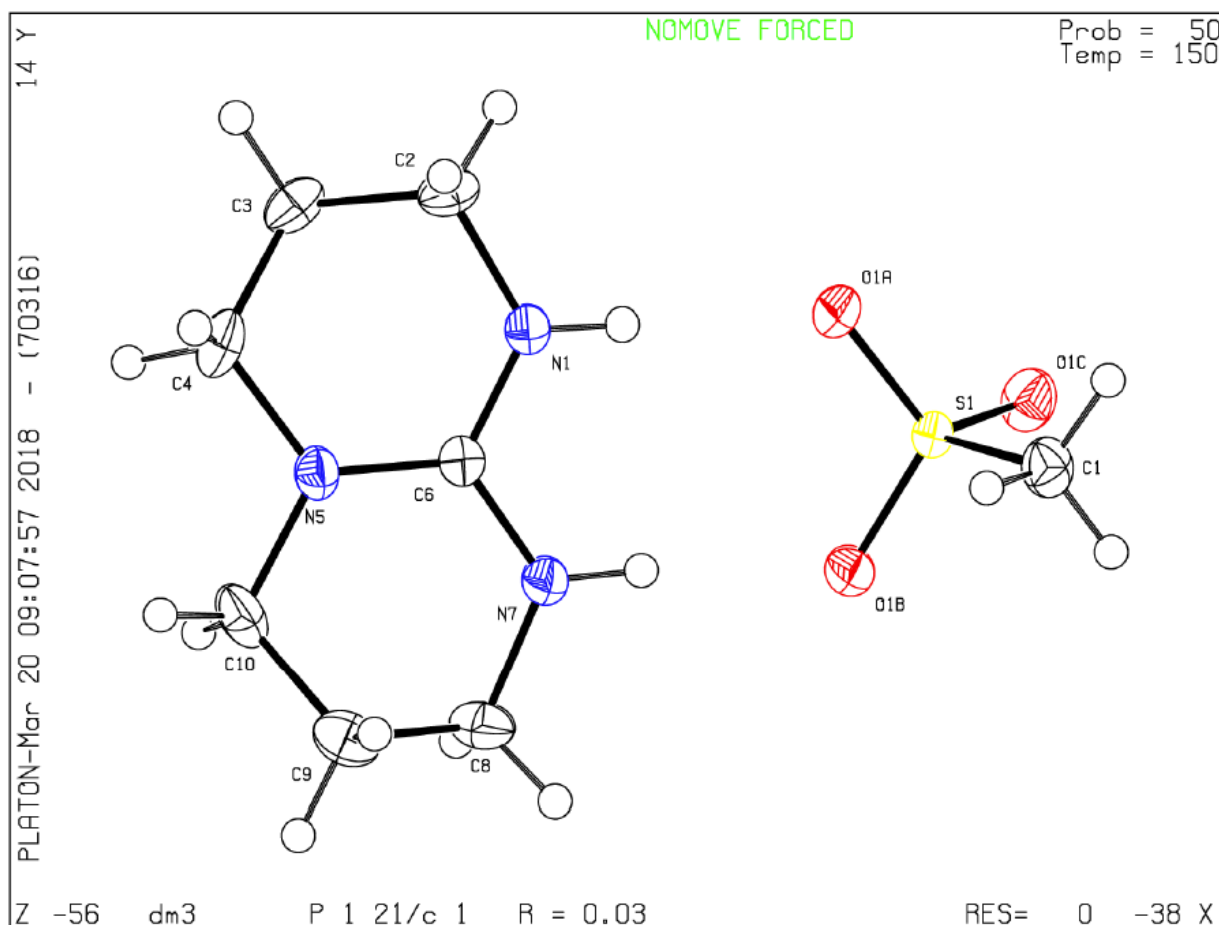


Figure S1.9. Crystal structure of TBD:MSA (1:1).

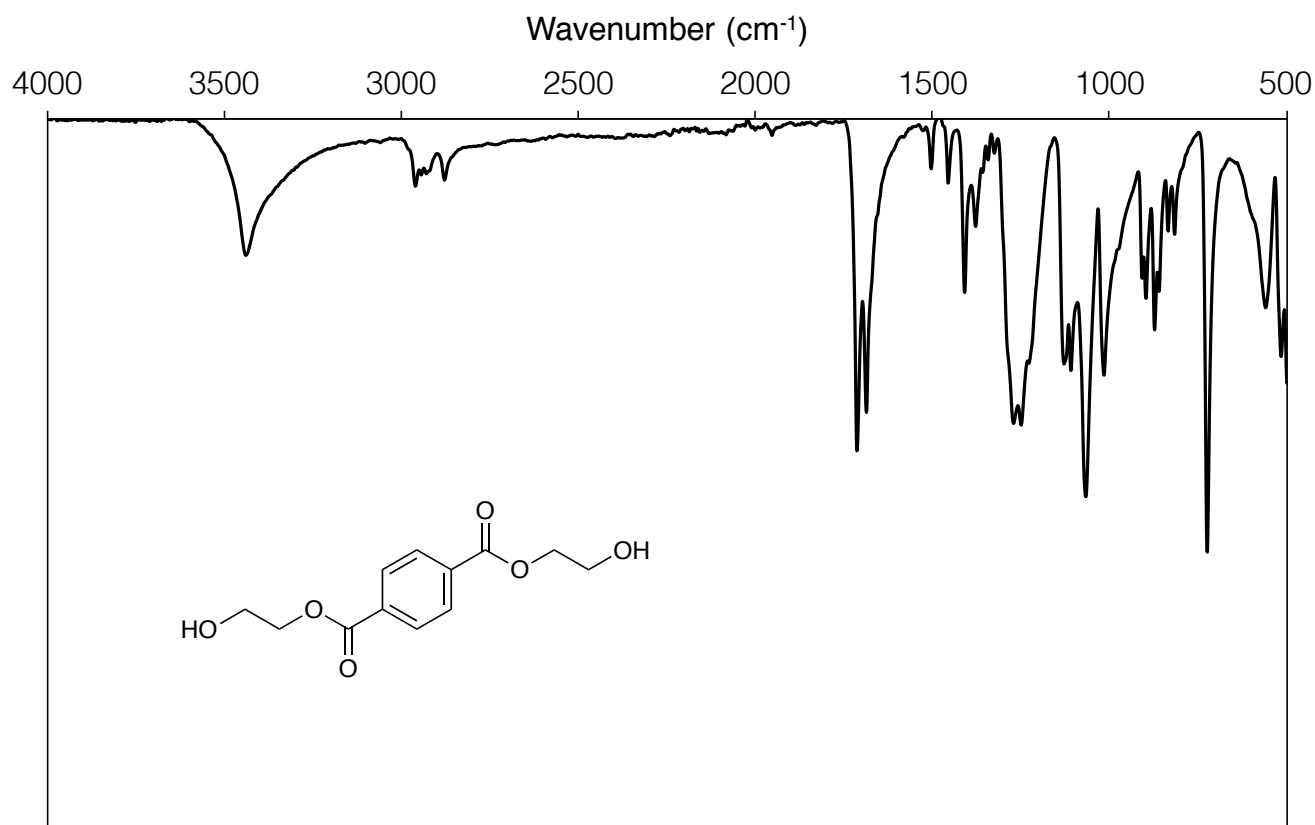
Table S1.1. Crystal data and structure refinement for TBD:MSA (1:1)

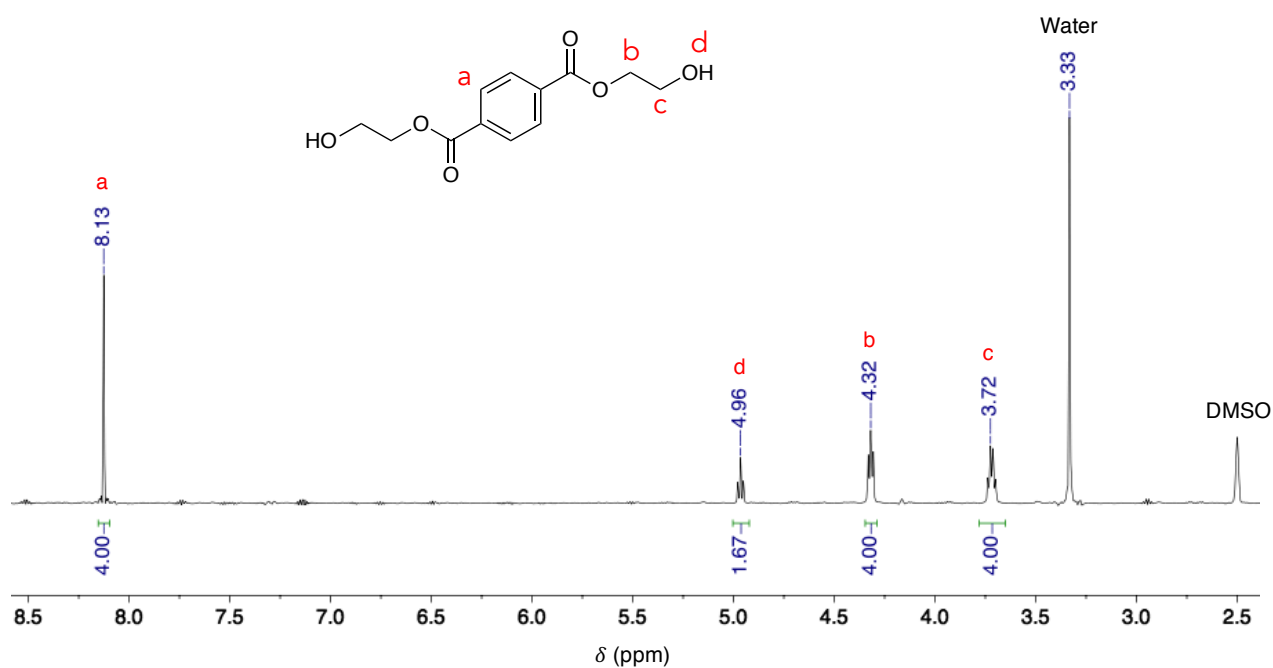
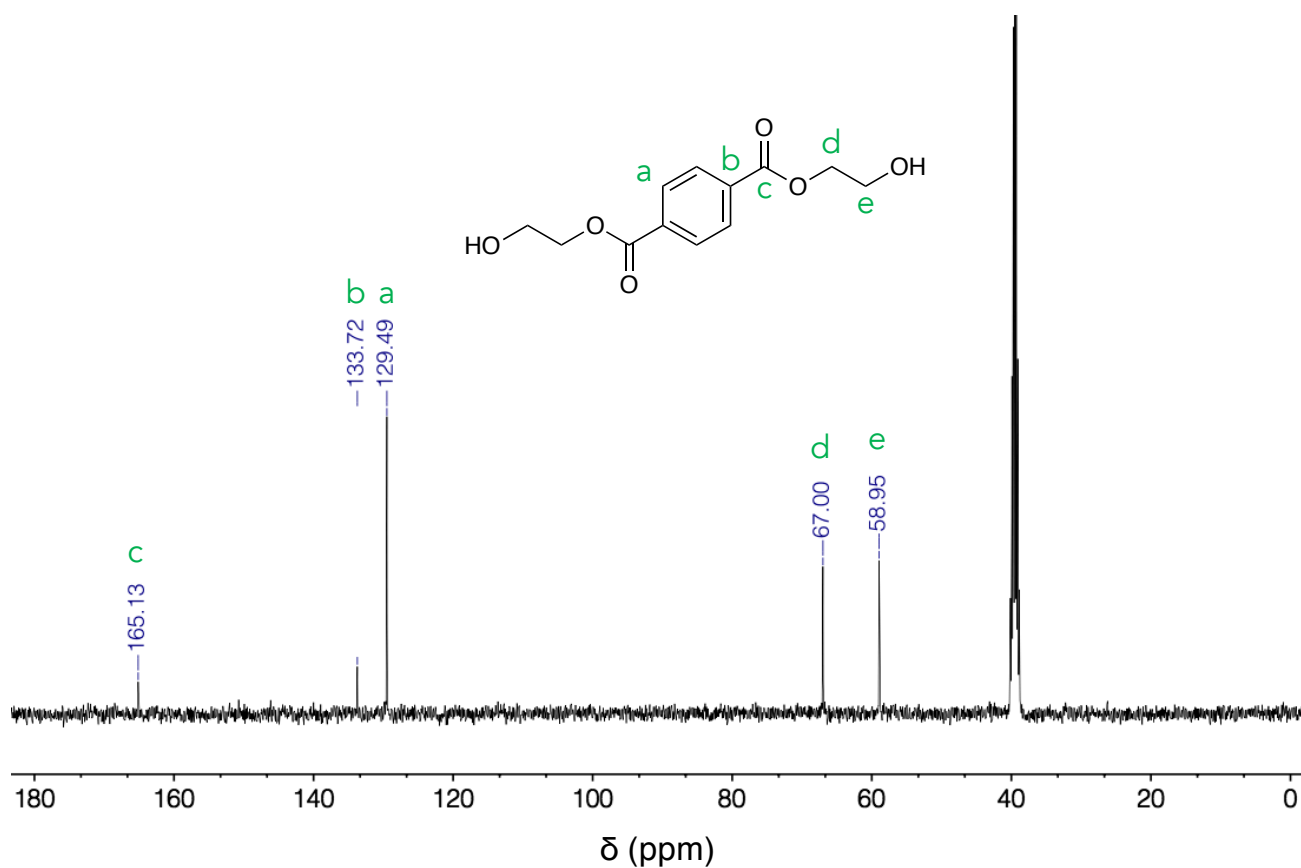
Identification code	dm3
Empirical formula	C ₈ H ₁₇ N ₃ O ₃ S
Formula weight	235.30
Temperature/K	150(2)
Crystal system	monoclinic
Space group	P2 ₁ /c
a/Å	7.83127(10)
b/Å	16.36158(17)
c/Å	8.81821(11)
α/°	90
β/°	104.5738(13)
γ/°	90
Volume/Å ³	1093.54(2)
Z	4
ρ _{calc} /cm ³	1.429
μ/mm ⁻¹	2.609

F(000)	504.0
Crystal size/mm ³	0.36 × 0.26 × 0.18
Radiation	CuKα (λ = 1.54184)
2θ range for data collection/°	10.814 to 156.952
Index ranges	-9 ≤ h ≤ 9, -20 ≤ k ≤ 20, -9 ≤ l ≤ 11
Reflections collected	14156
Independent reflections	2314 [R _{int} = 0.0307, R _{sigma} = 0.0145]
Data/restraints/parameters	2314/0/137
Goodness-of-fit on F ²	1.047
Final R indexes [I ≥ 2σ (I)]	R ₁ = 0.0341, wR ₂ = 0.0964
Final R indexes [all data]	R ₁ = 0.0347, wR ₂ = 0.0969
Largest diff. peak/hole / e Å ⁻³	0.34/-0.39

Table S1.2. Elemental analysis of TBD:MSA (1:1)

	Theoretical (%wt/wt)	Experimental (%wt/wt)
Carbon	40.8	40.4
Hydrogen	7.2	7.2
Nitrogen	17.8	17.7

Figure S1.10. FTIR spectrum of BHET (DMSO-*d*₆, 400 MHz, 298 K).

Figure S1.11. ^1H NMR spectrum of BHET (DMSO- d_6 , 400 MHz, 298 K).Figure S1.12. ^{13}C NMR spectrum of BHET (DMSO- d_6 , 400 MHz, 298 K).

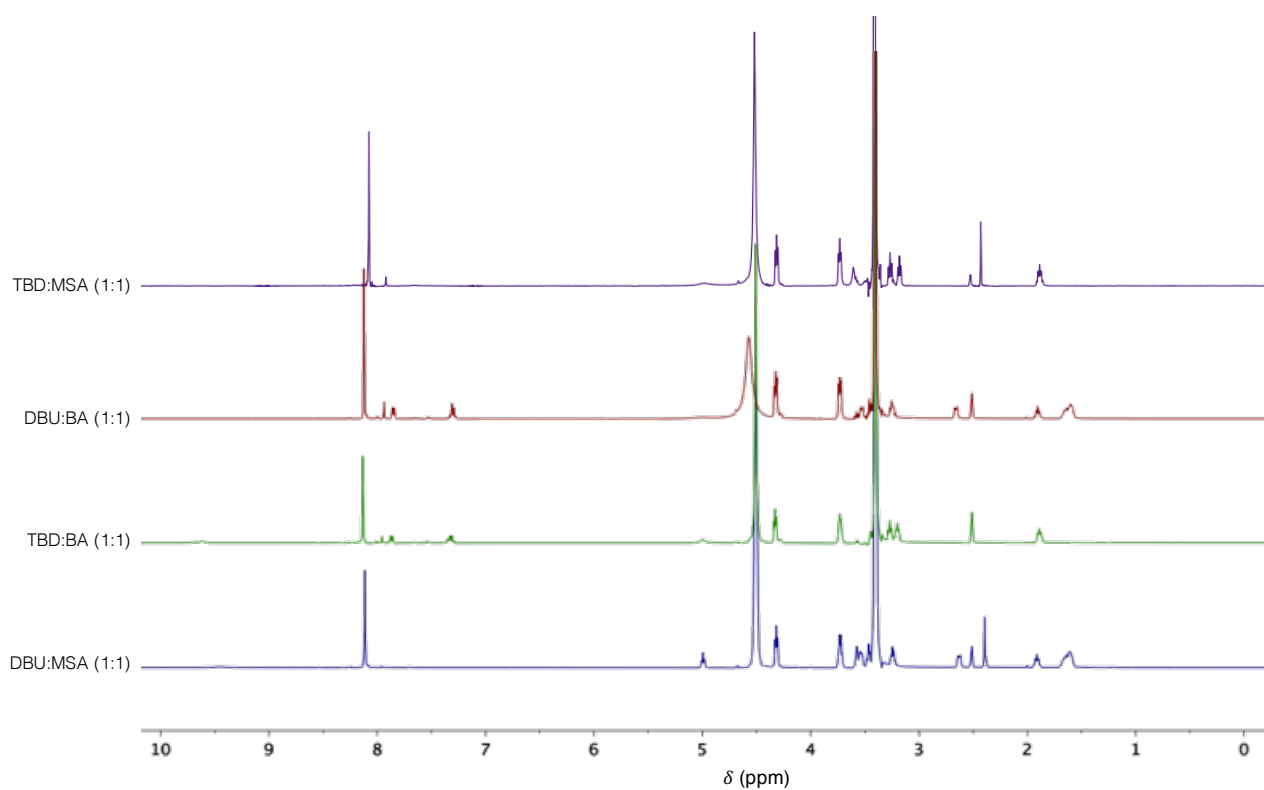


Figure S1.13. Stacked ^1H NMR spectra for the depolymerisation of PET (0.5 g, 2.60 mmol, 1 eq.) using different dual catalyst (0.5 eq.) with ethylene glycol (2.42 g, 39 mmol, 15 eq.) as reagent at 180 °C (DMSO- d_6 , 400 MHz, 298 K).

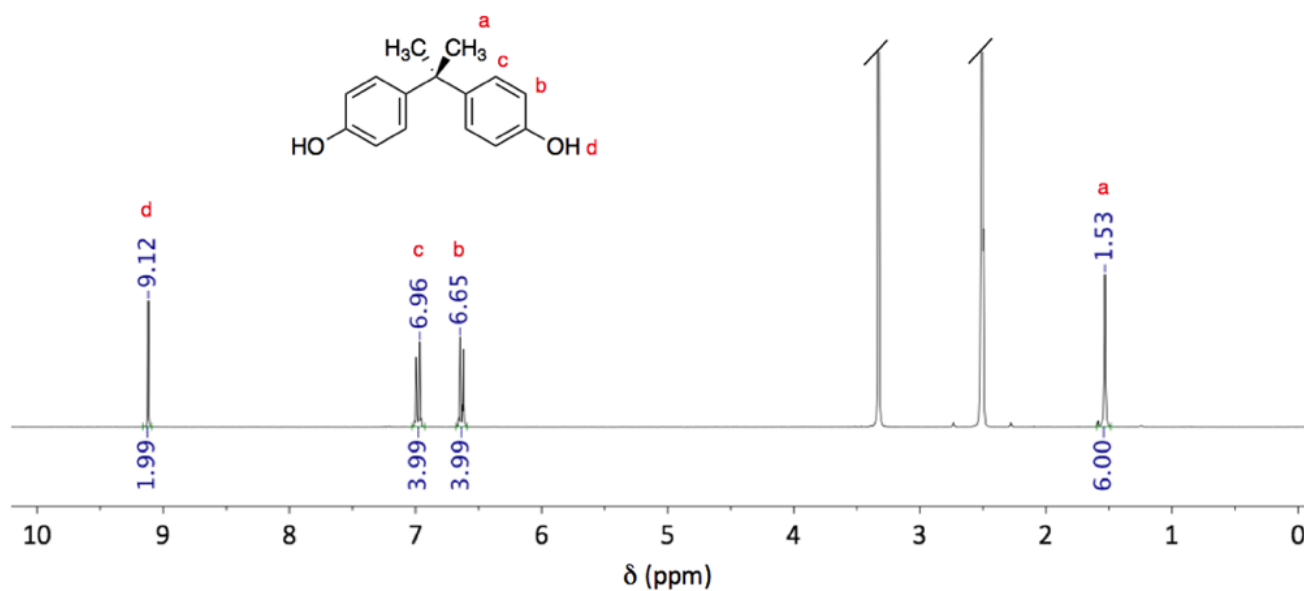


Figure S1.14. ^1H NMR spectrum of BPA (DMSO- d_6 , 400 MHz, 298 K).

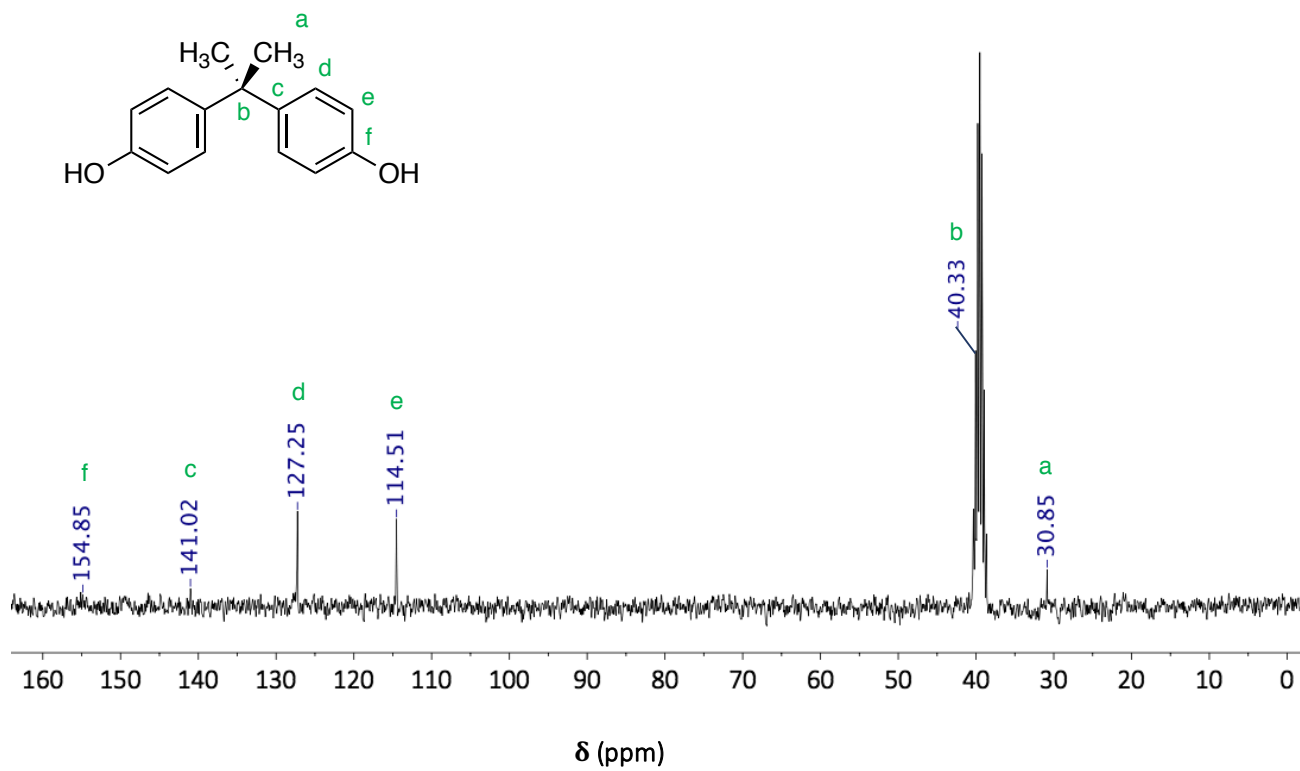


Figure S1.15. ^{13}C NMR spectrum of BPA (DMSO- d_6 , 400 MHz, 298 K).

Appendix Chapter 2

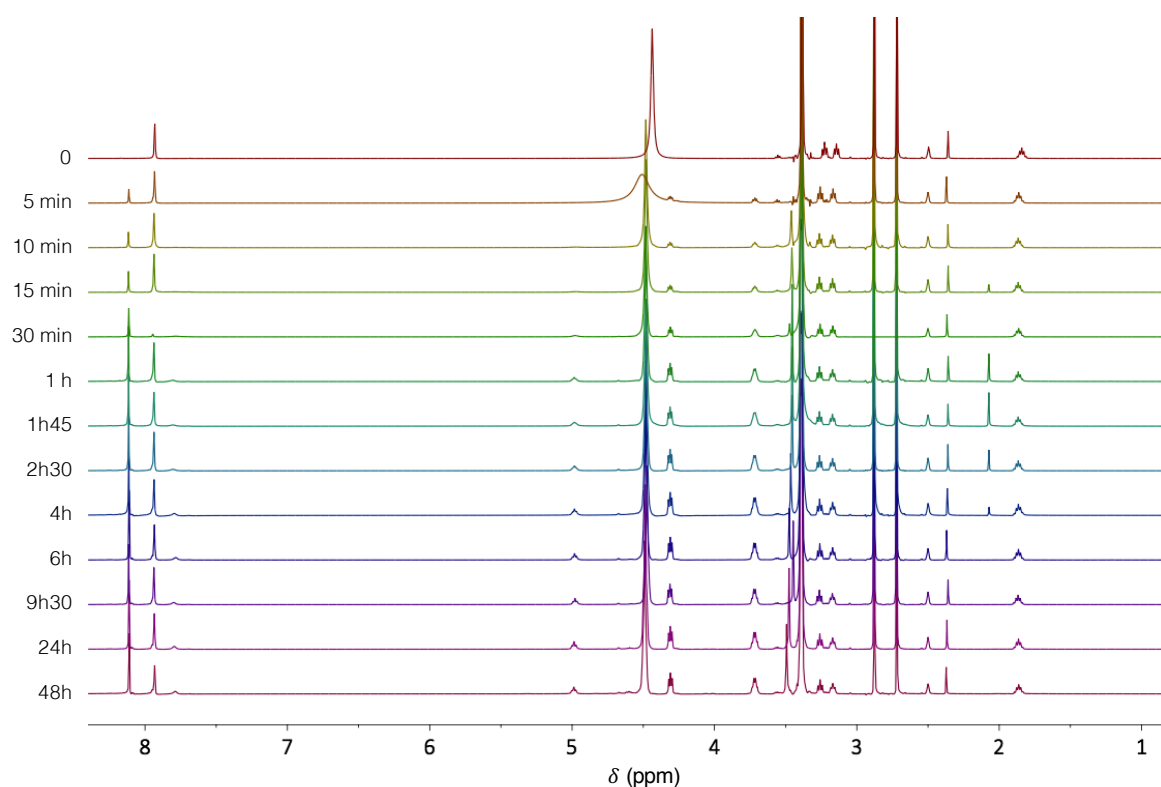


Figure S2.1. Stacked ¹H NMR spectra for the kinetic of the depolymerisation of PET (0.5 g, 2.60 mmol, 1 eq.) with ethylene glycol (2.42 g, 39 mmol, 15 eq.) as reagent using TBD:MSA (1:1) as catalyst (0.305 g, 1.30 mmol, 0.5 eq.) at 180 °C (DMSO-*d*₆, 400 MHz, 298 K).

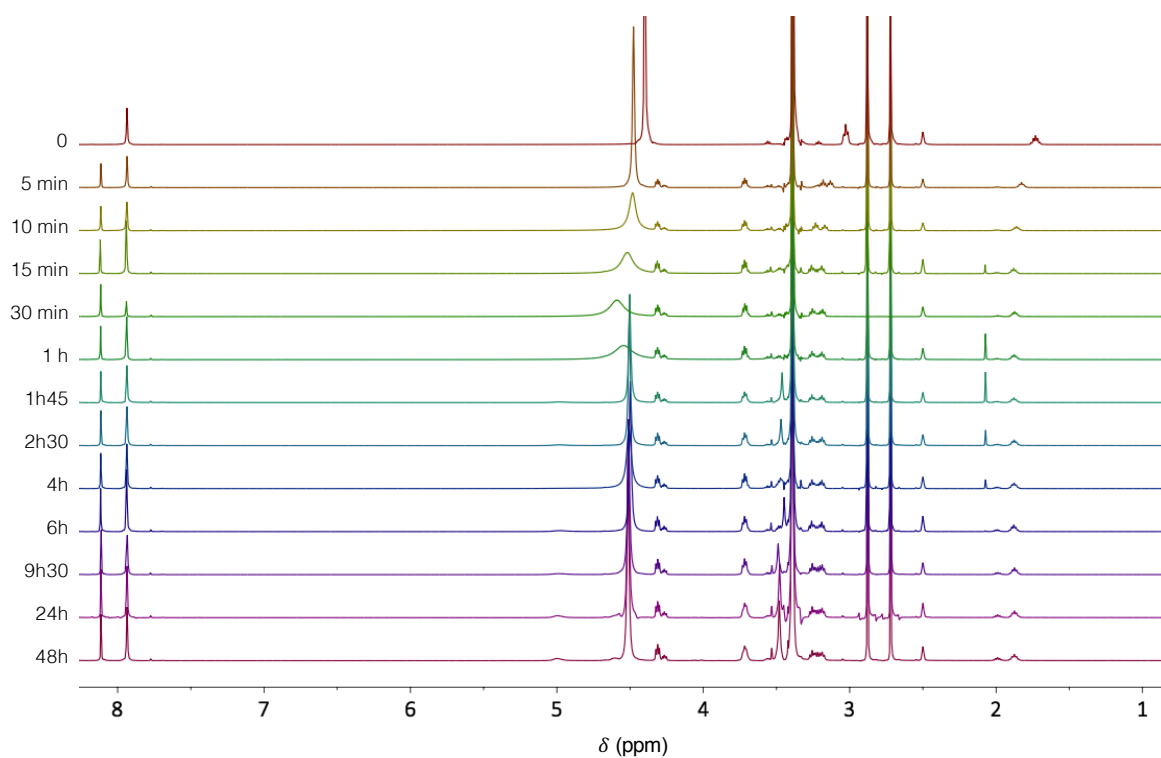


Figure S2.2. Stacked ¹H NMR spectra for the kinetic of the depolymerisation of PET (0.5 g, 2.60 mmol, 1 eq.) with ethylene glycol (2.42 g, 39 mmol, 15 eq.) as reagent using TBD as catalyst (0.181 g, 1.30 mmol, 0.5 eq.) at 180 °C (DMSO-*d*₆, 400 MHz, 298 K).

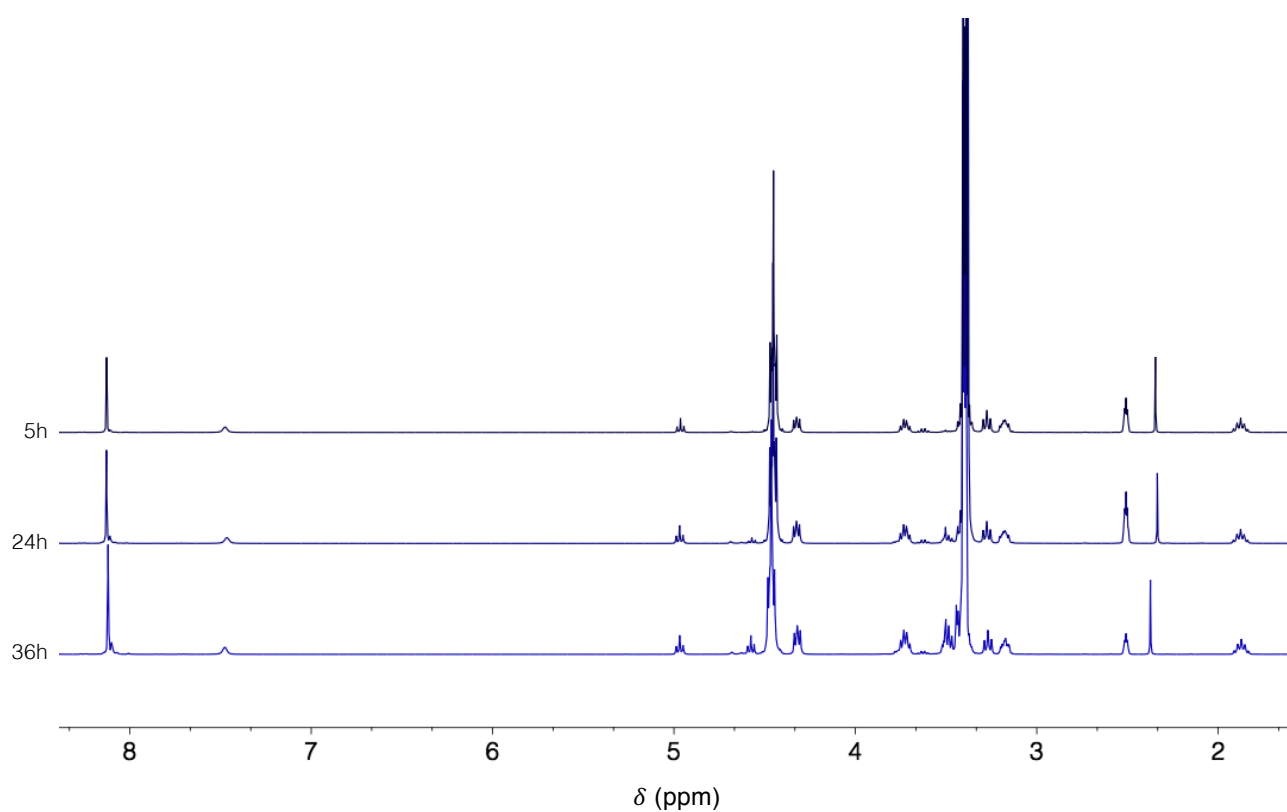


Figure S2.3. Stacked ¹H NMR spectra for the evolution of the depolymerisation of PET blue bottle pellets (0.5 g, 2.60 mmol, 1eq.) with ethylene glycol (2.42 g, 39 mmol, 15 eq.) as reagent using TBD:MSA (1:1) as catalyst (1.30 mmol, 0.5 eq.) at 180 °C (DMSO-*d*₆, 400 MHz, 298 K).

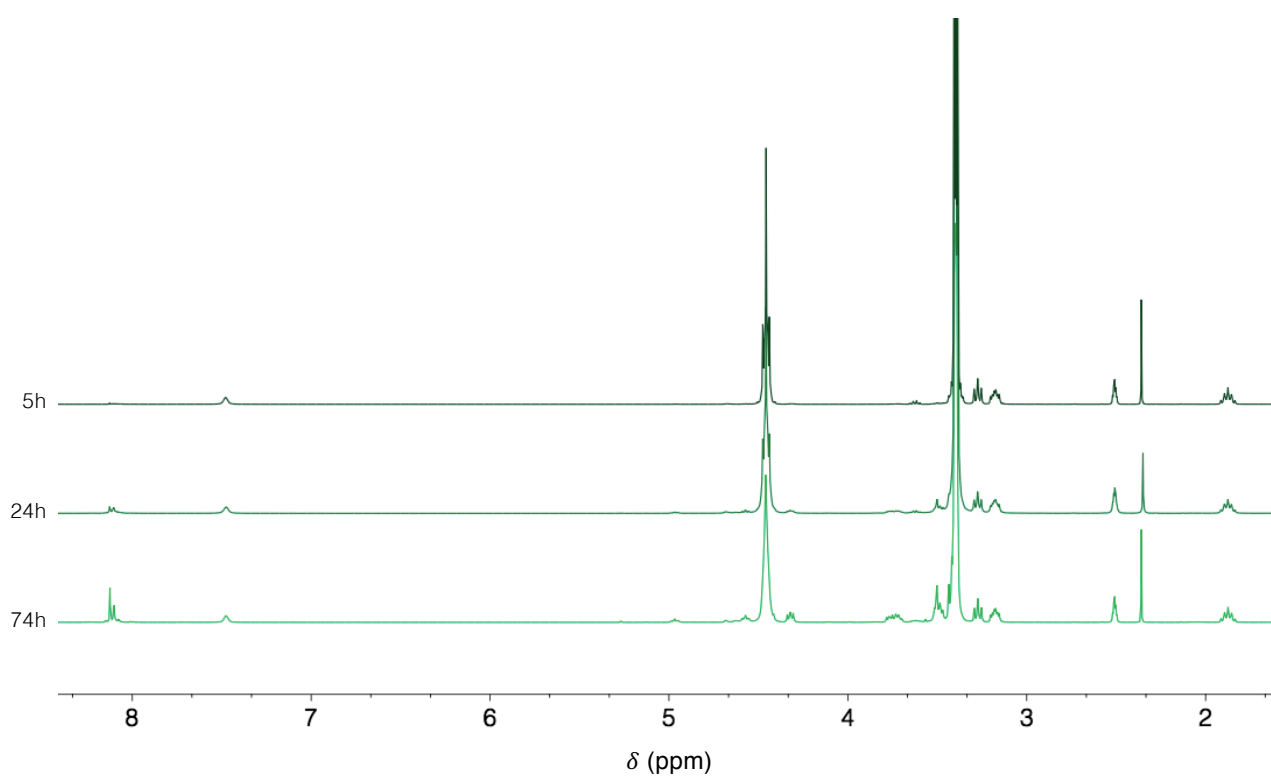


Figure S2.4. Stacked ¹H NMR spectra for the evolution of the depolymerisation of PET green bottle pellets (0.5 g, 2.60 mmol, 1eq.) with ethylene glycol (2.42 g, 39 mmol, 15 eq.) as reagent using TBD:MSA (1:1) as catalyst (1.30 mmol, 0.5 eq.) at 180 °C (DMSO-*d*₆, 400 MHz, 298 K).

Appendix Chapter 3

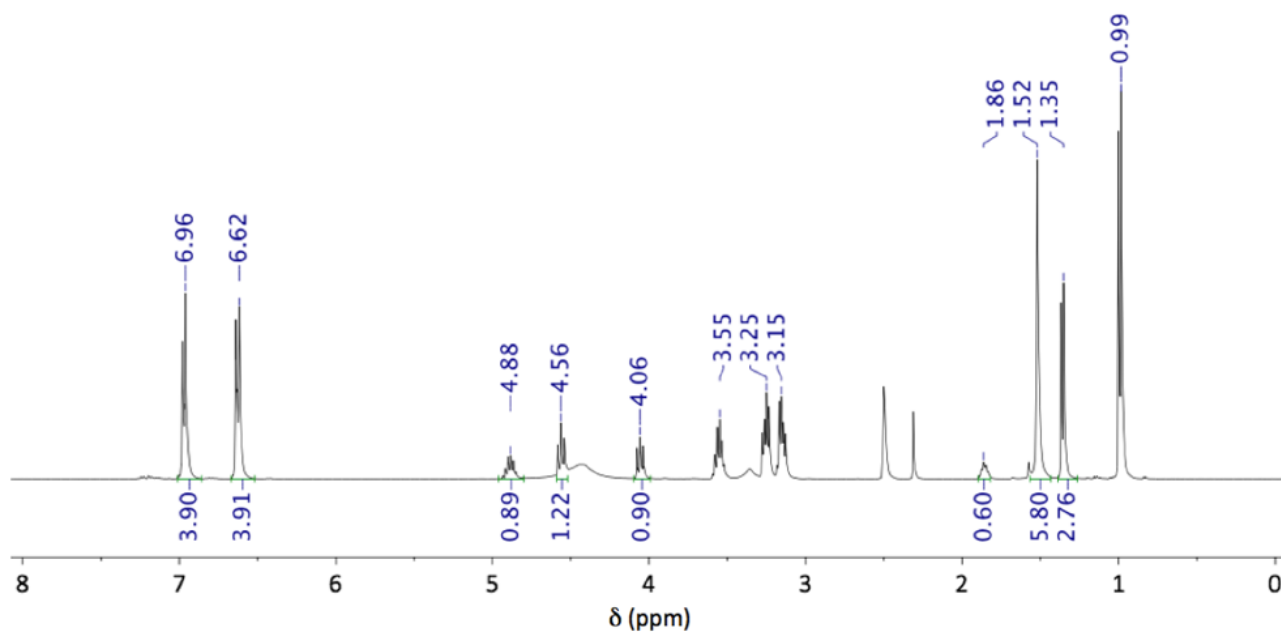


Figure S3.1. ^1H NMR spectrum of the crude product containing propylene carbonate (**2a**) ($\text{DMSO-}d_6$, 400 MHz, 298 K). Resonances assigned as: BPA – δ 6.96 (d, 4H, CH-C-C), 6.62 (d, 4H, CH-C-OH), 1.53 (s, 6H, CH_3); **2a** – δ 4.88 (m, 1H, CH), 4.56 (t, 1H, CH_2), 4.06 (t, 1H, CH_2), 1.35 (t, 3H, CH_3). Signals at $\delta = 3.55$, 3.25, 3.15 and 0.99 ppm correspond to residual reagent (**1a**), and signal at $\delta = 1.86$ ppm corresponds to TBD:MSA signal used as internal standard for calculating conversion.

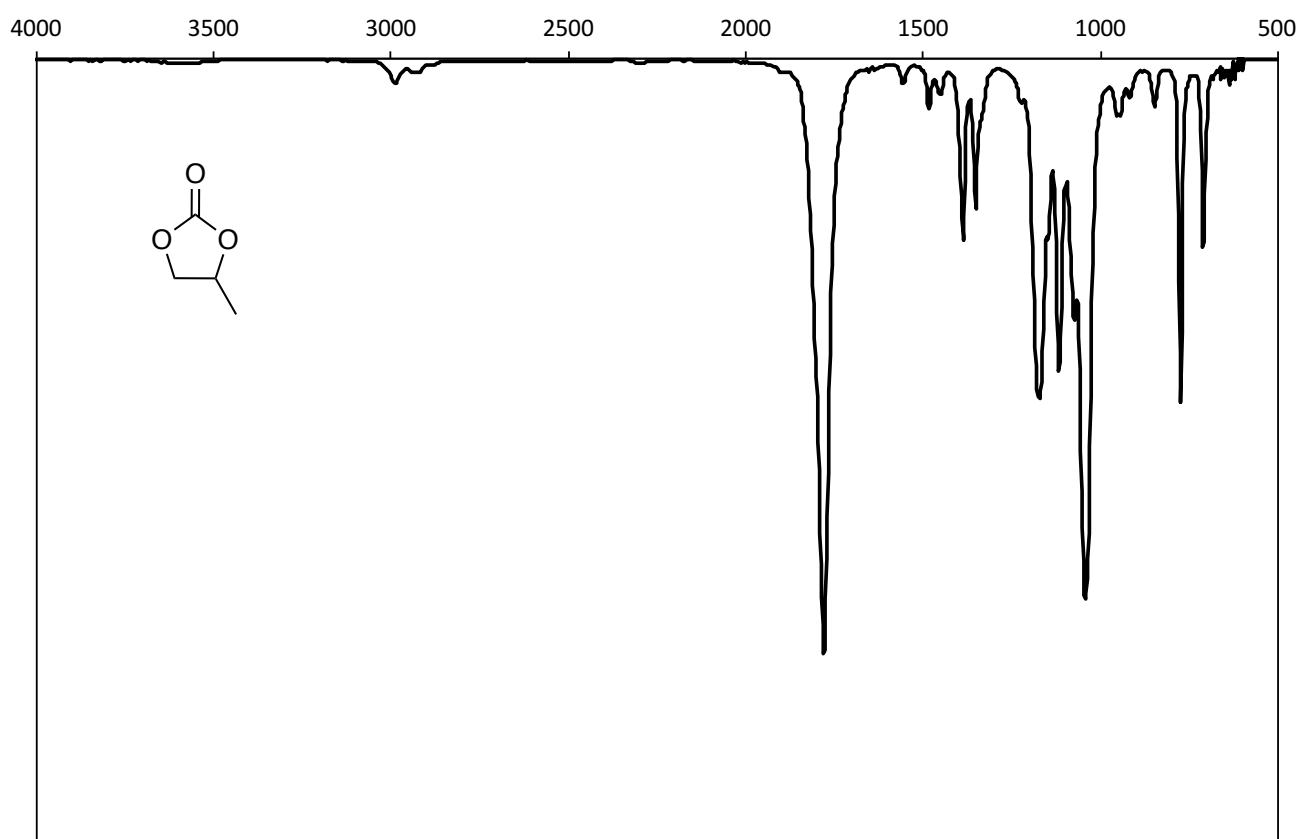


Figure S3.2. FT-IR spectrum of propylene carbonate (**2a**).

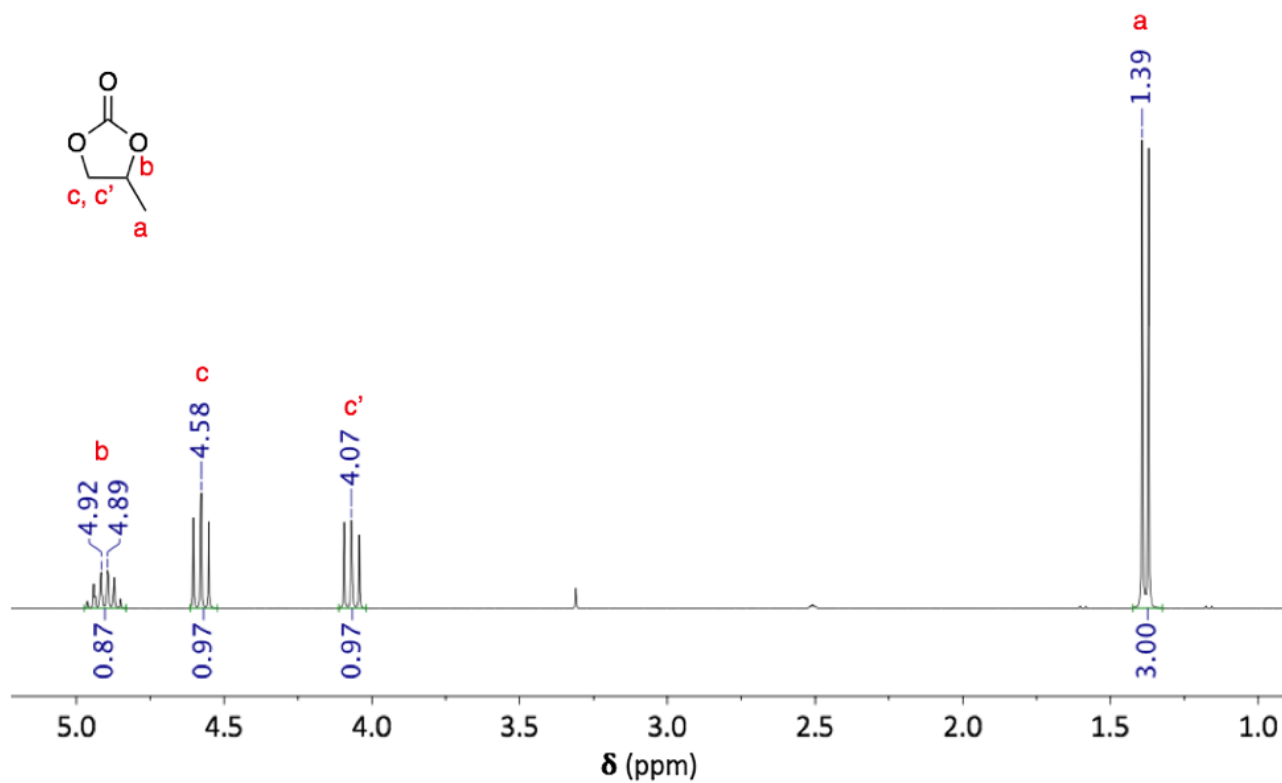


Figure S3.3. ¹H NMR spectrum of propylene carbonate (2a) (DMSO-*d*₆, 400 MHz, 298 K).

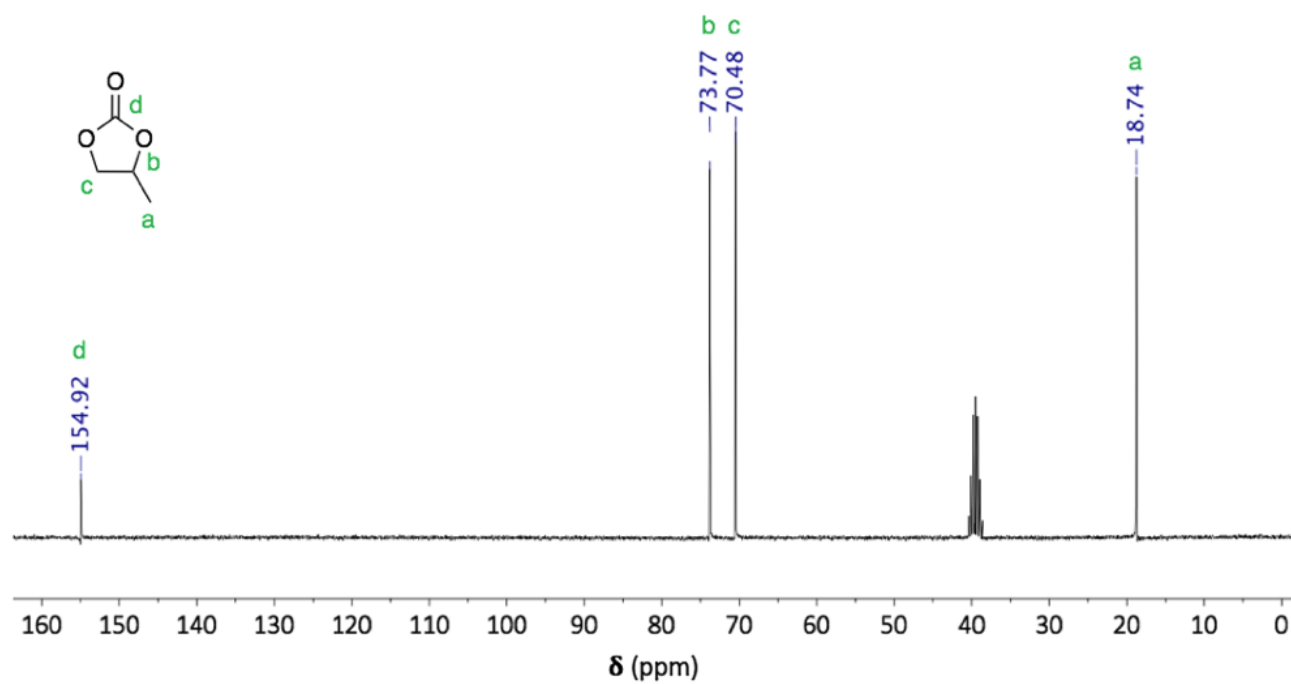


Figure S3.4. ¹³C NMR spectrum of propylene carbonate (2a) (DMSO-*d*₆, 400 MHz, 298 K).

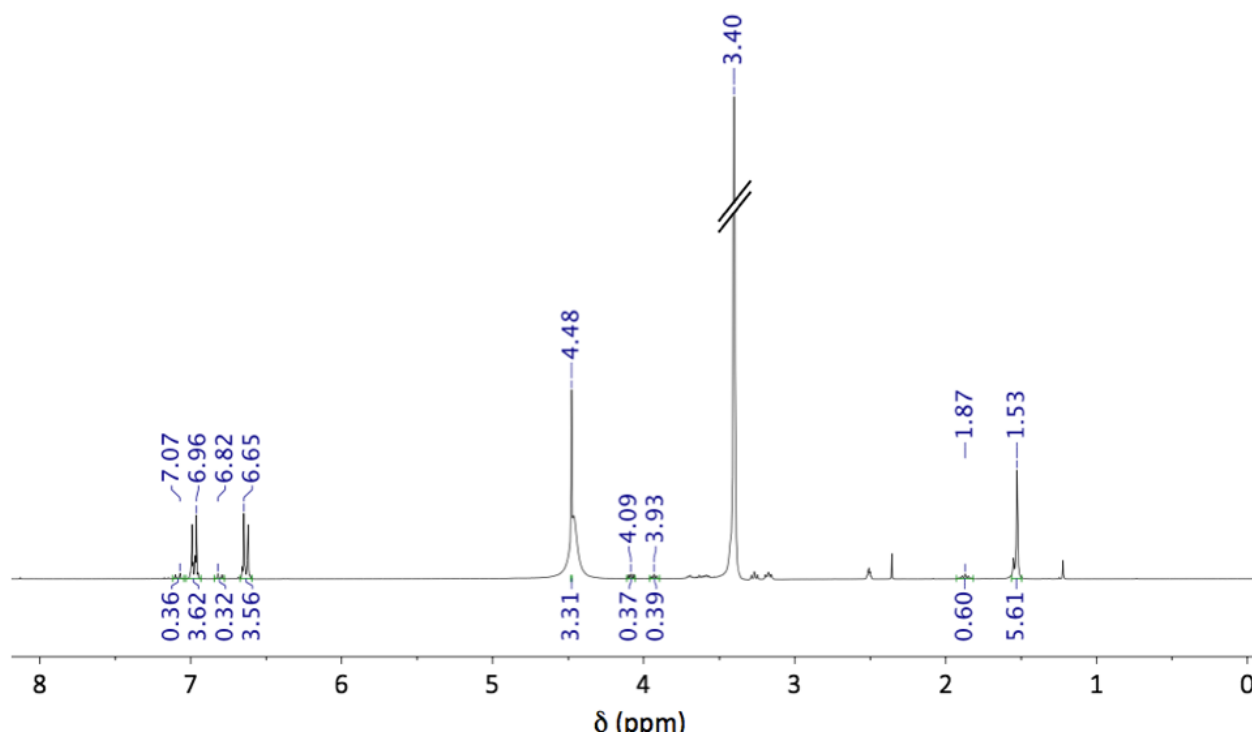


Figure S3.5. ^1H NMR spectrum of the crude product containing ethylene carbonate (**2b**) ($\text{DMSO-}d_6$, 400 MHz, 298 K). Resonances assigned as: **BPA** – δ 6.65 (d, 4H), 6.96 (d, 4H), 1.53 (s, 6H); **2b** – δ 4.48 (s, 4H, CH_2); **side product** – δ 7.07 (d, 4H), 6.82 (d, 4H), 4.09 (m, 4H), 3.93 (t, 4H). Signal at δ = 3.40 ppm corresponds to residual reagent (**1b**), and signal at δ = 1.87 ppm corresponds to TBD:MSA signal used as internal standard for calculating conversion.

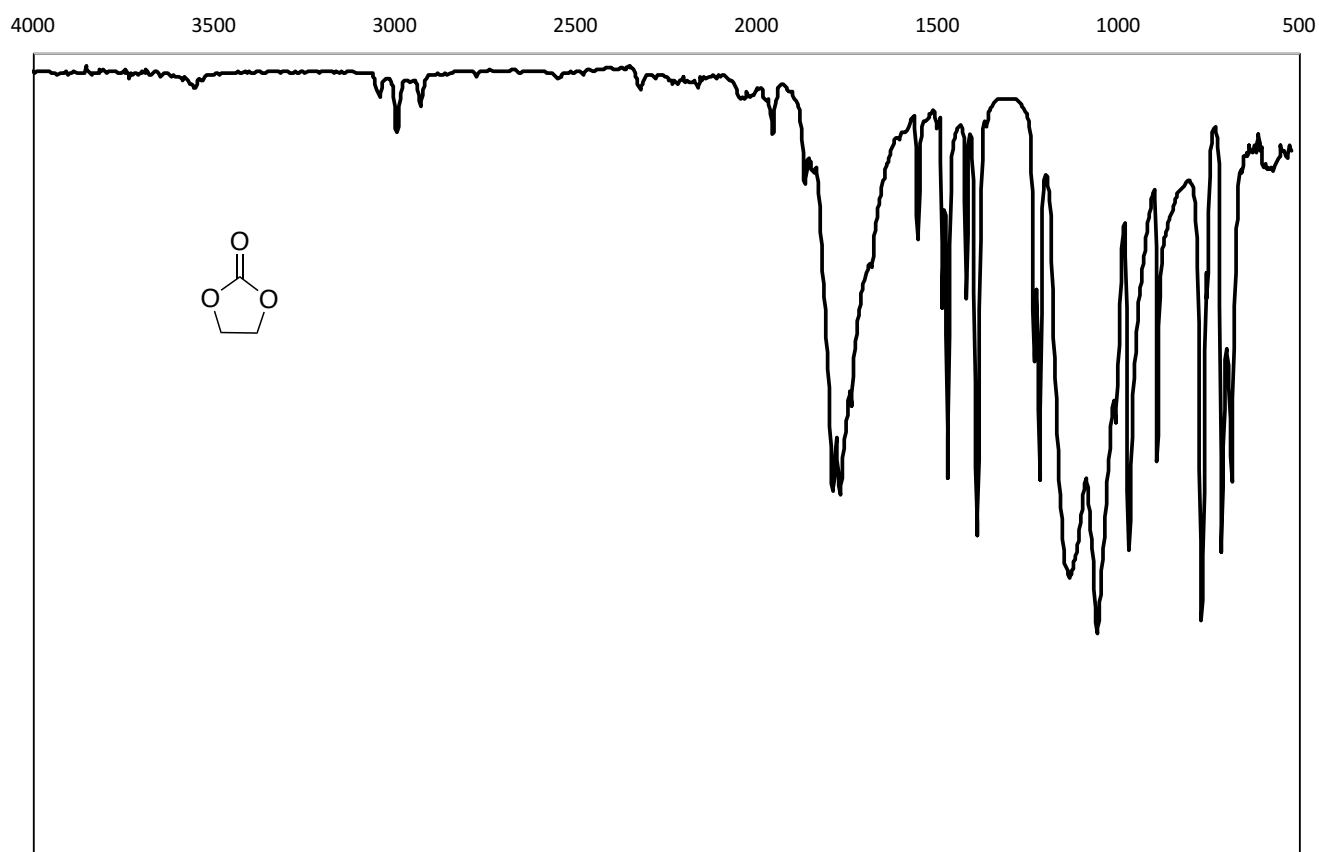


Figure S3.6. FT-IR spectrum of ethylene carbonate (**2b**).

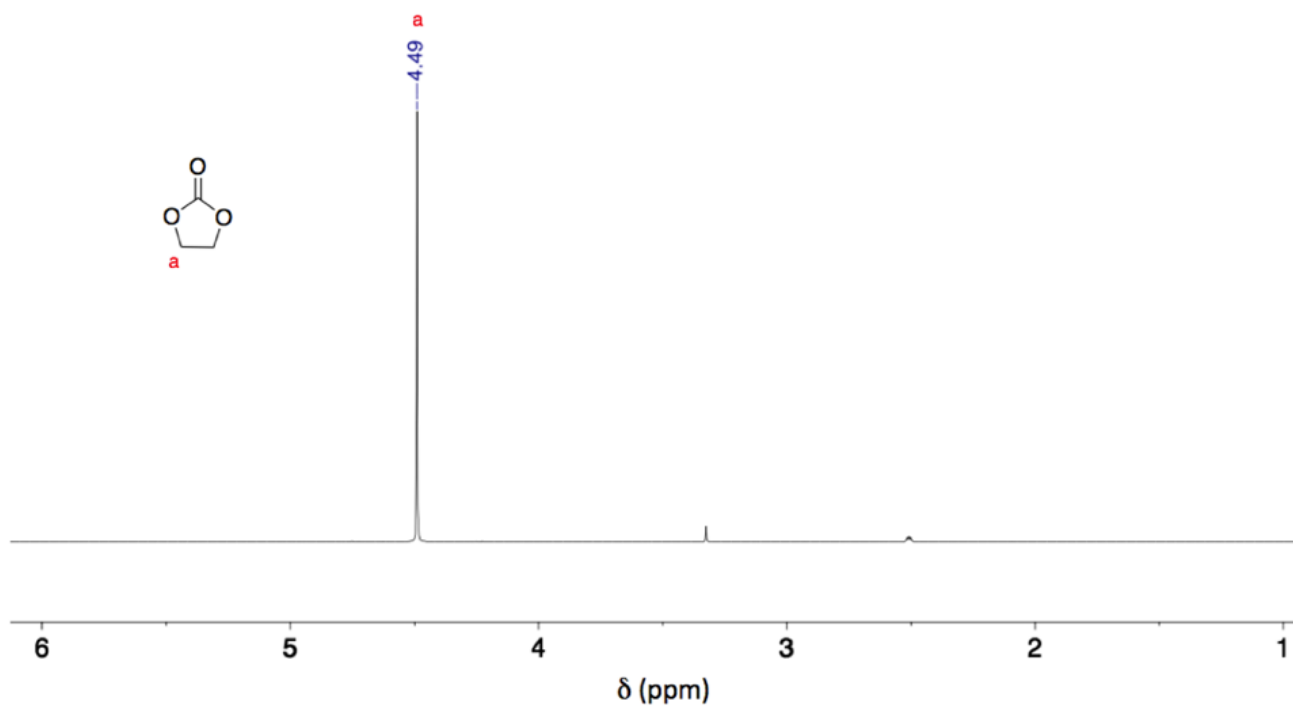


Figure S3.7. ^1H NMR spectrum of ethylene carbonate (2b) ($\text{DMSO-}d_6$, 400 MHz, 298 K).

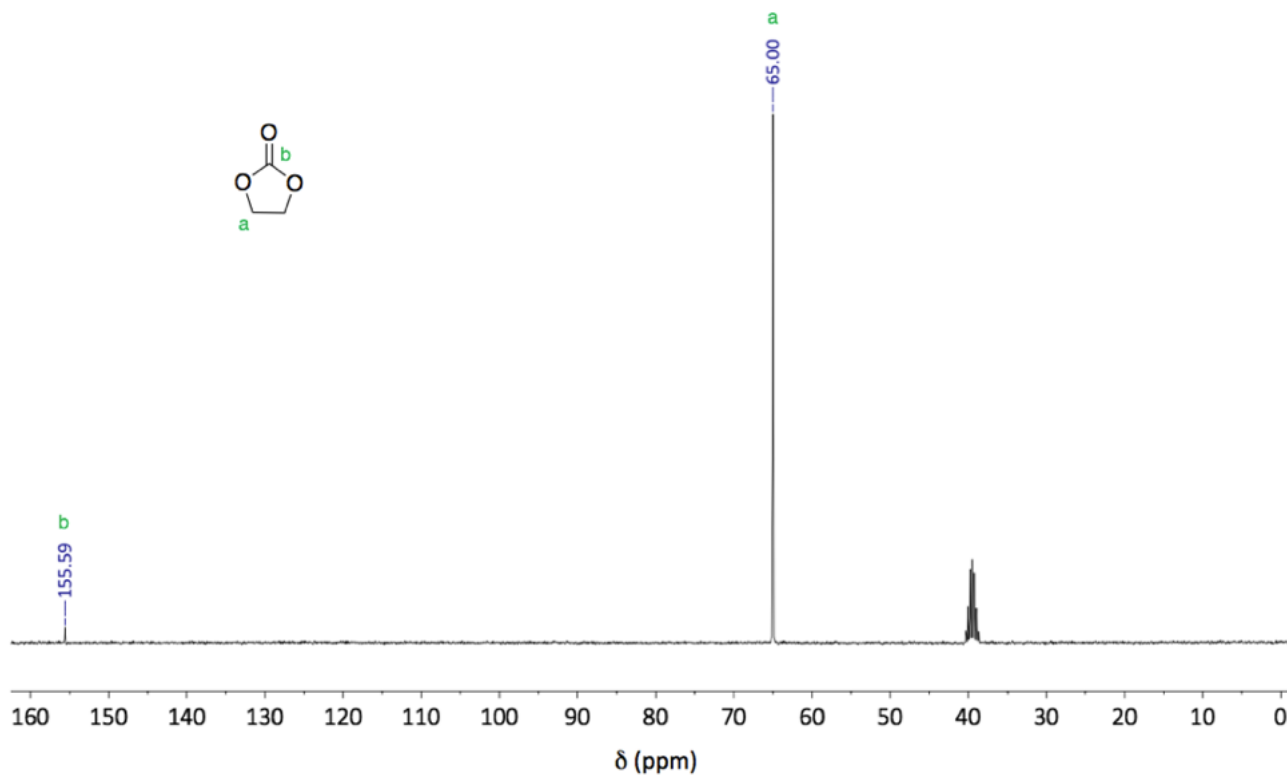


Figure S3.8. ^{13}C NMR spectrum of ethylene carbonate (2b) ($\text{DMSO-}d_6$, 400 MHz, 298 K).

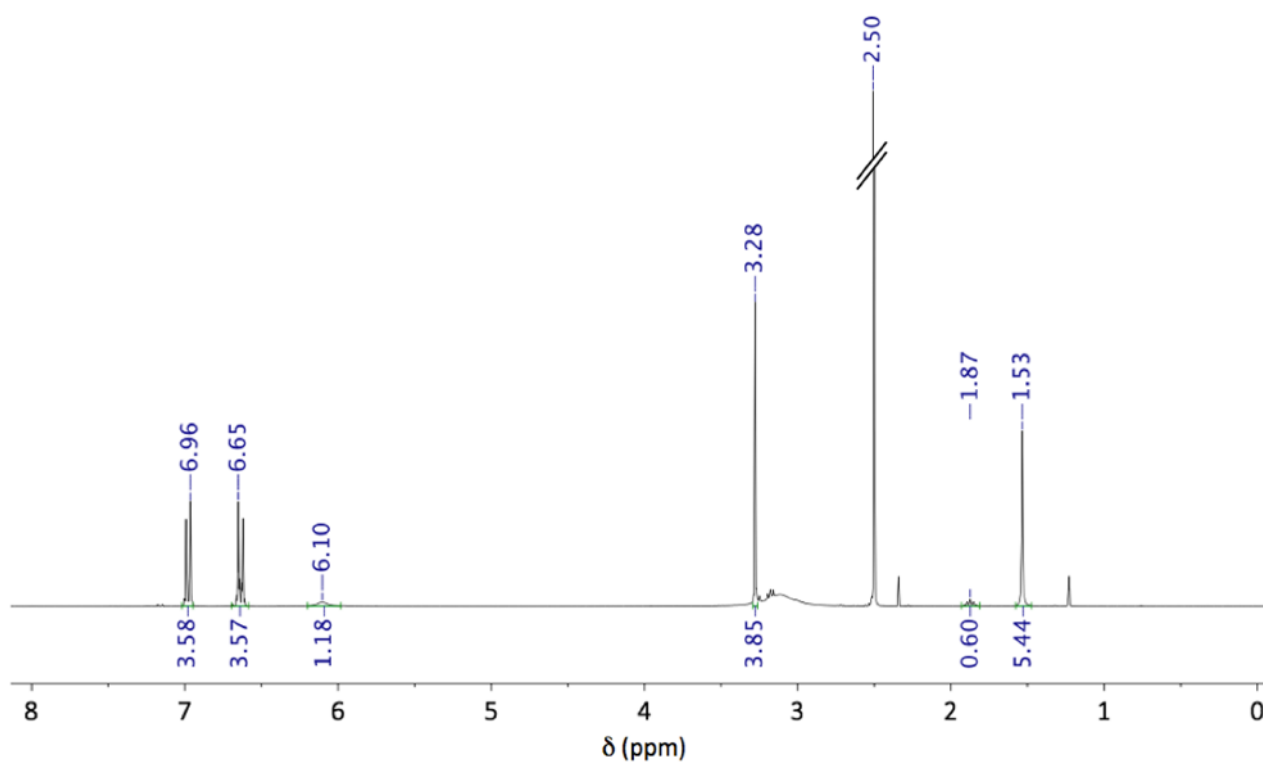


Figure S3.9. ^1H NMR spectrum of the crude product containing imidazolidin-2-one (**2c**) ($\text{DMSO-}d_6$, 400 MHz, 298 K). Resonances assigned as: **BPA** – δ 6.96 (d, 4H, CH-C-C), 6.65 (d, 4H, CH-C-OH), 1.53 (s, 6H, CH_3); **2c** – δ 6.10 (s, 4H, NH), 3.28 (s, 4H, CH_2). Signal at $\delta = 3.28$ ppm corresponds to residual reagent (**1c**), and signal at $\delta = 1.87$ ppm corresponds to TBD:MSA signal used as internal standard for calculating conversion.

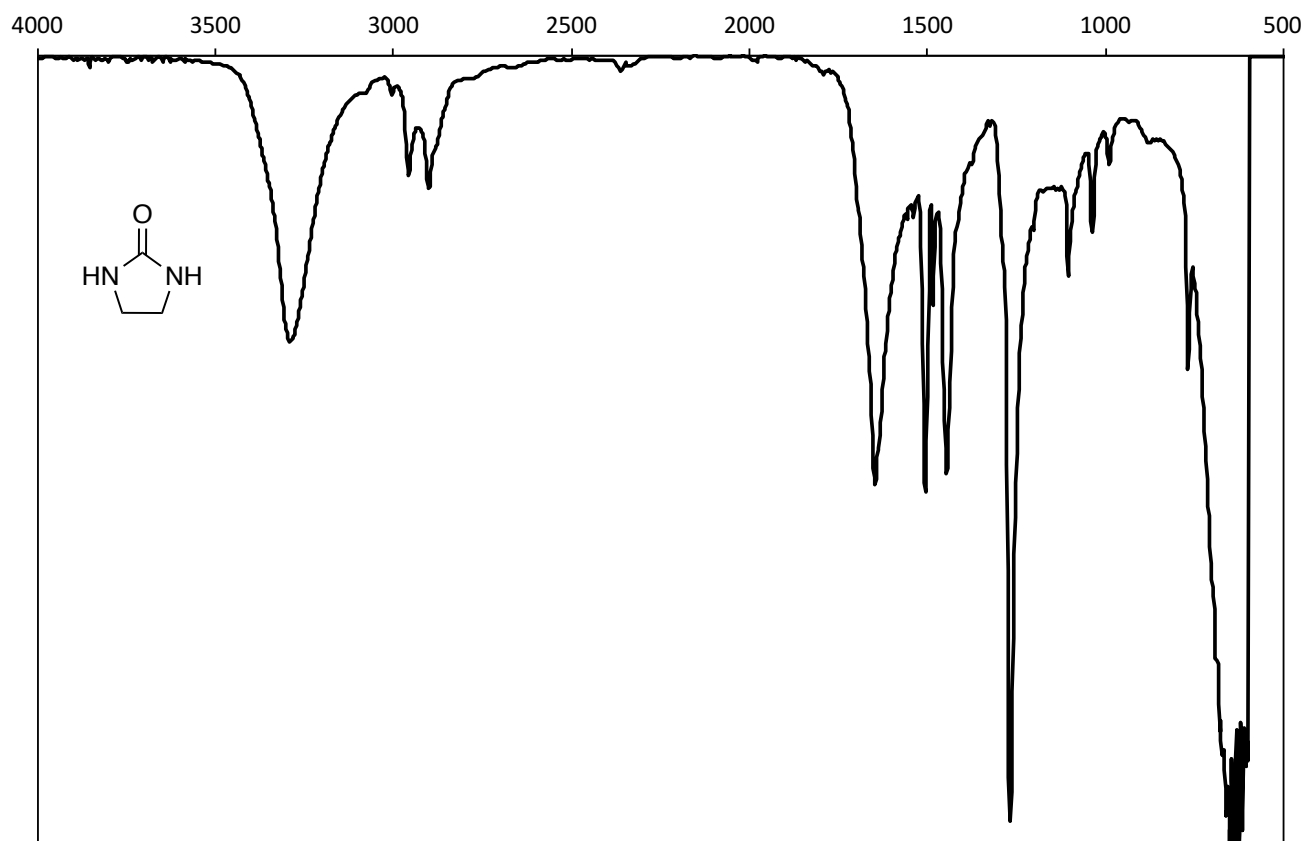


Figure S3.10. FT-IR spectrum of imidazolidin-2-one (**2c**).

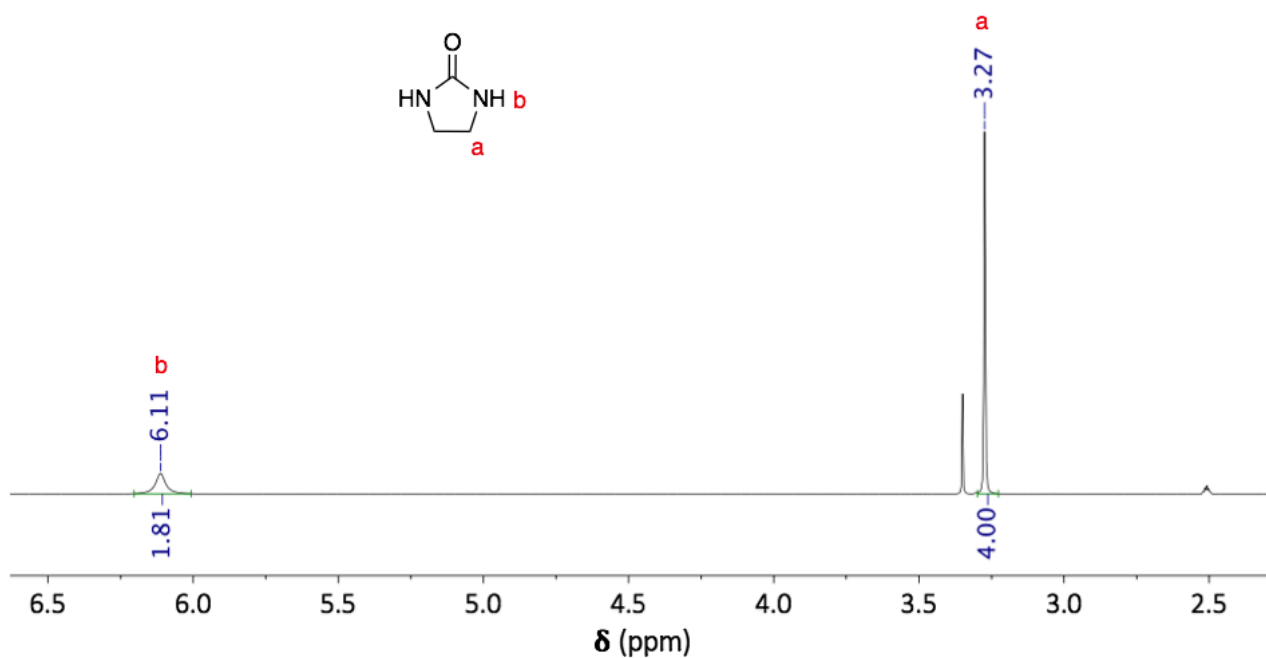


Figure S3.11. ¹H NMR spectrum of imidazolidin-2-one (2c) (DMSO-*d*₆, 400 MHz, 298 K).

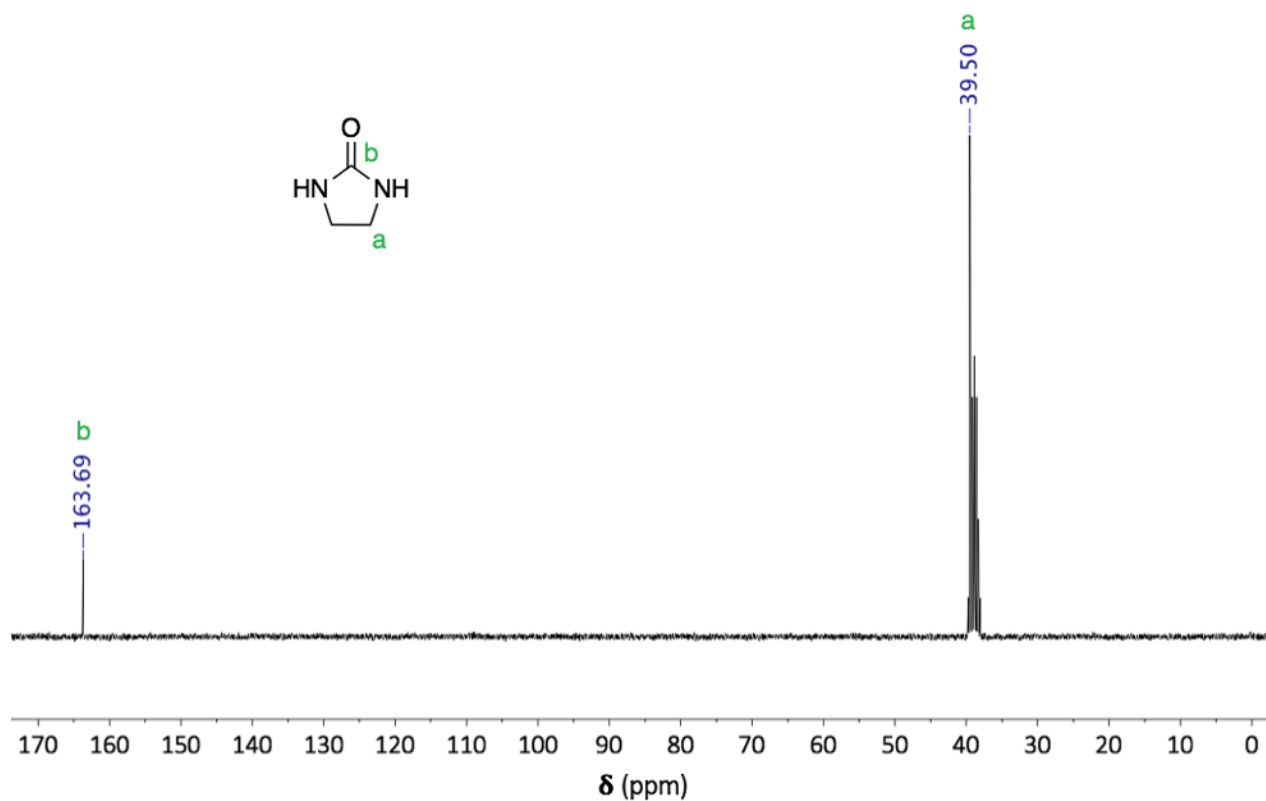


Figure S3.12. ¹³C NMR spectrum of imidazolidin-2-one (2c) (DMSO-*d*₆, 400 MHz, 298 K).

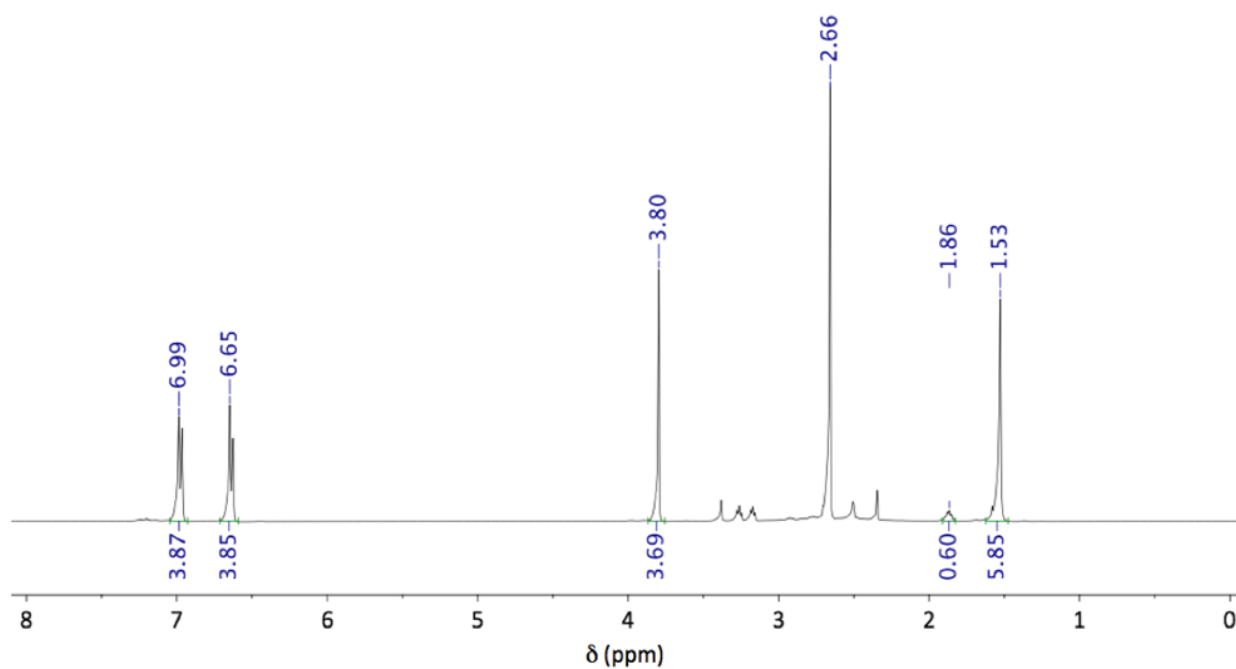


Figure S3.13. ¹H NMR spectrum of the crude product containing **3-dithiolan-2-one (2d)** (DMSO-*d*₆, 400 MHz, 298 K). Resonances assigned as: **BPA** – δ 6.99 (d, 4H, CH-C-C), 6.65 (d, 4H, CH-C-OH), 1.53 (s, 6H, CH₃); **2d** – δ 3.80 (s, 4H, CH₂). Signal at δ = 2.66 ppm corresponds to residual reagent (**1d**), and signal at δ = 1.86 ppm corresponds to TBD:MSA signal used as internal standard for calculating conversion.

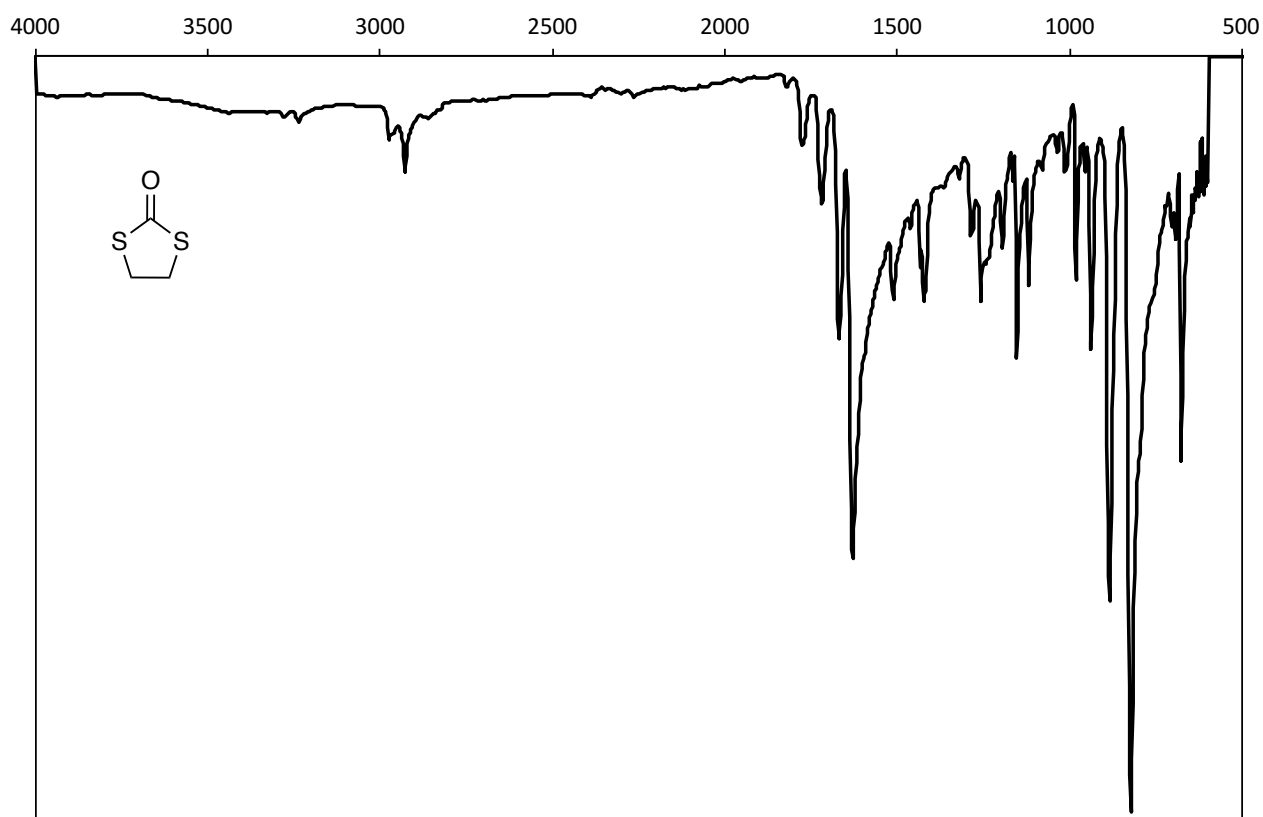


Figure S3.14. FT-IR spectrum of 3-dithiolan-2-one (**2d**).

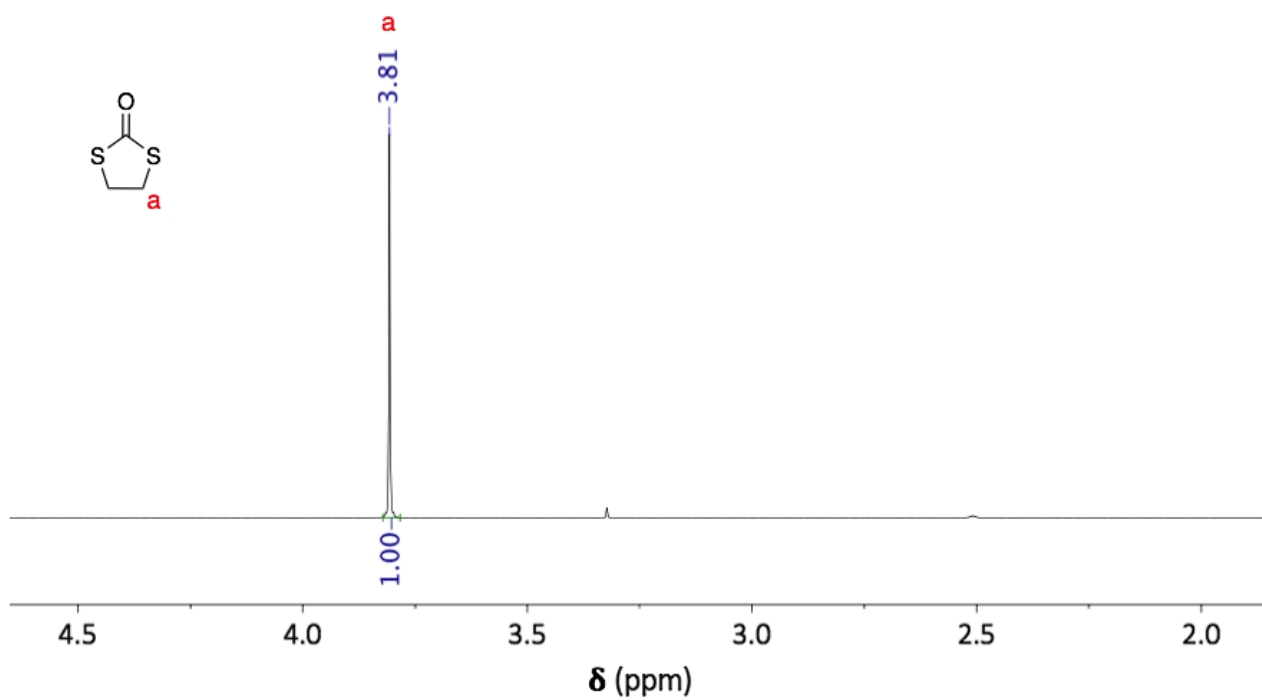


Figure S3.15. ¹H NMR spectrum of 3-dithiolan-2-one (2d) (DMSO-*d*₆, 400 MHz, 298 K).

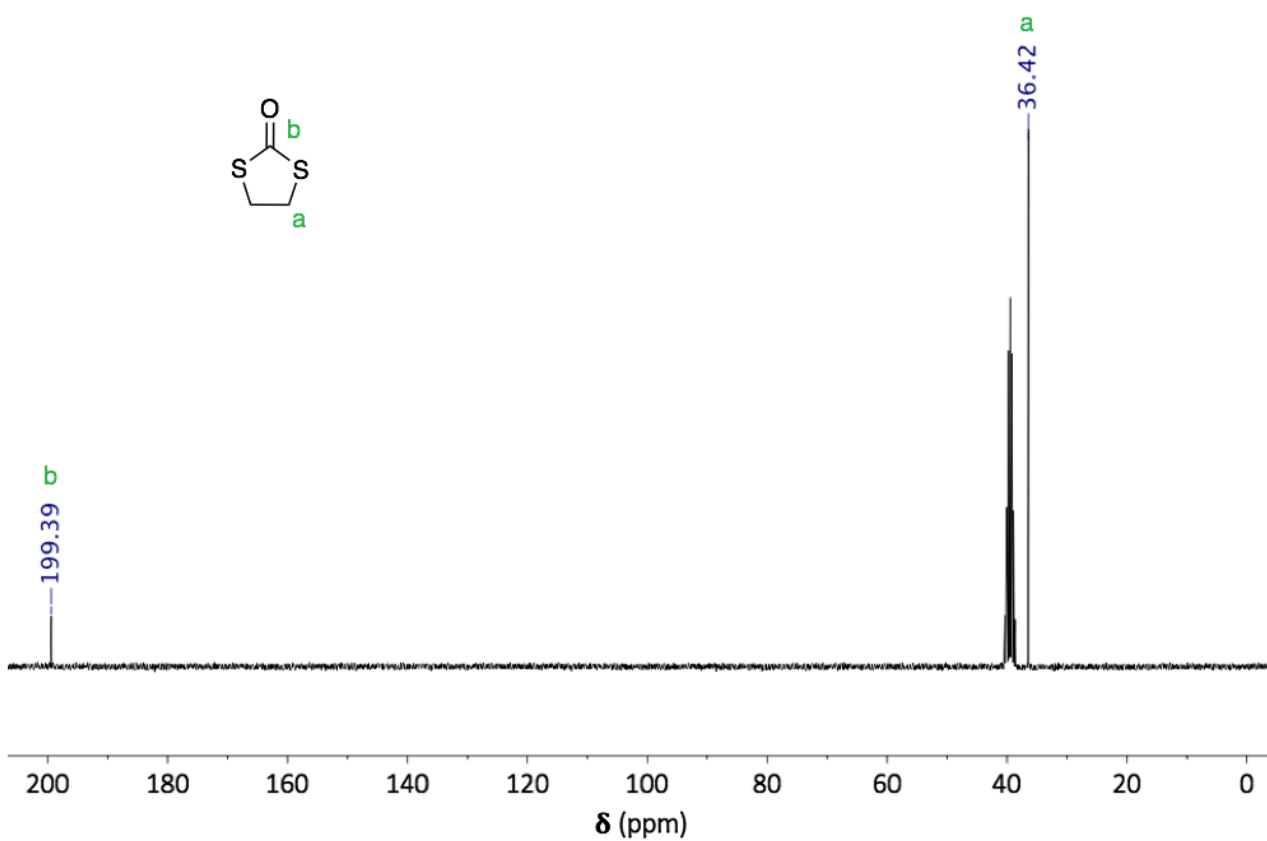


Figure S3.16. ¹³C NMR spectrum of 3-dithiolan-2-one (2d) (DMSO-*d*₆, 400 MHz, 298 K).

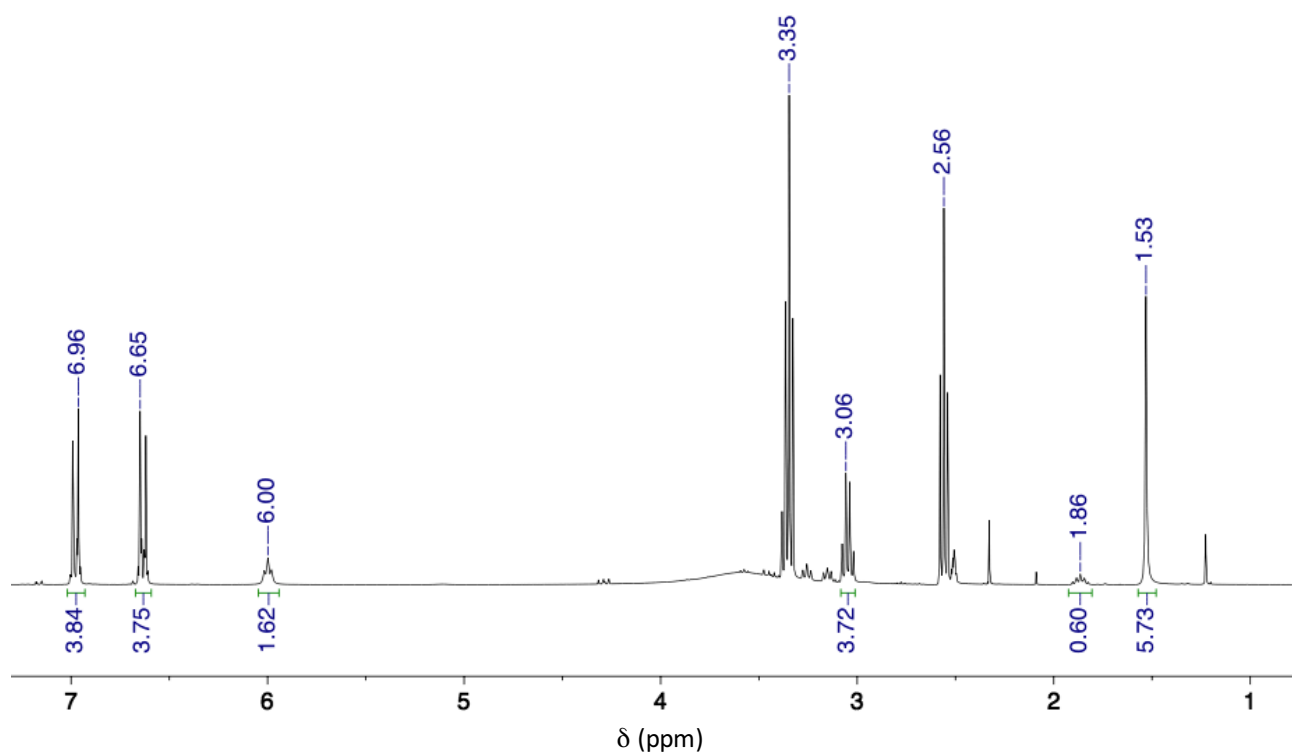


Figure S3.17. ^1H NMR spectrum of the crude product containing 1,3-bis(2-hydroxyethyl)urea (**2e**) ($\text{DMSO}-d_6$, 400 MHz, 298 K). Resonances assigned as: **BPA** – δ 6.96 (d, 4H, $\text{CH}-\text{C}-\text{C}$), 6.65 (d, 4H, $\text{CH}-\text{C}-\text{OH}$), 1.53 (s, 6H, CH_3); **2e** – δ 6.00 (t, 2H, NH), 3.35 (t, 4H, $\text{NH}-\text{CH}_2-\text{CH}_2-\text{OH}$), 3.06 (q, 4H, $\text{NH}-\text{CH}_2-\text{CH}_2-\text{OH}$). Signals at $\delta = 3.35$ and 2.56 ppm correspond to residual reagent (**1e**), and signal at $\delta = 1.86$ ppm corresponds to TBD:MSA signal used as internal standard for calculating conversion.

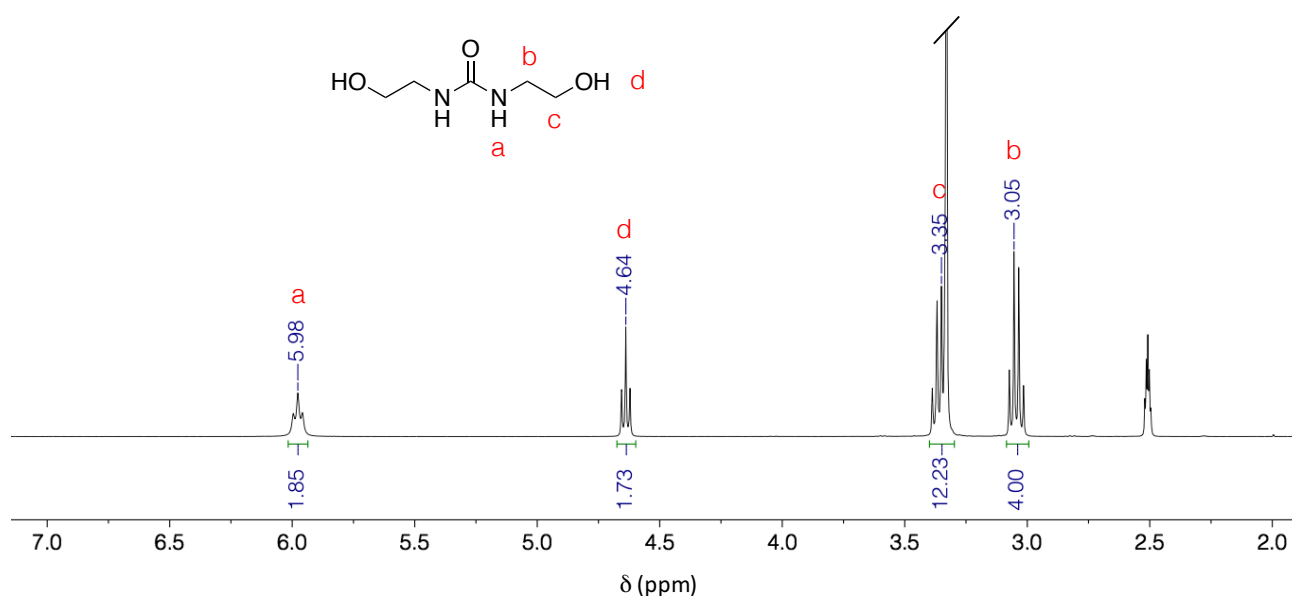


Figure S3.18. ^1H NMR spectrum of 1,3-bis(2-hydroxyethyl)urea (**2e**) ($\text{DMSO}-d_6$, 400 MHz, 298 K).

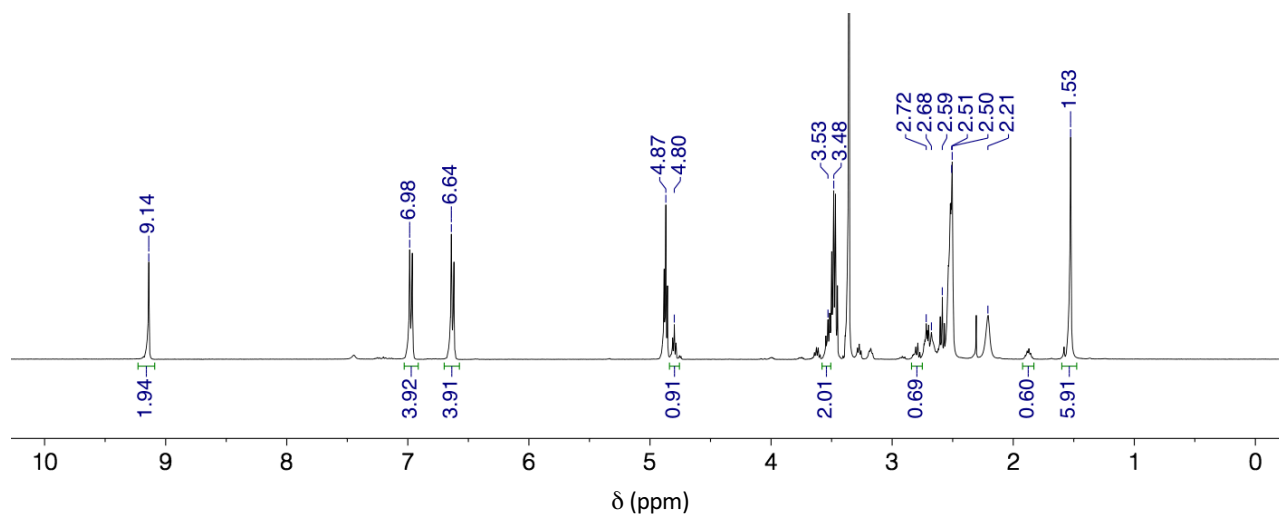


Figure S3.19. ^1H NMR spectrum of the crude product containing *S,S*-bis(2-hydroxyethyl) carbon dithioate (**2f**) (DMSO- d_6 , 400 MHz, 298 K). Resonances assigned as: **BPA** – δ 6.98 (d, 4H, *CH-C-C*), 6.64 (d, 4H, *CH-C-OH*), 1.53 (s, 6H, CH_3); **2f** – δ 4.80 (t, 2H, OH), 3.53 (m, 4H, *S-CH}_2\text{-CH}_2\text{-OH}*), 2.72 – 2.59 (m, 4H, *S-CH}_2\text{-CH}_2\text{-OH}*). Signals at δ = 4.89, 3.48, 2.68 – 2.51 and 2.21 ppm correspond to residual reagent (**1f**), and signal at δ = 1.86 ppm corresponds to TBD:MSA signal used as internal standard for calculating conversion.

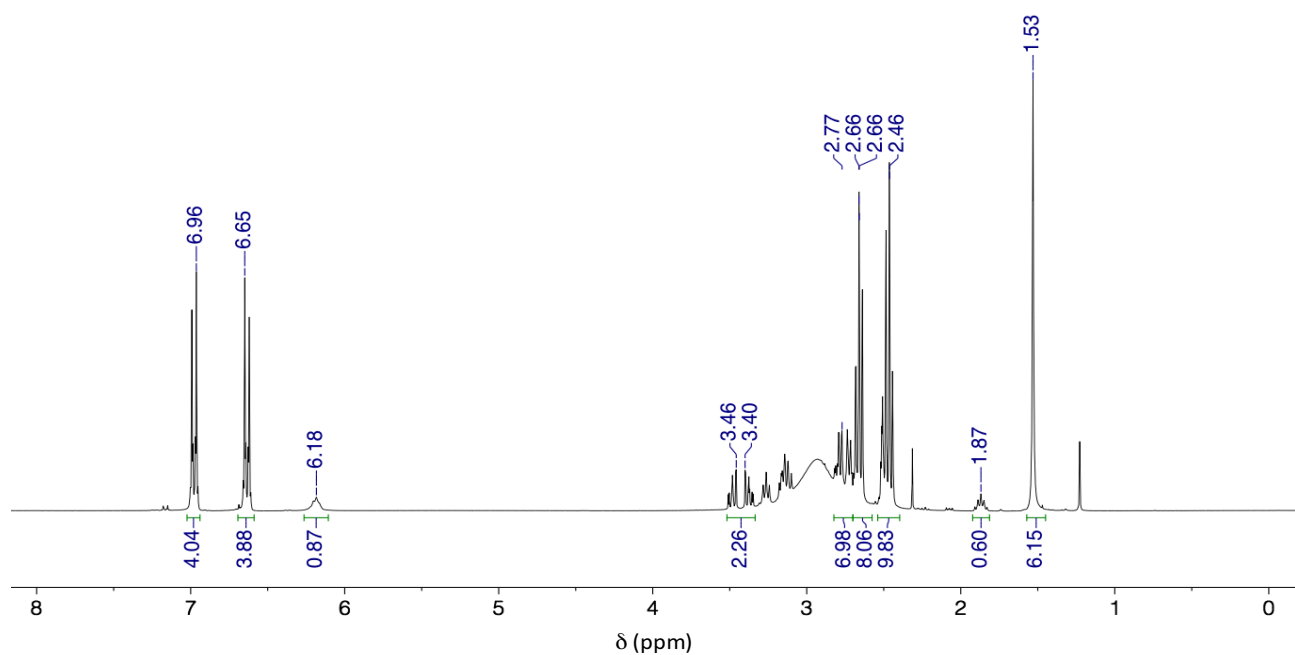


Figure S3.20. ^1H NMR spectrum of the crude product containing 1,3-bis(2-mercaptoethyl)urea (**2g**) (DMSO- d_6 , 400 MHz, 298 K). Resonances assigned as: **BPA** – δ 6.96 (d, 4H, *CH-C-C*), 6.65 (d, 4H, *CH-C-OH*), 1.53 (s, 6H, CH_3); **2g** – δ 6.80 (t, 2H, NH), 3.46 – 3.40 (dt, 4H, *NH-CH}_2\text{-CH}_2\text{-OH}*), 2.77 – 2.66 (dt, 4H, *NH-CH}_2\text{-CH}_2\text{-OH}*). Signals at δ = 2.66 and 2.46 ppm correspond to residual reagent (**1g**), and signal at δ = 1.87 ppm corresponds to TBD:MSA signal used as internal standard for calculating conversion.

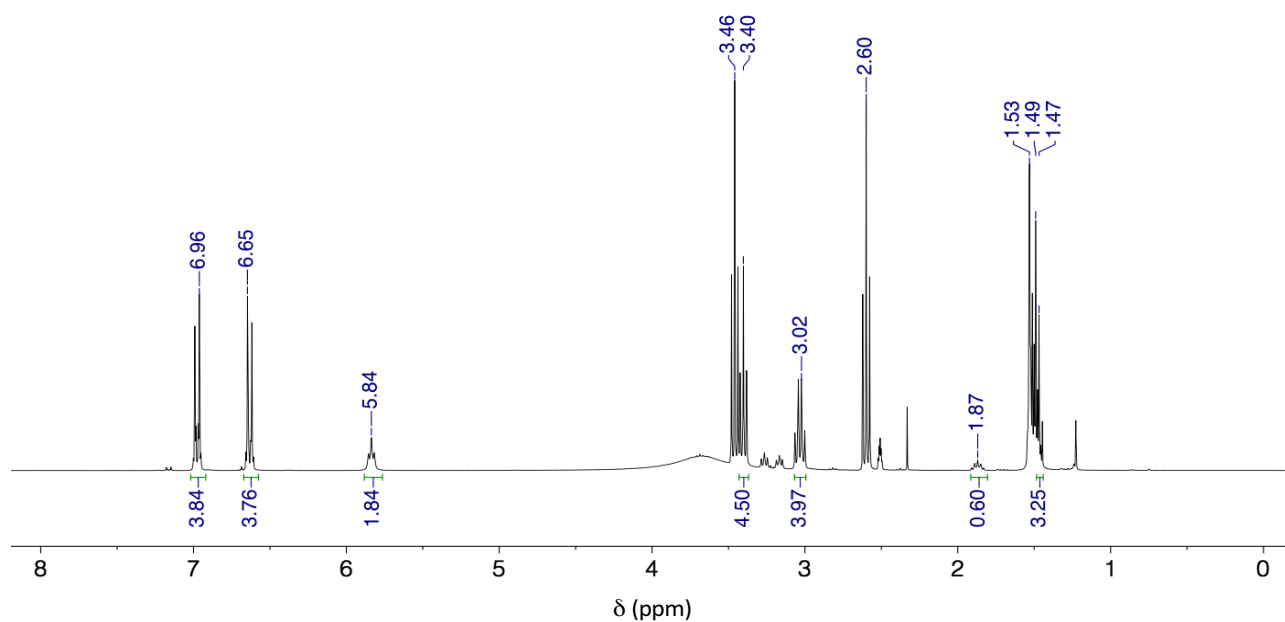


Figure S3.21. ^1H NMR spectrum of the crude product containing 1,3-bis(3-hydroxypropyl)urea (**2h**) (DMSO- d_6 , 400 MHz, 298 K). Resonances assigned as: **BPA** – δ 6.96 (d, 4H, CH-C-C), 6.65 (d, 4H, CH-C-OH), 1.53 (s, 6H, CH₃); **2h** – δ 5.84 (t, 2H, NH), 3.40 (t, 4H, CH₂-CH₂-OH), 3.02 (t, 4H, NH-CH₂-CH₂), 1.47 (t, 4H, NH-CH₂-CH₂). Signals at δ = 3.46, 2.60 and 1.49 ppm correspond to residual reagent (**1h**), and signal at δ = 1.87 ppm corresponds to TBD:MSA signal used as internal standard for calculating conversion.

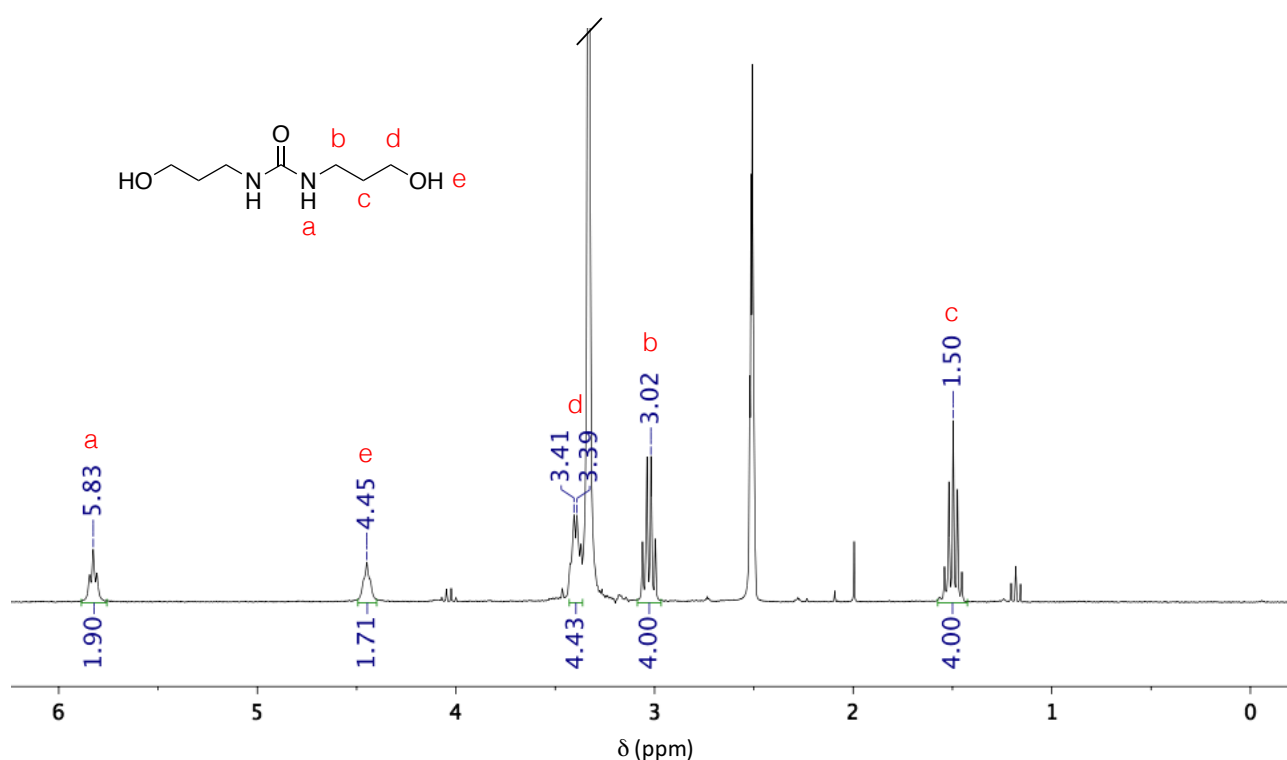


Figure S3.22. ^1H NMR spectrum of 1,3-bis(3-hydroxypropyl)urea (**2h**) (DMSO- d_6 , 400 MHz, 298 K). (DMSO- d_6 , 400 MHz, 298 K).

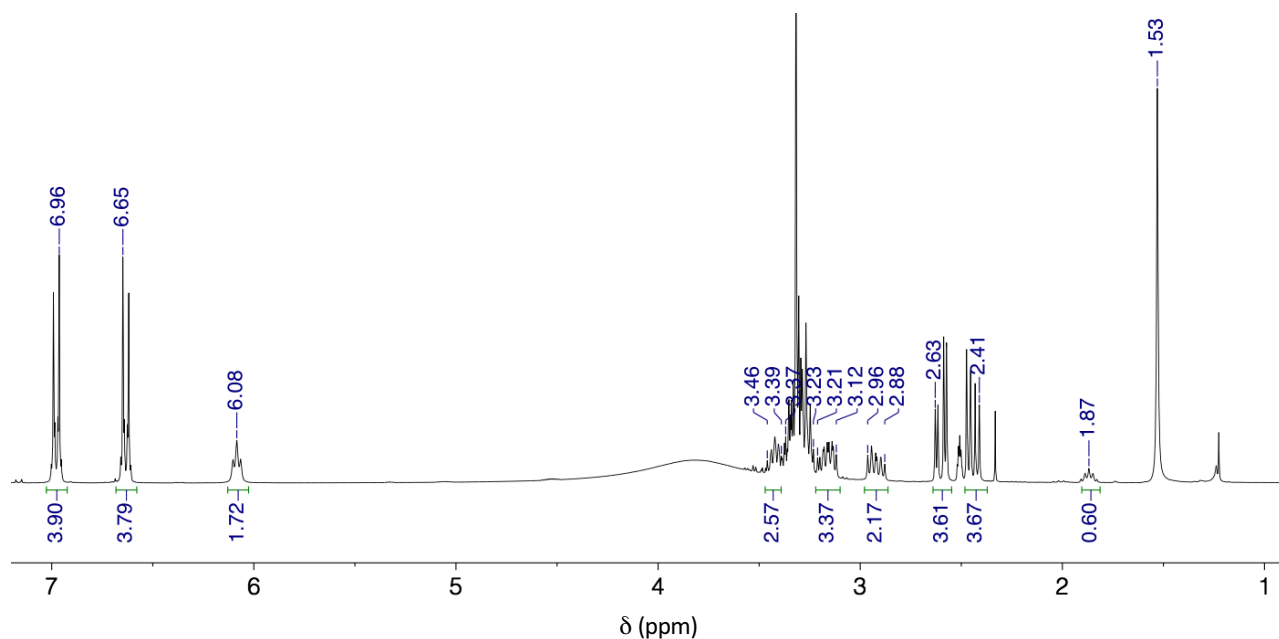


Figure S3.23. ^1H NMR spectrum of the crude product containing 1,3-bis(2-(2-hydroxyethoxy)ethyl) urea (**2i**) ($\text{DMSO-}d_6$, 400 MHz, 298 K). Resonances assigned as: BPA – δ 6.96 (d, 4H, CH-C-C), 6.65 (d, 4H, CH-C-OH), 1.53 (s, 6H, CH₃); **2i** – δ 6.08 (t, 2H, NH), 3.46 (m, 2H, CH₂-CH-CH₂), 3.23 (m, 4H, CH-CH₂-OH), 3.21 – 2.88 (t, 4H, CH₂-NH). Signals at δ = 3.23 – 3.37 and 2.41 – 2.63 ppm correspond to residual reagent (**1i**), and signal at δ = 1.87 ppm corresponds to TBD:MSA signal used as internal standard for calculating conversion.

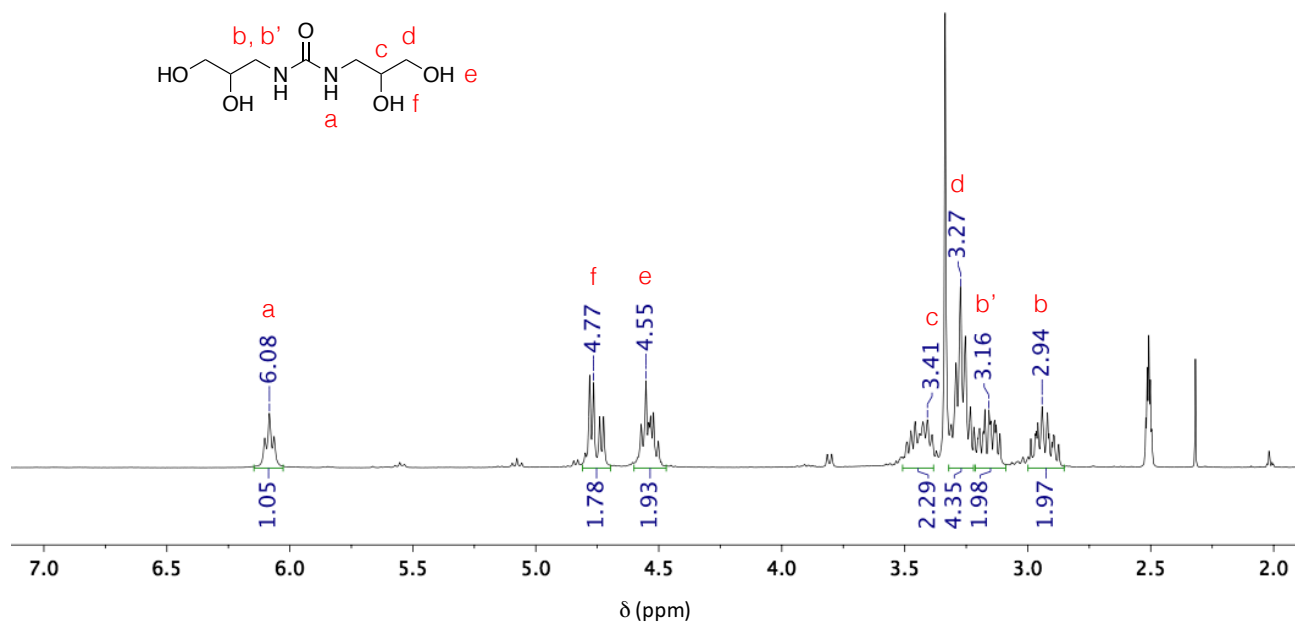


Figure S3.24. ^1H NMR spectrum of 1,3-bis(2-(2-hydroxyethoxy)ethyl) urea (**2i**) ($\text{DMSO-}d_6$, 400 MHz, 298 K).

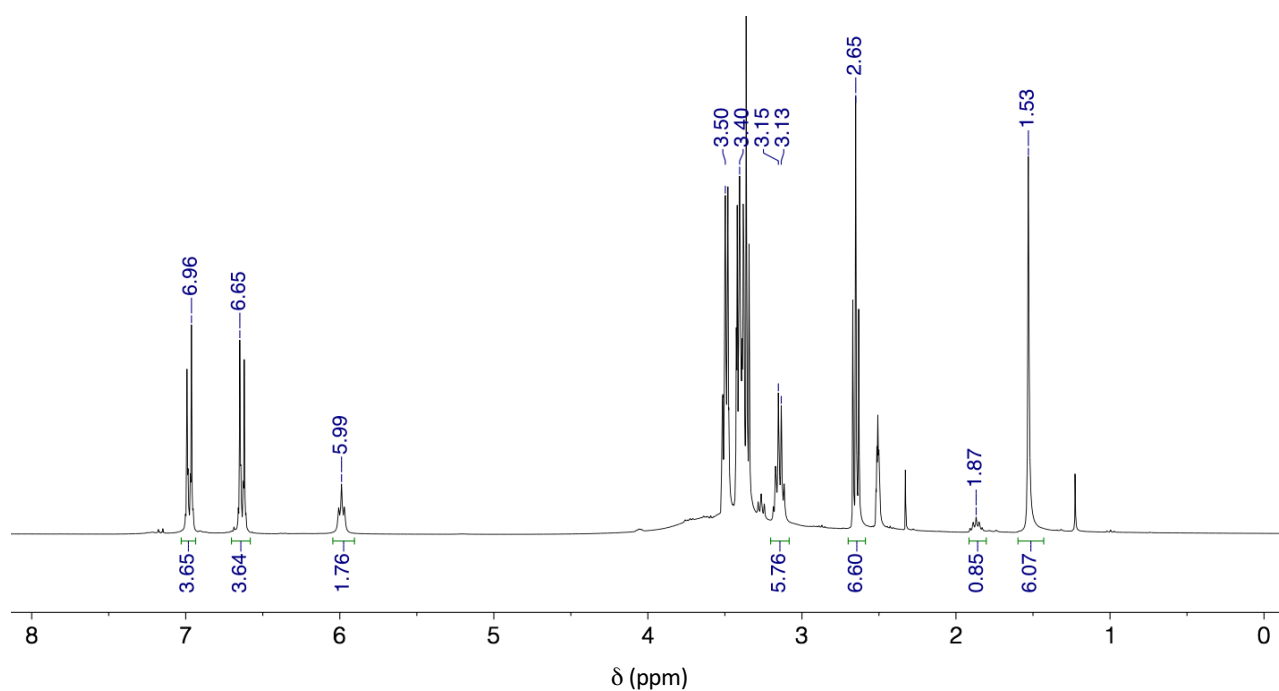


Figure S3.25. ^1H NMR spectrum of the crude product containing 1,3-bis(2,3-dihydroxypropyl)urea (**2j**) (DMSO- d_6 , 400 MHz, 298 K). Resonances assigned as: **BPA** – δ 6.96 (d, 4H, CH-C-C), 6.65 (d, 4H, CH-C-OH), 1.53 (s, 6H, CH₃); **2j** – δ 5.99 (t, 2H, NH), 3.50 (m, 2H, CH₂-OH), 3.40 (m, 4H, CH₂-O), 3.15 (m, 4H, CH₂-NH). Signals at δ = 2.65 ppm correspond to residual reagent (**1j**), and signal at δ = 1.87 ppm corresponds to TBD:MSA signal used as internal standard for calculating conversion.

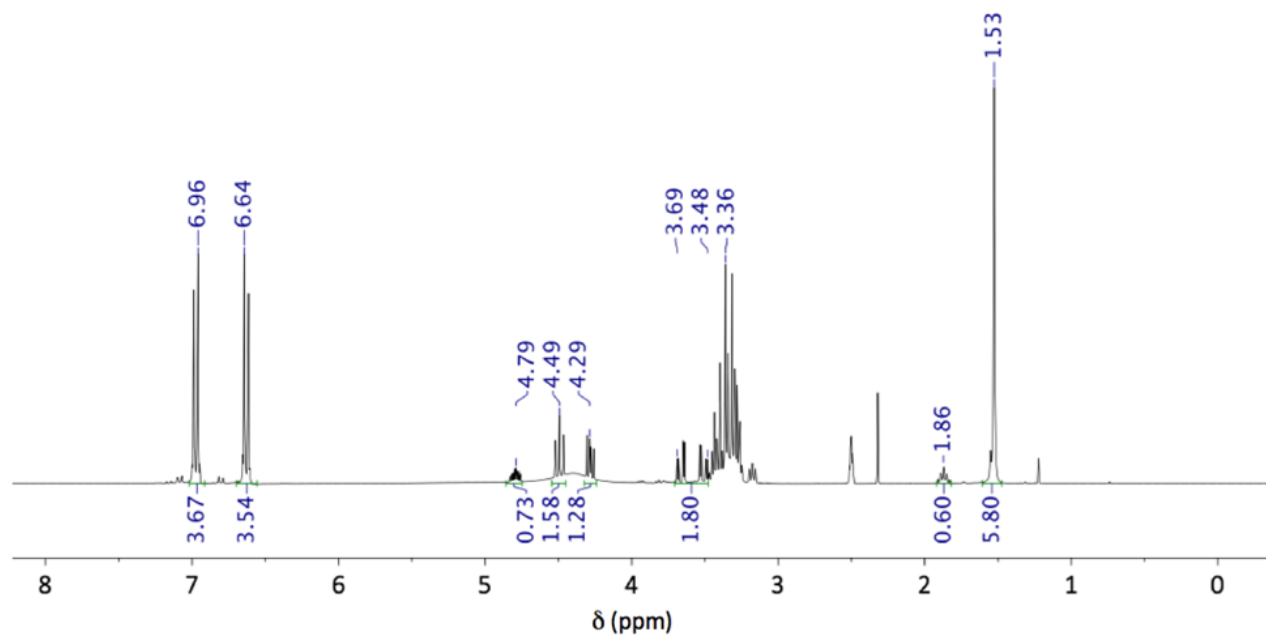


Figure S3.26. ^1H NMR spectrum of the crude product containing 4-(hydroxymethyl)-1,3-dioxolan-2-one (**2k**) (DMSO- d_6 , 400 MHz, 298 K). Resonances assigned as: **BPA** – δ 6.96 (d, 4H, CH-C-C), 6.64 (d, 4H, CH-C-OH), 1.53 (s, 6H, CH₃); **2k** – δ 4.79 (m, 1H, CH-O), 4.49 (t, 1H, CH₂-O), 4.29 (m, 1H, CH₂-O), 3.48-3.69 (dd, 2H, CH₂). Signal at δ = 3.36 ppm corresponds to residual reagent (**1k**), and signal at δ = 1.86 ppm corresponds to TBD:MSA signal used as internal standard for calculating conversion.

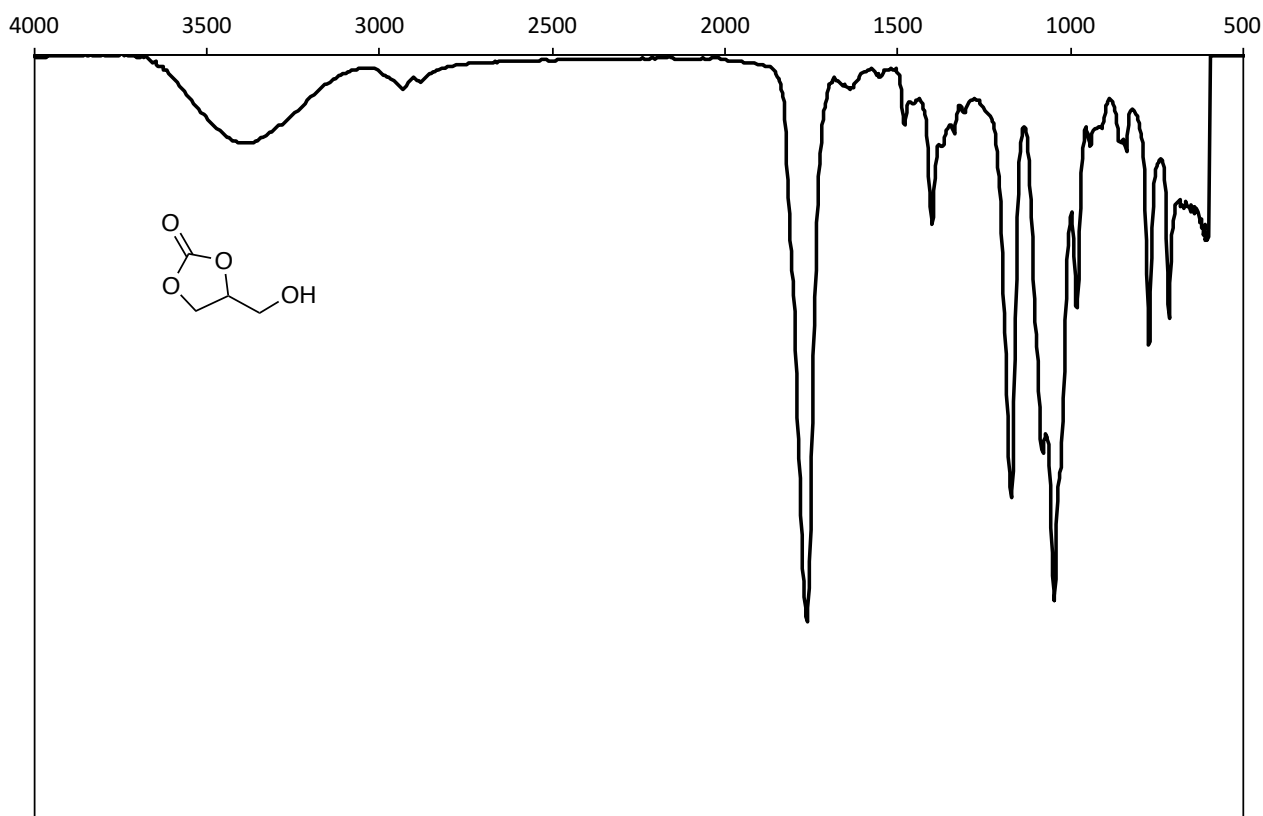


Figure S3.27. FT-IR spectrum of 4-(hydroxymethyl)-1,3-dioxolan-2-one (2k).

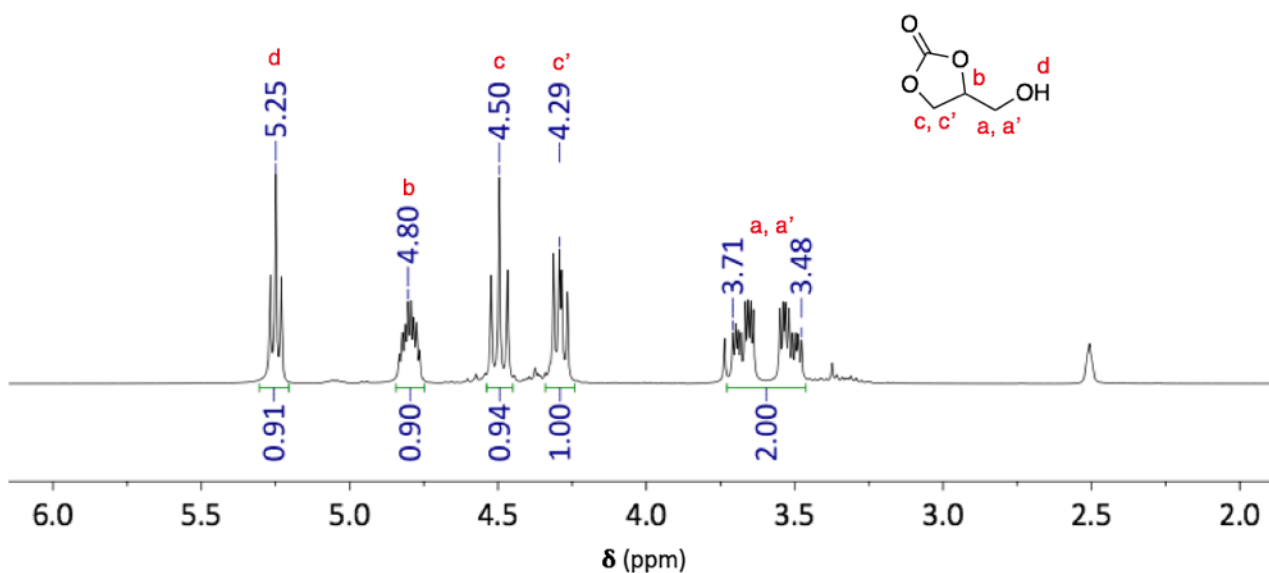


Figure S3.28. ^1H NMR spectrum of 4-(hydroxymethyl)-1,3-dioxolan-2-one (2k). (DMSO- d_6 , 400 MHz, 298 K).

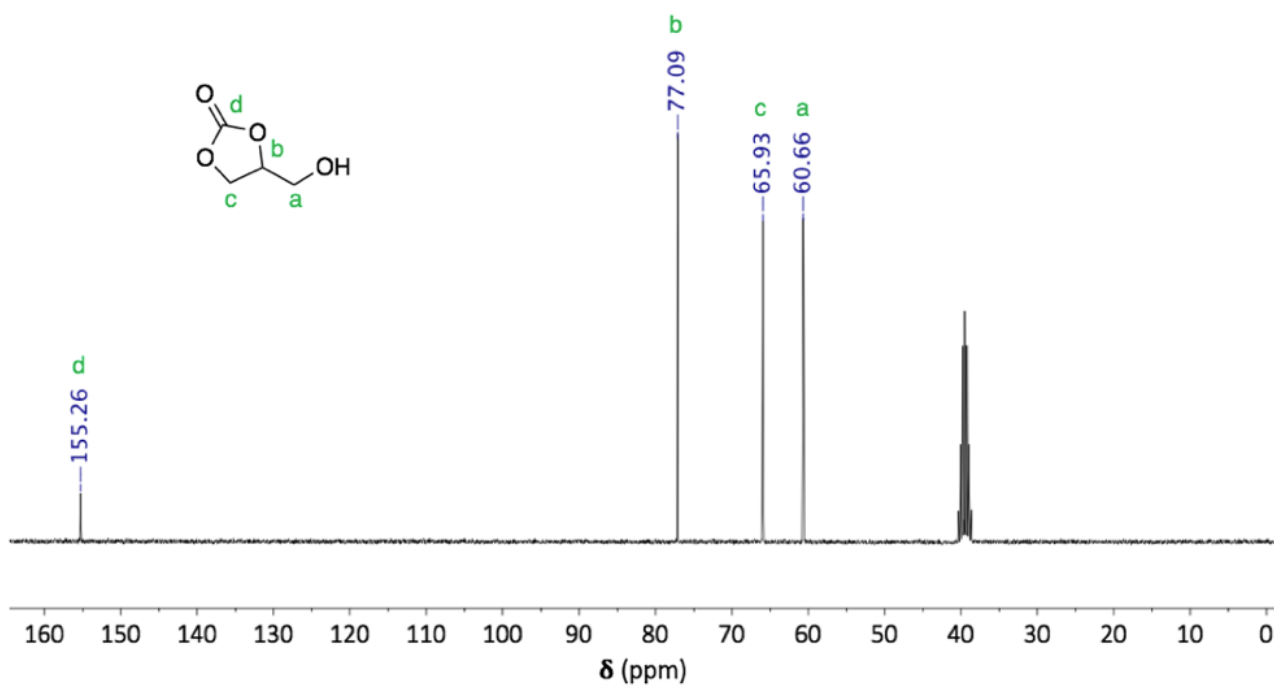


Figure S3.29. ^{13}C NMR spectrum of 4-(hydroxymethyl)-1,3-dioxolan-2-one (**2k**). (DMSO- d_6 , 400 MHz, 298 K).

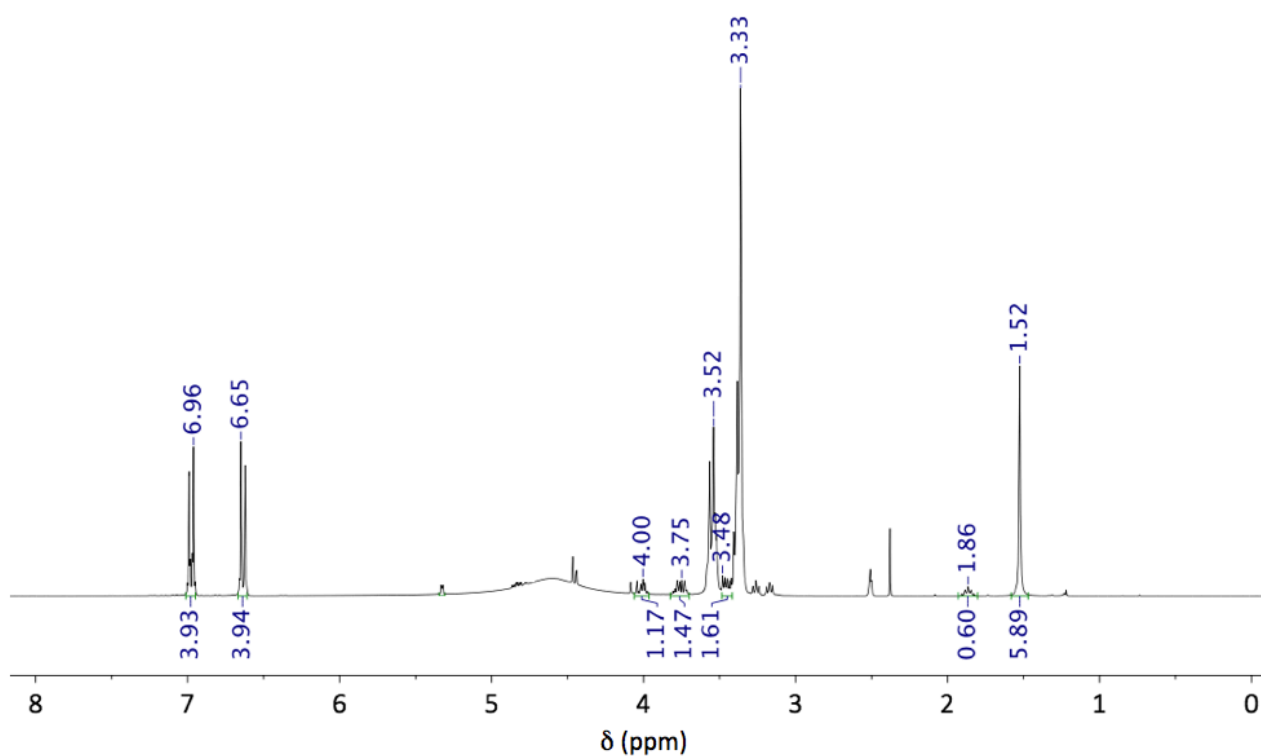


Figure S3.30. ^1H NMR spectrum of the crude product containing 4,5-bis(hydroxymethyl)-1,3-dioxolan-2-one (**2l**) (DMSO- d_6 , 400 MHz, 298 K). Resonances assigned as: BPA - δ 6.96 (d, 4H, CH-C-C), 6.65 (d, 4H, CH-C-OH), 1.53 (s, 6H, CH₃); **2l** - δ 4.00 (m, 2H, CH), 3.75 (m, 2H, CH₂), 3.48 (m, 2H, CH₂). Signals at δ = 3.52 and 3.33 ppm correspond to residual reagent (**1l**), and signal at δ = 1.86 ppm corresponds to TBD:MSA signal used as internal standard for calculating conversion.

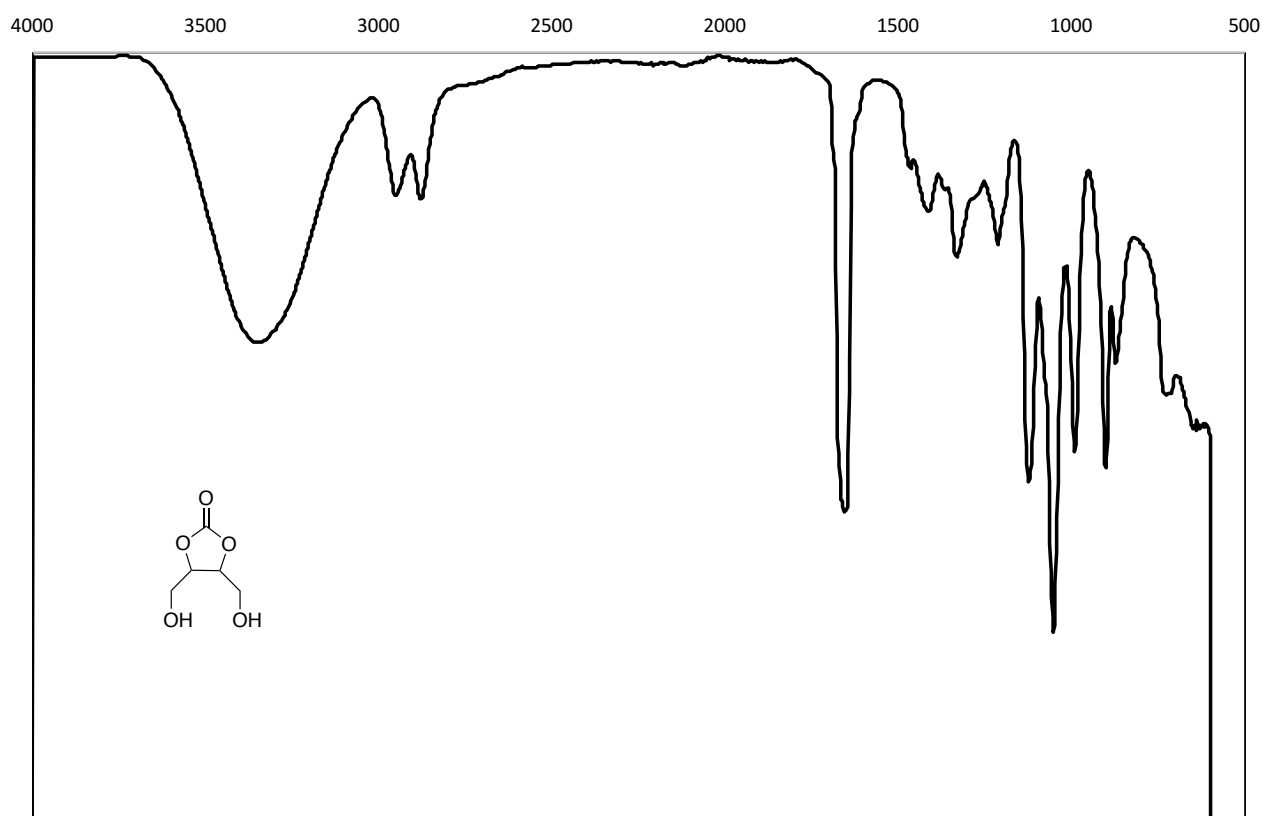


Figure S3.31. FT-IR spectrum of 4,5-bis(hydroxymethyl)-1,3-dioxolan-2-one (2I)

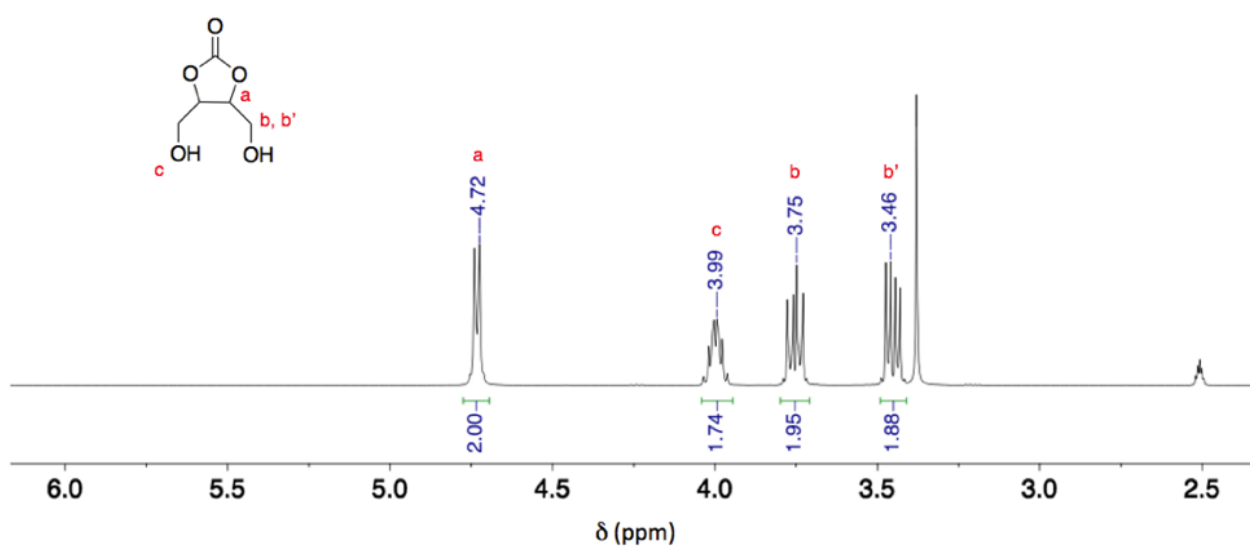


Figure S3.32. ^1H NMR spectrum of 4,5-bis(hydroxymethyl)-1,3-dioxolan-2-one (2I) ($\text{DMSO-}d_6$, 400 MHz, 298 K).

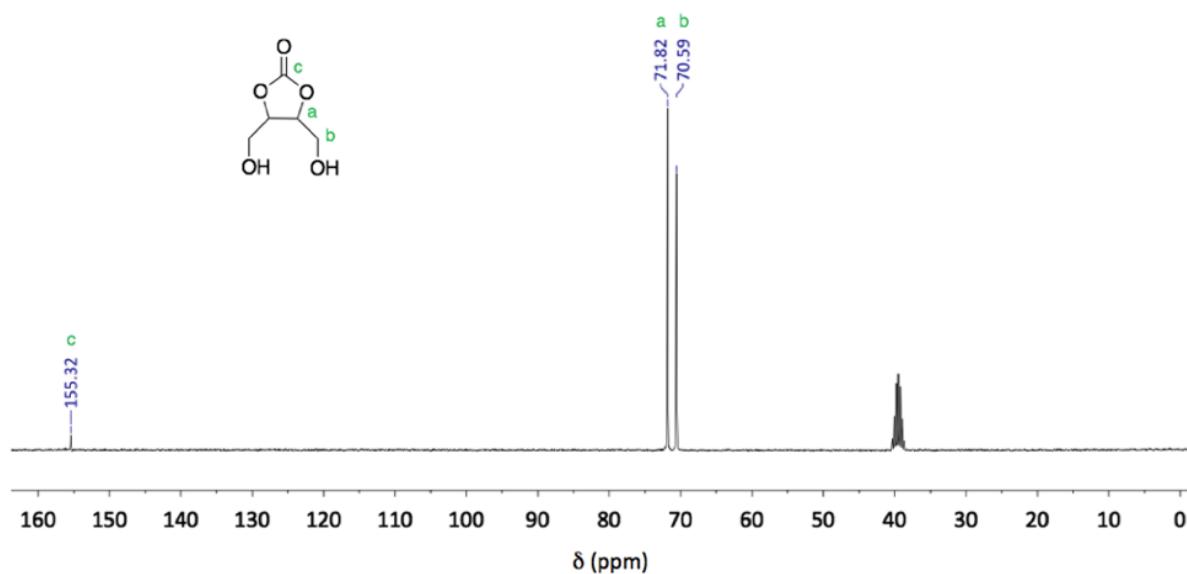


Figure S3.33. ^{13}C NMR spectrum of 4,5-bis(hydroxymethyl)-1,3-dioxolan-2-one (2l) (DMSO- d_6 , 400 MHz, 298 K).

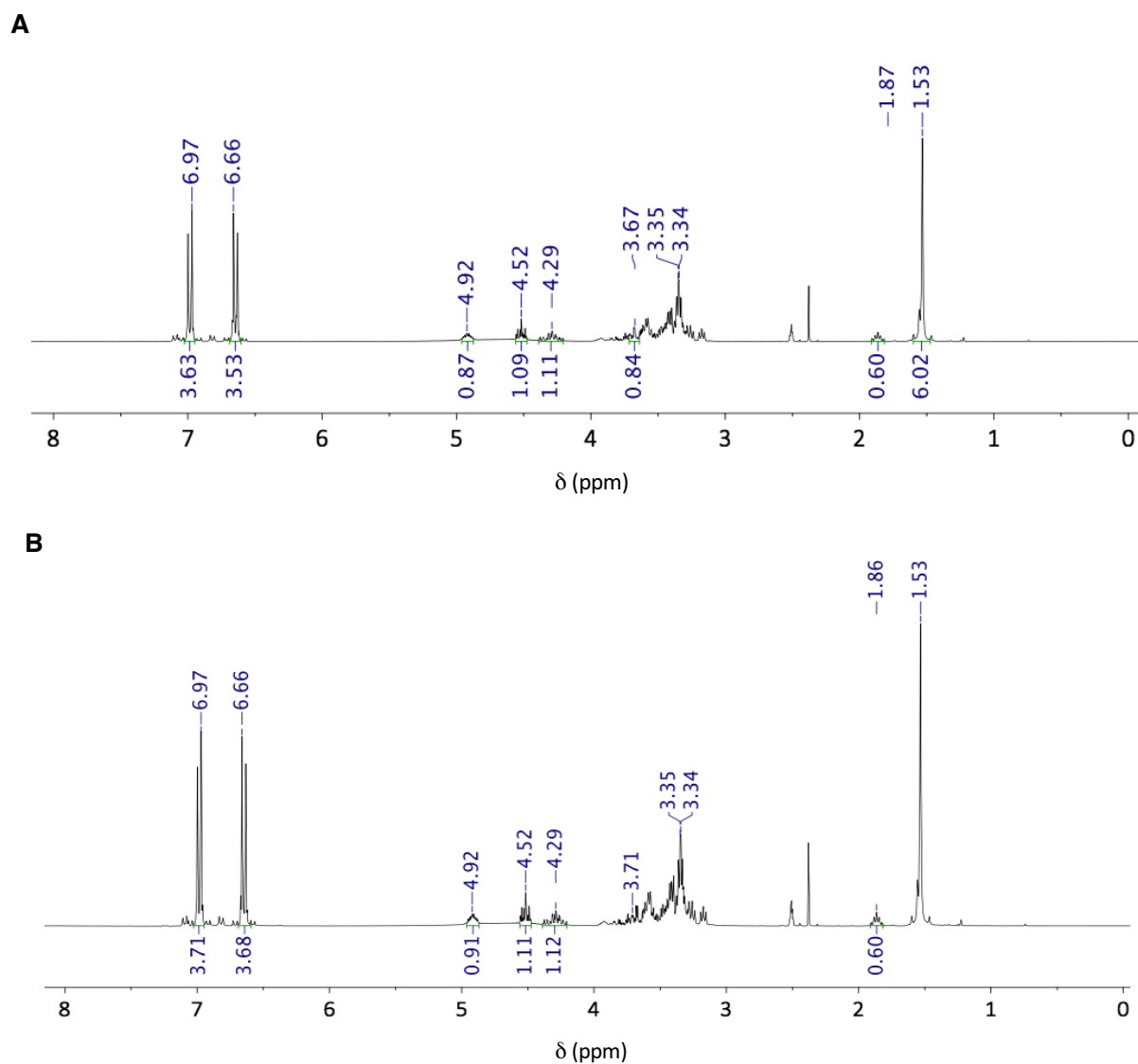


Figure S3.34. ^1H NMR spectrum of the crude product containing Diglycerol dicarbonate (2m) at (A) 160 °C and (B) 190 °C, (DMSO- d_6 , 400 MHz, 298 K). Resonances assigned as: BPA – δ 6.96 (d, 4H,

CH-C-C), 6.64 (d, 4H, *CH-C-OH*), 1.52 (s, 6H, CH_3); **2m** – δ 4.90 (m, 1H, *CH-O*), 4.51 (t, 1H, $\text{CH}_2\text{-O-C}$), 4.28 (t, 1H, $\text{CH}_2\text{-O-C}$), 3.55-3.66 (m, 4H, $\text{CH}_2\text{-O-CH}_2$). Signals at $\delta = 3.55$ and 3.34 ppm correspond to residual reagent (**1m**), and signal at $\delta = 1.87$ ppm corresponds to TBD:MSA signal used as internal standard for calculating conversion.

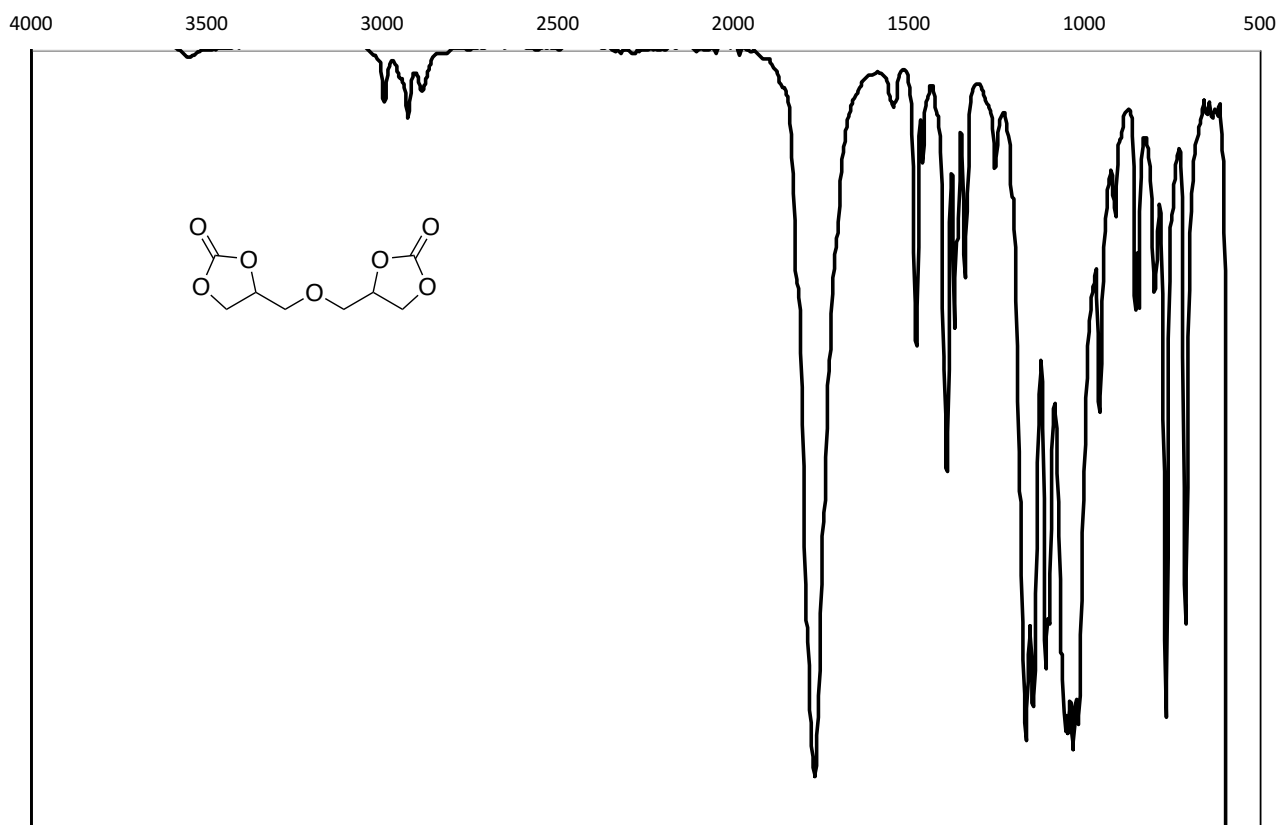


Figure S3.35. FT-IR spectrum of Diglycerol dicarbonate (**2m**).

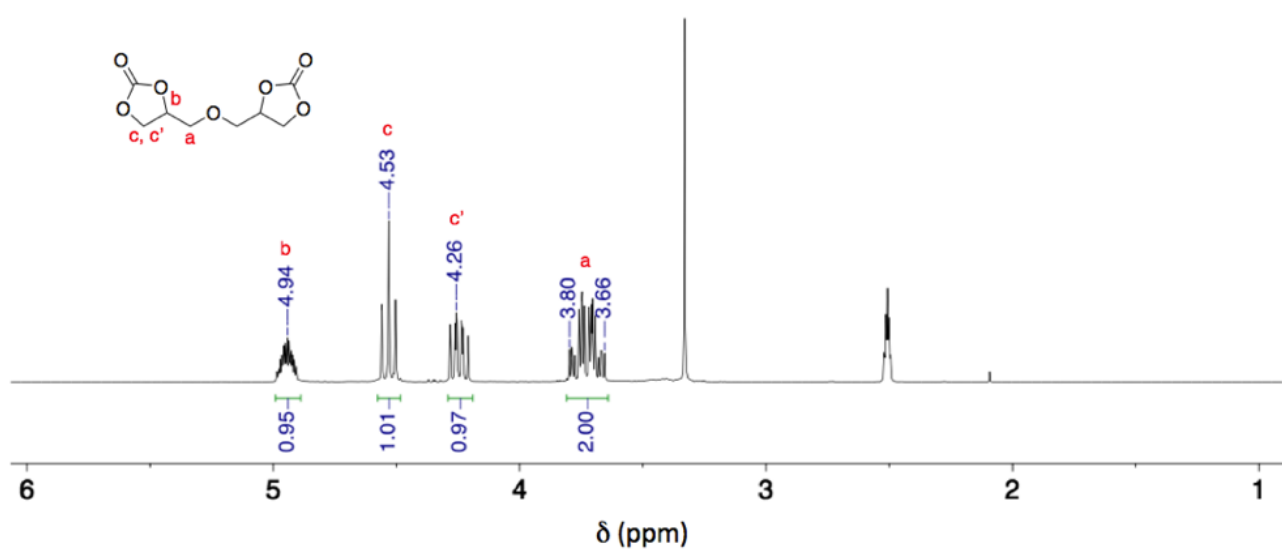


Figure S3.36. ^1H NMR spectrum of Diglycerol dicarbonate (**2m**) ($\text{DMSO-}d_6$, 400 MHz, 298 K).

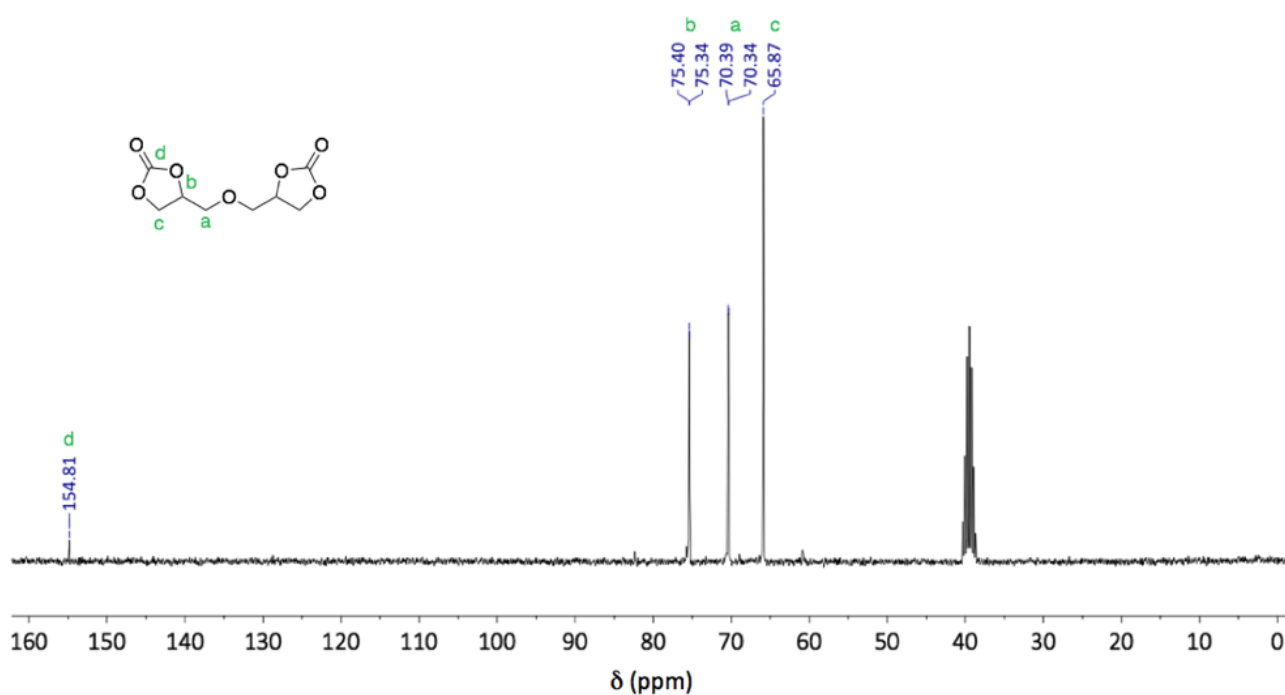


Figure S3.37. ^{13}C NMR spectrum of Diglycerol dicarbonate (**2m**) ($\text{DMSO-}d_6$, 400 MHz, 298 K).

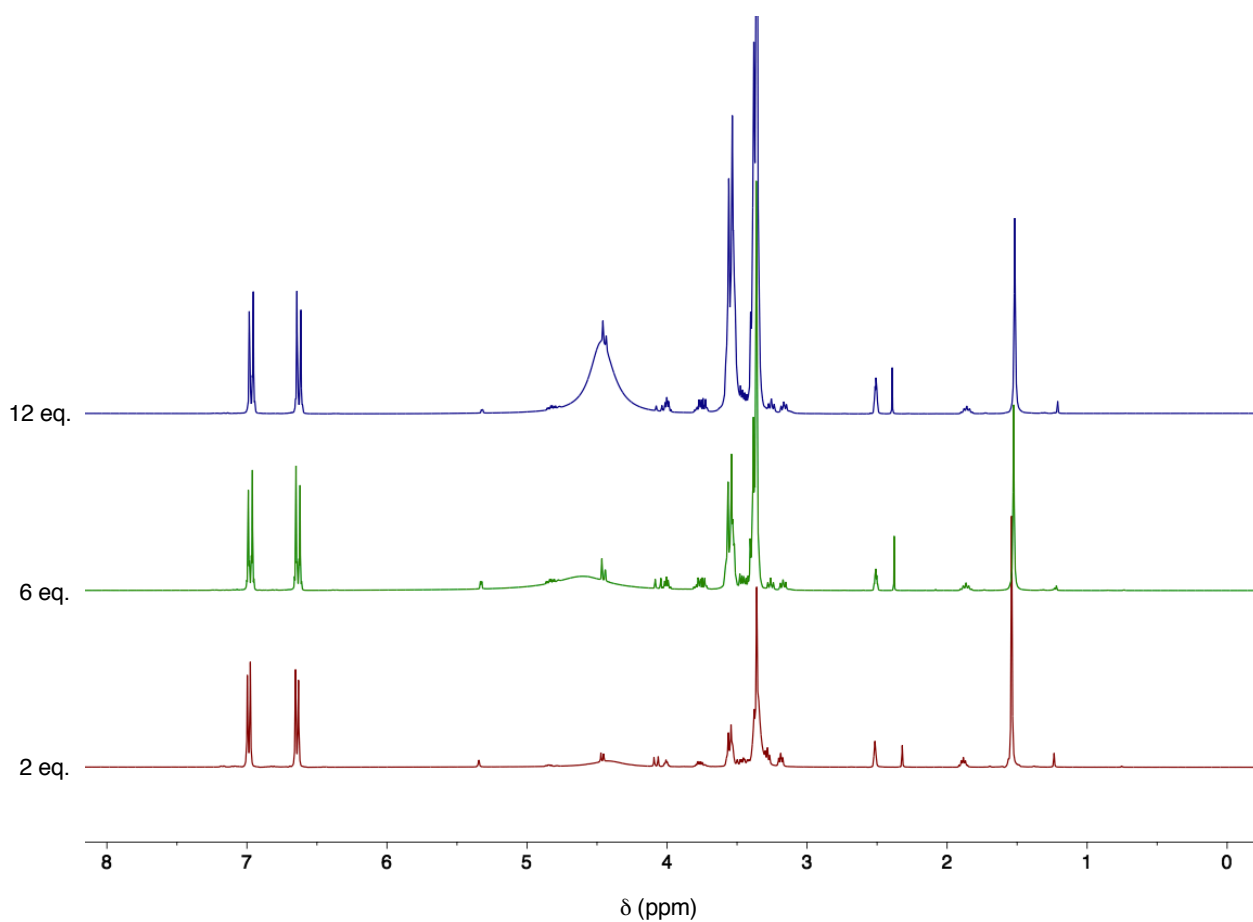


Figure S3.38. Stacked ^1H NMR spectrum of the crude product containing **2I** ($\text{DMSO-}d_6$, 400 MHz, 298 K) at 190 °C with different reagent contents. Resonances assigned as: **BPA** – δ 6.96 (d, 4H, CH-C-C), 6.65 (d, 4H, CH-C-OH), 1.53 (s, 6H, CH_3); **2I** – δ 4.00 (m, 2H, CH), 3.75 (m, 2H, CH_2), 3.48 (m, 2H, CH_2). Signals at δ = 3.52 and 3.33 ppm correspond to residual reagent (**1I**), and signal at δ = 1.86 ppm corresponds to TBD:MSA signal used as internal standard for calculating conversion.

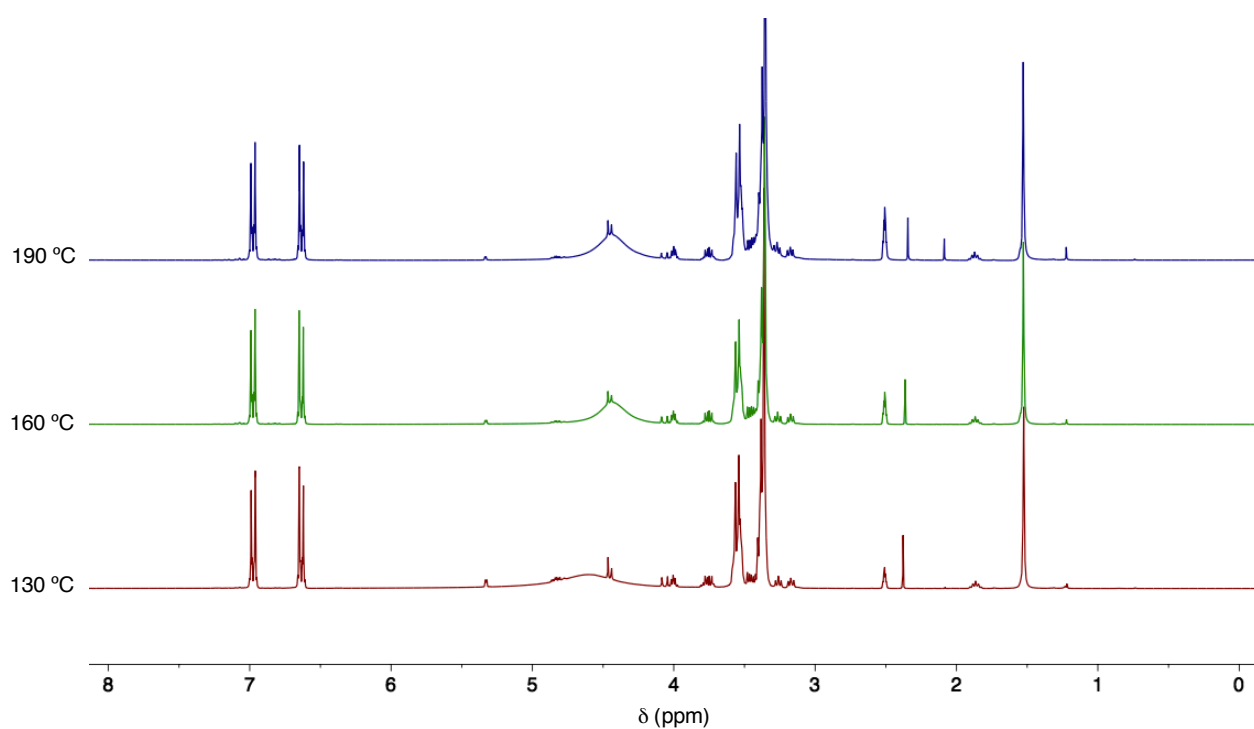


Figure S3.39. Stacked ^1H NMR spectra of the crude product containing **2I** ($\text{DMSO-}d_6$, 400 MHz, 298 K) at different temperatures with 6 eq. of reagent. Resonances assigned as: **BPA** – δ 6.96 (d, 4H, CH-C-C), 6.65 (d, 4H, CH-C-OH), 1.53 (s, 6H, CH_3); **2I** – δ 4.90 (m, 1H, CH-O), 4.51 (t, 1H, $\text{CH}_2\text{-O-C}$), 4.28 (t, 1H, $\text{CH}_2\text{-O-C}$), 3.55-3.66 (m, 4H, $\text{CH}_2\text{-O-CH}_2$). Signals at δ = 3.55 and 3.34 ppm correspond to residual reagent (**1I**), and signal at δ = 1.87 ppm corresponds to TBD:MSA signal used as internal standard for calculating conversion.

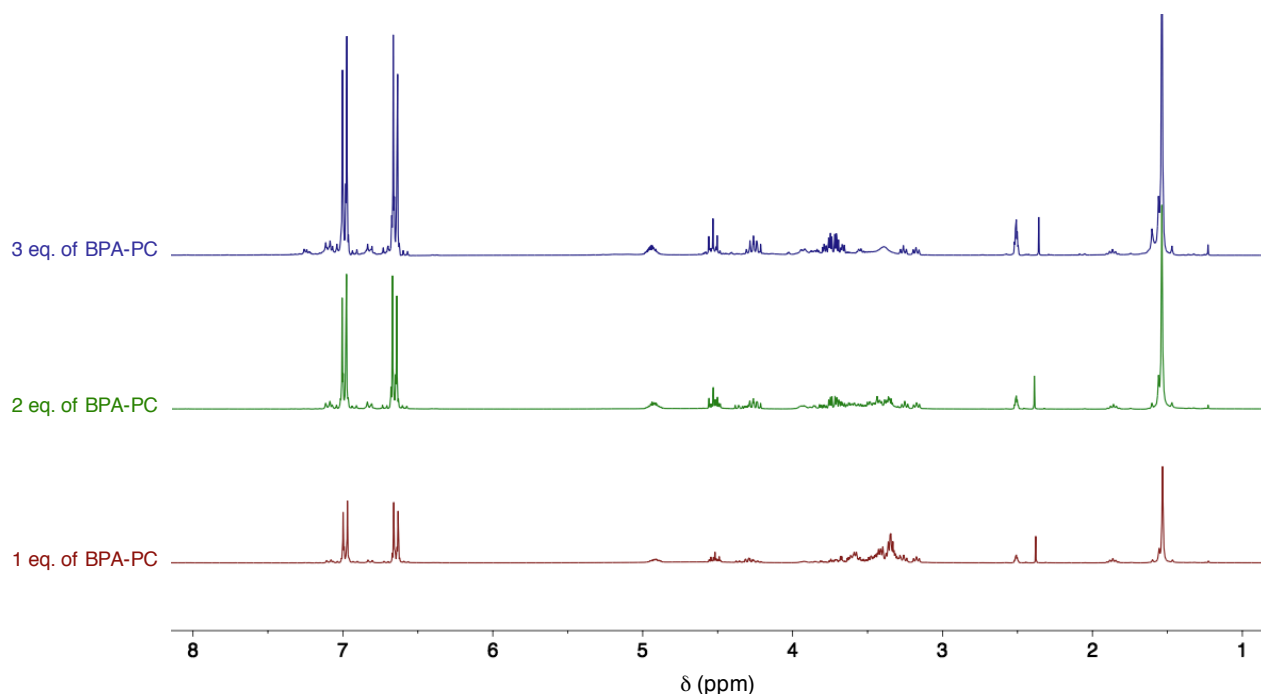


Figure S3.40. Stacked ^1H NMR spectra of the crude product containing **2m** ($\text{DMSO-}d_6$, 400 MHz, 298 K) at complete disappearance of each eq. of BPA-PC added. Resonances assigned as: **BPA** – δ 6.96 (d, 4H, CH-C-C), 6.65 (d, 4H, CH-C-OH), 1.53 (s, 6H, CH_3); **2m** – δ 4.90 (m, 1H, CH-O), 4.51 (t, 1H, $\text{CH}_2\text{-O-C}$), 4.28 (t, 1H, $\text{CH}_2\text{-O-C}$), 3.55-3.66 (m, 4H, $\text{CH}_2\text{-O-CH}_2$). Signals at δ = 3.55 and 3.34

ppm correspond to residual reagent (**1m**), and signal at $\delta = 1.87$ ppm corresponds to TBD:MSA signal used as internal standard for calculating conversion.

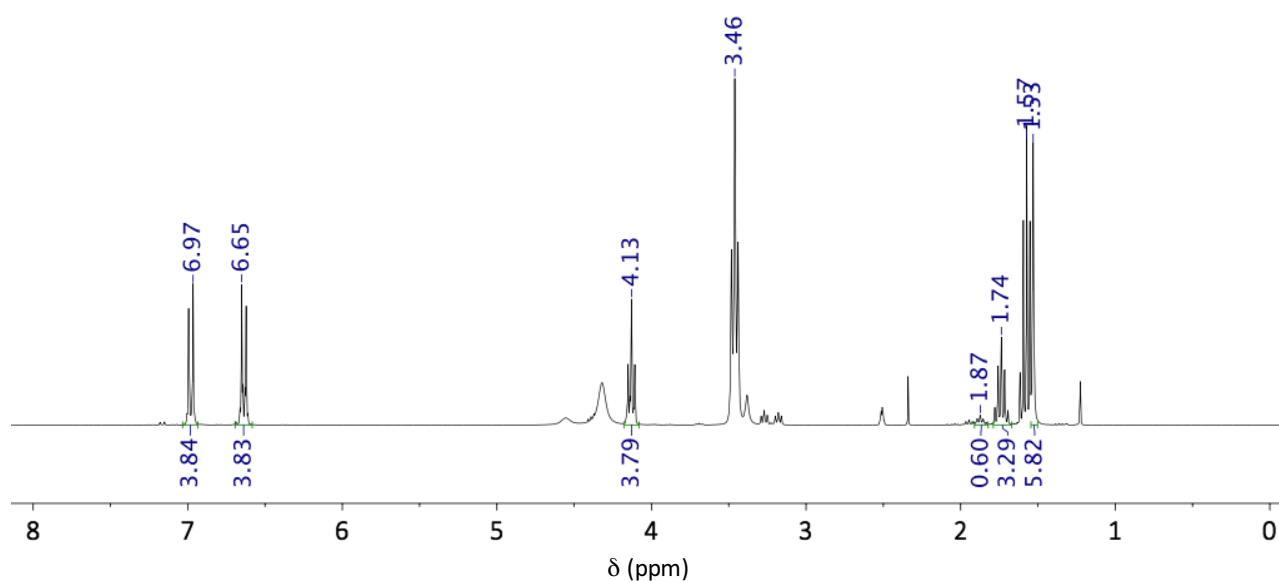


Figure S3.41. ^1H NMR spectrum of the crude product containing bis(3-hydroxypropyl) carbonate (DMSO- d_6 , 400 MHz, 298 K). BPA – δ 6.97 (d, 4H, CH-C-C), 6.65 (d, 4H, CH-C-OH), 1.53 (s, 6H, CH₃); bis(3-hydroxypropyl) carbonate – δ 4.13 (t, 4H, O-CH₂), 3.46 (t, 4H, CH₂-OH), 1.74 (m, 4H, CH₂-CH₂-CH₂). Signals at $\delta = 3.46$ and 1.57 ppm correspond to residual reagent (**1n**), and signal at $\delta = 1.87$ ppm corresponds to TBD:MSA signal used as internal standard for calculating conversion.

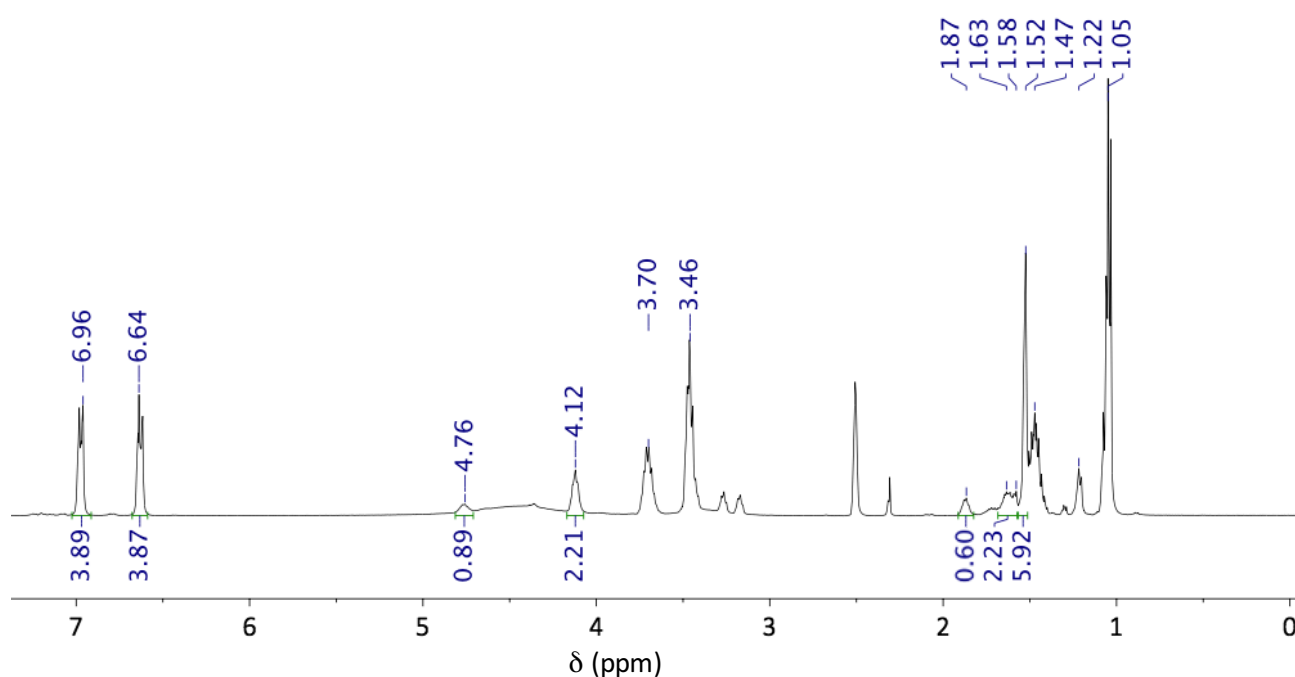


Figure S3.42. ^1H NMR spectrum of the crude product containing 4-methyl-1,3-dioxan-2-one (**2o**) (DMSO- d_6 , 400 MHz, 298 K). BPA – δ 6.96 (d, 4H, CH-C-C), 6.64 (d, 4H, CH-C-OH), 1.52 (s, 6H, CH₃); **2o** – δ 4.76 (m, 1H, CH-CH₃), 4.12 (m, 2H, O-CH₂-CH₂), 1.63 – 1.58 (m, 2H, CH₂-CH₂-CH), 1.06 (m, 3H, CH₃). Signal at $\delta = 3.36$ ppm corresponds to residual reagent (**1o**), and signal at $\delta = 1.87$ ppm corresponds to TBD:MSA signal used as internal standard for calculating conversion.

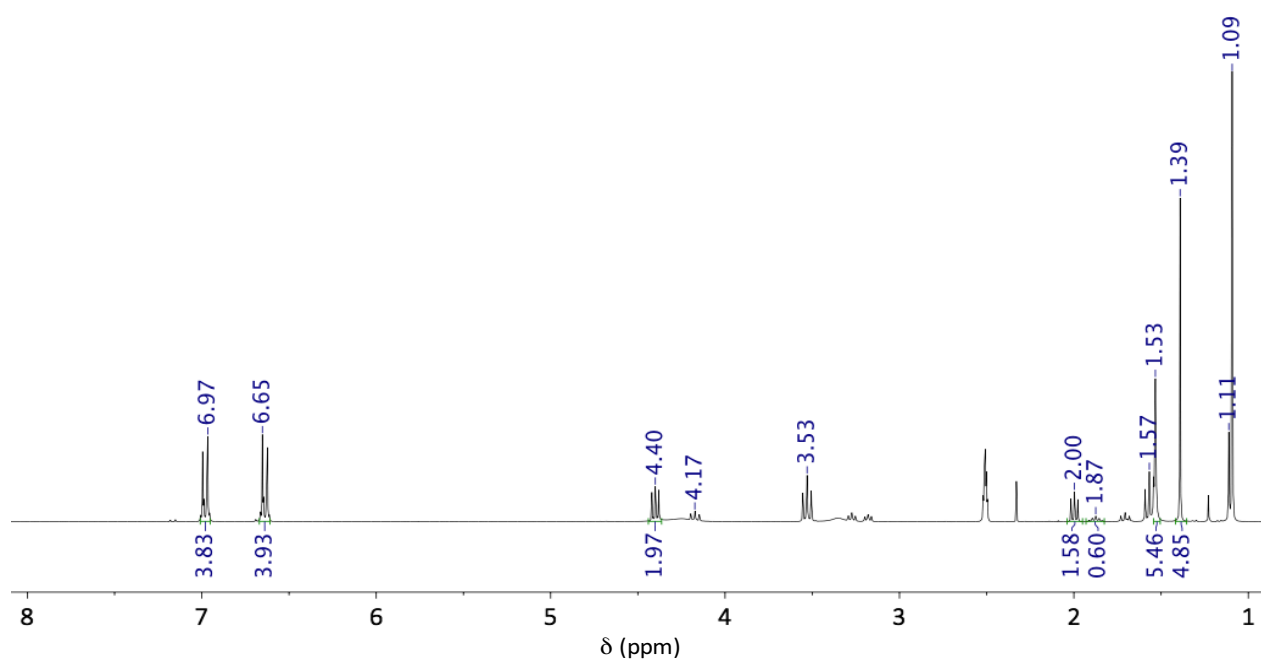


Figure S3.43. ^1H NMR spectrum of the crude product containing 4,4-dimethyl-1,3-dioxan-2-one (**2p**) ($\text{DMSO-}d_6$, 400 MHz, 298 K). **BPA** – δ 6.97 (d, 4H, CH-C-C), 6.65 (d, 4H, CH-C-OH), 1.53 (s, 6H, CH_3); **2p** – δ 4.40 (t, 2H, $\text{O-CH}_2\text{-CH}_2$), 2.00 (t, 2H, $\text{C-CH}_2\text{-CH}_2$), 1.39 (s, 6H, CH_3). Signal at $\delta = 3.53$, 1.57 and 1.09 ppm corresponds to residual reagent (**1p**), and signal at $\delta = 1.87$ ppm corresponds to TBD:MSA signal used as internal standard for calculating conversion.

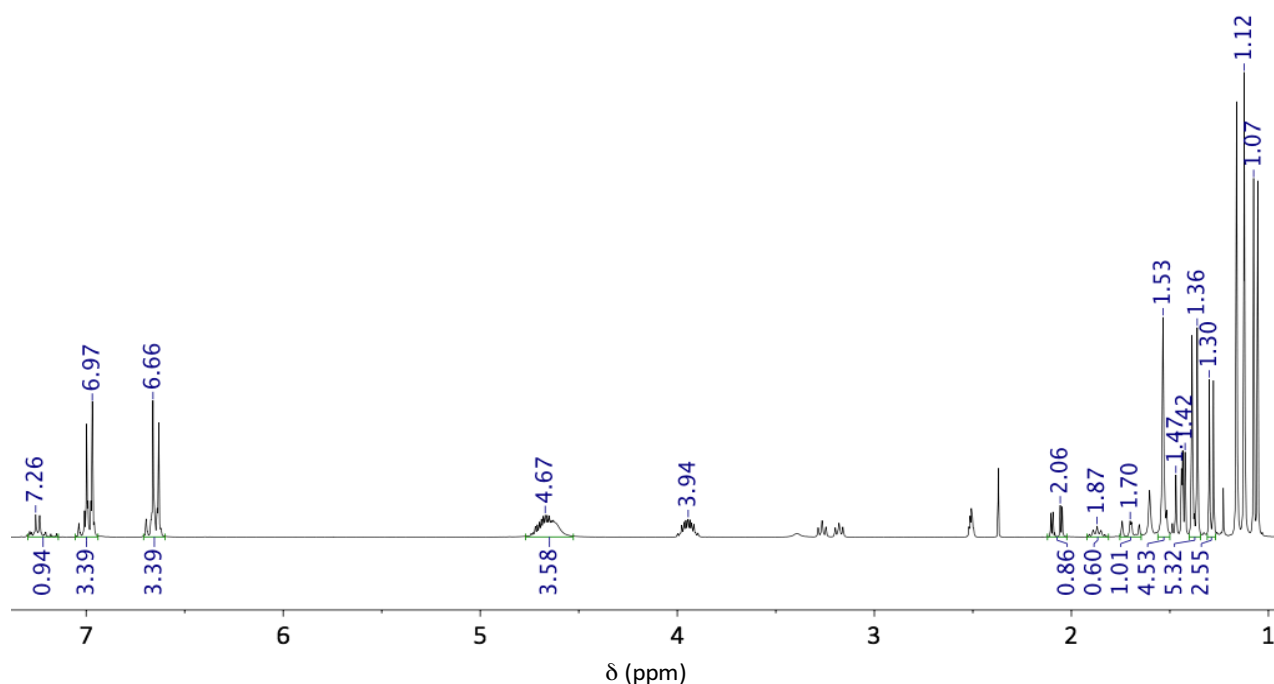


Figure S3.44. ^1H NMR spectrum of the crude product containing 4,4-dimethyl-1,3-dioxan-2-one (**2q**) ($\text{DMSO-}d_6$, 400 MHz, 298 K). **BPA** – δ 6.97 (d, 4H, CH-C-C), 6.66 (d, 4H, CH-C-OH), 1.53 (s, 6H, CH_3); **2q** – δ 4.67 (m, 1H, $\text{O-CH}_2\text{-CH}_2$), 1.70 (dd, 1H, $\text{C-CH}_2\text{-CH}$), 1.36 (d, 6H, CH_3), 1.30 (d, 3H, CH_3). Signal at $\delta = 3.94$, 1.47-1.42, 1.12 and 1.07 ppm corresponds to residual reagent (**1q**), signal at $\delta = 7.26$ ppm corresponds to side-product and signal at $\delta = 1.87$ ppm corresponds to TBD:MSA signal used as internal standard for calculating conversion.

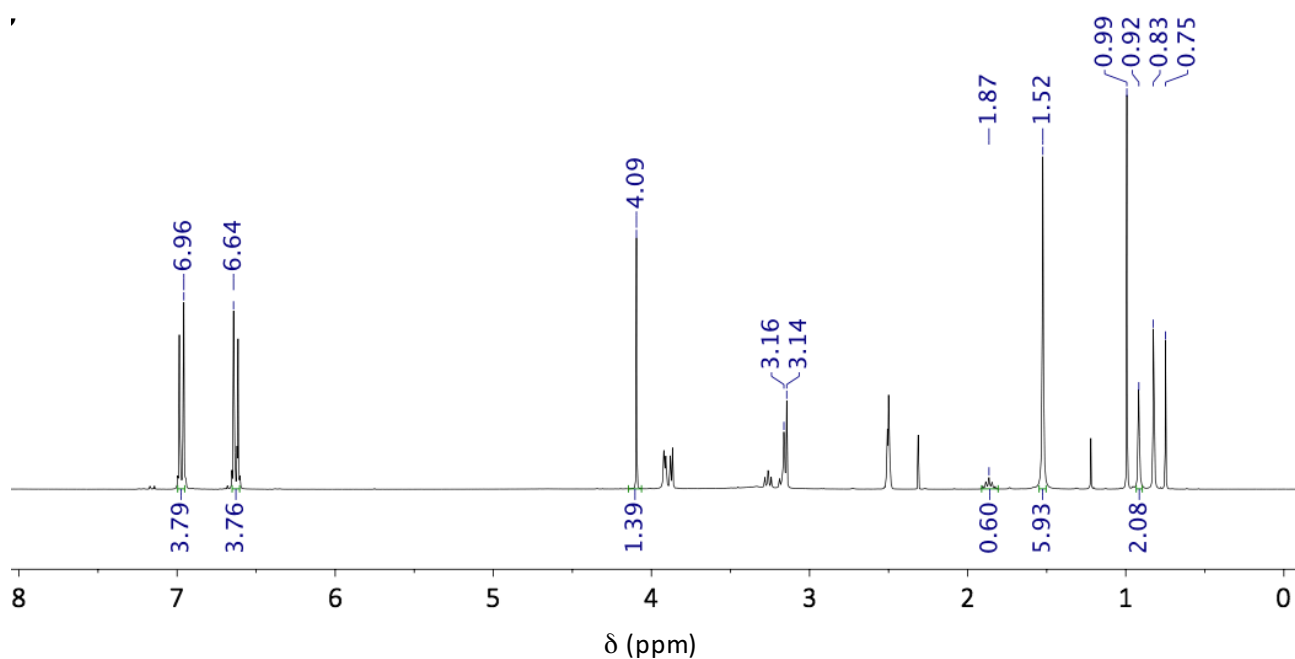


Figure S3.45. ^1H NMR spectrum of the crude product containing 5,5-dimethyl-1,3-dioxan-2-one (**2r**) (DMSO- d_6 , 400 MHz, 298 K). Resonances assigned as: **BPA** – δ 6.96 (d, 4H, CH-C-C), 6.64 (d, 4H, CH-C-OH), 1.52 (s, 6H, CH₃); **2r** – δ 4.09 (s, 1H, O-CH₂-CH₂), 0.92 (s 6H, CH₃). Signals at δ = 3.16 – 3.14, 0.83, 0.75 ppm correspond to residual reagent (**1r**), signal at δ = 3.87 ppm corresponds to linear carbonate and signal at δ = 1.87 ppm corresponds to TBD:MSA signal used as internal standard for calculating conversion.

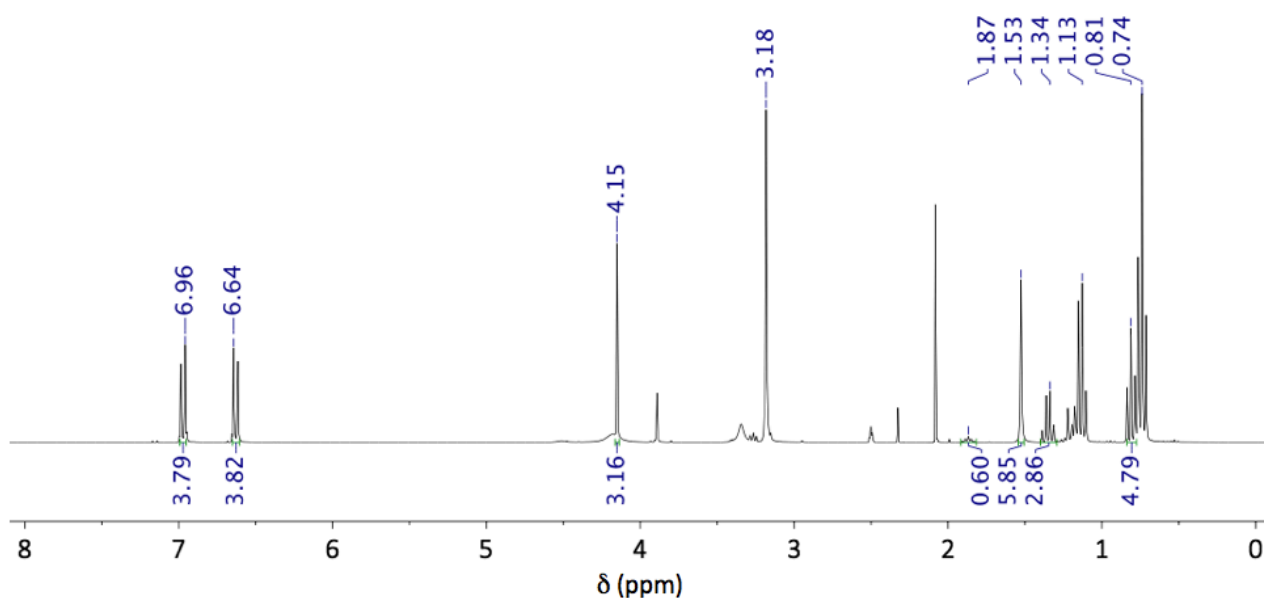


Figure S3.46. ^1H NMR spectrum of the crude product containing 5,5-diethyl-1,3-dioxan-2-one (**2s**) (DMSO- d_6 , 400 MHz, 298 K). Resonances assigned as: **BPA** – δ 6.96 (d, 4H, CH-C-C), 6.64 (d, 4H, CH-C-OH), 1.53 (s, 6H, CH₃); **2s** – δ 4.15 (s, 4H, CH-O), 1.34 (q, 4H, C-CH₂-CH₃), 0.81 (t, 6H, CH₂-CH₃). Signals at δ = 3.18, 1.13 and 0.74 ppm correspond to residual reagent (**1s**), signal at δ = 3.89 ppm corresponds to linear carbonate and signal at δ = 1.87 ppm corresponds to TBD:MSA signal used as internal standard for calculating conversion.

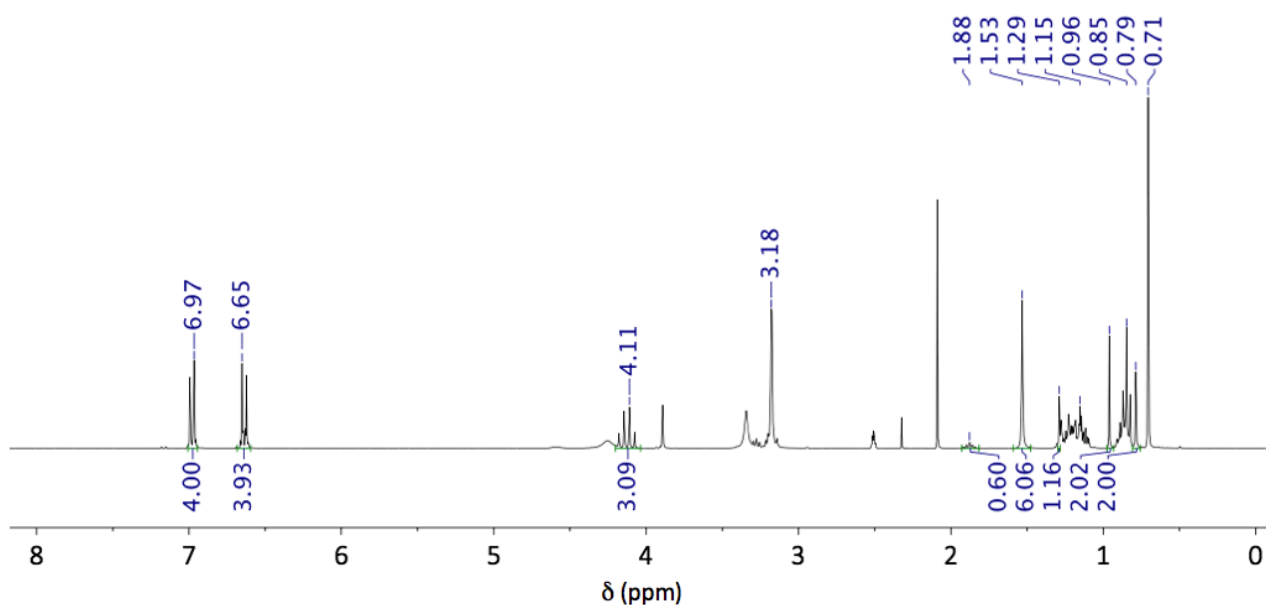


Figure S3.47. ^1H NMR spectrum of the crude product containing **5-methyl-5-propyl-1,3-dioxan-2-one (2t)** ($\text{DMSO-}d_6$, 400 MHz, 298 K). Resonances assigned as: **BPA** – δ 6.97 (d, 4H, CH-C-C), 6.65 (d, 4H, CH-C-OH), 1.53 (s, 6H, CH_3); **2t** – δ 4.11 (q, 4H, CH-O), 1.29 (m, 2H, $\text{C-CH}_2\text{-CH}_2$), 1.15 (m, 2H, $\text{C-CH}_2\text{-CH}_2$), 0.96 (s, 3H, C-CH_3), 0.79 (s, 3H, $\text{CH}_2\text{-CH}_3$). Signals at $\delta = 3.18$, 0.85 and 0.71 ppm correspond to residual reagent (**1t**), signal at $\delta = 3.89$ ppm corresponds to linear carbonate and signal at $\delta = 1.88$ ppm corresponds to TBD:MSA signal used as internal standard for calculating conversion.

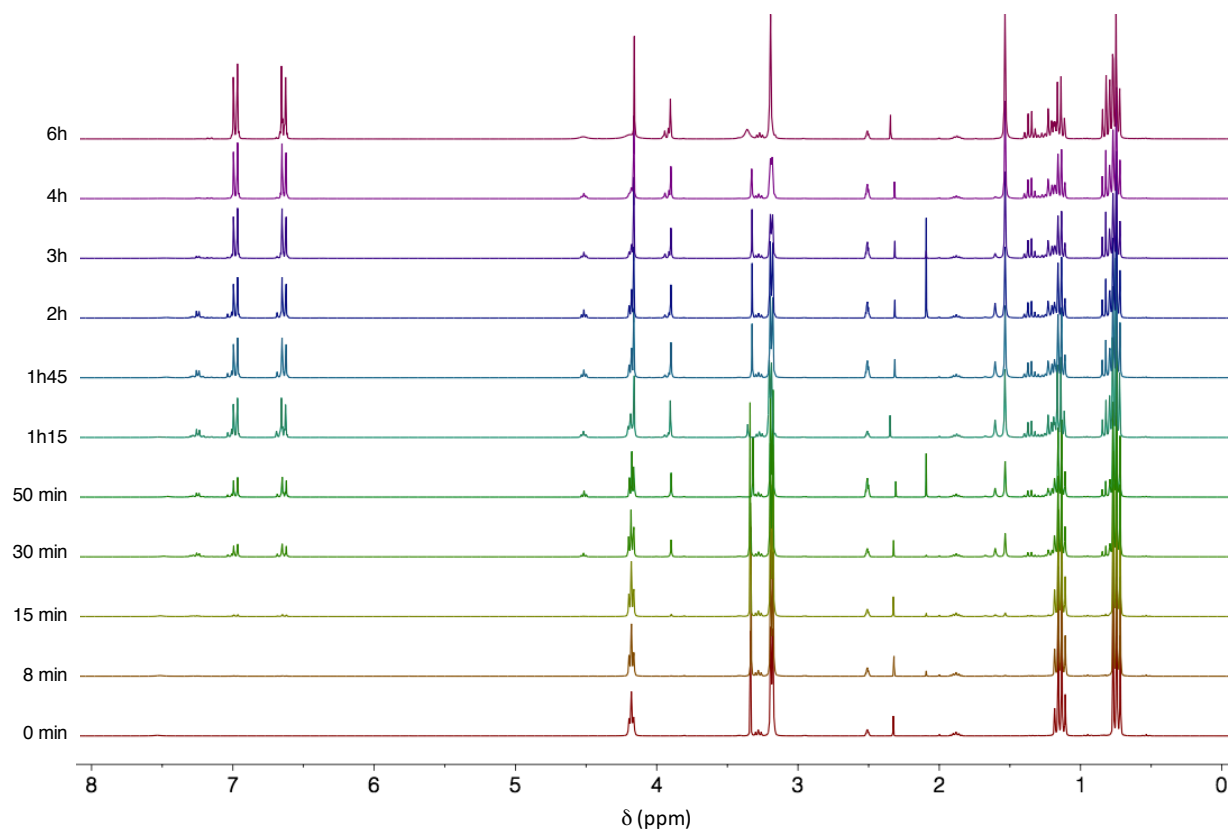


Figure S3.48. Stacked ^1H NMR spectra for the kinetic of the depolymerisation of BPA-PC (2 g, 7.80 mmol, 1eq.) with **1s** (3,1 g, 23.4 mmol, 3 eq.) as reagent using TBD:MSA (1:1) as catalyst (0.277 g, 1.18 mmol, 0.15 eq.) at 130 °C ($\text{DMSO-}d_6$, 400 MHz, 298 K).

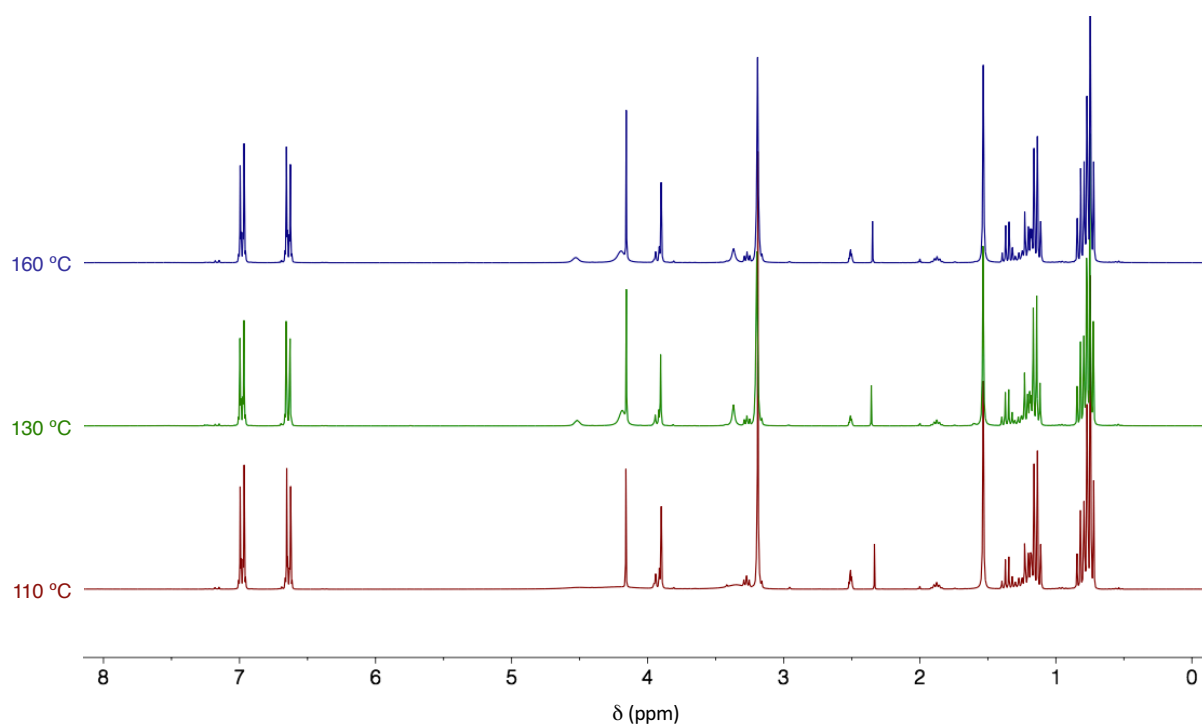


Figure S3.49. Stacked ¹H NMR spectra of the crude product containing **2s** (DMSO-*d*₆, 400 MHz, 298 K) at different temperatures. Resonances assigned as: **BPA** – δ 6.96 (d, 4H, CH-C-C), 6.64 (d, 4H, CH-C-OH), 1.53 (s, 6H, CH₃); **2s** – δ 4.15 (s, 4H, CH-O), 1.34 (q, 4H, C-CH₂-CH₃), 0.81 (t, 6H, CH₂-CH₃). Signals at δ = 3.18, 1.13 and 0.74 ppm correspond to residual reagent (**1s**), signal at δ = 3.89 ppm corresponds to linear carbonate and signal at δ = 1.87 ppm corresponds to TBD:MSA signal used as internal standard for calculating conversion.

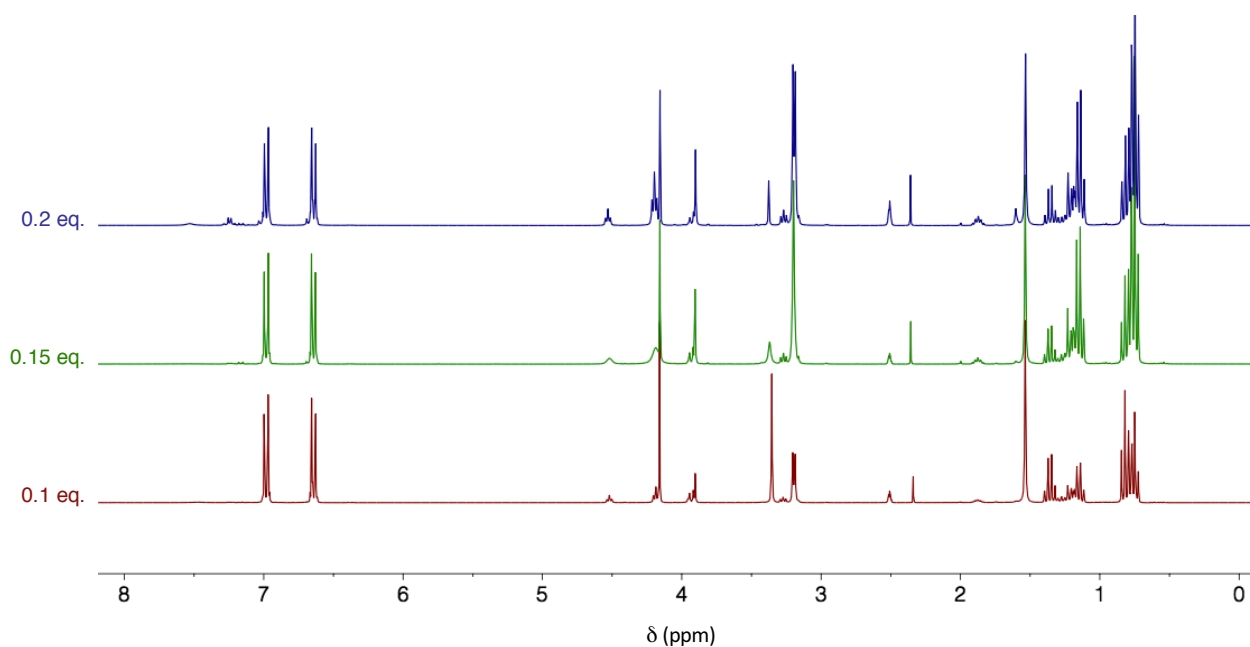


Figure S3.50. Stacked ¹H NMR spectra of the crude product containing **2s** (DMSO-*d*₆, 400 MHz, 298 K) at different catalyst contents. Resonances assigned as: **BPA** – δ 6.96 (d, 4H, CH-C-C), 6.64 (d, 4H, CH-C-OH), 1.53 (s, 6H, CH₃); **2s** – δ 4.15 (s, 4H, CH-O), 1.34 (q, 4H, C-CH₂-CH₃), 0.81 (t, 6H, CH₂-CH₃). Signals at δ = 3.18, 1.13 and 0.74 ppm correspond to residual reagent (**1s**), signal at δ = 3.89 ppm corresponds to linear carbonate and signal at δ = 1.87 ppm corresponds to TBD:MSA signal used as internal standard for calculating conversion.

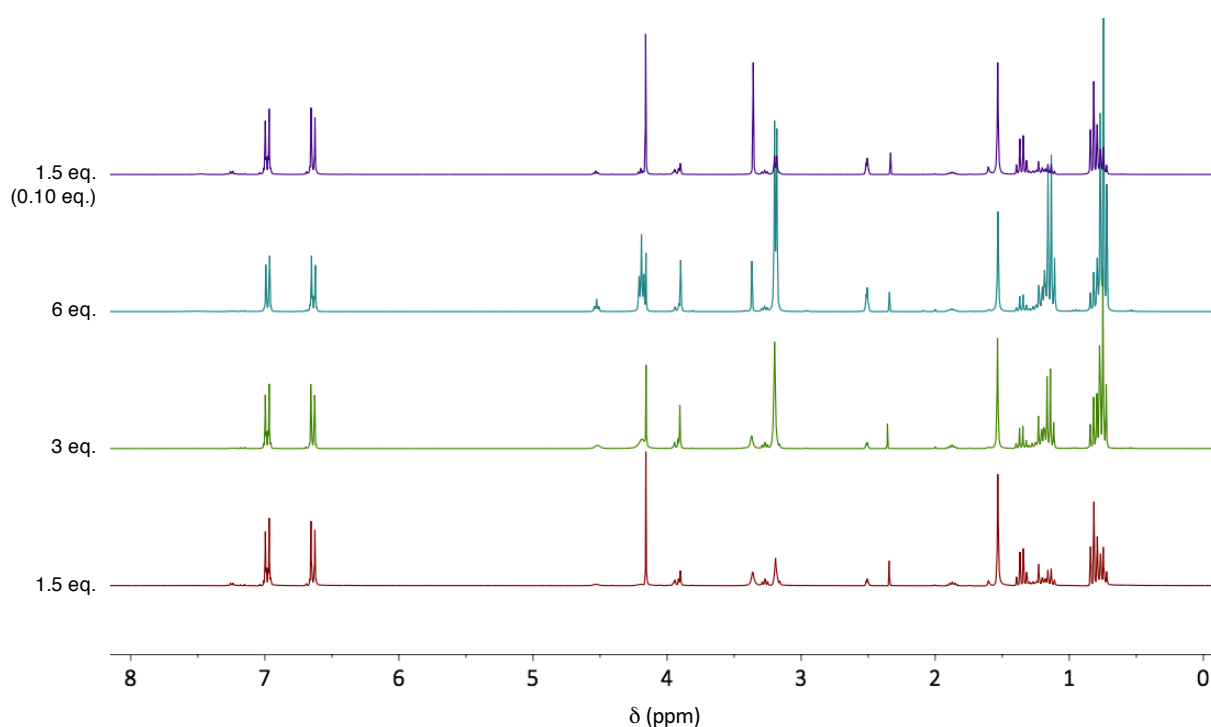


Figure S3.51. Stacked ¹H NMR spectra of the crude product containing **2s** (DMSO-*d*₆, 400 MHz, 298 K) at different reagent contents. Resonances assigned as: **BPA** – δ 6.96 (d, 4H, CH-C-C), 6.64 (d, 4H, CH-C-OH), 1.53 (s, 6H, CH₃); **2s** – δ 4.15 (s, 4H, CH-O), 1.34 (q, 4H, C-CH₂-CH₃), 0.81 (t, 6H, CH₂-CH₃). Signals at δ = 3.18, 1.13 and 0.74 ppm correspond to residual reagent (**1s**), signal at δ = 3.89 ppm corresponds to linear carbonate and signal at δ = 1.87 ppm corresponds to TBD:MSA signal used as internal standard for calculating conversion.

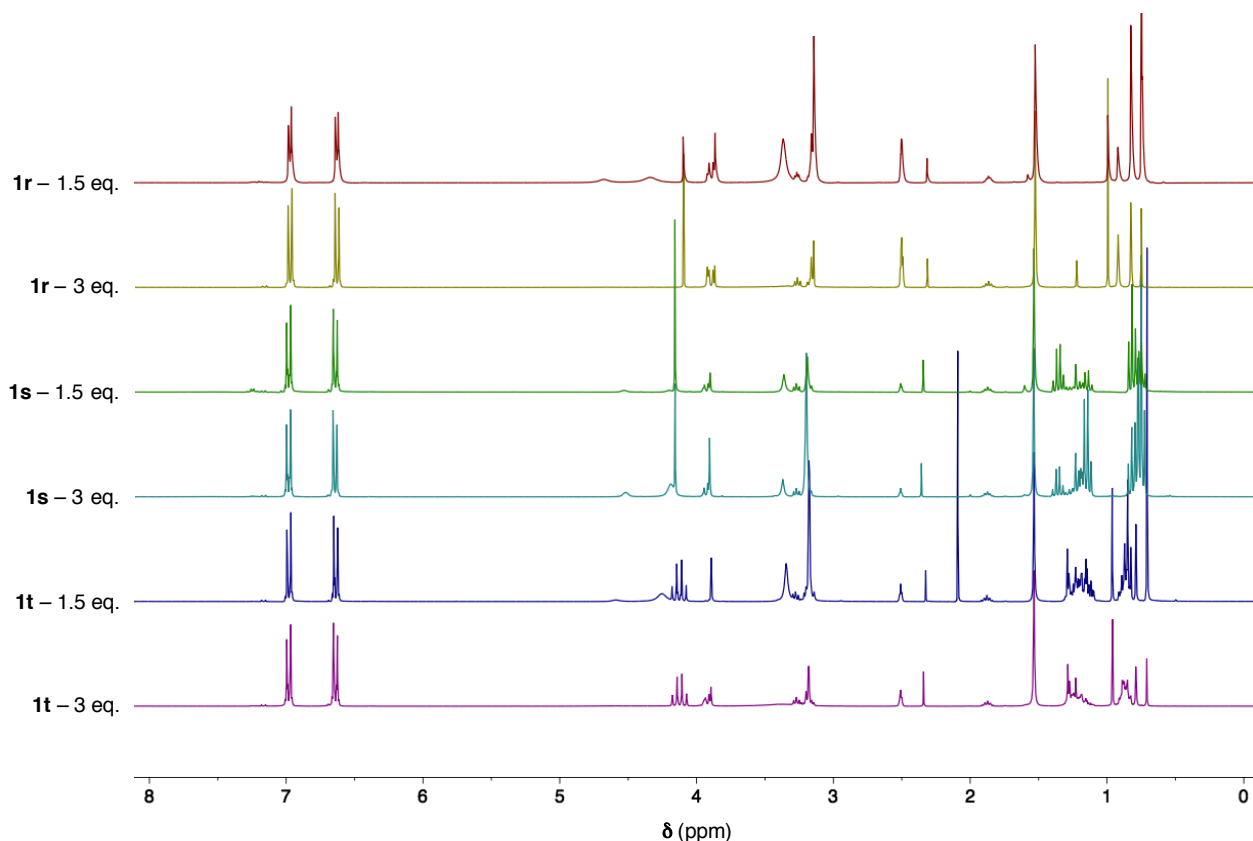


Figure S3.52. Stacked ¹H NMR spectra of the crude product containing **2r**, **2s** or **2t** (DMSO-*d*₆, 400 MHz, 298 K) at 130 °C with different reagent contents.

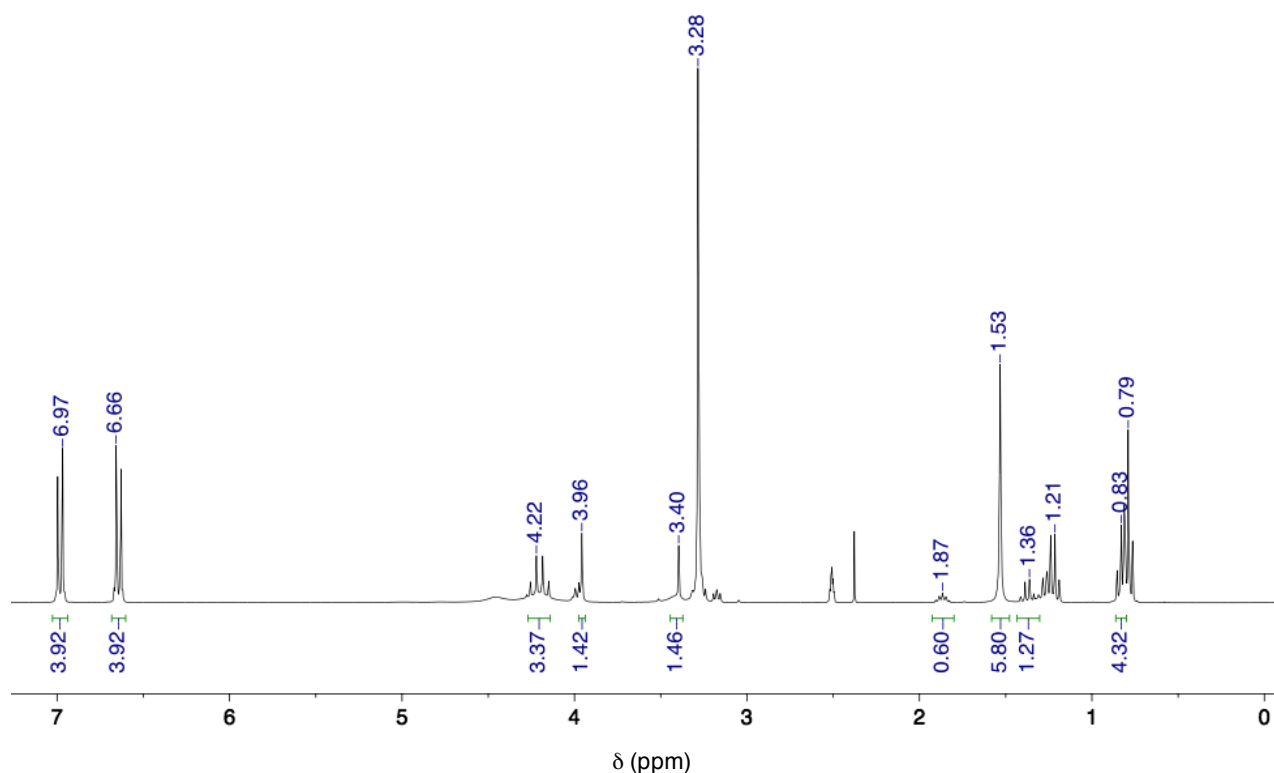


Figure S3.53. ¹H NMR spectrum of the crude product containing (**2u**) (DMSO-*d*₆, 400 MHz, 298 K). Resonances assigned as: **BPA** – δ 6.97 (d, 4H, CH-C-C), 6.66 (d, 4H, CH-C-OH), 1.53 (s, 6H, CH₃); **2u** – δ 4.22 (q, 4H, O-CH₂-C-CH₂-O), 3.40 (s, 2H, CH₂-OH), 1.36 (m, 2H, CH₂-CH₃), 0.83 (m, 6H, CH₂-CH₃). Signals at δ = 3.28, 1.21 and 0.79 ppm correspond to residual reagent (**1u**), signal at δ = 3.96 ppm corresponds to linear carbonate and signal at δ = 1.88 ppm corresponds to TBD:MSA signal used as internal standard for calculating conversion.

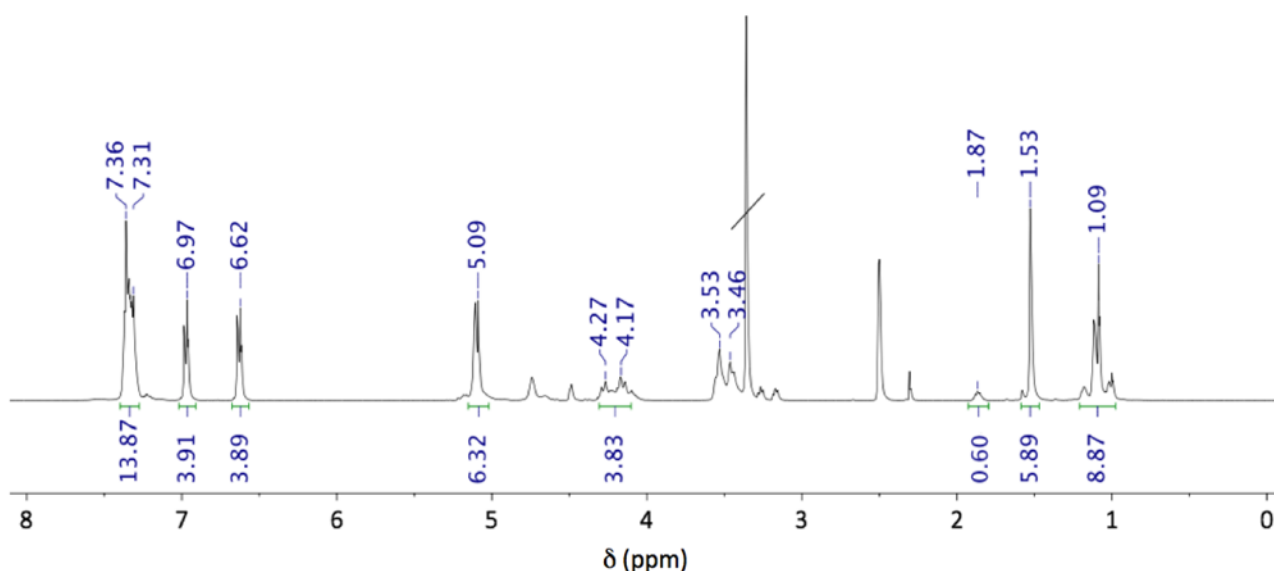


Figure S3.54. ¹H NMR spectrum of the crude product containing benzyl 5-methyl-2-oxo-1,3-dioxane-5-carboxylate (**2v**) (DMSO-*d*₆, 400 MHz, 298 K). Resonances assigned as: **BPA** – δ 6.97 (d, 4H, CH-C-C), 6.62 (d, 4H, CH-C-OH), 1.53 (s, 6H, CH₃); **2v** – δ 7.36 – 7.31 (m, 4H, O-CH₂-C-CH₂-O), 5.09 (m, 2H, O-CH₂-C-CH), 4.27 – 4.17 (m, 4H, O-CH₂-C-CH₂-O), 1.09 (s, 6H, CH₃). Signals at δ = 3.53 – 3.46 ppm correspond to residual reagent (**1v**), and signal at δ = 1.87 ppm corresponds to TBD:MSA signal used as internal standard for calculating conversion.

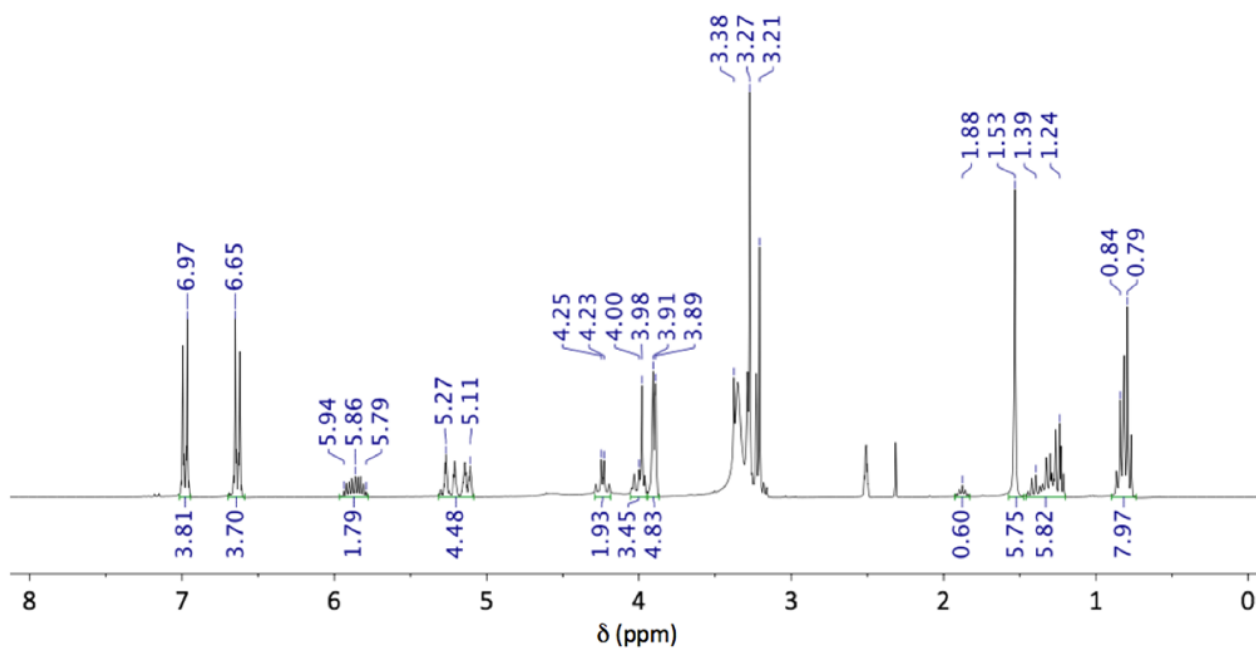


Figure S3.55. ^1H NMR spectrum of the crude product containing 5-((allyloxy)methyl)-5-ethyl-1,3-dioxan-2-one (**2w**) (DMSO- d_6 , 400 MHz, 298 K). Resonances assigned as: BPA – δ 6.97 (d, 4H, CH-C-C), 6.65 (d, 4H, CH-C-OH), 1.53 (s, 6H, CH₃); **2w** – δ 5.94 – 5.79 (m, 1H, CH=CH₂), 5.27 – 5.11 (m, 2H, CH=CH₂), 4.23 (q, 2H, O-CH₂-C-CH₂-O), 4.00 (m, 2H, O-CH₂-C-CH₂-O), 3.98 (s, 2H, O-CH₂-CH), 3.38 (s, 2H, O-CH₂-C) 1.39 (m, 2H, CH₂-CH₃), 0.84 (m, 6H, CH₂-CH₃). Signals at δ = 3.21 and 3.27 ppm correspond to residual reagent (**1w**), and signal at δ = 1.88 ppm corresponds to TBD:MSA signal used as internal standard for calculating conversion.

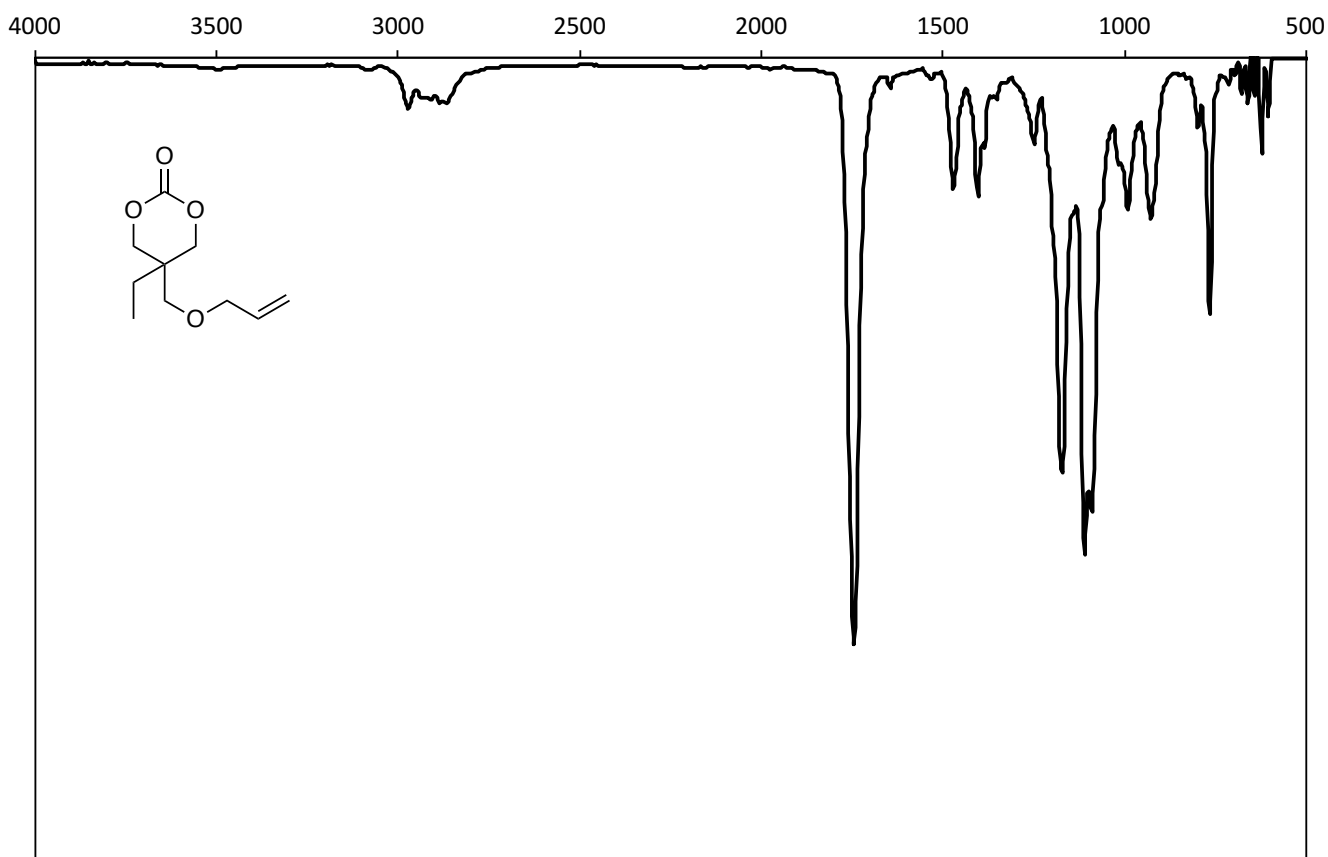


Figure S3.56. FT-IR spectrum of 5-((allyloxy)methyl)-5-ethyl-1,3-dioxan-2-one (**2w**).

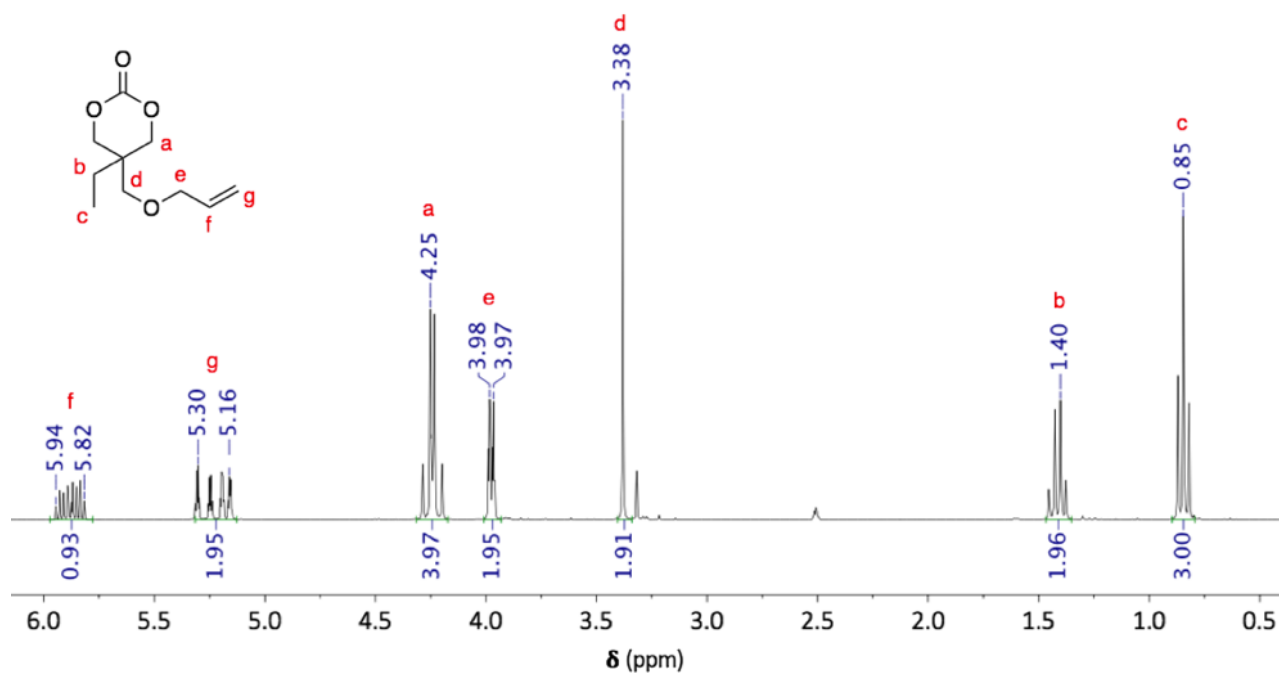


Figure S3.57. ¹H NMR spectrum of 5-((allyloxy)methyl)-5-ethyl-1,3-dioxan-2-one (**2w**) (DMSO-*d*₆, 400 MHz, 298 K).

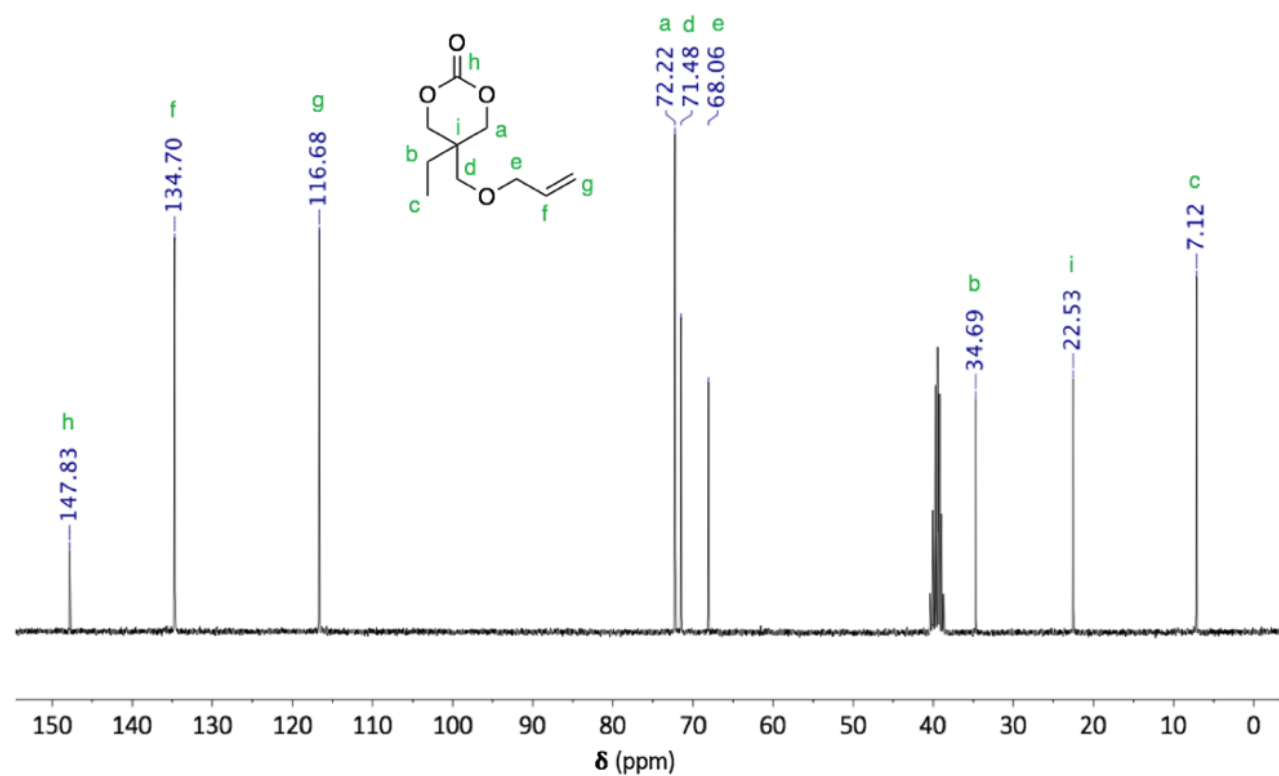


Figure S3.58. ¹³C NMR spectrum of 5-((allyloxy)methyl)-5-ethyl-1,3-dioxan-2-one (**2w**) (DMSO-*d*₆, 400 MHz, 298 K).

Appendix Chapter 4

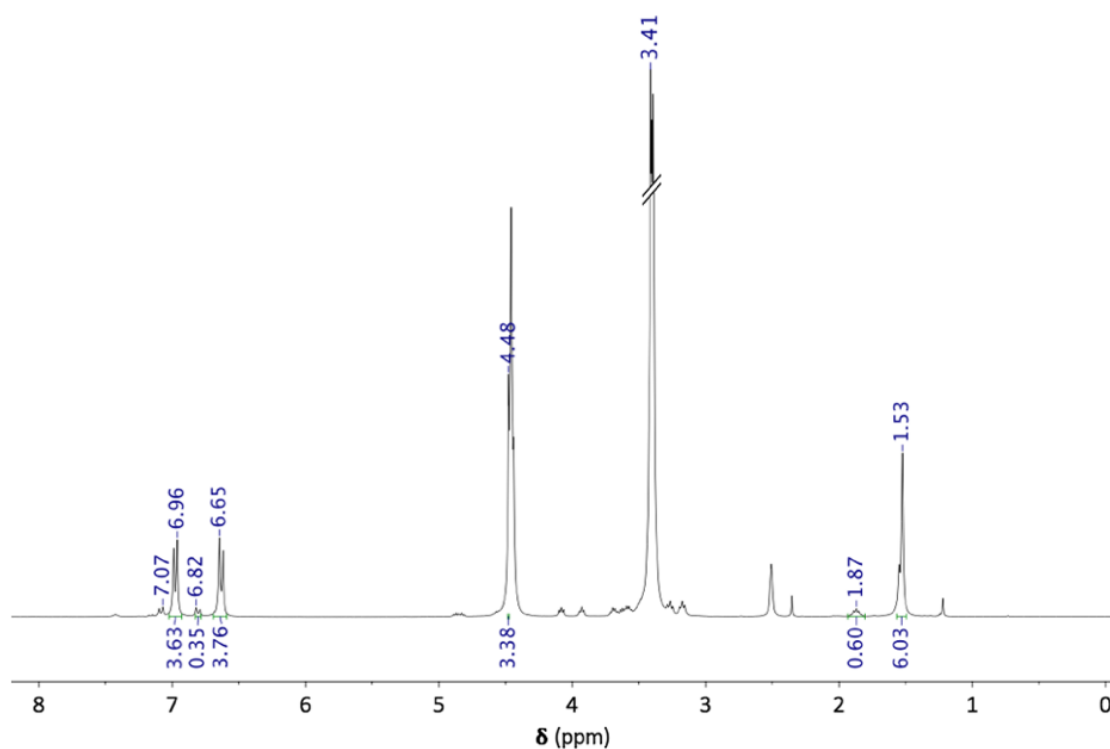


Figure S4.1. ^1H NMR spectrum of the crude product of BPA-PC depolymerisation using 16 eq. of ethylene glycol ($\text{DMSO-}d_6$, 300 MHz, 298 K). Resonances assigned as: **BPA** – δ 6.65 (d, 4H), 6.96 (d, 4H), 1.53 (s, 6H) – yield 94%; **ethylene carbonate** – δ 4.48 (s, 4H, CH_2).

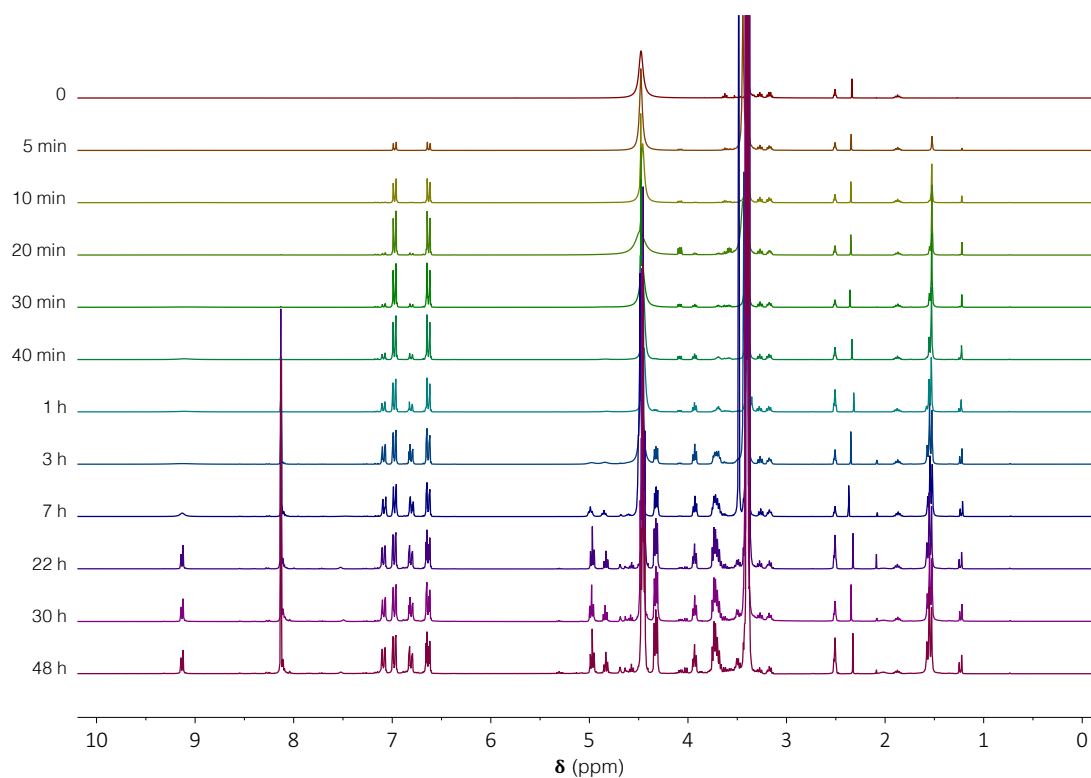


Figure S4.2. Stacked ^1H NMR spectra for the kinetic of the selective depolymerisation of BPA-PC (2 g, 7.80 mmol, 1 eq.) and PET (1.5 g, 7.80 mmol 1 eq.) using 0.15 eq. of TBD:MSA (1:1) as catalyst (0.277 g, 1.18 mmol) at 180 °C ($\text{DMSO-}d_6$, 400 MHz, 298 K).

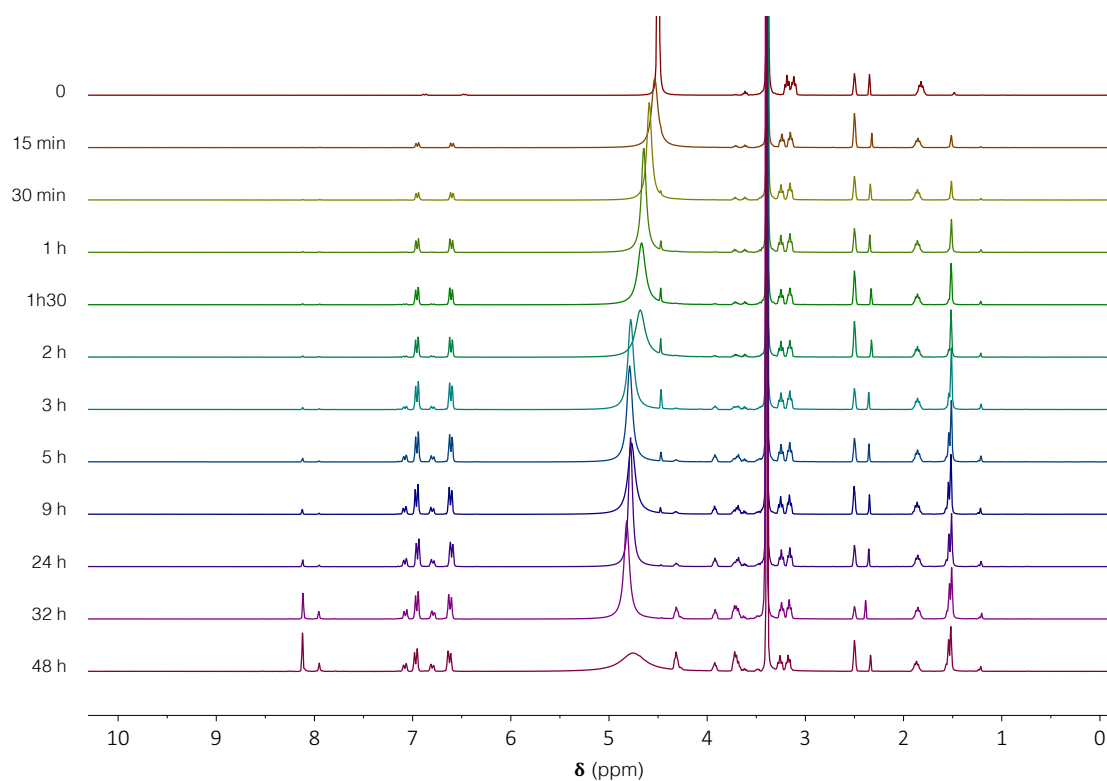


Figure S4.3. Stacked ¹H NMR spectra for the kinetic of the selective depolymerisation of BPA-PC (2 g, 7.80 mmol, 1eq.) and PET (1.5 g, 7.80 mmol 1 eq.) using 0.5 eq. of TBD:MSA (1:1) as catalyst (0.917 g, 3.90 mmol) at 130 °C (DMSO-*d*₆, 400 MHz, 298 K).

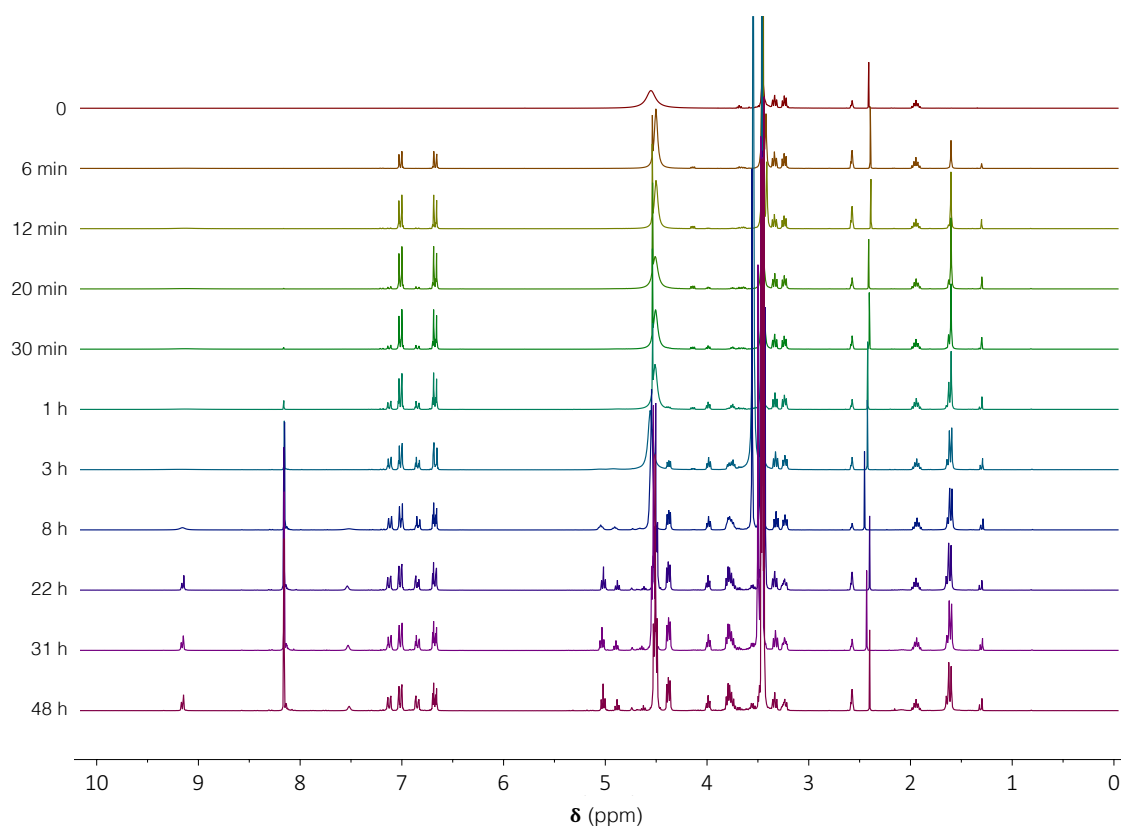


Figure S4.4. Stacked ¹H NMR spectra for the kinetic of the selective depolymerisation of BPA-PC (2 g, 7.80 mmol, 1eq.) and PET (1.5 g, 7.80 mmol 1 eq.) using 0.5 eq. of TBD:MSA (1:1) as catalyst (0.917 g, 3.90 mmol) at 180 °C (DMSO-*d*₆, 400 MHz, 298 K).

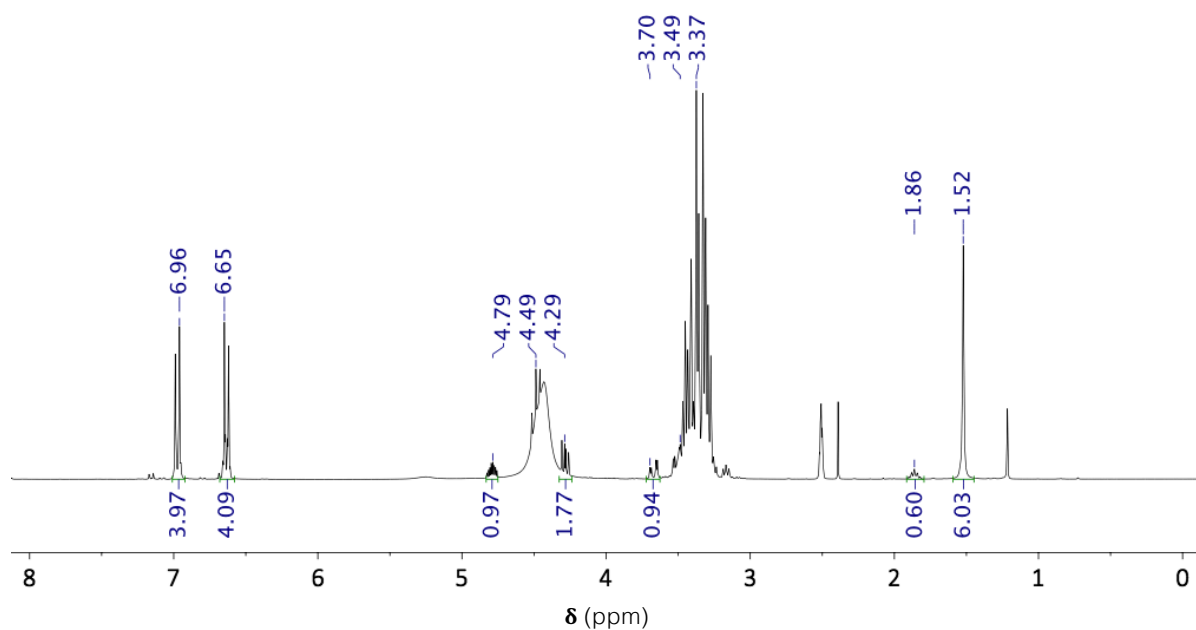


Figure S4.5. ^1H NMR spectrum of the selective depolymerisation of BPA-PC and PET using **1h** as reagent at the disappearance of PET pellets (DMSO- d_6 , 400 MHz, 298 K). Resonances assigned as: **BPA** – δ 6.96 (d, 4H, CH-C-C), 6.64 (d, 4H, CH-C-OH), 1.53 (s, 6H, CH₃); **2h** – δ 4.79 (m, 1H, CH-O), 4.49 (t, 1H, CH₂-O), 4.29 (m, 1H, CH₂-O), 3.49-3.70 (dd, 2H, CH₂). Signal at δ = 3.37 ppm corresponds to residual reagent (**1h**), and signal at δ = 1.86 ppm corresponds to TBD:MSA signal used as internal standard for calculating conversion.

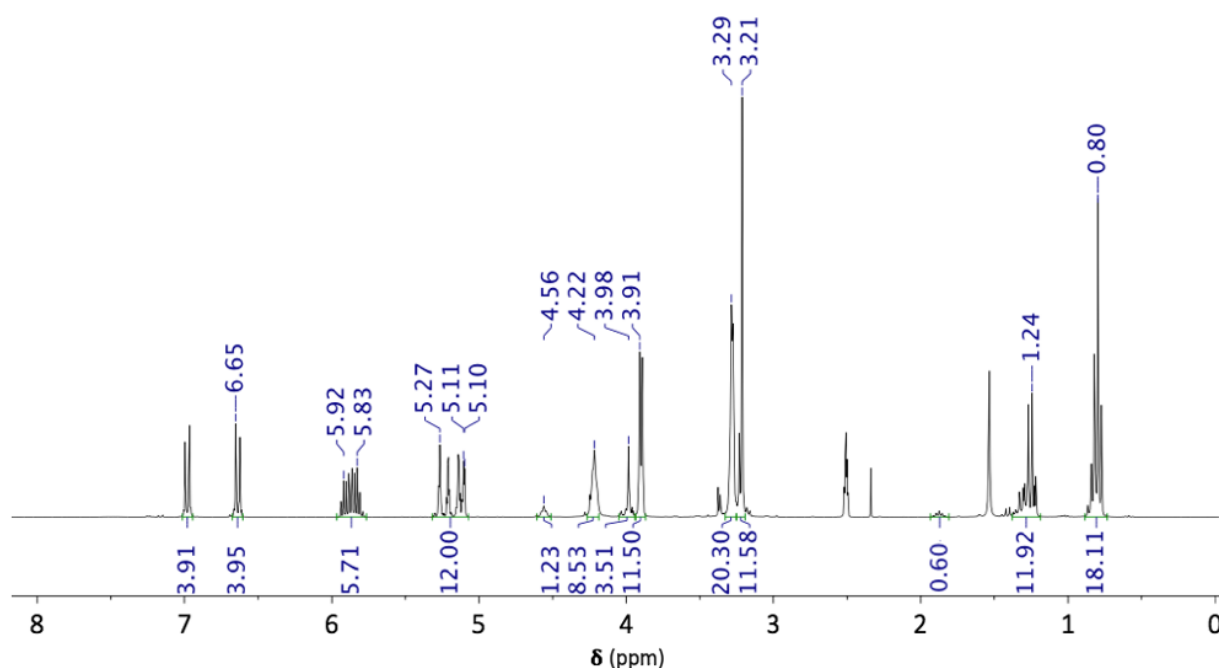


Figure S4.6. ^1H NMR spectrum of the selective depolymerisation of BPA-PC and PET using **1w** as reagent at the disappearance of PET pellets (DMSO- d_6 , 400 MHz, 298 K). Resonances assigned as: **BPA** – δ 6.65 (d, 4H), 6.96 (d, 4H), 1.53 (s, 6H); **2w** – δ 5.92 – 5.83 (m, 1H, CH=CH₂), 5.27 – 5.10 (m, 2H, CH=CH₂), 4.22 (q, 4H, O-CH₂-C-CH₂-O), 3.98 (s, 2H, O-CH₂-CH), 3.38 (s, 2H, O-CH₂-C) 1.39 (m, 2H, CH₂-CH₃), 0.84 (m, 6H, CH₂-CH₃). Signal at δ = 3.29 – 3.21 ppm corresponds to residual reagent (**1w**), and signal at δ = 1.86 ppm corresponds to TBD:MSA signal used as internal standard for calculating conversion.

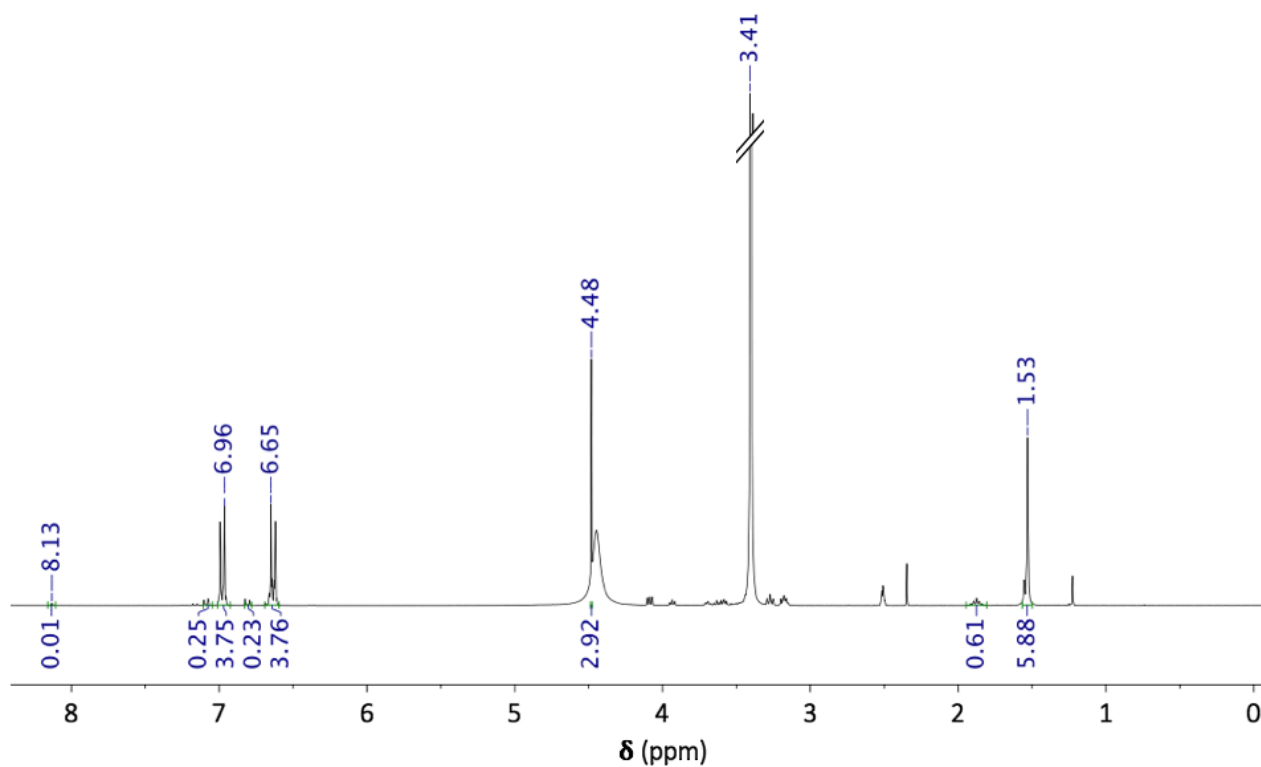


Figure S4.7. ¹H NMR spectrum of joint depolymerisations of BPA-PC and PET in the presence of PP pellets at the disappearance of BPA-PC pellets, (DMSO-*d*₆, 400 MHz, 298 K). Resonances assigned as: BPA – δ 6.65 (d, 4H), 6.96 (d, 4H), 1.53 (s, 6H); 2b – δ 4.48 (s, 4H, CH₂).

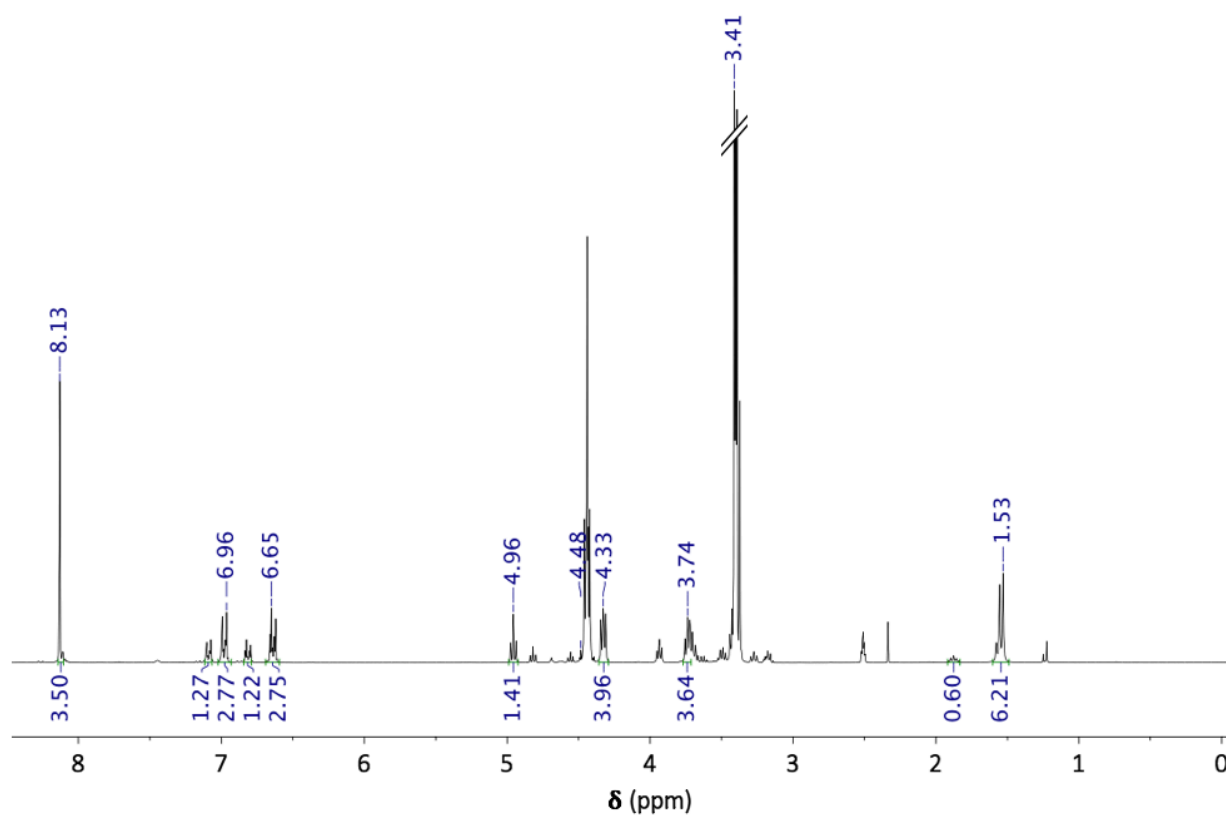


Figure S4.8. ¹H NMR spectrum of the joint depolymerisation of BPA-PC and PET in the presence of PP pellets at the disappearance of PET pellets (DMSO-*d*₆, 400 MHz, 298 K). Resonances assigned

as: **BPA** – δ 6.65 (d, 4H), 6.96 (d, 4H), 1.53 (s, 6H); **2a** – δ 4.48 (s, 4H, CH₂); **BHET** – δ 8.13 (s, 4H, CH), 4.96 (t, 2H, OH), 4.33 (t, 4H, O-CH₂), 3.74 (m, 4H, CH₂-OH).

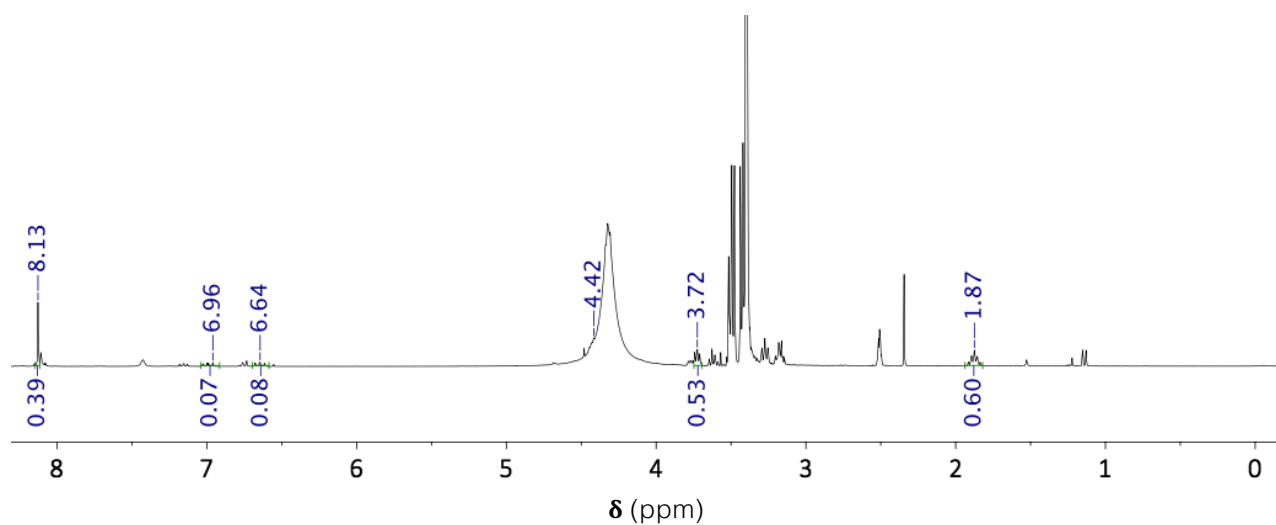


Figure S4.9. ¹H NMR spectrum of the joint depolymerisation of BPA-PC and PET in the presence of PVC pellets using 0.15 eq. of TBD:MSA (1:1) catalyst after 96 h (DMSO-*d*₆, 400 MHz, 298 K). Resonances assigned as: BPA – δ 6.64 (d, 4H), 6.96 (d, 4H), 1.53 (s, 6H); BHET – δ 8.13 (s, 4H, CH), 4.42 (s, 4H, O-CH₂), 3.72 (m, 4H, CH₂-OH).

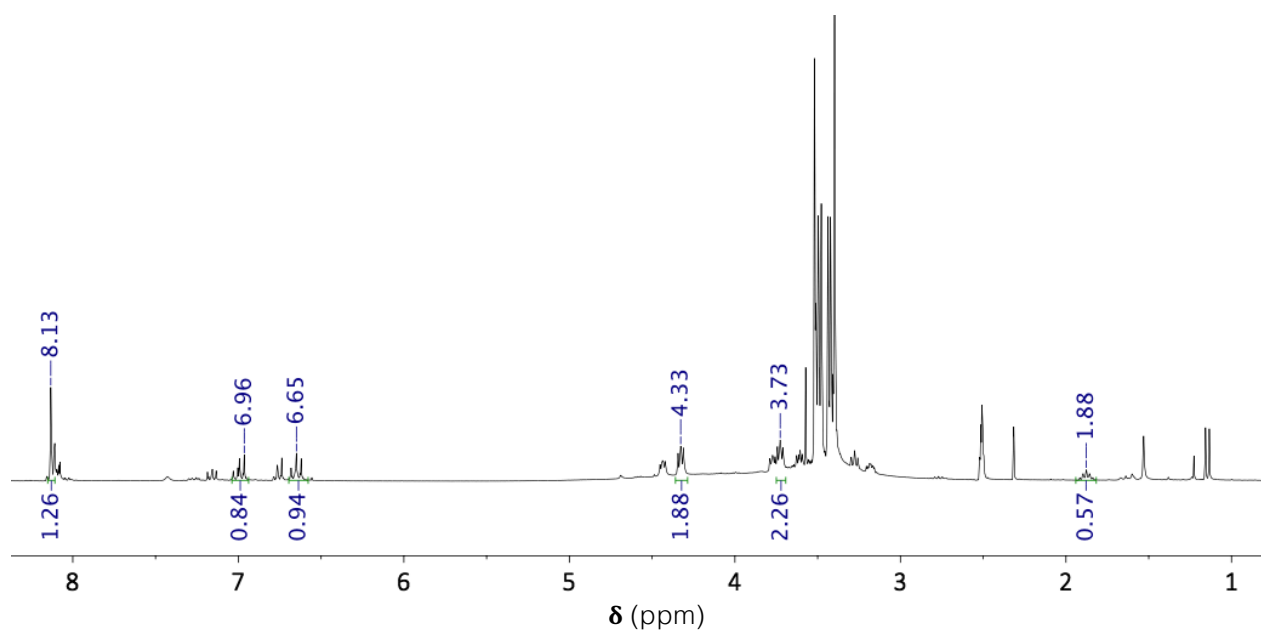


Figure S4.10. ¹H NMR spectrum of the joint depolymerisation of BPA-PC and PET in the presence of PVC pellets using 0.5 eq. of TBD:MSA (1:1) catalyst after 96 h (DMSO-*d*₆, 400 MHz, 298 K). Resonances assigned as: BPA – δ 6.64 (d, 4H), 6.96 (d, 4H), 1.53 (s, 6H); BHET – δ 8.13 (s, 4H, CH), 4.42 (s, 4H, O-CH₂), 3.72 (m, 4H, CH₂-OH).

A

Sample Identifier	Sample Description	Mw	Mn	Mw/Mn	Mz
IWTN/W000009777-1 Inj A	Sample 1	158,000	43,500	3.6	340,000
IWTN/W000009777-1 Inj B	Sample 1	155,000	44,800	3.5	330,000
IWTN/W000009777-1 Inj C	Sample 1	157,000	43,000	3.7	339,000
IWTN/W000009777-2 Inj A	Sample 2	151,000	41,100	3.7	323,000
IWTN/W000009777-2 Inj B	Sample 2	154,000	42,100	3.6	330,000
IWTN/W000009777-2 Inj C	Sample 2	153,000	41,000	3.7	328,000

B

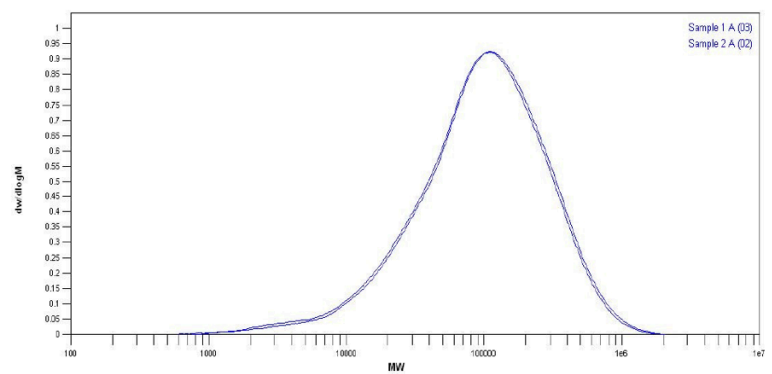


Figure S4.11. GPC analysis of PP before (Sample 1) and after (Sample 2) the selective depolymerisation of BPA-PC and PET (**A**) molecular weight for each samples and (**B**) plot of the molecular weight distribution.

Curriculum Vitae

Contact

Coralie Jehanno

+34 600 973 878 (SP) or +33 659 483 200 (FR)

coralijeh@gmail.com

Working experiences

Dec 2015 – July 2019

POLYMAT • San Sebastian, SPAIN

PhD student as part of 'Innovative polymers' group under the guidance of Dr. Fernando Ruipérez and Dr. Haritz Sardon. **Depolymerisation of oxygen-containing polymers using innovative organocatalysts.** Project is part of SUSPOL European program and funded by Marie Curie researcher fellowship.

Jan – July 2018

Universities of Warwick & Birmingham • UK

Secondment in Prof. Andrew Dove laboratory as part of the European SUSPOL co-tutelle program. **Selective chemical recycling of commodity polymers from mixed plastic streams.**

March – July 2017

IBM Almaden research center • San José, CA, USA

Visiting researcher in Dr. James Hedrick laboratory. **Synthesis of functionalised cyclic carbonate derived from the recycling of a commodity polymer: BPA-PC.**

April – Sept 2015

TOTAL • Lyon area, FRANCE

Research intern in the lubricant department. **Screening of bio-sourced molecules for improving lubrication performance of transmission. Study of molecular structure, formulation and mechanical tests.**

Curriculum Vitae

Jul – Nov 2014

King Abdullah University of Science and Technology (KAUST) • Thuwal, SAUDI ARABIA

Research placement in Supramolecular and Micellar group on the KAUST Catalysis Center under the guidance of Pr. Valentin Rodionov. **Polymerisation and characterisation of enzyme-inspired amphiphilic copolymers for catalytic applications.**

Aug 2013

'Projets Solidaires', Humanitarian association • Banfora, BURKINA FASO

One-month volunteer on a sustainable energy project for a humanitarian association from Bordeaux. **Feasibility study on the possibility to develop bio-based charcoal for daily consumption in adapted oven in Burkina Faso – Mali area.**

Education

2015 – 2019

Universidad del País Vasco (UPV) • San Sebastian, SPAIN

University of Warwick • UK

PhD in applied chemistry and polymeric materials in co-tutelle between the universities of the Basque country, Spain, and Warwick, UK. PhD supervised by Dr. Fernando Ruipérez and Dr. Haritz Sardon in the university of the Basque Country and Prof. Matthew I. Gibson and Prof. Andrew P. Dove in the university of Warwick.

2012 – 2015

Graduate School of Chemistry, Biology and Physics (ENSCBP) • Bordeaux, FRANCE

Master's Degree in Chemistry and Physics obtained in September 2015

2010 – 2012

Graduate School of Chemistry (ENSCR) • Rennes, FRANCE

Two-year intensive undergraduate course in Maths, Physics and Chemistry in an international class.

Skills

Laboratory

Spectroscopy (NMR, UV, IR)

Chromatography (GC, HPLC)

Thermogravimetric analysis

Polymer analysis techniques (GPC, DLS)

Microscopy techniques (TEM, AFM)

Organic chemistry, synthesis of polymers, depolymerisation.

Computer

ChemDraw, MestreNova, Gwyddion, Origin

Word, Excel, PowerPoint

Basic knowledge of Linux, Gaussian 16, GaussView, Molden

Languages

French – native speaker

English & Spanish – fluent writing and speaking

References

Pr. Andrew P. Dove

Professor of Chemistry

School of Chemistry – University of Birmingham

Edgbaston

B15 2TT Birmingham, UK

+44(0)121 414 2768

a.dove@bham.ac.uk

Dr. Fernando Ruipérez

Research Associate

POLYMAT - University of the Basque Country UPV/EHU

Centro Joxe Mari Korta, Avda. de Tolosa, 72

20018 Donostia-San Sebastian, SPAIN

+34 943 01 5985

fernando.ruiperez@polymat.eu

Dr. Haritz Sardon

Research Associate

POLYMAT – University of the Basque Country UPV/EHU

Departamento de Química aplicada - Procesos Polimerizacion

Universidad del País Vasco - Facultad de Química, Paseo Manuel Lardizabal,

3

20018 Donostia-San Sebastian, SPAIN

+34 943 01 5303

haritz.sardon@ehu.es

Dr. James Hedrick

Group leader

Advance Organic materials

IBM Research – Almaden

San José, CA, USA

+1 408 927 1632

hedrick@us.ibm.com

Dr. Valentin Rodionov

Assistant professor of Chemical Science

KAUST Catalysis Center (KCC)

King Abdullah University of Science and Technology - KAUST

+966-2-808-4592

valentin.rodionov@kaust.edu.sa

Bibliography

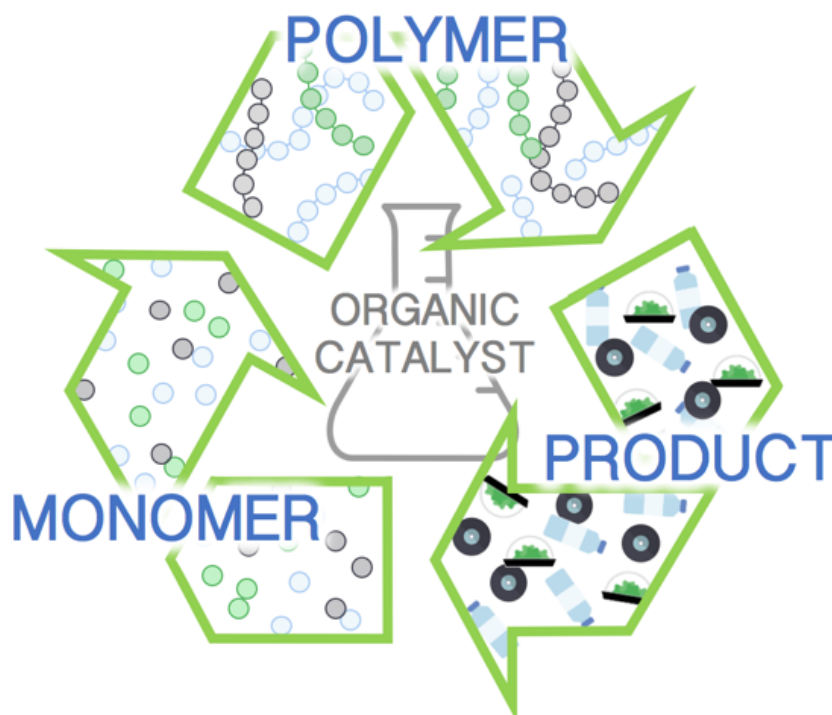
1. Chemical sorting of PET and BPA-PC by solvent-free, selective depolymerization.

Coralie Jehanno, Daniele Mantione, Maria C. Arno, Fernando Ruipérez, James L. Hedrick, Andrew P. Dove, Haritz Sardon. *Submitted*

2. Dynamic polymer network points the way to truly recyclable plastics.

Coralie Jehanno, Haritz Sardon. *Nature*, **2019**, 568 (7753), 467.

3. Organocatalysis for depolymerisation



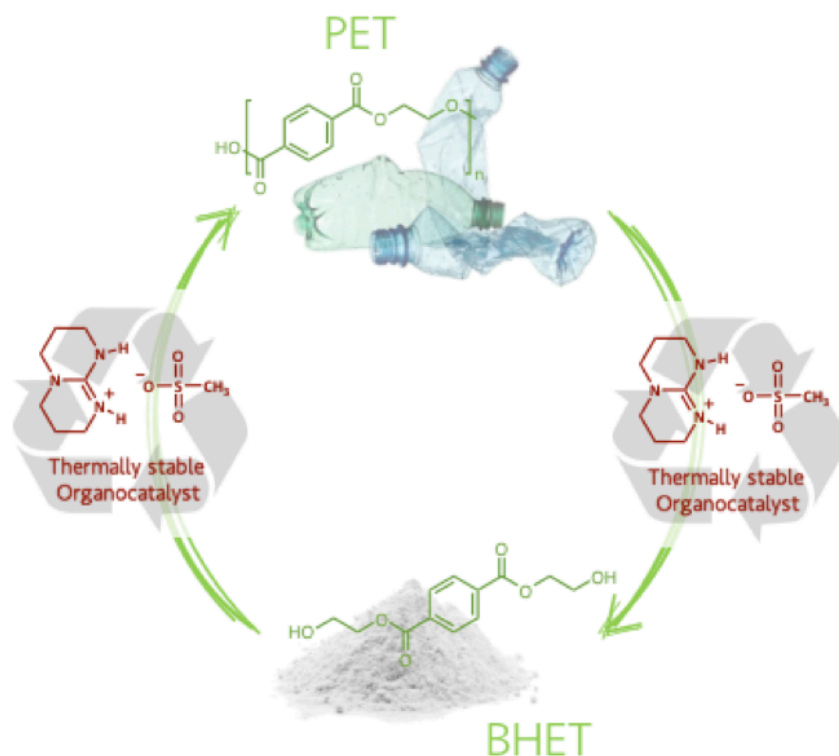
Coralie Jehanno, Maria M. Pérez-Madrugal, Jeremy Demarteau, Haritz Sardon, Andrew P. Dove, *Polym. Chem.*, **2018**, 10 (2), 172.

4. Organic catalysis for polymerisation. *Polymer Chemistry Series*, **2018**, Editors: Andrew P. Dove, Haritz Sardon, Stefan Naumann.

Chapter 14 – Organocatalysis for depolymerisation

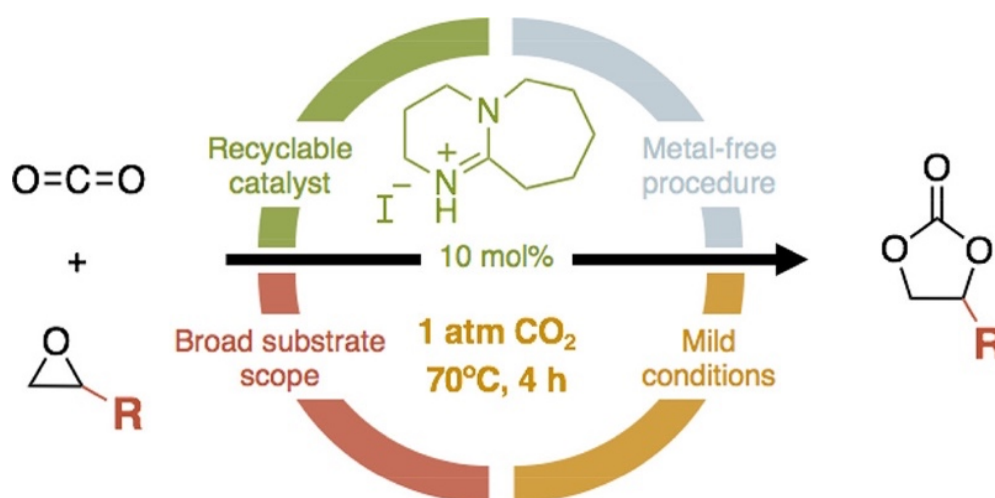
Coralie Jehanno, Jeremy Demarteau, Andrew P. Dove, 607 – 633.

5. Organocatalysed depolymerisation of PET in a fully sustainable cycle using thermally stable protic ionic salt.



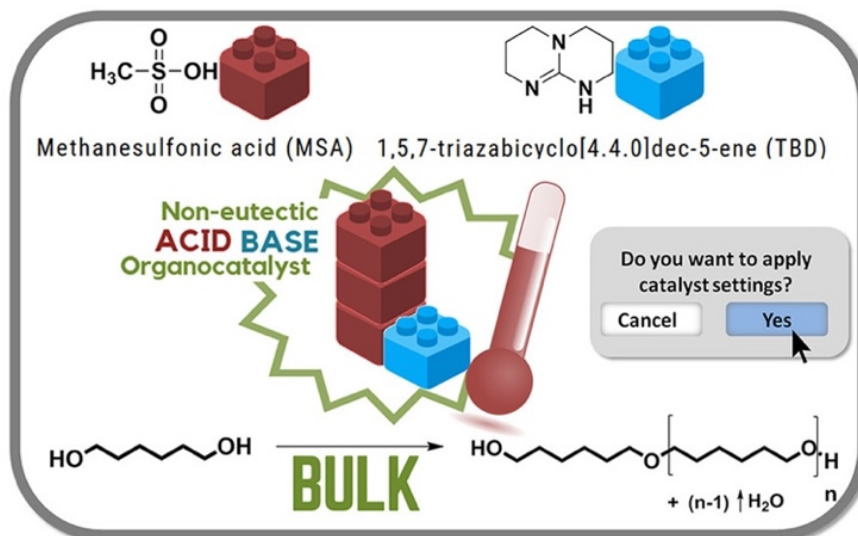
Coralie Jehanno, Irma Flores, Andrew P. Dove, Alejandro J. Müller, Fernando Ruipérez, Haritz Sardon, *Green Chem.*, **2018**, 20 (6), 1205.

6. Rational study of DBU salts for the CO₂ insertion into epoxides for the synthesis of cyclic carbonates.



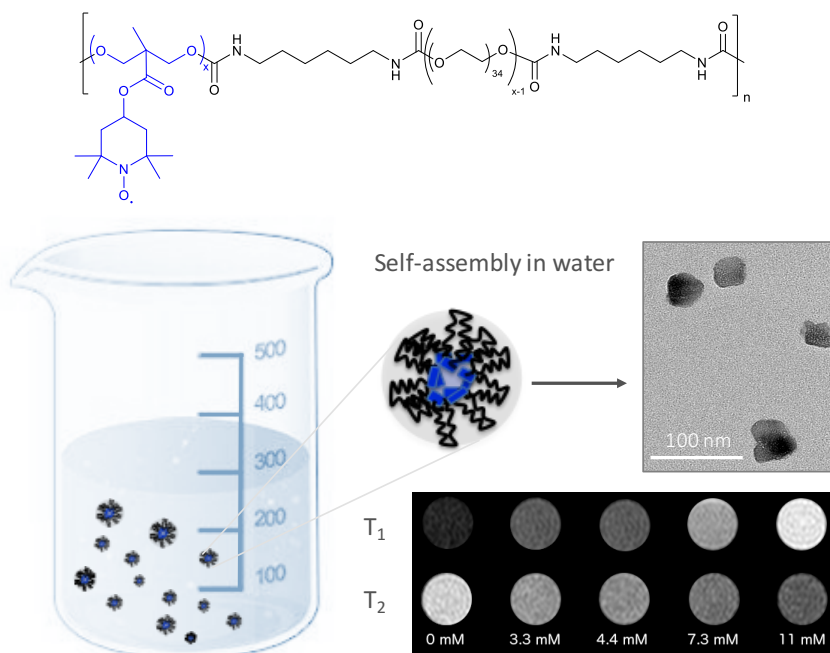
Noé Fanjul Mosteirín, **Coralie Jehanno**, Fernando Ruipérez, Haritz Sardon; Andrew P. Dove, DOI: 10.1021/acssuschemeng.9b01300, *ACS Sus. Chem. Eng.*, **2019**.

7. Polyether Synthesis by Bulk Self-Condensation of Diols Catalyzed by Non-Eutectic Acid-Base Organocatalysts.



Andere Basterretxea, Elena Gabirondo, **Coralie Jehanno**, Haijin Zhu, Irma Flores, Alejandro Muller, Agustin J. Etxeberria, David Mecerreyes, Olivier Coulembier, Haritz Sardon, *ACS Sus. Chem. Eng.*, **2019**, 7 (4), 4103.

8. Polyurethane based organic macromolecular contrast agents (PU-ORCAs) for magnetic resonance imaging.



Sofiem Garmendia, Daniele Mantione, Silvia Alonso-de Castro, **Coralie Jehanno**, Luis Lezama, James L. Hedrick, David Mecerreyes, Luca Salassa, Haritz Sardon, *Polym. Chem.*, **2017**, 8, 2693.

Conference contributions

March 2019

Which sustainable future for plastics? • Mons, BELGIUM

Presentation of a **poster** entitled “An innovative organocatalyst for the depolymerisation of commodity polymers: from plastic wastes to valuable monomers”.

October 2018

ECNP European centre for nanostructured polymers • San Sebastian, SPAIN

Oral presentation entitled “An innovative organocatalyst for the depolymerisation of commodity polymers: from plastic wastes to valuable monomers”.

Organisation committee

September 2018

GEP2018 Grupo especializado de polímeros • Huelva, SPAIN

Oral presentation entitled “An innovative organocatalyst for the depolymerisation of commodity polymers: from plastic wastes to valuable monomers”.

September 2017

3rd EuCheMS Congress on Green and Sustainable Chemistry • University of York, UK

Presentation of a **poster** entitled “Innovative organocatalyst for depolymerisation and subsequent polymerisation of poly(ethylene terephthalate) in a fully sustainable cycle”.

April 2017

ACS • San Francisco, CA, USA

Curriculum Vitae

September 2016

SUSPOL conference • Brussel, BELGIUM

Presentation of a **poster** entitled "Depolymerisation of Poly(ethylene terephthalate) using innovative protic ionic liquids as catalyst".

July 2016

Warwick Polymer Conference • University of Warwick, UK

Presentation of a **poster** entitled "Nitroxide radical chemistry for polymerisation and depolymerisation catalysis".

